

FLUID BORNE NOISE  
IN VANE TYPE  
HYDRAULIC TRANSMISSION SYSTEMS

TO MUM, DAD, SIS AND GRANDMA  
FOR ENCOURAGEMENT AND SUPPORT  
TO PURSUE THE WORK I ENJOYED

FLUID BORNE NOISE  
IN VANE TYPE  
HYDRAULIC TRANSMISSION SYSTEMS

by

GERALD GIM LEE SEET, B.Sc, M.Sc, AMIMechE.

A thesis submitted for the degree of  
Doctor of Philosophy

Department of  
Mechanical & Production Engineering  
The University of Aston in Birmingham

NOVEMBER 1984

**THE UNIVERSITY OF ASTON IN BIRMINGHAM**

**FLUID BORNE NOISE IN VANE TYPE HYDRAULIC TRANSMISSION SYSTEMS**

**GERALD GIM LEE SEET**

A thesis submitted for the degree of Doctor of Philosophy, 1984.

**SUMMARY**

A computer model was developed for a radial vane pump, possessing a new configuration with twin abutments and retractable vanes. The model computes the flow and pressure histories of the segment and port, based on compressibility, leakage and geometry effects. The equation describing the general flow processes is a non-linear first order differential equation, and under specific conditions can be simplified or approximated to a form amenable to a quick solution. The program incorporates a separate algorithm enabling the utilisation of this time saving feature. The combined effects of compressibility, and of segment and port compression mis-match results in high levels of fluid flow ripple. Resistive flow paths (relief grooves), enable correct segment compression by providing adequate leakage from the ports. The program was used to assess the levels of flow ripple and the effectiveness of relief grooves.

Direct measurement of flow ripple is hindered by requirements of high dynamic response, and existing techniques are expensive and complicated. However, dynamic pressure measurements may be used to determine the flow ripple levels. The relationship between the dynamic levels of flow and pressure is dependant on standing wave and other system effects. A technique, utilising transmission line theory, has been developed which enables the deconvolution of individual flow ripples from standing wave and superposition effects.

The pump model has been found to correlate well with actual measurements. Using the model, silencing grooves have been found to be effective in reducing the amplitude of the flow ripple over a wide range of operating conditions. In the pump tested, a 5.4 dB reduction was achieved. Greater reductions are expected under more typical conditions. In tests, the technique of wave deconvolution was effective in recovering the required data with a typical error of 5 percent.

**KEYWORDS**

FLUID BORNE NOISE, FLOW RIPPLE, VANE PUMP MODEL  
HYDRAULIC TRANSMISSION, IMPEDANCE MODEL

## ACKNOWLEDGEMENT

The author wishes to make note of, and extend his most sincere thanks to all who have provided assistance and support during the duration of the project. Due to the nature of the work, many were involved. There are, however, a few who warrant special mention due to their particular involvement during the final stages of this work.

Professor K. Foster and Dr. J. Penny are particularly acknowledged for their technical and moral support which they have so readily provided, especially so in the light of increasing workload.

Technical assistance is indispensable to any research project. It is essential in order to complement the efforts of the researcher, and to enable the work to progress at a faster rate. To these roles, the efforts of Barry, Brian, Malcolm and many others, are acknowledged.

The staff and fellow research students, in particular Andy, are formally acknowledged for their friendship and advice.

The author is indebted to the University of Aston in Birmingham and the Ministry of Defence (Foxhill) for the financial assistance they provided in the form of a research studentship award.

## LIST OF CONTENTS

	Page
SYNOPSIS	i
ACKNOWLEDGEMENTS	ii
LIST OF CONTENTS	iii
LIST OF FIGURES	x
LIST OF TABLES	xiv
NOMENCLATURE	xv
<b>CHAPTER 1 - INTRODUCTION</b>	
1.1 Outline of Overall Research Programme	2
1.2 Noise Generation in Pumps	4
1.3 Relief Grooves	5
1.4 Modelling for Noise	6
1.5 Fundamental Noise Measurements	8
1.6 Structure of the Thesis	9
<b>CHAPTER 2 - A SURVEY OF RELEVANT LITERATURE</b>	
2.1 The Noise Problem in Hydraulics	12
2.1.1 Noise Source and its Propagation	12
2.2 Predicting Fluid Borne Noise in Pumps	15
2.2.1 Relevance to Current Work	19
2.3 Hydraulic Transmission Lines	21
2.3.1 Relevance to Current Work	25
<b>CHAPTER 3 - THE PUMP MODEL</b>	
3.1 Introduction	28
3.2 Description of Pump Model	28

3.2.1	Basic Definitions	30
3.2.2	Description of Segment History	31
3.2.3	Line Flow Ripple	33
3.2.4	Line Pressure Ripple	34
3.2.5	Effects of Silencing Grooves	34
3.3	Fundamental Flow Equations	35
3.3.1	Laminar Flow Between Parallel Plates	35
3.3.2	Laminar Flow Between Moving Parallel Plates	35
3.3.3	Laminar Flow Through an Orifice	36
3.4	Flow and Pressure Equations	36
3.4.1	General Compressible Flow and Pressure Equations	37
3.4.2	General Segment Flow and Pressure Equation	38
3.5	Analytical Solution	40
3.6	Solution of Flow-Pressure equation	42
3.6.1	Flow-Pressure Equation With Zero Port Area	43
3.6.2	Linearised Flow-Pressure Equation Without Flow Reversal	44
3.6.3	Linearised Flow-Pressure Equation With Flow Reversal	46
3.7	System Modelling Scheme	48
 <b>CHAPTER 4 - TRANSMISSION LINE MODEL</b>		
4.1	Introduction	51
4.2	The Fourier Transform	53
4.3	Wave Propagation Theory	55

4.4	Transmission Line Model	58
4.5	Lossless Anechoic Line	61
4.6	Pump-Motor Transmission Model	63
4.7	Solving the Standing Wave Equation	66
4.7.1	Removing Standing Wave Effects	66
4.7.2	Uncoupling Wave Superposition Effects	72

## CHAPTER 5 - COMPUTER IMPLEMENTATION

5.1	Introduction	76
5.2	Computer System Configuration	78
5.3	Suite of Programs	80
5.4	Datafile Structure	82
5.4.1	Parameter Datafile	84
5.4.2	Process Datafile	88
5.5	Program VFLGEN	91
5.6	Program VMODEL	92
5.7	Program VPLOT	112

## CHAPTER 6 - STANDARD PUMP SIMULATIONS

6.1	Introduction	115
6.2	Line Pressure Effects	117
6.2.1	Pressure Effects on Segment History	117
6.2.2	Pressure Effects on Flow Ripple	119
6.3	Speed Effects	121
6.3.1	Speed Effects on Segment History	121
6.3.2	Speed Effects on Flow Ripple	123
6.4	Vane Tip Clearance Effects	125
6.4.1	Vane Tip Effects on Segment History	125
6.4.2	Vane Tip Effects on Flow Ripple	127

6.5	Fluid Viscosity Effects	127
6.5.1	Viscosity Effects on Segment History	130
6.5.2	Viscosity Effects on Flow Ripple	130
6.6	Fluid Bulk Modulus Effects	133
6.6.1	Modulus Effects on Segment History	133
6.6.2	Modulus Effects on Flow Ripple	133
6.7	End-Plate Clearance Effects	135
6.7.1	End-Plate Effects on Segment History	135
6.7.2	End-Plate Effects on Flow Ripple	137
6.8	General Conclusions	137

## **CHAPTER 7 - RELIEF GROOVES**

7.1	Introduction	140
7.2	Groove Profiles	140
7.3	Groove Profile Effects	143
7.3.1	Profile Effects on Segment History	145
7.3.2	Profile Effects on Flow Ripple	147
7.4	Groove Length Effects	150
7.4.1	Length Effects on Segment History	150
7.4.2	Length Effects on Flow Ripple	150
7.5	Inlet Groove Effects	152
7.5.1	Inlet Effects on Segment History	152
7.5.2	Inlet Effects on Flow Ripple	154
7.6	Speed Effects	154
7.6.1	Speed Effects on Segment History	157
7.6.2	Speed Effects on Flow Ripple	157
7.7	Line Pressure Effects	157
7.7.1	Pressure Effects on Segment History	160
7.7.2	Pressure Effects on Flow Ripple	160

7.8	End-Plate Effects	163
7.8.1	End-Plate Effects on Segment History	163
7.8.2	End-Plate Effects on Flow Ripple	163
7.9	Optimum Groove Criteria	164

## **CHAPTER 8 - EXPERIMENTAL WORK**

8.1	Introduction	171
8.1.1	Data Acquisition and Analysis System	171
8.1.2	Pump System Schematic	175
8.1.3	Transmission Line System Schematic	175
8.2	Pump Model Correlation	176
8.2.1	Harmonic Analysis of Pump Data	179
8.2.2	Time Average Analysis of Pump Data	180
8.3	Correlation of Pump Performance Data	180
8.3.1	Performance of Standard Pump	185
8.3.2	Performance of Silenced Pump	191
8.4	Conclusion on Pump Model	192
8.5	Acquiring Transmission Line Data	196
8.5.1	Standing Wave Data	199
8.6	Conclusion on Transmission Line Model	203
8.7	Procedure for the Deconvolution of Pressure Ripples	204

## **CHAPTER 9 - CONCLUSION**

9.1	Conclusion	208
9.1.1	Conclusion on Pump Model	208
9.1.2	Conclusion on Transmission Model	210
9.2	Recommendation for Further Work	212

## APPENDICES

### Appendix A - Geometrical Relationships for Pump Model

A.1	Cam Actuation Profile	216
A.2	Silencing Groove Geometry	218
A.3	Port Geometry	221
A.4	Segment Geometry	223

### Appendix B - Algorithm for Analytical Solution

B.1	Introduction	231
B.2	Algorithm 1	232
B.3	Algorithm 2	233
B.3.1	Starting Point for Equation (3.6.13) at Branch (A.2.1)	235
B.3.2	Starting Point for Equation (3.6.19) at Branch (A.2.3)	236
B.4	Algorithm 3	237
B.5	Algorithm 4	238
B.5.1	Starting Point for Equation (3.6.13) at Branch (A.4.1)	239
B.5.2	Starting Point for Equation (3.6.13) at Branch (A.4.3)	240
B.6.1	Algorithm for Solving for Root of non-linear equation	242
B.6.2	Modified Regula-Falsi Method	244
B.6.3	Newton-Raphson Method	246
B.6.4	Algorithm for the solution of the root of the equation	246

## **Appendix C - Listing of Pump Model Programs**

C.1	Program VFLGEN	251
C.2	Program VMODEL	258
C.3	Program VPLOT	294

## **Appendix D - Simulation Run**

D.1	Introduction	304
D.2	Datafile Preparation	305
D.3	Process Simulation	307
D.4	Graphical Output	308

## **REFERENCES**

List of Abbreviations	314
List of References	315

## LIST OF FIGURES

Figure	Title	Page
3.2.1	Vane Pump Schematic	7
3.2.2	Basic Definitions	29
3.7.1	System Modelling Scheme	48
4.2.1	Forms of the Fourier Transform	52
4.2.2	Fourier Transform of Pressure Pulse	54
4.4.1	Simple Hydraulic Circuit	57
4.4.2	Equivalent Impedance Circuit	57
4.6.1	Pump-Motor Transmission System	64
5.2.1	Computer System Configuration	77
5.3.1	Program Interconnection	79
5.4.1	Parameter Datafile Structure	83
5.4.2	Process Datafile Structure	87
5.5.1	Flow Chart of Program Vflgen : Sheet 1	89
5.5.2	Flow Chart of Program Vflgen : Sheet 2	90
5.6.1	Flow Chart of Program Vmodel : Sheet 1	93
5.6.2	Flow Chart of Program Vmodel : Sheet 2	95
5.6.3	Flow Chart of Program Vmodel : Sheet 3	96
5.6.4	Flow Chart of Program Vmodel : Sheet 4	97
5.6.5	Flow Chart of Program Vmodel : Sheet 5	98
5.6.6	Flow Chart of Program Vmodel : Sheet 6	99
5.6.7	Flow Chart of Program Vmodel : Sheet 7	102
5.6.8	Flow Chart of Program Vmodel : Sheet 8	104
5.6.9	Flow Chart of Program Vmodel : Sheet 9	107
5.6.10	Flow Chart of Program Vmodel : Sheet 10	108
5.7.1	Flow Chart of Program Vplot : Sheet 1	110

5.7.2	Flow Chart of Program Vplot : Sheet 2	111
6.2.1	Mean Line Pressure Effects on Segment History	116
6.2.2	Mean Line Pressure Effects on Flow Ripple	118
6.3.1	Shaft Speed Effects on Segment History	120
6.3.2	Shaft Speed Effects on Flow Ripple	122
6.4.1	Vane Clearance Effects on Segment History	124
6.4.2	Vane Clearance Effects on Flow Ripple	126
6.5.1	Fluid Viscosity Effects on Segment History	128
6.5.2	Fluid Viscosity Effects on Flow Ripple	129
6.6.1	Fluid Bulk Modulus Effects on Segment History	131
6.6.2	Fluid Bulk Modulus Effects on Flow Ripple	132
6.7.1	End-Plate Clearance Effects on Segment History	134
6.7.2	End-Plate Clearance Effects on Flow Ripple	136
7.2.1	Groove Flow Area Vs Groove Position	141
7.2.2	Change in Groove Flow Area Vs Groove Position	142
7.3.1	Outlet Groove Profile Effects on Segment History	144
7.3.2	Outlet Groove Profile Effects on Flow Ripple	146
7.4.1	Outlet Groove Length Effects on Segment History	148
7.4.2	Outlet Groove Length Effects on Flow Ripple	149
7.5.1	Inlet Groove Effects on Segment History	151
7.5.2	Outlet Groove Effects on Flow Ripple	153
7.6.1	Speed Effects on Segment History of Silenced Pump	155
7.6.2	Speed Effects on Flow Ripple of Silenced Pump	156
7.7.1	Mean Line Pressure Effects on Segment History of Silenced Pump	158
7.7.2	Mean Line Pressure Effects on Flow Ripple of Silenced Pump	159
7.8.1	End-Plate Clearance Effects on Segment History of Silenced Pump	161

7.8.2	End-Plate Clearance Effects on Flow Ripple of Silenced Pump	162
7.9.1	Segment History of the Silenced Pump	165
7.9.2	Flow Ripple of the Silenced Pump	166
8.1.1	Data Acquisition and Analysis System	170
8.1.2	Pump System Schematic	173
8.1.3	Transmission Line Schematic	174
8.2.1	Outlet Spectrum of Unsilenced Pump	177
8.2.2	Outlet Spectrum of Silenced Pump	178
8.3.1	Performance Correlation of Standard Pump at 700 rpm	181
8.3.2	Performance Correlation of Standard Pump at 1050 rpm	182
8.3.3	Performance Correlation of Standard Pump at 1400 rpm	183
8.3.4	Performance Correlation of Silenced Pump at 700 rpm	187
8.3.5	Performance Correlation of Silenced Pump at 1050 rpm	188
8.3.6	Performance Correlation of Silenced Pump at 1400 rpm	189
8.4.1	End-Plate Clearance Effects on Outlet Spectrum	193
8.4.2	Outlet Spectrum of Standard and Silenced Pump	194
8.5.1	Anechoic Data	197
8.5.2	Spectral Map of Reverberant Chamber	198
8.5.3	Standing Wave in Reverberant Chamber	200
A.1.1	Cam Profile Geometry	215
A.2.1	Groove Geometry	217
A.3.1	Port Geometry	220
A.4.1	Segment Geometry	222
B.1.1	Algorithm 1	228
B.1.2	Algorithm 2	229
B.1.3	Algorithm 3	229
B.1.4	Algorithm 4	230
B.3.1	Starting Values for Branch (A.2.1)	234

B.3.2	Starting Values for Branch (A.2.3)	236
B.5.1	Starting Values for Branch (A.4.1)	239
B.5.1	Starting Values for Branch (A.4.3)	241
B.6.1	Modified Regula-Falsi Method	243
B.6.2	Newton-Raphson Method	245
B.6.3	Algorithm for Solving Roots of Equation - Sheet 1	247
B.6.4	Algorithm for Solving Roots of Equation - Sheet 2	248
D.2.1	Parameter Datafile Contents	305
D.4.1	Graphical Output of Pump Process - Sheet 1	310
D.4.2	Graphical Output of Pump Process - Sheet 2	311

## LIST OF TABLES

Table	Title	Page
8.3.1	Quantitative Correlation Between Simulated and Measured Flow Ripple - Standard	184
8.3.2	Quantitative Correlation Between Simulated and Measured Flow Ripple - Silenced	190
8.5.1	Quantitative Correlation Between Anechoic and Derived Pressure Amplitudes	201

## NOMENCLATURE

The following list summarises the notations used throughout the main thesis. Where it was necessary to use the same variables to represent different parameters, the list provides the alternative definitions and the context in which the variables appear (in brackets). Local constants and variables do not appear in this list. They are defined locally in the text where they appear.

A	Cross-sectional area
$A_d$	Amplitude component of reflection constant at datum
$A_s$	Amplitude component of reflection constant at source
$A_t$	Amplitude component of reflection constant at termination
$A_x$	Amplitude component of reflection constant at x
b	Plate width
$C_d$	Coefficient of discharge
d	Mean pipe diameter
D	Orifice diameter
$D_i$	Inlet orifice diameter
$D_o$	Outlet orifice diameter
Dir	Pressure gradient sign
Dir <sub>d</sub>	Pressure gradient sign at dominant port
Dir <sub>i</sub>	Pressure gradient sign at inlet
Dir <sub>o</sub>	Pressure gradient sign at outlet
e	Naperian constant
h	Plate separation (pump)
h	Pipe wall thickness (transmission line)
$H_1$	Leading vane clearance
$H_2$	Trailing vane clearance
$H_3$	End-plate clearance

L	Pipeline length (transmission line)
L	Vane, rotor width (pump)
$L_3$	End-plate land length
ln	Natural logarithm
m	mass
P	Pressure
$P_d$	Pressure at dominant port (pump)
$P_d$	Pressure at datum position (transmission line)
$P_E$	Pressure at start of line
$P_i$	Inlet port pressure
$P_{mx}$	Pressure at x due to motor
$P_o$	Outlet port pressure
$P_{px}$	Pressure at x due to pump
$P_t$	Pressure at termination
$P_x$	Pressure at position x
$P_1$	Pressure at position 1
$P_2$	Pressure at position 2
$P'_o$	Pressure at outlet with characteristic line
Q	Flow
$Q_e$	Entrained flow
$Q_{in}$	Flow into volume
$Q_l$	Leakage flow
$Q_o$	Orifice flow
$Q_{out}$	Flow from volume
$Q_s$	Flow at source (transmission line)
$Q_s$	End-plate leakage (pump)
$Q_{sm}$	Flow at source due to motor
$Q_{sp}$	Flow at source due to pump
$Q_t$	Flow at termination

$Q_v$	Viscous flow
$Q_x$	Flow at position $x$
$Q'_o$	Flow at outlet with characteristic line
$R$	Line resistance
$t$	Time
$U$	Relative surface velocity
$V$	Volume
$W$	Vane width
$W_3$	End-plate land width
$x$	Position from start of line
$Z$	Impedance
$Z_o$	Characteristic impedance of pipeline
$Z_r$	Variable at point of flow reversal
$Z_s$	Source impedance
$Z_{sm}$	Source impedance due to motor
$Z_{sp}$	Source impedance due to pump
$Z_t$	Termination impedance
$\beta$	Bulk modulus
$\beta'$	Effective bulk modulus
$\gamma$	Wave propagation constant
$\mu$	Coefficient of absolute viscosity
$\omega$	Angular velocity
$\rho$	Fluid density
$\rho_s$	Source reflection constant
$\rho_{sm}$	Source reflection constant due to motor
$\rho_{sp}$	Source reflection constant due to pump
$\rho_t$	Termination reflection constant
$\rho_{tm}$	Termination reflection constant due to motor
$\rho_{tp}$	Termination reflection constant due to pump

$\theta_1$	Angle at position 1
$\theta_2$	Angle at position 2
$\theta_d$	Phase component of reflection constant at datum
$\theta_r$	Angle at point of flow reversal
$\theta_s$	Phase component of reflection constant at source
$\theta_t$	Phase component of reflection constant at termination
$\theta_x$	Phase component of reflection constant at x

## **CHAPTER 1 : INTRODUCTION**

- 1.1 Outline of Overall Research Programme
- 1.2 Noise Generation in Pumps
- 1.3 Relief Grooves
- 1.4 Modelling for Noise
- 1.5 Fundamental Noise Measurements
- 1.6 Structure of the Thesis

## 1.1 Outline of Overall Research Programme

The work described in this thesis forms but part of an extensive Ministry of Defence research and development programme, on high power marine hydraulic propulsion systems. The programme of work, which was commissioned in 1973, was conceived to study the feasibility of employing hydrostatic transmission systems in medium to large sized Naval vessels. These hydraulic transmission systems were required to replace the conventional propeller shaft and mechanical gearbox systems currently employed in these vessels. With these systems numerous advantages were anticipated for the intended Naval applications.

With the absence of the constraint imposed by a heavy rigid drive shaft, hydraulic transmission can provide a system of high flexibility and improved ship manoeuvrability. In conventional systems, it is essential to locate the prime-mover and propeller in close proximity. The equipment layout is also heavily dictated by the shaft and gearbox configuration. With hydraulic transmission, it is physically possible to locate the prime-mover and drive at opposite ends of the vessel and coupled flexibly by high pressure hydraulic hoses.

There are further advantages to be derived from a system which is flexibly coupled. The problem of structurally transmitted noise from the prime-mover, is practically removed and greater design flexibility of the system is afforded. The propeller and drive may be contained in a pod and designed as an integral unit. This could be mounted so as to enable the vessel greater manoeuvrability and stability. A propeller pod capable of 180 degree rotation enables reversed thrust without the need for a reversible pitch propeller screw. Entangled or damaged propellers can be dealt with simply by a quick decoupling and replacing the entire drive units, a distinct advantage recognised

during servicing and repair.

Through a system of valves and cross-links, additional prime-movers can be switched into and removed from the network. Damaged sections can be removed and serviced without affecting the operation of the entire system. By this method a highly efficient system can be made to operate.

The above are but some of the advantages that can be derived from a hydraulic transmission system. The direct shaft transmission has one significant advantage, its mechanical efficiency approaches 100 percent. With commercially available hydraulic systems, of small power, the efficiency is, at best, of the order 80-85 percent under optimum running condition. The capacity for the generation of severe fluid and structurally borne noise is another problem to be considered. At one end of the transmission line, fluid at greater volume and lower pressure is compressed, and at the other end the fluid is expanded to a lower pressure. These operations, if not performed precisely, are potential noise sources. Provided the levels of losses in mechanical efficiency and noise are kept low, these disadvantages would be offset by the advantages cited earlier.

The research programme involved four establishments, the Universities of Aston and Birmingham, Normalair Garrett Ltd. (Yeovil) and the Ministry of Defence (Foxhill), in a project co-ordination capacity. In physical terms, the project involved the design, development and testing of a 1 MW. motor and a 100 KW. pump.

As the motor was intended to be incorporated into a propeller boss and provide direct drive to the screw, the external diameter and size was critical. Due to this constraint on size and that of requiring high

efficiency, a new motor configuration was required. This motor designed by Jones (1), can be described as being a derivation of two radial vane pumps whose rotors are turned inside out and fixed together through a central plate.

The pump is of the radial vane configuration, with twin abutments and retractable vanes. This gives the pump the qualities of a large swept volume, for a given pump dimension, and also a radially balanced rotor shaft. The pump operation and physical geometry are described later in the thesis (chapter 3 and appendix A). The initial design work is attributed to Burgess (2) and Wuerzer (3).

Normalair Garrett was essentially assigned the task of constructing, developing and testing of the motor and its associated test rig. To them was also entrusted the preliminary design of a 1 MW. radial vane pump. The University of Birmingham was principally assigned the task of further design, development and testing of the 100 KW. radial vane pump and its test rig. The University of Aston was responsible for all noise work at the various research establishments. Primarily the work consisted of modelling the radial vane pump to identify its noise potential, and in the designing of silencing grooves to minimise the noise levels. Included in this brief, was the responsibility of designing all the data acquisition and noise analysis systems relating to the overall project. Attempts to fulfil the second task, resulted in the study of waveforms under the influence of standing waves.

## **1.2 Noise Generation in Pumps**

In a hydraulic system, the positive displacement pump has the potential of being the main noise source. Noise is an unwanted by-product of

the energy conversion process, Stecki (4) and BISHOPP (5). The pumping action is basically one of taking finite quantities of fluid at low pressure and injecting into a high pressure outlet. This repeated action produces a continuous flow of fluid with a superimposed flow fluctuation. As a consequence of the system impedance, there results a pressure fluctuation in the system. This pressure fluctuation in turn results in transmission of both structural and fluid borne noise.

In a pump there is a further mechanism of noise generation. Under ideal conditions, the pockets of fluid are raised to the outlet pressure before they are permitted to communicate with the system pressure. This results in a smooth transition of fluid pressure from the low inlet to the high outlet. The process of compressing the fluid and taking it to the level of the outlet is known as 'pre-compression'. Ideally, fluid is discharged smoothly into the system. In cases of mis-matched segment and port pressures very vigorous back-flow of fluid can occur at the instant segment and port communicate. This results in the generation of fluid borne noise. Cavitation of the fluid, and also erosion of the pump walls and elements can occur, in extreme cases. Similar effects are observable at the inlet, and are appropriate to the case of motors. The key to quiet pump operation is therefore to seek a smooth transfer of low pressure fluid to a high pressure outlet.

### 1.3 Relief Grooves

The importance of adequate pre-compression for quiet pump operation has been explained (section 1.2). By appropriately timing the instant at which the port begins to communicate with the segment volume, adequate pre-compression levels can be achieved for a very narrow range of operating conditions. Unfortunately, the pre-compression requirements

are dependant on a number of parameters. These are system pressure, fluid bulk modulus, viscosity, operating speed and temperature. The effects of temperature are a consequence of its effects on fluid modulus and viscosity. As it is unacceptable to design pumps with a narrow quiet operating range, a more tolerant means of ensuring adequate pre-compression is desired.

Relief or silencing grooves is a means of coping with the problem and provides for quiet operation under wide operating conditions. Relief grooves are resistive pathways which provide controlled communication between the port and segment before direct port communication occurs. To a lesser extent, relief groove operations are also dependant on the fluid and operating parameters for optimum pre-compression. Although these grooves provide adequate silencing over a wide range of conditions, it is still desirable to optimise their parameters for the mean required operating conditions. The groove parameters and their effects are studied in chapter 7 and appendix A.

#### **1.4 Modelling for Noise**

The main objective of mathematical modelling is to minimise the trial and error stage of product development. It can be used to evaluate alternative designs and the performance of a degraded system, Iyengar (6).

In recent years the cost of digital computers has fallen considerably and the concept of personal computers have become a reality. The fall in computing costs have been offset by a corresponding increase in the general cost of research, and product development.

Product performance has also taken on new dimensions. A product is

appraised not just on its immediate tasks but in its ability to satisfy numerous legislation as regards safety, user comfort, noise and other undesirable effects. The developed product must, in addition, be cost competitive and economic to run. In view of such severe demands on product performance, increasing use is made of mathematical modelling and other design aids. These are being accepted as necessary tools in design, Foster (7) and Hooke et al.(8). In recent years, both manager and designer have become aware of the cost savings to be derived from the use of computer analysis and design aids.

Recently noise has been given ever increasing attention. Manufacturers have been placed under considerable pressure to develop quieter fluid power systems. The significance of noise is even greater due to the move towards higher operating pressures and speeds.

In this thesis, a radial vane pump model has been developed which enables the prediction of both flow and pressure histories. This model was used to study the effects of various parameters on the potential for noise generation. Various groove profiles were simulated to obtain the optimum groove parameters for the required operating conditions.

In the modelling of such hydraulic devices, one major problem is obtaining the solution of the system equations. The fundamental equations are generally non-linear first order differential equations with no analytical solution. A numerical solution method is therefore required. As the equations are generally 'stiff', implying an equation where parameters change at widely different rates, very long computation times are required. This program applies a sophisticated semi-analytical solution technique. The significance of parameters are checked by the computer program, and where appropriate, solves the linearised forms of the equations. This technique results in a

considerable saving of computation time.

### 1.5 Fundamental Noise Measurements

In hydraulic pumps, one of the most important parameter defining the potential for noise output is the flow fluctuation. This parameter is difficult to measure directly as the majority of flow measuring transducers are unable to meet the high dynamic response required. Where equipment or techniques are available, these tend to be very expensive, difficult to operate or both. The problem can be overcome by measuring the pressure fluctuations and correlating the measurement to flow using the transmission line theory. With this 'solution' comes a different type of problem. O'Neal et al.(9).

The fundamental relationships relating flow and pressure are complex and the parameters difficult to determine. The complexity of the relationships are due to standing wave effects in the presence of reverberant conditions. Where the standing wave effects are removed, the relationships are greatly simplified.

In the measurement of pump fluid borne noise potential it has become acceptable to quote pressure ripple levels under anechoic conditions. It is, however, possible to calculate the flow ripple levels from a knowledge of the line characteristic impedance, source impedance and the pressure ripple levels. Anechoic termination conditions are obtained by connecting long hydraulic lines to the ports, so as to remove the effects of reflection at the line termination. As pressure ripple levels are a function of the line and termination conditions, it is also necessary to specify the line diameter and other termination conditions. It is, however, accepted that the quieter pump under

anechoic condition is also quieter under any other operating condition.

Where it is not possible to analyse a pump or system under anechoic conditions, it is not sufficient to attempt a measurement of the fluid borne noise by simply measuring the pressure at a particular point in the line, and analysing the waveform. Under reverberant conditions, the waveform is a function of position. Since the anechoic condition pressure data is the parameter of interest and is needed to correlate to flow measurements, the fundamental pressure data must be unravelled from the effects of standing waves. Once this fundamental pressure fluctuation is determined, the flow fluctuation can be determined from a knowledge of the line and source impedances. In most instances, however, the pump potential is commonly presented in terms of the pressure ripple.

In this thesis, standing waves in transmission systems are studied (chapter 4), for the purpose of unravelling reverberant noise data. This enables the identification of the noise potential of individual pumps and motors in a reverberant system.

## **1.6 Structure of the Thesis**

The thesis is divided into nine chapters and four appendices. The present chapter serves to introduce the theme and subjects relating to the thesis. Various topics are briefly discussed qualitatively, while details are omitted, to be elaborated on in later chapters. In chapter two, a survey is presented of relevant literature by other researchers. Their work is summarised and the relevance to this work is highlighted. In chapters three and four, the theory relating to the vane pump and transmission line models are developed respectively. In chapter three,

the general flow equations are first derived and further developed to the linearised form. This provides greater computational efficiency. In addition to developing the general transmission line model, the latter chapter also presents the equations and techniques appropriate to its implementation, for unravelling standing wave effects. The pump model computer program is detailed in chapter five. The main structure is presented and discussed, with the aid of flow charts. The chapters six and seven, presents the simulations performed by the developed vane pump computer model. The former chapter deals with simulations relating to the standard pump, and the latter those incorporating silencing grooves. Various effects are studied with the emphasis on flow fluctuations and the minimising of the noise potential. Chapter eight describes the data acquisition and analysis system developed, together with experimental results. Experimental results are presented for correlating with the pump model predictions, and the transmission line model is verified experimentally. The final chapter, summarises the overall work, and presents its conclusion.

In the appendices, listings are provided of the computer programs developed together with other details, which though necessary, are felt likely to provide a distraction from the main flow of the thesis.

## **CHAPTER 2 : A SURVEY OF RELEVANT LITERATURE**

- 2.1 The Noise Problem in Hydraulics
  - 2.1.1 Noise Source and its Propagation
- 2.2 Predicting Fluid Borne Noise  
in Pumps
  - 2.2.1 Relevance to Current Work
- 2.3 Hydraulic Transmission Lines
  - 2.3.1 Relevance to Current Work

## **2.1 The Noise Problem in Hydraulics**

In recent years, the problem of noise has been receiving increasing attention. Noise levels which were previously considered 'acceptable' are now considered as socially unacceptable or even hazardous. Under the current 'Health and Safety at Work Act', excessive noise at work can constitute an offence. It is currently also recognised that noise reduces the operator's performance and productivity levels. The reduction in general noise levels is therefore both necessary and desirable.

Although it has long been recognised that the reduction of noise is desirable, manufacturers of hydraulic components and plants have often overlooked this aspect of design, in their quest for higher power to weight ratios. The unacceptable neglect of noise aspects in hydraulic design has been recognised, and efforts made to overcome this trend. This has taken the form of a concerted research and development effort by both industry and research establishments. In view of the current concern regarding noise levels, the noise specification is becoming of increasing importance to the selection of equipment. The manufacturer of quieter equipment would have an edge over his competitor, and in the present competitive climate, could provide the necessary difference between success and failure of a product.

### **2.1.1 Noise Source and its Propagation**

In a hydraulic circuit, the pump and valves are potentially the major sources of noise. Although the noise levels from valves can be much higher than in pumps, more effort has been directed towards reducing the noise levels from pumps. The noise spectrum from valves are broad

band, Crook et al.(10). In contrast, the spectrum of pump noise is narrow band with components occurring at harmonics of the fundamental frequency. Broad band noise is potentially less of a problem as the energy is spread out over a wider spectrum. In general, it is less annoying in terms of human comfort and less likely to induce severe vibrations in adjacent structures.

Noise emanating from hydraulic equipment can generally be recognised as consisting of three components; air-borne noise (ABN), fluid borne noise (FBN) or structurally borne noise (SBN). Air-borne noise is radiated directly from the casing, structural borne noise is transmitted via the mountings, and fluid borne noise is transmitted via the fluid along the inlet and outlet lines. As both fluid and structurally borne noise components have the potential of being converted to air-borne noise, efforts to silence a hydraulic system must be directed at all three components. The method of reducing noise which is most applicable to the general industrial user would be that of noise isolation. The long term and probably the most effective method must be that of reducing noise at its source. This method, however, is more appropriate to manufacturers.

Much work has been undertaken in the study of noise isolation and its reduction at source. The transmission of structural borne noise through pump and valve mountings have been studied by Heron et al.(11). This work demonstrated the advantages to be obtained, in terms of reducing air-borne noise levels, by the implementation of vibration isolation techniques. The two main pathways for structurally borne noise was shown to be the walls of fluid lines and mountings. Fluid borne noise has been studied analytically by Longmore (12). He derived equations which enabled the pressure and flow fluctuations, as well as wall

vibrations in hoses to be predicted. The analysis was reported to be consistent with experimental measurements. Crook et al.(13) has studied the transmission of air-borne noise in hydraulic lines due to fluid flow fluctuation. The effects of tube bore and material rigidity on the level of air-borne noise were investigated. It was shown that, in the absence of structural vibrations, lower air-borne noise emission levels can result from the use of rigid or nylon hose in preference to rubber hydraulic hose. The use of smaller bore rigid or hydraulic hoses also results in lower noise levels. In the case of non-straight pipe configurations, fluid borne flow fluctuation can induce high levels of structural vibration. This effect has been studied and reported by Hughes (14). He discusses the mechanisms involved and attributes it to the oscillatory forces generated in the line due to dynamic pressure differences.

No less effort has gone into the study of noise generation at source, in both valves and pumps. The design of a quiet valve has been reported by Donaldson (15). In a valve, fluid is made to change its pressure and flow velocity. If the process is not performed gradually, cavitation can occur and noise will be generated. The valve reported by Donaldson controls this process by lengthening the flow path. This provides for a controlled dissipation of the pressure energy and thus produces a more ideal condition for the process. Much has also been done in the study of noise in pumps. One of the earlier works was by Helgestad et al.(16) who studied the axial piston pumps extensively both theoretically and experimentally. Martin et al.(17) studied the problem of optimum port plate timing for axial piston pumps. For a pump operating under a very narrow operating envelope, smooth operation can be obtained by appropriate timing of the port plate. This is, however, not a practical solution as most pumps operate under a wide range of operating

conditions. Correctly designed relief grooves were shown to be effective in providing smooth operations under a wider envelope. In addition to operating conditions, the fluid being pumped has an affect on the optimum condition. This has been studied by Kelsey et al.(18). Using a computer program, the output flow ripple from a piston pump has been simulated for a variety of fluids. Kelsey demonstrated that a pump designed for quiet operation using mineral oil would result in high noise levels when using fire resistant fluids. This is due to the significant differences in the fluid properties of the two mediums.

## **2.2 Predicting Fluid Borne Noise in Pumps**

Interest in the modelling of hydraulic pumps dates to the mid-1920s with the publication in 1926, by Brown (19), relating to gear pump design. A simple equation was provided which enabled the delivery to be estimated. The work by Meldahl (20) can however be considered, Fielding et al.(21), as being the foundation to much of the future work. Meldahl derived, an equation describing ideal delivery flow and considered the problem of trapped fluid. He suggested that pathways in the pump case could be used to relieve the trapped volume in the meshing teeth. Besides Meldahl, there has been many other names which have become associated with gear pump analysis. Some of which are Mukherjee et al.(22), Merritt (23) and Hadekel (24).

Later in 1953, Bloch (25) investigated the flow, forces and pressure fluctuations in axial piston fluid transmission. In this work many assumptions were made in order that the equations could be solved. Two other early researchers were Zaichenko et al.(26) and Yamaguchi(27). In the work by Zaichenko an approximate method was formulated, whereby

the dimensions of shaped restrictors could be estimated for the use of reducing the flow ripple.

In the earlier analysis, true simulations were not possible due to the absence of automated computing facilities. Researchers from necessity tended to include numerous simplifications in their models. Accurate simulations have only been possible with the widespread availability of cheap computing power. Helgestad et al.(28) in 1974, originated a computer model based on the theory for pressure transients in axial piston pumps. This model enabled the cylinder pressures and port flows to be predicted analytically. The theory was devised for the case of a volume of fluid in the cylinder being displaced by the piston via a portplate. The pump was modelled as being connected to two oil volumes, one at the inlet and outlet respectively. The resulting mathematical model was a non-linear differential equation. This was solved using a variable step Runge-Kutta method. Due to the 'stiffness' of the equation, the solution required an excessively long time, and faced the possibility of numerical instability, resulting in a wasted simulation run. This model was later developed by Kakoullis (29). He modified the theory and computer program to include the simulation of the swash plate moments and torque transients. Attempts to correlate the theoretical and experimental results were rewarded with limited success.

The work by Halgestad and Kakoullis, on the axial piston pump, was subsequently developed by Hannan (30). He re-wrote the computer program while modifying both the fundamental model and the solution technique. The modified program was cited by Foster et al.(31), in which a good theoretical model of an axial piston pump was described. The program was shown to predict flow, force and pressure fluctuation, with good

correlation to practice. A forty fold savings in program execution cost was also reported.

In this adaptation of the axial piston pump program, the inlet and outlet port conditions of the model was changed, together with the technique applied to the solution of the differential equation. The inlet model was simplified and a constant port pressure was assumed. The outlet was modelled as being an anechoic termination, using transmission line theory. This technique of considering pressure fluctuations in terms of impedance and transmission line theory was applied by Willekens (32). In this work, he showed that the effects of viscosity could be neglected in this context. Modelling an anechoic termination has the advantage that, a practically anechoic termination is fairly easily realised.

In the early model the Runge-Kutta method, which was used to solve the non-linear differential equation, was found to be very time consuming. Hannan in an effort to minimise the computation time utilised a semi-analytical method to solve the equation. The method in effect reduces the problem to one involving the solution of a transcendental equation. This is achieved by employing a step-wise solution where leakage is considered to be constant over the step length. This method undoubtedly introduces an element of error. Providing that the step length is sufficiently small, this error is not significant. This assumption is particularly appropriate to an axial pump, as leakage is typically only a small component of the total flow for a major part of the pump history. Where leakage is significant, there is no port flow. Under this condition the equation can be solved analytically. The semi-analytical method, therefore, consists of an inspection of the parameters and identifying the conditions, to which the appropriate

equations and solutions are applied.

Recently, another attempt has been made to quantify the pump flow ripple from an axial piston pump, Kogima et al.(33). In this analysis, however, a simple semi-empirical method was used. The back-flow was modelled as a triangular function with the fluid compressibility effects occurring totally at the instant of port communication. A good correlation was reported between the experimental and theoretical observations. This demonstrates the dominant effects of fluid compressibility on the pump flow ripple.

Three years after Helgestad reported of his axial pump computer program, Fielding et al.(34), reports another computer program capable of predicting the flow fluctuations from an external gear pump. This enabled the study of parameters which affect the fluid flow ripple, and thus the potential for fluid borne noise generation. In this program, the flow due to the meshing of the gear teeth were calculated for each gear increment. At each rotor position, the port flow and pressure in the tooth spaces were calculated, whilst considering the summed effects of variations in trapped volume, tooth tip leakage, entrained and port flows. In addition the effects of trapped volume during double tooth meshing and gear eccentricity were considered. Ideal inlet and outlet conditions were assumed, together with a constant inlet pressure and an anechoic outlet termination. The effects of cavitation, end-plate leakage and fluid compressibility were ignored. Provided the pump inlet pressure is sufficiently boosted, cavitation effects can be neglected. Significant end-plate leakage and compressibility effects can however alter the results significantly. The program was reported to provide good qualitative correlation to experimental data. Discrepancies were attributed to experimental error, the assumption of ideal inlet and

outlet conditions, and wave effects.

The gear pump program has since been further developed and reported by Bidhendi et al.(35). In this paper, a refined model is presented and the program re-structured to make the execution more amenable for design and verification analysis. Although ideal port conditions and the anechoic outlet termination are maintained, the theoretical model has been further refined and modified to include the necessary effects of end-plate leakage, cavitation and fluid compressibility, within the adjacent tooth space. A constant end-plate clearance is assumed, which Fielding et al.(36) has shown this to be a valid assumption in an experimental investigation. Compressibility within the meshing volume was not considered. In addition the hydraulic moments and shaft forces are also computed. Although a limited correlation to practical data was made, the program has been demonstrated, especially with its graphical data presentation techniques, to be ideal for providing the starting point in design applications.

### **2.2.1 Relevance to Current Work**

Radial vane pumps have traditionally been considered as potentially quiet machines. This has resulted in the relative neglect of noise studies relating to vane machines. Recently, a theoretical model for a balanced vane pump has been published by Kogima et al.(37). In this work an attempt was made to model the flow ripple whilst considering the effects of fluid compressibility, variations in trapped volume, vane tip leakage and port flows. The effects of entrained flow and end-plate leakage were not considered. A further simplification, was made in the derivation of the port flow equation. The line pressures

were assumed constant. This would result in an underestimation of the flow ripple. In the solution of the flow equations, the Runge-Kutta method was used. The disadvantages of this method of solution has been described in the previous sections.

The vane pump described in this thesis employs a new and novel configuration. The model developed considers the additional effects of vane tip entrained flow and end-plate leakage. In addition, the model overcomes the need for assuming constant line pressures by reiterating the port and line calculations. For the solution of the flow equations, a semi-analytical solution was used, giving a significant savings in computational time.

The goal set for the development of this radial vane pump computer model was to determine its potential for quiet operation, and to study the effects of relief groove configuration on the flow ripple from this pump.

The mathematical equation defining the pump processes are fundamentally the same in all the three types of pumps. The differences lies in the dominance of the various parameters and consequently in the method to which the equations can be solved. In the piston pump, long solution time was shown to be a problem in the formulation of an engineering application program. This problem led to the implementation of the semi-analytical solution technique, which significantly reduces the computation time. As mentioned earlier, this technique is only valid when leakage flow is only a small percentage of the combined flow parameters. In the vane pump, the leakage is not necessarily a minor component. The significance of the various parameters changes, and depends on both the relative leakage parameters and its history during the pump cycle.

In the vane pump program, it is not valid to approximate the solution to one where leakage is constantly a small factor during the entire pumping cycle. This program incorporates a sophisticated algorithm which identifies the condition prevailing, selects and monitors the subsequent solution. This algorithm, therefore, permits for an accurate solution, with the best possible speed advantage.

### 2.3 Hydraulic Transmission Lines

The application of transmission line theory in hydraulics, is not new. Constantinesco (38), in 1922, was first to suggest its application in the context of fluid power. In general, however, the significance of the transmission line theory to hydraulics, is not widely appreciated, Bowns et al.(39). Due to the increasing interest in measuring fluid borne pump noise, recent years have seen the transmission line theory used to model simple hydraulic circuits. The general equation (2.3.1) defining the pressure wave amplitude  $P_x$  in a pipeline is complex and contains a number of difficult to derive parameters.

$$P_x = \frac{Q_s Z_o Z_s}{Z_s + Z_o} \left( \frac{e^{\gamma x} + \rho_t e^{-\gamma(2L - x)}}{1 - \rho_s \rho_t e^{-2\gamma L}} \right) \quad (2.3.1)$$

Where  $Q_s$  is the flow at source ( $x = 0$ ),  $Z_o$  the line impedance and  $Z_s$  the source impedance.  $\rho_s$  and  $\rho_t$  are the source and termination reflection coefficients respectively.  $L$  is the line length and  $\gamma$  the wave propagation constant.

Under special conditions, the equation is simplified and is of the form commonly applied in the testing of hydraulic pumps, some of these were by Bowns et al.(40), Edge (41) and Iyengar et al.(42). Applications of

the complicated general form of the equation are significantly few.

In a pipeline, the pressure at any point, is a sum of the pressure waves travelling up and down the line. A wave initiated at source travels along the line until it is reflected at the termination. This wave then travels up back to the source, where a further reflection occurs. The process is repeated until all the energy is dissipated. The effect of the multiple reflection is to generate a standing wave with nodes and antinodes at half wavelength separations along the length of the line.

Conesco (43) in their work on fluid acoustic filters, applied the transmission line theory, in an attempt to unravel the effects of standing waves. In the derivation of their model, a simplification was applied, whereby only a single incident and reflected wave was assumed. Multiple reflections were ignored. With this simple model, solution for the incident and reflected wave amplitudes, proceeds with the obtaining of the maximum and minimum (node and antinode) amplitude of the standing wave. Two methods were used. The first consisted of trailing a hydrophone along the line and noting its amplitude. The second used an analytical method whereby the required amplitudes were computed from a set of three fixed transducer readings.

While still maintaining the theme of evaluating fluid borne noise attenuators, O'Neal et al.(44) improved on the solution techniques for obtaining the parameter estimates. He formulated an analysis which enabled a more accurate estimate, using a set of six fixed transducer readings at known position. In addition to increasing accuracy, the fixed transducer method enables higher pressure measurements, which were not possible using the moving hydrophone method. This work was detailed in another publication, O'Neal et al.(45).

In a later work by Henderson (46), also on the subject of fluid borne attenuators, the solution technique was further improved. He applied a numerical technique which minimised on the error between the observed and computed values based on the parameter estimates. This technique enabled the identification of faulty transducer and apply low weighting to these readings. In this work 20 fixed pressure transducers were used enabling accurate monitoring of the pressure levels in the line.

In the publications cited, arguments were not forwarded to substantiate the assumptions, which were required in formulating the reduced standing wave equation used in the analysis. Such approximations would result in erroneous results, if strong multiple reflections were present in the line. In the work by Henderson, a substantial line length was used. This was indicated to be over 30 metres. Under this condition it is reasonable to assume only a single reflection occurring at the termination. With the Conesco and O'Neal work, however, there appear conditions whereby a system of multiple reflection would be more representative of the conditions prevailing.

In the work by McCandlish et al.(47) and later by Tilley (48), the full general standing wave equation was solved in an effort to determine the fluid borne noise characteristics of simple hydraulic systems. The work described methods which enabled the unknown parameters to be determined, either by relatively simple experiments or calculations. The general standing wave equation for multiple reflections condition, contains five unknown parameters, the source and line impedances, the source and termination constants, and the wave propagation constant. The source impedance can, however, be obtained from a knowledge of the line impedance and source reflection coefficient. Although all the parameters are fundamentally complex (containing both amplitude and

phase components) and basically frequency dependant, the line impedance and the wave propagation can be easily calculated with sufficient accuracy, Bowns et al.(39). The remaining two unknown parameters must, however, be determined experimentally from a set of simultaneous equations to derive the flow fluctuations at any point in the line.

In the work by McCandlish, the primary intention was to design a series of experiments to determine the unknown parameters. With these the fluid flow fluctuations could be derived. This was achieved in two stages. If the pressure at any two points in the same line are divided, the equation reduces to that containing only the termination and the wave propagation constants, equation (2.3.2).

$$\frac{P_1}{P_2} = \frac{e^{-\gamma x_1} + \rho_t e^{-\gamma(2L - x_1)}}{e^{-\gamma x_2} + \rho_t e^{-\gamma(2L - x_2)}} \quad (2.3.2)$$

Where  $P_1$  and  $P_2$  are pressure levels at position  $X_1$  and  $X_2$  respectively.

As the wave propagation constant can be estimated with sufficient accuracy, the termination constant is determined. To improve the statistical accuracy, McCandlish applied the mean value from a set of experiments with different line lengths. With the solution of the termination constant, the source reflection constant can be obtained by solving the equation (2.3.1) with data from tests at two different line length, but under similar operating conditions. Again statistical accuracy was improved by applying the mean value from a number of solutions.

Numerous methods have been suggested to enable the assessment of pump pressure ripple. Fielding et al.(21) and Bowns et al.(62) provides a summary. All these methods exploit the special conditions which simplify the standing wave equation (2.3.1), by avoiding the standing wave condition. These techniques can be classed either 'acoustically reflectionless' or 'high impedance' delivery lines.

The 'acoustically reflectionless' or 'anechoic' delivery line can be achieved by one of three methods. The most practical being the use of a long pipe line. The use of a quarter wavelength line or matching termination impedances, are other ways of achieving reflectionless termination conditions. These methods are, however, less practical as pump outputs are seldom, if ever, of a single frequency and therefore requiring a different line configuration for each frequency component.

The 'anechoic' transmission line equation at ( $x = 0$ ) reduces to:

$$P_o = \frac{Q_s Z_o Z_s}{Z_s + Z_o} \quad (2.3.3)$$

The high impedance delivery line technique attempts to further simplify the transmission line equation of (2.3.3). By using small bore delivery lines (increasing the line impedance) reflections at the termination can be made negligible in comparison to the pressure fluctuations at the pump outlet. This condition leads to the pipe impedance being much greater than that of the source impedance.

Simplification of equation (2.3.3) results in:

$$P_o = Q_s Z_s \quad (2.3.4)$$

On the basis of simplicity, the high impedance method appears to be more favourable as it does not require knowledge of the line impedance,

$Z_0$ . The 'anechoic line' technique also requires handling of long hose lengths, in the region of 30 metres. This can prove to be a hindrance in conditions of limited space. The impedance of low friction lines can, however, be estimated with sufficient accuracy, Bowns et al.(39).

The high impedance delivery line technique has, however, an underlying disadvantage. Under conditions of high flowrates, low outlet pressures or high source impedance, it is difficult to ensure that  $Z_0$  is much greater than  $Z_s$ . The high delivery impedance requirements can require pump testing under non typical operating conditions, and thus non typical results. There are also differences to be found in both the amplitude and character of the frequency spectrum of the pump output. The pressure ripple measured at the pump outlet is greater for the case of the 'high impedance' than for the 'anechoic' line. In cases of a noisy environment, this can be an advantage. The accentuation of the low frequency harmonics is, however, a distinct disadvantage.

### 2.3.1 Relevance to Current Work

The standing wave equation, derived from the transmission theory, for the condition of multiple reflection is used to determine the fluid borne noise potential of two hydraulic machines, connected by a steel transmission line. In this application a situation existed which made it not feasible to connect the hydraulic machines to long anechoic terminations for the testing of its noise potential. As this data was required, a method had to be devised which could provide this by some other means. An additional problem encountered was that the two machines had the same physical configuration and operated at the same speed. For machines operating at different speeds, the problem is greatly simplified. Components due to each machine can then be easily identified, when operating at frequencies whose harmonic components do not coincide.

In this work, it was envisaged that by the use of a combination of the techniques applied in the work by Henderson and McCandlish above, a procedure could be formulated to derive the required data. In the procedure developed, a system of eight pressure transducers were positioned along the line. From these transducer readings, the standing wave effects were removed by solving the standing wave equations. The resultant waveform at this stage is a combination of the fluctuation due to the two connected machines. This can be uncoupled by performing three tests under similar operating conditions, but with different phasing between the two machines, and solving a set of simultaneous equations. The effects of mixing two pump outputs on the pressure ripple has been earlier studied by the author, Taylor et al.(49).

## CHAPTER 3 : THE PUMP MODEL

- 3.1 Introduction
- 3.2 Description of Pump Model
  - 3.2.1 Basic Definitions
  - 3.2.2 Description of Segment History
  - 3.2.3 Line Flow Ripple
  - 3.2.4 Line Pressure Ripple
  - 3.2.5 Effects of Silencing Grooves
- 3.3 Fundamental Flow Equations
  - 3.3.1 Laminar Flow Between Parallel Plates
  - 3.3.2 Laminar Flow Between Moving Parallel Plates
  - 3.3.3 Laminar Flow Through an Orifice
- 3.4 Flow and Pressure Equations
  - 3.4.1 General Compressible Flow and Pressure Equations
  - 3.4.2 General Segment Flow and Pressure Equation
- 3.5 Analytical solution
- 3.6 Solution of Flow-Pressure equation
  - 3.6.1 Flow-Pressure Equation With Zero Port Flow
  - 3.6.2 Linearised Flow-Pressure Equation Without Flow Reversal
  - 3.6.3 Linearised Flow-Pressure Equation With Flow Reversal
- 3.7 System Modelling Scheme

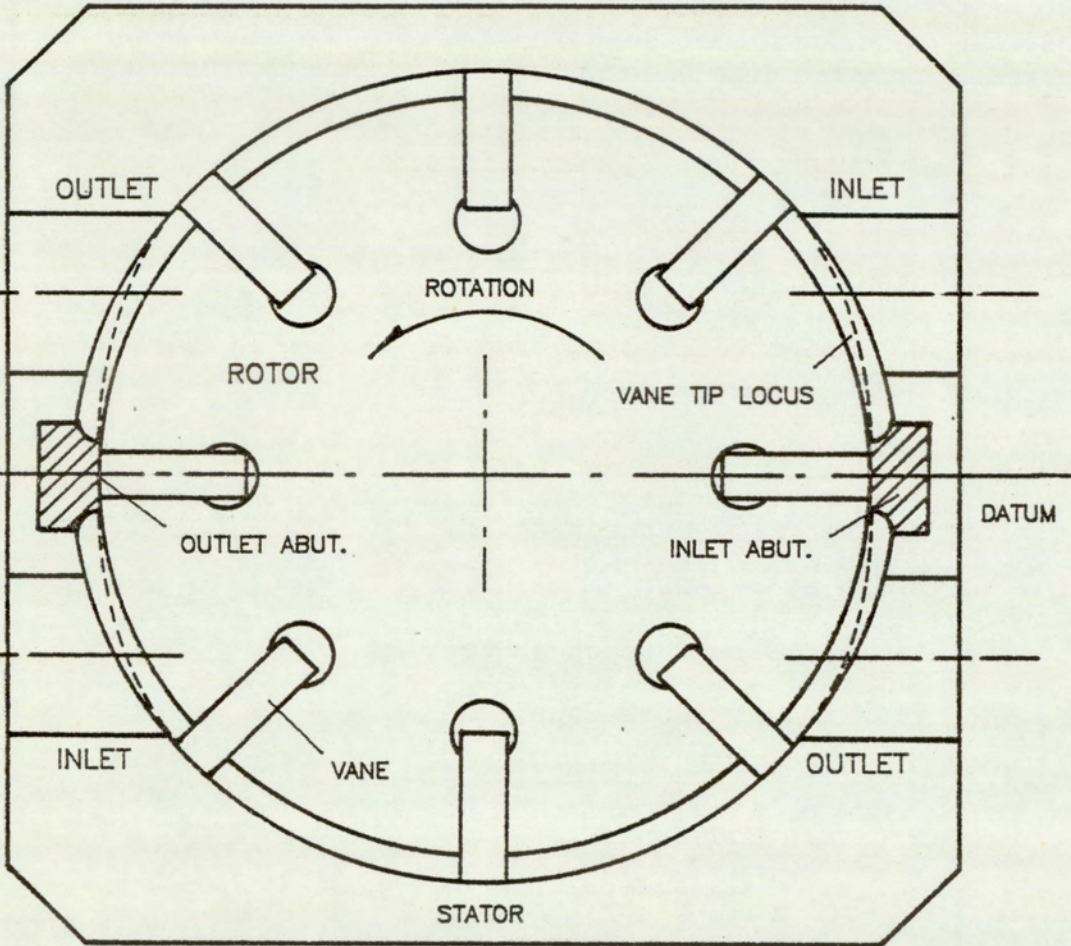


FIG.3.2.1 VANE PUMP SCHEMATIC

### 3.1 Introduction

This chapter deals with the theory and analysis techniques necessary for the implementation of the mathematical pump model on a computer. The theory relating to the termination is dealt with separately in chapter 4, which deals with the topic of transmission line. In the section that follows, the events relating to a pump cycle are briefly described whilst omitting the details. The detailed theory is dealt with in the subsequent sections. In these, the fundamental classical fluid mechanics equations are presented, and followed by a derivation of the 'Flow-Pressure' equations relating to the pump. The final section describes the scheme of the pump model.

### 3.2 Description of Pump Model

The model is best described in terms of the segment history as the rotor turns through one revolution. A segment is defined as the fluid volume bounded between one vane edge and its adjacent, vane or abutment edge. The pumping cycle occurs over five segment pitches (for an 8 vane machine) and due to the symmetry of the pump it is sufficient to consider only one complete cycle, instead of a full 360 degree rotor rotation. This can be appreciated when referred to the pump schematic of figure (3.2.1). In general the number of segment pitches per cycle is half the number of vanes plus one. This model is developed for a general machine having an even number of vanes, two abutments and symmetric about the abutment centreline.

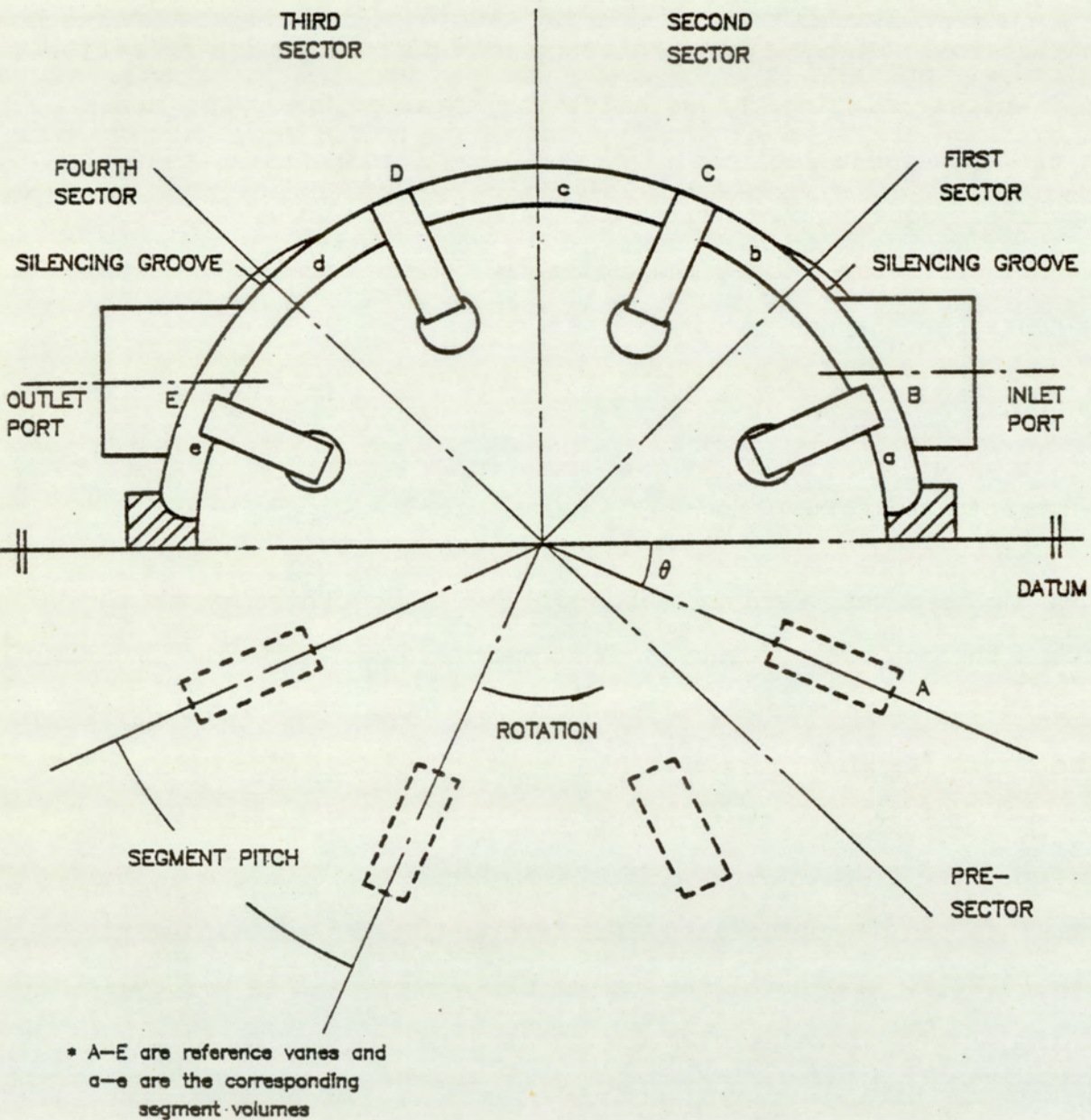


FIG.3.2.2 BASIC DEFINITIONS

### 3.2.1 Basic Definitions

Before we proceed with the detailed model description the following terms must be defined. These are presented pictorially in figure (3.2.2).

**Segment Position:** This is referenced by the angular position of the trailing vane centreline with respect to the centreline of the inlet abutment at the pump centre.

**Segment Pitch:** This is defined as the angle subtended at the centre of the pump by the centrelines of two adjacent vanes.

**Segment Volume:** In the angular position 0 degrees to minus one segment pitch, the segment volume is defined as the volume bounded by the trailing edge of the leading vane and the forward edge of the associated abutment. This definition is valid until the segment volume reduces to zero, then the segment becomes undefined. In the region zero degrees, to the position when the trailing vane just sweeps below the outlet abutment, the segment volume is defined as the volume bounded by the trailing edge of the leading vane and the leading edge of the trailing vane. From this position till when the leading edge of the trailing vane meets the outlet abutment, the segment volume is defined as the volume bounded by the outlet abutment and the leading edge of the trailing vane. The segment is not defined after this position.

**Pre-Sector:** This is the angular region bounded by minus one vane pitch and zero degree.

**First Sector:** This is the angular region bounded by zero degree and one vane pitch.

**Second Sector:** This is the angular region bounded by one and two vane pitches.

**Third Sector:** This is the angular region bounded by the upper limit

of the second sector and PI-(one vane pitch).

Fourth Sector: This is the angular position bounded by the upper limit of the third sector and PI.

### 3.2.2 Description of Segment History

The cycle starts with the pre-sector. The model is undefined until the trailing edge of the leading vane has completely swept past the inlet abutment. The vane is currently in the fully retracted position. As the rotor proceeds, the leading vane is advanced outwards until the operating vane clearance is reached. This motion is controlled by the cam actuation profile. Until the segment volume is exposed to the inlet port, the only flow into and out from the segment volume is via the leakage and entrainment paths, across the forward vane tip, end-plate and inlet abutment. There is another leakage path, the intervane leakage path. This is not included as it is considered unnecessary for the purpose for which this model is required.

As the rotor turns there is an increase in the segment volume which results in a temporary fall in the segment pressure. The consequence of this is to increase the pressure difference across the segment boundary, and thus the leakage flow into the segment volume. This added leakage soon brings the segment pressure to a new dynamic equilibrium. Once the vane has swept across the inlet port, the segment begins to communicate with the inlet port introducing another flow path. During this part of the cycle, fluid is directly being drawn into the segment. Due to the resistance to flow at the inlet port orifice, the segment pressure is lower than the inlet port pressure. If at any instant the flow area is too small for the level of flow,

cavitation will occur and introduce air bubbles into the system. By the time the rotor has completed this sector, the vane would have been fully extended to its working clearance.

In the first few degrees of the first sector history, the leading boundary is the leading vane and the trailing boundary is at the inlet abutment. The mechanism of flow is, as in the pre-sector, due to pressure and entrainment effects. Fluid is being drawn into the segment volume. Similarly as before, if the flow area is too small cavitation will occur. After the trailing vane has cleared the inlet abutment, there is a change in condition at the trailing boundary. The new trailing boundary is the trailing vane of the segment. In the early stages of the segment history, the trailing vane is fully retracted. The vane is gradually extended until it achieves working clearance. This occurs just before the inlet flow area reduces to zero. Following this, the process of fluid compression can begin. Before the fluid pressure can rise, however, any air bubbles in the fluid caused by earlier cavitation, must be collapsed.

In the second sector, as in the later stages of the previous sector history, fluid compression is taking place. At this stage, the segment does not communicate with the ports. The only flow occurring are via the leakage paths. As the rotor progresses, there is a net flow into the segment due to the effects of compressibility, and the pressure slowly rises. If there is no silencing groove, this segment behavior continues for a few degrees into the third sector.

In the early part of the third sector history, the segment pressure continues to rise gradually. At the moment the segment begins to communicate with the outlet port, there is a sudden surge of fluid into the segment, causing a corresponding increase in segment pressure.

Further rotor movement forces fluid from this contracting segment volume through the outlet port. Besides port flow, there is also the leakage across the vane and the end-plate boundaries. At this stage the leading vane begins to retract into the rotor, and permits the vane to pass below the outlet abutment. Until the time the leading vane tip meets the outlet abutment, the leading boundary is the leading vane of the segment. After this point the leading boundary is the outlet abutment. The trailing boundary is at the segment trailing vane.

At the start of the fourth sector, the trailing vane is fully extended. The vane tip is, however, retracting as it rotates forward. The fluid flow is initially dominated by port flow effect. As the vane tip retracts, the leakage to the trailing segment increases and the outlet flow decreases. At the end of the sector history, the segment flow is entirely leakage. The leading boundary is the outlet abutment and the trailing boundary is the trailing vane. The segment history is undefined when the trailing segment begins to pass under the outlet abutment.

### **3.2.3 Line Flow Ripple**

The instantaneous port flow is a summation of the flows into the segments in communication with the port. At the inlet port, fluid is drawn in by segments in the pre and first sectors. The outlet flow is derived from segments in the third and fourth sectors. If silencing grooves are incorporated, there would also be a flow component from the segment in the second sector. The flow rate from each segment is dependant on the pressure difference across the port orifice, the available flow area and the fluid density.

### 3.2.4 Line Pressure Ripple

The pressure variations measured in the line can be described using the transmission line theory. The equations relating pressure variation and flow is complex. It is, however, significantly simplified when applied to a lossless 'Anechoic Line', whose characteristic impedance is much greater than that of the source. Under this condition the pressure variation at the pump outlet becomes only a product of the flow and the characteristic line impedance. The characteristic line impedance is a function of the fluid bulk modulus, fluid density and the line cross-sectional area.

### 3.2.5 Effects of Silencing Grooves

Consider the case of the eight segment pump. If the forward and trailing vanes have the same clearances, then by the time the segment has swept through the second quadrant, the segment pressure would only have attained a pressure of less than half that of the mean port pressures. At the instant the segment communicates with the outlet port there is a large flow surge into the segment. This is to compensate for the volume lost due to the compressibility of the fluid. This abrupt change of state is a source of fluid flow ripple, and thus fluid borne noise. If the pressure in the segment can be gradually raised to that of the outlet port, the initial surge can be suppressed resulting in a flow ripple of lower magnitude and potentially result in a much quieter pump. The segment pressure can be profiled by permitting a controlled leakage path between the segment and port. By changing the form and dimensions of the grooves, an 'optimum' groove can be defined.

### 3.3 Fundamental Flow Equations

This section presents the fundamental dynamic equations used in the derivation of the 'flow-pressure' equations. These equations and the conditions of validity are commonly known. A formal presentation is thus considered to be unnecessary. References to these equations can be found in most books dealing with the fundamentals of fluid mechanics. A suitable reference is Massey (50).

#### 3.3.1 Laminar Flow Between Parallel Plates

The laminar flow of a viscous fluid,  $Q_v$  between two parallel plates, in the absence of end effects, is given by:

$$Q_v = \frac{bh^3(P_1 - P_2)}{12\mu L} \quad (3.3.1)$$

Where  $b$  and  $L$  are the width and length of the plates respectively,  $h$  is the plate separation,  $\mu$  the coefficient of absolute viscosity, and  $P_1$ ,  $P_2$  are the up, and down stream hydrostatic pressures.

#### 3.3.2 Laminar Flow Between Moving Parallel Plates

Entrained flow also known as 'Couette Flow' is caused by the relative movement of a boundary under viscous effects. In the absence of edge effects, the entrained flow  $Q_e$  is given by:

$$Q_e = \frac{bhU}{2} \quad (3.3.2)$$

Where  $b$  is the plate width,  $h$  is the plate clearance and  $U$  the relative

plate velocity.

### 3.3.3 Laminar Flow Through an Orifice

The flow through an orifice is derived from Bernoulli's equation for an inviscid fluid. The orifice flow  $Q_o$  is given by:

$$Q_o = \frac{\text{Dir} \cdot C_d \pi D^2}{4} \sqrt{\frac{2|P_1 - P_2|}{\rho}} \quad (3.3.3)$$

and  $\text{Dir} = \text{Sgn}(P_1 - P_2)$

Sgn is defined as:

$\text{Sgn}(x) = 1 ; x > 0$

$\text{Sgn}(x) = 0 ; x = 0$

$\text{Sgn}(x) = -1 ; x < 0$

Where  $C_d$  is the coefficient of discharge,  $D$  the orifice diameter,  $\rho$  the fluid density and  $P_1, P_2$  the up and down stream hydrostatic pressure respectively.

### 3.4 Flow and Pressure Equations

In this section the general flow and pressure equation for a viscous compressible fluid is developed. The first of two sub-sections develops the equation for a general control volume. The second applies the equation to the modelling of the pump segment pressure.

### 3.4.1 General Compressible Flow and Pressure Equation

Consider a quantity of fluid having absolute density  $\rho$  and volume  $V$ .

The mass  $m$  is given by:

$$m = \rho V \quad (3.4.1)$$

Differentiating the equation (3.4.1) with respect to time  $t$  gives:

$$\frac{dm}{dt} = \rho \frac{dV}{dt} + V \frac{d\rho}{dt} \quad (3.4.2)$$

The isentropic bulk modulus  $\beta$  is defined:

$$\beta = \rho \frac{dP}{d\rho} \quad (3.4.3)$$

The mass flow rate into a control volume is related to the flow across its boundary by:

$$\frac{dm}{dt} = \rho(Q_{in} - Q_{out}) \quad (3.4.4)$$

Where  $Q_{in}$  and  $Q_{out}$  are the flow in and out of the control volume.

Equating equations (3.4.2) to (3.4.4) and re-arranging gives:

$$Q = \frac{dV}{dt} + \frac{V}{\rho} \frac{d\rho}{dt} \quad (3.4.5)$$

Where  $Q = Q_{in} - Q_{out}$

Substituting equation (3.4.3) and (3.4.5) and re-arranging gives:

$$\frac{dP}{dt} = \frac{\beta}{V} \left( Q - \frac{dV}{dt} \right) \quad (3.4.6)$$

The angular velocity  $\omega$  is given by:

$$\omega = \frac{d\theta}{dt} \quad (3.4.7)$$

Where  $\theta$  is the angular position.

By using the above relationship, we obtain the flow-pressure equation with respect to angular position:

$$\frac{dP}{d\theta} = \frac{\beta}{\omega V} \left( Q - \omega \frac{dV}{d\theta} \right) \quad (3.4.8)$$

### 3.4.2 General Segment Flow and Pressure Equation

In the application of equation (3.4.8) to the modelling of the segment pressure of the pump, the variable  $Q$ , has two components.

$$Q = Q_1 + Q_0$$

Where  $Q_1$  is the total leakage and  $Q_0$  the total port flow from the segment volume.

The component  $Q_1$  consists of three sub-components:

$$Q_1 = Q_e + Q_v + Q_s$$

Where  $Q_e$  and  $Q_v$  are the entrained and viscous leakage across the vane tips, and  $Q_s$  is the end-plate leakage.

The equation (3.4.8) then takes the form:

$$\frac{dP}{d\theta} = \frac{\beta}{\omega V} \left( Q_e + Q_v + Q_s + Q_0 - \omega \frac{dV}{d\theta} \right) \quad (3.4.9)$$

From equation (3.3.1), (3.3.2) and (3.3.3) we obtain the equation relating to  $Q_e$ ,  $Q_v$ ,  $Q_s$  and  $Q_o$ .

$$Q_e = \frac{UL}{2}(H_2 - H_1)$$

$$Q_v = \frac{L}{12\mu} \left( \frac{(H_1)^3}{W} (P_1 - P) + \frac{(H_2)^3}{W} (P_2 - P) \right) + 2 \frac{L_3}{12\mu} \left( \frac{(H_3)^3}{W_3} (P_3 - P) \right)$$

$$Q_o = - \frac{C_d \pi}{4} \sqrt{\frac{2}{\rho}} \left( \text{Dir}_o \cdot (D_o)^2 \sqrt{|P - P_o|} + \text{Dir}_i \cdot (D_i)^2 \sqrt{|P - P_i|} \right)$$

Where  $\text{Dir}_o = \text{Sgn}(P - P_o)$

$\text{Dir}_i = \text{Sgn}(P - P_i)$

The subscripts 1,2 relates to the leading and trailing boundaries and subscript 3 relates to the end-plate boundary.  $U$ ,  $L$  are the vane tip linear velocity and vane length.  $L_3$  is the end-plate land length.  $W$  is the vane tip width and  $W_3$  is the end-plate land width.  $H_1$ ,  $H_2$ ,  $H_3$  are the surface clearances.  $P$  is the vane main segment pressure and  $P_1$ ,  $P_2$  are the pressures at the adjacent segments.  $P_3$  is the case pressure.  $P_o$ ,  $P_i$  are the outlet and inlet pressures respectively.

With the substitution of  $Q_e$ ,  $Q_v$ ,  $Q_s$  and  $Q_o$  the equation (3.4.9) can be written as:

$$\begin{aligned} \frac{dP}{d\theta} = & K_5 + K_6(P_1 - P) + K_7(P_2 - P) + K_8(P_3 - P) \\ & - \text{Dir}_o \cdot K_9 \sqrt{|P - P_o|} - \text{Dir}_i \cdot K_{10} \sqrt{|P - P_i|} \end{aligned} \quad (3.4.10)$$

Where:

$$K_1 = \frac{\beta}{\omega V} \qquad K_2 = \frac{L(H_1)^3}{12\mu W}$$

$$K_3 = \frac{L(H_2)^3}{12\mu W}$$

$$K_4 = \frac{L_3(H_3)^3}{12\mu W_3}$$

$$K_5 = K_1 \left( \frac{UL}{2} (H_2 - H_1) - \omega \frac{dV}{d\theta} \right)$$

$$K_6 = K_1 K_2$$

$$K_7 = K_1 K_3$$

$$K_8 = 2K_1 K_4$$

$$K_9 = K_1 \frac{C_d \pi}{4} \sqrt{\frac{2}{\rho}} (D_o)^2$$

$$K_{10} = K_1 \frac{C_d \pi}{4} \sqrt{\frac{2}{\rho}} (D_i)^2$$

### 3.5 Analytical Solution

The equation (3.4.9) is a non-linear first order differential equation and in its current form cannot be solved analytically. A numerical technique must be employed to solve for the segment pressure. Another problem arises as a consequence of the stiffness of the equation. The term 'stiffness' implies an equation where parameters change at widely different rates. When a numerical solution is applied to a stiff equation, very small iterative steps must be taken or instability will occur. Small step computation incur the penalty of extremely long computation time. A method due to Gear (51) is available which gives a significant improvement in the time required for the solution of stiff differential equations. This method incorporates an automatic starting procedure and a sophisticated iterative solution of the predictor equation. Even with this technique, the required computation time could

prove excessive for the average engineering application. One way round this problem is to linearise the flow-pressure equation.

If the flow through the dominant port is much larger than that due to the secondary port and leakage, these latter components can be held constant over a small step change in  $\theta$ . Provided sufficiently small steps are taken, there will not be any significant loss in accuracy. The step-wise form of the equation (3.4.10) is given as:

$$\frac{dP}{d\theta} = K_{11} - \text{Dir}_d \cdot K_{12} \sqrt{|P - P_d|} \quad (3.5.1)$$

Where  $d$  denotes the dominant port,  $K_{11}$  is the cumulative constant representing the leakage,  $K_{12}$  is the secondary flow at the start of the step and;

$$K_{12} = K_9 \quad ; \quad |P - P_o| > |P - P_i|$$

$$K_{12} = K_{10} \quad ; \quad |P - P_o| < |P - P_i|$$

In the work by Hannan (30), a similar technique, was implemented for an axial piston pump. This was found to have a considerable saving in time when compared with a similar model using the standard 'Runge-Kutta' method of solving differential equations. A time saving factor of 50 was quoted in a comparison made by Foster (52).

With the vane pump model, there can be identified three different conditions of operation, in respect of the importance of the various variables. The first is one of having dominant port flow, and negligible secondary port and leakage flow. The second condition is one with zero port area. The third is one of significant port and leakage flow. For the first condition, the step-wise method described earlier can be used to solve for the segment pressures. The particular flow-pressure equation with zero flow area can be solved directly

analytically. The third condition however cannot be accurately modelled using the approximate flow-pressure equation. The equation must be solved using a numerical solution for a first order non-linear differential equation.

In the computer implementation of the pump model, an algorithm is developed which tests for the significance of the various variables. This algorithm, which is described in detail in chapter 5, then identifies the condition which best describes the conditions operating and the corresponding solution technique required. It is worth mentioning that for the eight vane machine, the segment can communicate simultaneously with both ports only if long silencing grooves are incorporated for both the inlet and outlet ports.

### **3.6 Solution of Flow-Pressure Equation**

This section deals with the solution of the various forms of the flow-pressure equations. The first sub-section, deals with the case of zero port area. This reduces the equation to a form which is amenable to a direct analytical solution. The latter sub-sections deal with the solution of the linearised flow-pressure equations. In solving this equation two conditions must be considered. The first is for the case of no flow reversal within the step, and the second for that with flow reversal.

### 3.6.1 Flow-Pressure Equation With zero Port Flow

When the port area is zero, the equation (3.4.10) is reduced to:

$$\begin{aligned}\frac{dP}{d\theta} &= K_5 + K_6(P_1 - P) + K_7(P_2 - P) + K_8(P_3 - P) \\ &= -(K_6 + K_7 + K_8)P + K_5 + K_6P_1 + K_7P_2 + K_8P_3\end{aligned}$$

This is a linear first order differential equation of the form:

$$\frac{dP}{d\theta} = -BP + A \tag{3.6.1}$$

Where  $A = K_5 + K_6P_1 + K_7P_2 + K_8P_3$   
 $B = K_6 + K_7 + K_8$

Re-arranging equation (3.6.1) gives:

$$\frac{dP}{A - BP} = d\theta \tag{3.6.2}$$

Using the substitution:

$$Z = A - BP \tag{3.6.3}$$

Differentiating both sides gives:

$$dZ = -B.dP \tag{3.6.4}$$

Substituting equation (3.6.3) and (3.6.4) into (3.6.2) gives:

$$\frac{dZ}{BZ} = -d\theta$$

Integrating both sides between the limits  $Z_1, \theta_1$  and  $Z_2, \theta_2$  gives:

$$\begin{bmatrix} \ln z \\ z \end{bmatrix} \begin{matrix} z_2 \\ z_1 \end{matrix} = -B \begin{bmatrix} \theta \\ \theta \end{bmatrix} \begin{matrix} \theta_2 \\ \theta_1 \end{matrix} \quad (3.6.5)$$

Re-arranging and using the relation:

$$e^{\ln x} = x \quad (3.6.5)$$

gives:

$$z_2 = z_1 e^{-B(\theta_2 - \theta_1)} \quad (3.6.7)$$

From equation (3.6.3):

$$P_2 = \frac{(A - z_2)}{B} \quad (3.6.8)$$

### 3.6.2 Linearised Flow-Pressure equation Without Flow Reversal

The linearised step-wise form of the flow-pressure equation (3.5.1) was given as:

$$\frac{dP}{d\theta} = K_{11} - \text{Dir} \cdot K_{12} \sqrt{|P - P_d|} \quad (3.6.9)$$

Let

$$(\text{Dir} \cdot U)^2 = \text{Dir}(P - P_d) \quad (3.6.10)$$

Differentiating equation (3.6.10) on both sides gives:

$$\text{Dir} \cdot 2U \cdot du = dP \quad (3.6.11)$$

Substituting equation (3.6.10) and (3.6.11) into (3.6.9) gives:

$$\frac{\text{Dir.}2U.dU}{K_{11} - \text{Dir.}K_{12}U} = d\theta$$

Re-arranging and factorising gives:

$$\left( -\frac{2}{\text{Dir.}K_{12}} + \frac{2K_{11}}{\text{Dir.}K_{12}(K_{11} - \text{Dir.}K_{12}U)} \right) dU = \text{Dir.}d\theta$$

Integrating between the limits  $U_1, \theta_1$  and  $U_2, \theta_2$  gives:

$$-\frac{2(U_2 - U_1)}{\text{Dir.}K_{12}} - \frac{2K_{11}}{(\text{Dir.}K_{12})^2} \ln \left( \frac{K_{11} - \text{Dir.}K_{12}U_2}{K_{11} - \text{Dir.}K_{12}U_1} \right) = \text{Dir.}(\theta_2 - \theta_1)$$

Let

$$Z_1 = K_{11} - \text{Dir.}K_{12}U_1$$

$$Z_2 = K_{11} - \text{Dir.}K_{12}U_2 \quad (3.6.12)$$

Substituting equation (3.6.12) gives:

$$\frac{\text{Dir.}2(Z_2 - Z_1)}{(K_{12})^2} - \frac{\text{Dir.}2K_{11}}{K_{12}} \ln \left( \frac{Z_2}{Z_1} \right) - (\theta_2 - \theta_1) = 0 \quad (3.6.13)$$

From equation (3.6.10):

$$P_2 = P_d + \text{Dir.}(U_2)^2$$

Substitute equation (3.6.12) gives:

$$P_2 = P_d + \text{Dir.} \left( \frac{K_{11} - Z_2}{\text{Dir.}K_{12}} \right)^2 \quad (3.6.14)$$

At the beginning of the step,  $Z_1$  of the equation (3.6.13) is known.  $Z_2$  can be solved using a numerical solution method (eg. Newton-Raphson). Knowing  $Z_2$  the segment pressure  $P_2$ , at the end of the step is found by

substitution into equation (3.6.14)

### 3.6.3 Linearised Flow-Pressure equation With Flow Reversal

In equation (3.5.1) Dir represents the direction of flow through the dominant port at the start of the step. If Dir and  $K_{11}$  are not of the same sign, there is a possibility of flow reversal, within the step. At the point of reversal, the segment pressure, P is equal to the port pressure  $P_d$ .

The conditions at the point of flow reversal are:

$$\begin{aligned} \text{Sgn}(\text{Dir} \cdot K_{11}) &= -1 \\ P &= P_d \end{aligned} \quad (3.6.15)$$

Substitute equation (3.6.15) into (3.6.14) gives:

$$Z_r = K_{11}$$

Where subscript r refers to the point of reversal.

Substituting the value of  $Z_r$  into the equation (3.6.13) gives the angular value,  $\theta_r$  at the point of reversal:

$$\theta_r = \theta_1 + \frac{\text{Dir} \cdot 2}{(K_{12})^2} (K_{11} - Z_1) - \frac{\text{Dir} \cdot 2K_{11}}{(K_{12})^2} \ln \left( \frac{K_{11}}{Z_1} \right) \quad (3.6.16)$$

The condition for flow reversal within a step is given by:

$$\theta_r < \theta_1 + \Delta\theta \quad (3.6.17)$$

Where  $\Delta\theta$  is the angular step interval.

If  $\theta_r > \theta_1 + \Delta\theta$ , flow reversal occurs after the end of the step. The

segment pressure  $P_2$  at the end of the step can be found using the equation (3.6.13) and (3.6.14) for the condition of no flow reversal within the step. If  $\theta_r = \theta_1 + \Delta\theta$ , the flow reversal occurs at the end of the step and the segment pressure,  $P_2$  is the port pressure,  $P_d$  at the start of the step.

For the condition of flow reversal, it is necessary to solve the equation (3.6.13) for the limits  $\theta_1$  to  $\theta_r$  and  $\theta_r$  to  $\theta_2$ . The equation (3.6.13) for the first condition, gave equation (3.6.16). The equation for the second set of limits gives:

$$-\frac{\text{Dir}.2}{(K_{12})^2} (Z_2 - K_{11}) + \frac{\text{Dir}.2K_{11}}{(K_{12})^2} \ln\left(\frac{Z_2}{K_{11}}\right) - (\theta_2 - \theta_r) = 0 \quad (3.6.18)$$

Substituting equation (3.6.16) into (3.6.18) eliminates  $\theta_r$  and gives:

$$-\frac{\text{Dir}.2}{(K_{12})^2} \left[ Z_1 + Z_2 - 2K_{11} + K_{11} \ln\left(\frac{(K_{11})^2}{Z_1 Z_2}\right) \right] - (\theta_2 - \theta_1) = 0 \quad (3.6.19)$$

By replacing Dir with -Dir in equation (3.6.14) we obtain the corresponding equation for  $P_2$  for the condition of flow reversal. The equation is:

$$P_2 = P_d - \text{Dir} \left( \frac{Z_2 - K_{11}}{\text{Dir}.K_{12}} \right)^2 \quad (3.6.20)$$

The solution of the equations for the condition with flow reversal is the same as that for without flow reversal. Equation (3.6.19) is solved for  $Z_2$  using a numerical technique. With  $Z_2$  the segment pressure,  $P_2$  at the end of the step is given by equation (3.6.20).

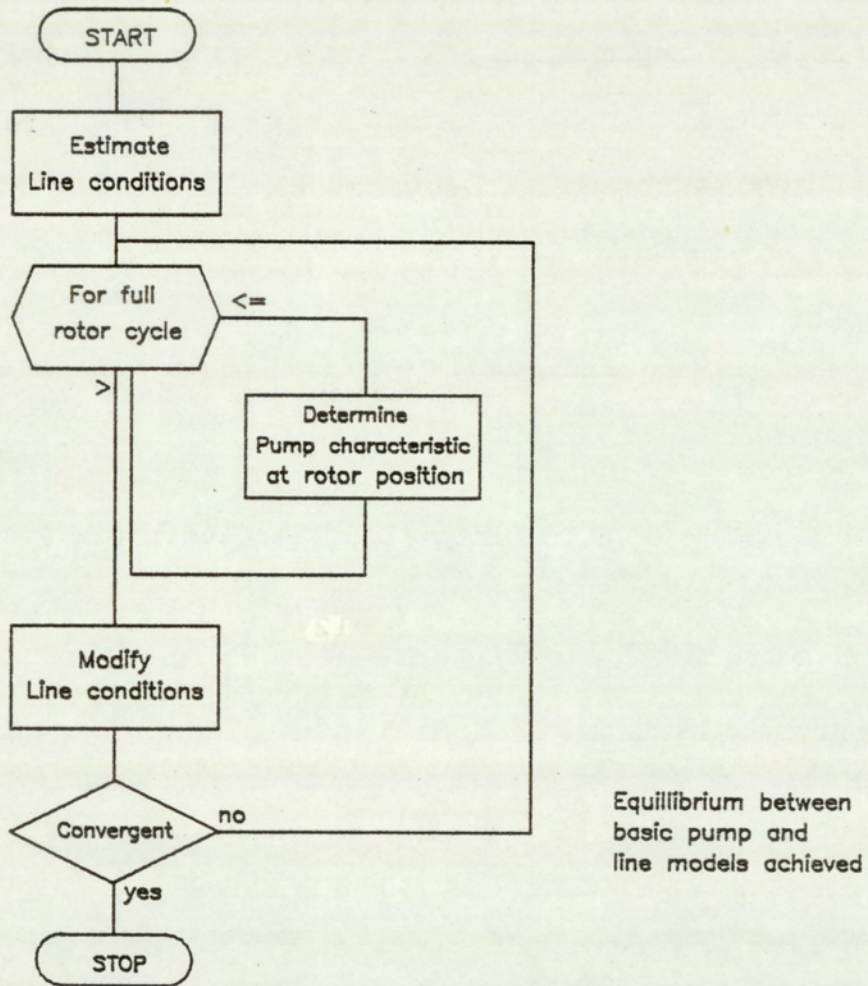


FIG.3.7.1 SYSTEM MODELLING SCHEME

### 3.7 System Modelling Scheme

The outputs of a pump are dependant on the inlet and outlet line conditions and line conditions are dependant on the pump flow conditions. This therefore necessitates the reiteration of both the basic pump and line model till convergence is achieved between the two models. In this simulation program, the anechoic line is modelled as the termination condition. This is done both from a point of ease of modelling and from the accepted practice of testing pump noise using anechoic line terminations. The resulting system model is referred in subsequent references as the 'pump model'.

The scheme of the pump model is shown in figure (3.7.1) and starts with an estimate of the line conditions. Using this estimate condition, the pump conditions of segment pressure and port flows are determined for the full pump cycle. With a knowledge of the port flows, the line conditions are corrected and another pass is made at simulating the pump conditons, under this new line condition. This is repeated till convergence is achieved between consecutive port conditions.

## CHAPTER 4 : THE TRANSMISSION LINE

- 4.1 Introduction
- 4.2 The Fourier Transform
- 4.3 Wave Propagation Theory
- 4.4 Transmission Line Model
- 4.5 Lossless Anechoic Line
- 4.6 Pump-Motor Transmission Model
- 4.7 Solving the Standing Wave Equation
  - 4.7.1 Removing Standing Wave Effects
  - 4.7.2 Uncoupling Wave Superposition Effects

## 4.1 Introduction

In the investigation of fluid borne noise in hydraulic systems, it is necessary to determine the dynamic flow fluctuations of the system. In a typical eight vane machine operating at 3000 rpm., the significant frequency components typically extends up to the tenth harmonic. This requires a flow monitoring system with a dynamic response in excess of 4000 Hz. Flow transducers in general have poor dynamic response. Sophisticated flow measuring techniques - for example, hot film anemometers or laser anemometers - can provide the required dynamic response but they are difficult and expensive to implement. In contrast measurement of dynamic pressure fluctuations is relatively simple and cheap. There is available commercially a wide range of suitable transducers with very high specifications. By the use of transmission line theory, a mathematical relationship can be derived which relates pressure to flow fluctuation. The application of transmission line theory in hydraulics is not new. In 1922, Constantinesco (38) suggested such applications in the field of fluid power. Latterday applications include Foster et al.(53), Oldenburger et al.(54) and Iyengar(55). In his paper on 'Pressure Ripple Propagation', Bowns et al.(39) outlines the application, and compares the various forms of the basic equations.

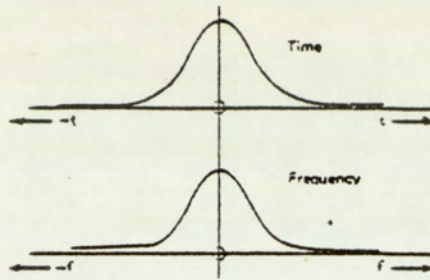
In this chapter the transmission line theory will be applied to three different systems, a lossless anechoic line, a simple transmission system and a pump-motor transmission network. The anechoic line condition is used in the modelling of the pump model termination. The two other conditions are required for the experimental work on the measurement of fluid borne noise in the hydraulic transmission systems.

A brief introduction to the Fourier transform is included in this chapter as an appreciation of the basic concepts is essential to the

a) Fourier Integral

$$X(f) = \int_{-\infty}^{\infty} x(t) e^{-j2\pi ft} . dt$$

$$x(t) = \int_{-\infty}^{\infty} X(f) e^{j2\pi ft} . dt$$

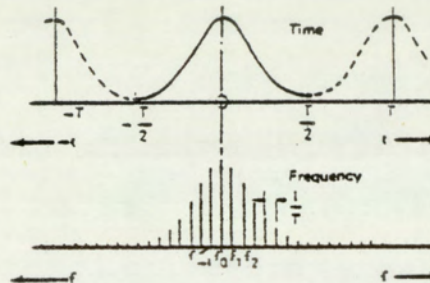


Infinite and continuous in time and frequency domain

b) Fourier Series

$$X(f_k) = \frac{1}{T} \int_{-T/2}^{T/2} x(t) e^{-j2\pi f_k t} . dt$$

$$x(t) = \sum_{k=-\infty}^{\infty} X(f_k) e^{j2\pi f_k t}$$

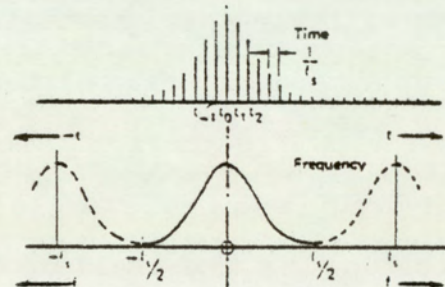


Periodic in time and discrete in frequency domain

c) Sampled Functions

$$X(f) = \sum_{k=-\infty}^{\infty} x(t_n) e^{-j2\pi ft_n}$$

$$x(t_n) = \frac{1}{f_s} \int_{-f_s/2}^{f_s/2} X(f) e^{j2\pi ft_n} . df$$

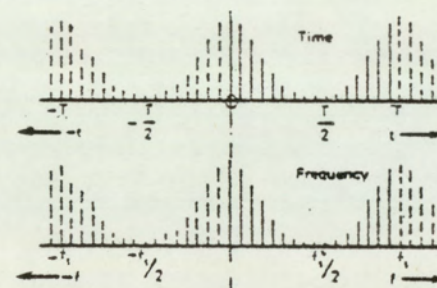


Discrete in time and periodic in frequency domain

d) Discrete Fourier Series

$$X(f_k) = \frac{1}{N} \sum_{n=0}^{N-1} x(t_n) e^{-jz}$$

$$x(t_n) = \sum_{k=0}^{N-1} X(f_k) e^{jz}$$



Where  $z = \frac{2\pi nk}{N}$

Discrete and periodic in time and frequency domain

Fig.4.2.1 FORMS OF THE FOURIER TRANSFORMS

understanding of the analytical and experimental analysis that follow. Numerous books are available on the subject. 'Applied Time Series' by Otnes et al.(56) is a suitable reference on the practical aspects.

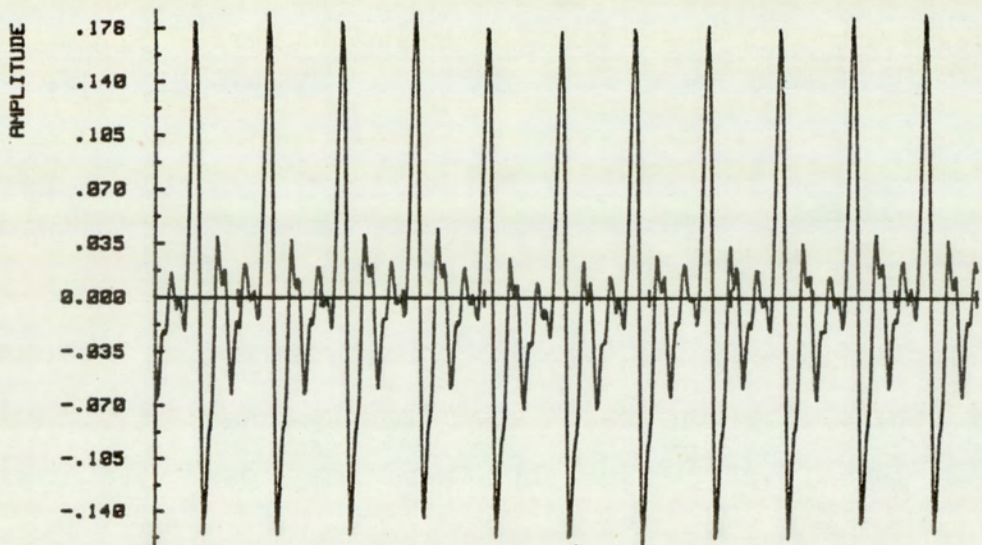
## 4.2 The Fourier Transform

In brief the Fourier transform is the conversion of time domain data to the frequency domain. The conversion from the frequency to the time domain is the inverse Fourier transform. There are, however, a number of different forms of the Fourier transform depending on the type of signal analysed. This is summarised in figure (4.2.1).

The most general of all is the Integral transform. This transform can be applied to any realistic signal. Periodic and non-periodic signals can be suitably transformed. This transform necessitates a knowledge of the series to be defined between infinite limits and thus reduces its application to short duration transient signals. The domain for both frequency and time are continuous for this version of the transform.

When dealing with periodic signals, the signal can be defined by one period of the time signal. The Fourier transform for periodic signals take the form of the Fourier series. In this form the time domain is continuous and periodic, and the frequency domain discrete and infinite.

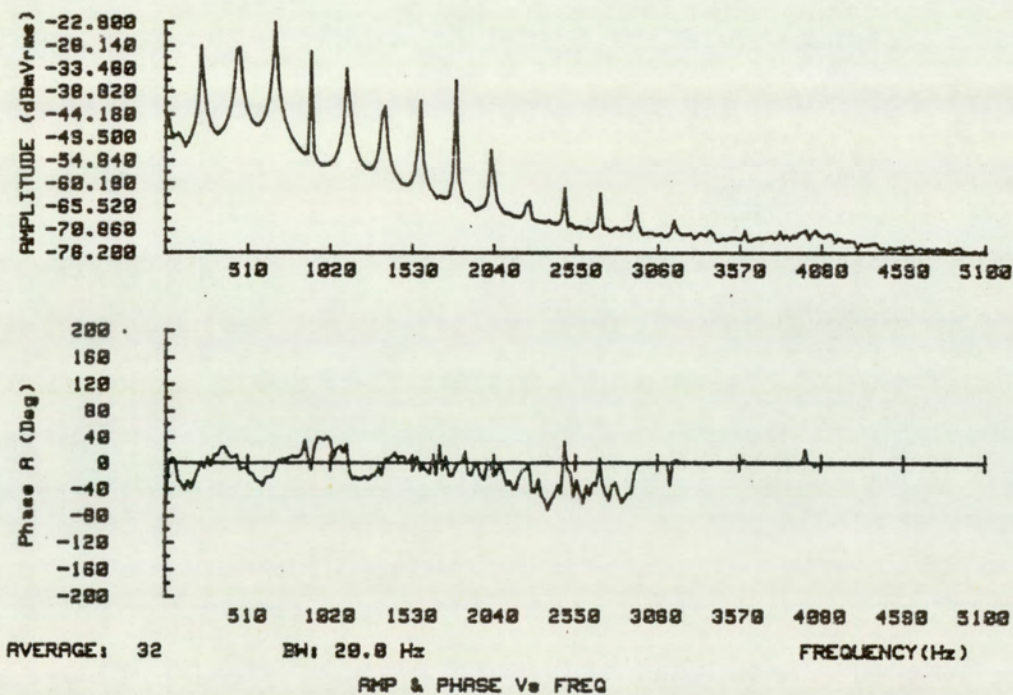
For discrete and non-periodic time data the sampled function transform is used. The time domain of this transform is discrete and infinite, and the frequency domain continuous and periodic. Due to the symmetry and periodicity in the frequency spectrum, a component of the



ALTERNATE SAMPLES AFTER FILTER

Time Axis

a) Time Domain Signal



b) Frequency Domain Signal

Fig.4.2.2 FOURIER TRANSFORM OF PRESSURE PULSE

frequency in the continuous time signal will appear at frequencies of multiple intervals of the sampling frequency.

As a means of avoiding the possible ambiguities of the frequency content of the signal, the time domain signal is band limited before transforming by passing through a low pass filter. This filter is usually referred to as an antialiasing filter with a cut off point set at a value slightly less than half that of the sampling frequency.

The final and possibly the most useful form, for use in digital signal analysis is the discrete Fourier transform. This transform is applied to discrete and periodic signals in both the frequency and time domain. N points in the time domain are transformed to N points in the frequency domain. Due to the symmetry of the frequency domain, only half of these frequency points are independent. The number of valid frequency points is however further reduced due to the effects of the antialiasing filters.

The figure (4.2.2) demonstrates the forward discrete Fourier transform of an actual pressure pulse from a piston pump. Figure (4.2.2a) shows the time signal after passing through the low pass antialiasing filter and figure (4.2.2b), the amplitude and phase spectrum of the transformed signal.

### **4.3 Wave Propagation Theory**

The one dimensional plane wave propagation theory can be used to study the transmission of flow and pressure in fluid lines. The validity of the analysis depends on the conditions of linearity and compactness being satisfied. By these conditions, it is implied that the disturbances

are sufficiently small for their squares to be negligible, and that the source region is small when compared to the size of the wavelength. The wave equation is derived from continuity and force equilibrium equations.

From continuity :

$$-\frac{\partial Q}{\partial x} = -\frac{A}{\beta} \frac{\partial P}{\partial t} \quad (4.3.1)$$

Where  $Q$  is the volume flow rate,  $A$  is the cross-sectional area,  $\beta$  the bulk modulus and  $P$  pressure.  $x$  and  $t$  relates to position and time respectively.

From equilibrium of forces:

$$-\frac{\partial P}{\partial x} = QR + \frac{\rho}{A} \frac{\partial Q}{\partial t} \quad (4.3.2)$$

From equations (4.3.1) and (4.3.2), the wave equations are obtained:

$$\frac{\partial^2 Q}{\partial x^2} = \gamma^2 Q$$

and

$$\frac{\partial^2 P}{\partial x^2} = \gamma^2 P \quad (4.3.3)$$

Where the propagation constant  $\gamma$  is given by:

$$\gamma = \sqrt{\frac{A}{\beta} \left( R + \frac{\rho}{A} j\omega \right)} \quad (4.3.4)$$

Where  $R$  is the line resistance and  $\omega$  the wave frequency in angular units.

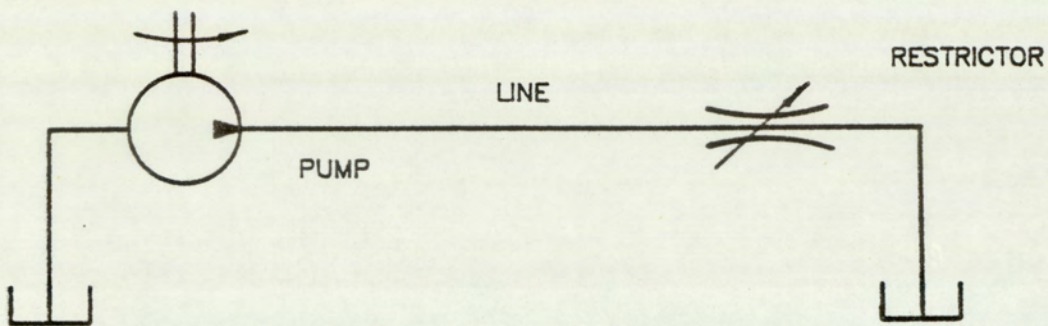


FIG 4.4.1 SIMPLE HYDRAULIC CIRCUIT

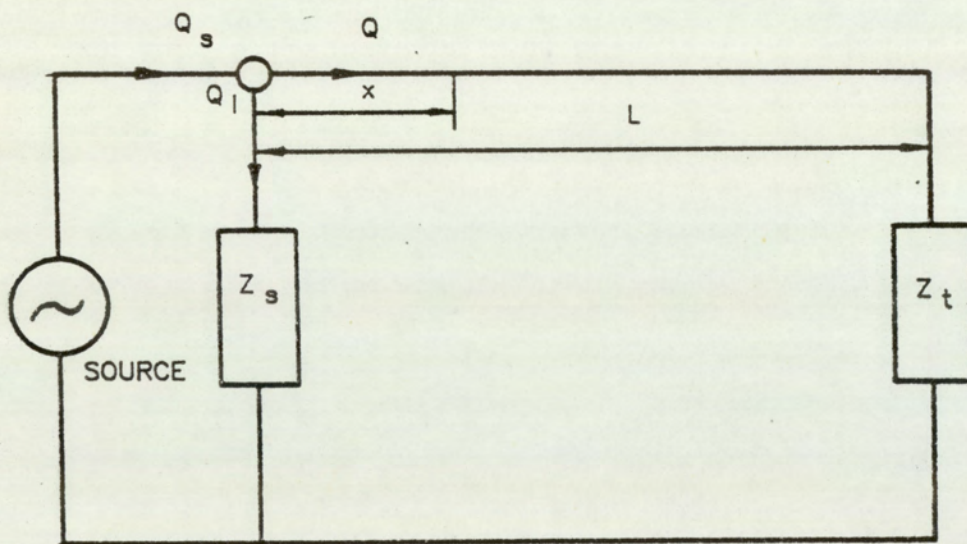


Fig.4.4.2 EQUIVALENT IMPEDANCE CIRCUIT

The general solution to the wave equation is :

$$P_x = Fe^{-\gamma x} + He^{\gamma x} \quad (4.3.5)$$

$$Q_x = \frac{1}{Z_0} \left( Fe^{-\gamma x} - He^{\gamma x} \right) \quad (4.3.6)$$

Where F and H are constants, and  $Z_0$  is the general characteristic line impedance, defined by :

$$Z_0 = \sqrt{\begin{pmatrix} R + \rho & -j\omega \\ A & A \end{pmatrix} \begin{pmatrix} A & -j\omega \\ \beta & \beta \end{pmatrix}^{-1}} \quad (4.3.7)$$

Also

$$Q = -\frac{P}{Z} \quad (4.3.8)$$

Where Z is the general impedance.

#### 4.4 Transmission Line Model

The figure (4.4.1) shows a simple hydraulic circuit consisting of a pump connected to a length of pipe and terminating at a pressure relief valve. Consider a pressure wave emanating from the pump and travelling towards the line termination at the speed of sound. As any waveform can be transformed to a series of sine waves by the Fourier series it is sufficient to visualise a simple sine wave in place of the complex pump wavelet. As the wave travels along the pipe it is attenuated, the degree of which depends on the line friction. At the termination the wave is reflected back towards the pump. The wave will continue to be reflected up and down the line until its energy is completely

dissipated. The result of this complex interaction of incident and reflected waves is to produce a standing wave. If a pressure transducer is moved along the length of the pipe, it will detect a pressure wave of varying amplitude. At points corresponding to nodes, a minimum signal will be detected, while at points midway between two consecutive nodes, a maximum signal will be detected. These are the antinode points. For a perfect line with zero attenuation and complete reflection at the ends, the signal would be zero at the nodes and tending to infinity at the antinodes.

The impedance circuit of figure (4.4.2) is the equivalent of the simple hydraulic circuit of figure (4.4.1). The wave propagation theory enables the derivation of a mathematical equation defining the flow and pressure fluctuation, as a function of the pump and termination characteristic, and the line dependant parameters. The pump and termination characteristics are the source and termination impedance, and the reflection coefficients. The line parameters are the wave propagation constant and the line impedance.

At the beginning of the line  $x = 0$ . Substitution of this condition reduces equation (4.3.5) to:

$$P_E = F + H \tag{4.4.1}$$

Where  $P_E$  is the pressure at the start of the line (or the pump outlet). At the end of the line, the termination impedance,  $Z_t$  is given by:

$$Z_t = \frac{P_t}{Q_t} \tag{4.4.2}$$

Where  $P_t$  and  $Q_t$  are pressure and flow fluctuations at the termination.

Substitution of the condition  $x = L$  into equation (4.3.5) gives:

$$P_t = Fe^{-\gamma L} + He^{\gamma L} \quad (4.4.3)$$

$$Q_t = \frac{1}{Z_0} \left( Fe^{-\gamma L} - He^{\gamma L} \right) \quad (4.4.4)$$

Further substitution of  $P_t$  and  $Q_t$  into equation (4.4.2) gives:

$$Z_t = Z_0 \left( \frac{Fe^{-\gamma L} + He^{\gamma L}}{Fe^{-\gamma L} - He^{\gamma L}} \right) \quad (4.4.5)$$

If the termination constant,  $\rho_t$  is defined as:

$$\rho_t = \frac{Z_t - Z_0}{Z_t + Z_0} \quad (4.4.6)$$

and the equation (4.4.1), (4.4.5), (4.4.6) are solved, the constants F and H can be determined.

$$F = \frac{P_E e^{2\gamma L}}{\rho_t + e^{2\gamma L}} \quad (4.4.7)$$

$$H = \frac{P_E \rho_t}{\rho_t + e^{2\gamma L}} \quad (4.4.8)$$

Substitution of equations (4.4.7) and (4.4.8) into (4.3.5) and (4.3.6) gives:

$$P_x = P_E \left( \frac{e^{-\gamma x} + \rho_t e^{-\gamma(2L - x)}}{1 + \rho_t e^{-2\gamma L}} \right) \quad (4.4.9)$$

$$Q_x = \frac{P_E}{Z_0} \left( \frac{e^{-\gamma x} - \rho_t e^{-\gamma(2L - x)}}{1 + \rho_t e^{-2\gamma L}} \right) \quad (4.4.10)$$

but

$$Q_s = \frac{P_E}{Z_s} \quad (4.4.11)$$

The source reflection coefficient  $\rho_s$  can similarly be defined as:

$$\rho_s = \frac{Z_s - Z_o}{Z_s + Z_o} \quad (4.4.12)$$

Using the substitutions equations (4.4.11) and (4.4.12) transforms the equations (4.4.9) and (4.4.10) into:

$$P_x = \frac{Q_s Z_o Z_s}{Z_s + Z_o} \left( \frac{e^{-\gamma x} + \rho_t e^{-\gamma(2L - x)}}{1 - \rho_s \rho_t e^{-2\gamma L}} \right) \quad (4.4.13)$$

$$Q_x = \frac{Q_s Z_s}{Z_s + Z_o} \left( \frac{e^{-\gamma x} - \rho_t e^{-\gamma(2L - x)}}{1 - \rho_s \rho_t e^{-2\gamma L}} \right) \quad (4.4.14)$$

The above equations defines the pressure and flow fluctuation at any point in the transmission line in terms of the source flow , pump and termination characteristics and the line parameters. The relationships are appropriate to variables at individual frequency components. With the exception of length, all the other variables are frequency dependant.

#### 4.5 Lossless Anechoic Line

In a typical hydraulic line, the internal wall of the pipe is usually smooth. This results in low pipe friction. For a system with negligible pipe friction, substitution of  $R = 0$  into equation (4.3.7) gives:

$$Z_0 = \sqrt{\frac{\rho\beta}{A^2}} \quad (4.5.1)$$

Where  $Z_0$  is the characteristic line impedance for a lossless line. This is independent of frequency.

The wave propagation constant for a pipe of negligible friction is obtained by substituting  $R = 0$  into equation (4.3.4):

$$\gamma = j\omega \sqrt{\frac{\rho}{\beta}} \quad (4.5.2)$$

For an anechoic condition, the termination reflection coefficient is effectively zero. Substitution of  $\rho_t = 0$  into equations (4.4.13) and (4.4.14) gives:

$$P_x = \frac{Q_s Z_0 Z_s}{Z_s + Z_0} e^{-\gamma x} \quad (4.5.3)$$

$$Q_x = \frac{Q_s Z_s}{Z_s + Z_0} e^{-\gamma x} \quad (4.5.4)$$

Where  $P_x$  and  $Q_x$  are the pressure and flow fluctuations at position  $x$  in a lossless and anechoic line.

At the pump outlet,  $x = 0$ . Substitution of this condition into equation (4.5.3) and (4.5.4) gives:

$$P_0 = \frac{Q_s Z_0 Z_s}{Z_s + Z_0} \quad (4.5.5)$$

$$Q_o = \frac{Q_s Z_s}{Z_s + Z_o} \quad (4.5.6)$$

Where  $Q_o$ ,  $P_o$  are the flow and pressure fluctuations at the pump outlet.

The characteristic line impedance  $Z_o$ , is generally found in practice to be small in magnitude when compared with the source impedance  $Z_s$ .

This reduces the equation (4.5.5) and (4.5.6) to:

$$P'_o = Q_s Z_o \quad (4.5.7)$$

$$Q'_o = Q_s \quad (4.5.8)$$

Where  $Q'_o$  and  $P'_s$  are the flow and pressure fluctuations at the pump outlet.

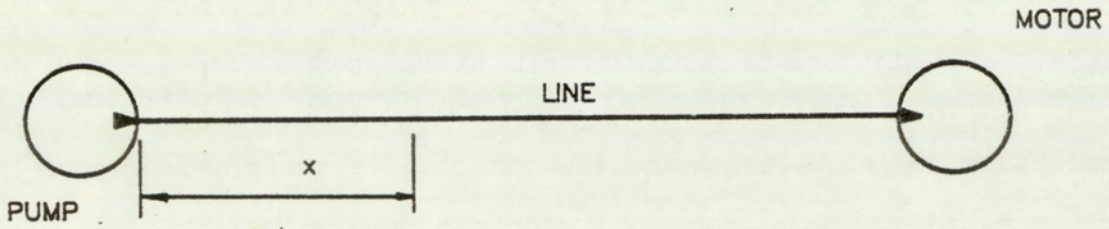
For a flexible pipe, the bulk modulus of the fluid is effectively reduced, and is given by:

$$\frac{1}{\beta'} = \frac{1}{\beta} + \frac{d}{Eh} \quad (4.5.9)$$

Where  $\beta'$  is the effective bulk modulus,  $d$  the mean pipe diameter,  $E$  the elastic modulus of the pipe material and  $h$  the pipe wall thickness.

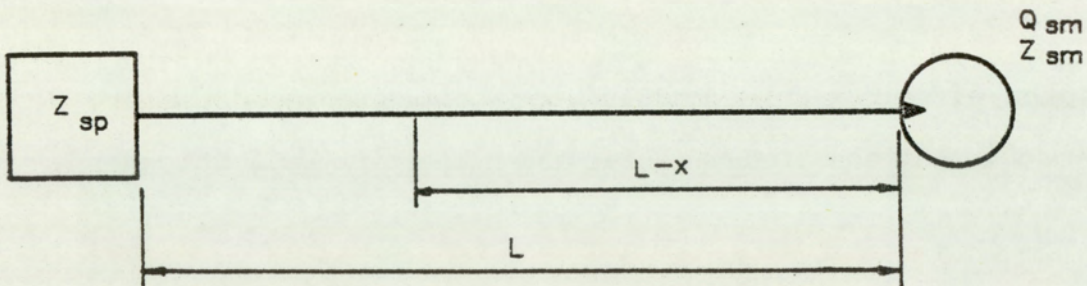
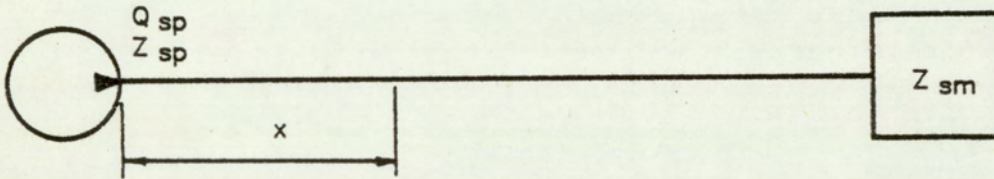
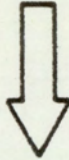
#### 4.6 Pump-Motor Transmission Model

In a pump-motor transmission line, there are two sources of flow ripples. A model for the transmission line can be derived using the principle of superposition. The pressure measured at any point in the line can be considered as being the sum of pressure fluctuations due



a) Integral Pump-Motor System

$$P_x = P_{px} + P_{mx}$$



b) Equivalent Pump-Motor Sub-system

Fig.4.6.1. PUMP-MOTOR TRANSMISSION SYSTEM

to the individual flow ripple generators. The figure (4.6.1) shows a simple hydraulic pump-motor system and its equivalent sub-systems.

The total pressure fluctuation  $P_x$ , at point  $x$  in the line is given by:

$$P_x = P_{px} + P_{mx} \quad (4.6.1)$$

Where  $P_{px}$  is the pressure ripple component due to the pump and  $P_{mx}$  is the component due to the motor.

Substitution of the local variables in the equations (4.4.13) and (4.4.14) gives  $P_{px}$  and  $P_{mx}$ , in terms of its source and line characteristics.

$$P_{px} = \frac{Q_{sp} Z_o Z_{sp}}{Z_{sp} + Z_o} \left( \frac{e^{-\gamma x} + \rho_{tm} e^{-\gamma(2L - x)}}{1 - \rho_{sp} \rho_{tm} e^{-2\gamma L}} \right) \quad (4.6.2)$$

$$P_{mx} = \frac{Q_{sm} Z_o Z_{sm}}{Z_{sm} + Z_o} \left( \frac{e^{-\gamma(L - x)} + \rho_{tp} e^{-\gamma(L + x)}}{1 - \rho_{sm} \rho_{tp} e^{-2\gamma L}} \right) \quad (4.6.3)$$

Where  $Q_{sp}$  and  $Q_{sm}$  are source flows,  $Z_{sp}$  and  $Z_{sm}$  are source impedances, and  $\rho_{sp}$  and  $\rho_{sm}$  are the line termination constants. The subscripts  $p$ ,  $m$  denote pump and motor quantities respectively.

Provided that the pump and motor components are sufficiently separated, in the frequency domain, the equations (4.6.2) and (4.6.3) enables the deconvolution of the pump and motor components from the standing wave effects. If the pump and motor are operating under conditions where the frequency components overlap, the required components cannot be obtained directly. It can, however, still be determined from measurements made from at least three different and independant phase conditions. This is described in the following section.

## 4.7 Solving the Standing Wave Equation

This section describes a technique for separating the effects of individual pump and motor, operating under conditions where there is overlap of the frequency components and under reverberant conditions. The technique involves a solution in two parts. The first sub-section deals with the removal of the standing wave effects to obtain the equivalent data to that from an anechoic condition. The second enables the deconvolution of the individual effects of the pump and motor.

### 4.7.1 Removing Standing Wave Effects

The general standing wave equation given by equation (4.4.13) can be written as:

$$P_x = P_o \left( \frac{e^{-\gamma x} + \rho_t e^{-\gamma(2L - x)}}{1 - \rho_s \rho_t e^{-2\gamma L}} \right) \quad (4.7.1)$$

Where

$$P_o = \frac{Q_s Z_s Z_o}{Z_s + Z_o} \quad (4.7.2)$$

$P_o$  is the pressure fluctuation measured at the pump outlet when connected to an anechoic line of characteristic impedance  $Z_o$ .

The equation (4.7.1) can be solved from a set of four complex simultaneous equations. The technique is, however, not to be recommended as an accurate solution is dependant on exact values being available. Errors in measurement would result in significant errors in the solution. A solution based on the estimation of parameters by the method of Least-squares is more appropriate, due to its tolerance

against measurement errors. A suitable method employed in this solution is the 'Least-Squares Linear-Taylor Differential-correction' technique. Although a detailed references is provided by McCalla (57), the technique is reproduced in summary.

Assume the function:

$$y = f(x, C_0, C_1, \dots, C_m) \quad (4.7.3)$$

Where  $x, y$  are relating variables and  $C_0, C_1, \dots, C_m$  are non-linear independant parameters.

Assume also a set of data  $x_i, y_i, (i = 0, n)$ , with  $y$  possessing an element of measurement error.

If the true values of the parameters were known, the residual error  $r_i$ , can be determined at each value of  $x_i$ .

The true residuals are given by:

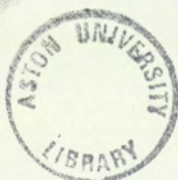
$$r_i = f(x, C_0, C_1, \dots, C_m) - y_i \quad (i = 0, n) \quad (4.7.4)$$

For a set of estimates of the unknown parameters,  $C'_k$ , the 'computed' residuals,  $R_i$  are given by:

$$R_i = f(x, C'_0, C'_1, \dots, C'_m) - y_i \quad (i = 0, n) \quad (4.7.5)$$

The problem is to obtain improved estimates values of  $C_k$ , for the data  $x_i, y_i$ , the initial estimate  $C'_k$  and the computed residuals  $R_i$ . Provided that the initial estimates are sufficiently close, this can be accomplished by a differential correction technique based on Least-squares.

By expanding the function about  $(C'_0, C'_1, \dots, C'_m)$  using the linear Taylor-Series expansion, the following is obtained:



$$\begin{aligned}
f(x, C_0, C_1, \dots, C_m) &= f(x, C'_0, C'_1, \dots, C'_m) + \frac{\partial f}{\partial C_0} (C_0 - C'_0) \\
&\quad + \frac{\partial f}{\partial C_1} (C_1 - C'_1) + \dots + \frac{\partial f}{\partial C_m} (C_m - C'_m)
\end{aligned}
\tag{4.7.6}$$

By using the relationships:

$$\begin{aligned}
\delta C_k &= C_k - C'_k \\
\frac{\partial f_i}{\partial C_k} &= \frac{\partial f}{\partial C'_k} \Big|_{x = x_i, C_k = C'_k}
\end{aligned}
\tag{4.7.7}$$

From the equations (4.7.3) to (4.7.7), and by minimising the square of the residual error  $r_i$ , the following relationship is derived.

$$C_0 \sum_i \frac{\partial f_i}{\partial C_k} \frac{\partial f_i}{\partial C_0} + \dots + C_m \sum_i \frac{\partial f_i}{\partial C_k} \frac{\partial f_i}{\partial C_m} = - \sum_i \frac{\partial f_i}{\partial C_k} R_i \quad (k = 0, m)
\tag{4.7.8}$$

The solution of equation (4.7.8), provides  $(C_0, C_1, \dots, C_m)$ , and is the amount of change required of  $(C'_0, C'_1, \dots, C'_m)$  to obtain the 'true' parameter solution,  $(C_0, C_1, \dots, C_m)$ . If the required change for any parameter is larger than the accepted error term, the procedure is repeated using the new estimate.

The solution of equation (4.7.1), contains 5 complex variables. For a lossless line, the wave propagation constant is effectively dependant only on the frequency and speed of sound, in the fluid. The number of unknowns are thus reduced to 4. For a first estimate the speed of sound can be calculated from the effective bulk modulus.

Although it is theoretically possible to obtain a solution to this equation, experience has shown that the technique is very prone to instability, when applied to an equation with a large number of unknowns. Better solution stability is obtained by re-arranging the equations to reduce the number of unknowns.

By expressing the pressure fluctuation  $P_x$  with respect to that at a chosen reference,  $P_d$  ( $x = x_d$ ), the equation (4.7.1) is reduced to one containing only two complex unknowns:

$$\frac{P_x}{P_d} = \frac{e^{-\gamma x} + \rho_t e^{-\gamma(2L - x)}}{e^{-\gamma x_d} + \rho_t e^{-\gamma(2L - x_d)}} \quad (4.7.9)$$

The complex parameters can be expressed in terms of its amplitude and phase components, where:

$$\begin{aligned} \rho_s &= A_s e^{j\theta_s} & \rho_t &= A_t e^{j\theta_t} \\ P_x &= A_x e^{j\theta_x} & P_d &= A_d e^{j\theta_d} \end{aligned}$$

Using the above substitution, equation (4.7.9) can be expressed in terms of its amplitude relationships:

$$\frac{A_x}{A_d} = \sqrt{\frac{1 + (A_t)^2 + 2A_t \cos[2(\omega/c)(L - x) - \theta_t]}{1 + (A_t)^2 + 2A_t \cos[2(\omega/c)(L - x_d) - \theta_t]}} \quad (4.7.10)$$

The above equation can be written as:

$$f(A_t, \theta_t) = \frac{A_x}{A_d} = \sqrt{\frac{U}{V}}$$

Where:

$$U = 1 + (A_t)^2 + 2A_t \cos[2(\omega/c)(L - x) - \theta_t]$$

$$V = 1 + (A_t)^2 + 2A_t \cos[2(\omega/c)(L - x_d) - \theta_t]$$

The partial derivatives are:

$$\frac{\partial f}{\partial A_t} = \frac{1}{2(V)^2} \sqrt{\frac{V}{U}} \left( V \frac{\partial U}{\partial A_t} - U \frac{\partial f}{\partial A_t} \right) \quad (4.7.11)$$

Where:

$$\frac{\partial U}{\partial A_t} = 2A_t + 2\cos[2(\omega/c)(L - x) - \theta_t]$$

$$\frac{\partial V}{\partial A_t} = 2A_t + 2\cos[2(\omega/c)(L - x_d) - \theta_t]$$

$$\frac{\partial f}{\partial \theta_t} = \frac{1}{2(V)^2} \sqrt{\frac{V}{U}} \left( V \frac{\partial U}{\partial \theta_t} - U \frac{\partial f}{\partial \theta_t} \right) \quad (4.7.12)$$

Where:

$$\frac{\partial U}{\partial \theta_t} = 2A_t \sin[2(\omega/c)(L - x) - \theta_t]$$

$$\frac{\partial V}{\partial \theta_t} = 2A_t \sin[2(\omega/c)(L - x_d) - \theta_t]$$

Substitution of the equations (4.7.11) and (4.7.12) into (4.7.8), and employing the Least-square technique enables the solution of the line termination parameters  $A_t$ , and  $\theta_t$ . The solution then proceeds

to solve for the remaining unknowns.

The full standing wave equation (4.7.1) can similarly be written in terms of its amplitude and phase components:

$$\frac{A_x}{A_o} = \sqrt{\frac{1 + (A_t)^2 + 2A_t \cos[2(\omega/c)(L - x) - \theta_t]}{1 + (A_t A_s)^2 + 2A_t A_s \cos[-2(\omega/c)L + \theta_t + \theta_s]}} \quad (4.7.13)$$

$$\begin{aligned} \frac{\theta_x}{\theta_o} &= \tan^{-1} \left( \frac{\sin(-\omega x/c) + A_t \sin[(-\omega/c)(2L - x) + \theta_t]}{\cos(-\omega x/c) + A_t \cos[(-\omega/c)(2L - x) + \theta_t]} \right) \\ &+ \tan^{-1} \left( \frac{A_t A_s \sin[(-2L)(\omega/c) + \theta_t + \theta_s]}{A_t A_s \cos[(-2L)(\omega/c) + \theta_t + \theta_s] - 1} \right) \end{aligned} \quad (4.7.14)$$

Where  $A_x$ ,  $A_o$  are the amplitude and  $\theta_x$ ,  $\theta_o$  the phase components of  $P_x$ ,

$P_o$  respectively. The above equation can similarly be written as:

$$f(A_s, \theta_s) = A_x = A_o \sqrt{\frac{U}{V}}$$

Where:

$$U = 1 + (A_t)^2 + 2A_t \cos[2(\omega/c)(L - x) - \theta_t]$$

$$V = 1 + (A_t A_s)^2 + 2A_t A_s \cos[-2(\omega/c)L + \theta_t + \theta_s]$$

The partial derivatives are:

$$\frac{\partial f}{\partial A_o} = \sqrt{\frac{U}{V}} \quad (4.7.15)$$

$$\frac{\partial f}{\partial A_S} = -A_O \frac{\partial U}{2V^2} \sqrt{\frac{V}{U}} \frac{\partial V}{\partial A_S} \quad (4.7.16)$$

$$\frac{\partial V}{\partial A_S} = 2A_S(A_T)^2 - 2A_T \cos[-2(\omega/c)L + \theta_T + \theta_S]$$

$$\frac{\partial f}{\partial \theta_S} = -A_O \frac{U}{2V^2} \sqrt{\frac{V}{U}} \frac{\partial V}{\partial \theta_S} \quad (4.7.17)$$

$$\frac{\partial V}{\partial \theta_S} = 2A_S A_T \sin[-2(\omega/c)L + \theta_T + \theta_S]$$

Similar to the solution for the first two unknowns, substitution of the equations (4.7.15) to (4.7.17) into (4.7.8) and employing the Least-square technique, enables the solution of the remaining unknowns.

At this stage, the full amplitude spectrum has been recovered from the effects of the standing wave. Substitution of the unknown parameters into equation (4.7.14), gives the phase relationships. The next stage is that of unravelling the effects of wave superposition. This is handled in the next sub-section.

#### 4.7.2 Uncoupling Wave Superposition Effects

Assume two periodic signals  $Y_1$  and  $Y_2$ , defined as follows:

$$Y_1 = A_1 \sin(\omega t)$$

$$Y_2 = A_2 \sin(\omega t + \sigma)$$

Superpositioning of the two sine waves results in  $Y$ , where:

$$\begin{aligned}
 Y &= Y_1 + Y_2 \\
 &= A \sin(\omega t + \delta)
 \end{aligned}$$

Assume the superposition of the two waveforms of amplitudes  $A_1$  and  $A_2$ , at three different phase lag conditions. Let the resultant amplitude  $A$ , be  $A'_1, A'_2, A'_3$  at the corresponding phase,  $\delta$  of  $\alpha, \alpha + \varphi_2, \alpha + \varphi_3$ . These conditions provide the equations:

$$(A'_1)^2 = (A_1)^2 + (A_2)^2 + 2A_1A_2 \cos \alpha \quad (4.7.18)$$

$$(A'_2)^2 = (A_1)^2 + (A_2)^2 + 2A_1A_2 \cos(\alpha + \varphi_2) \quad (4.7.19)$$

$$(A'_3)^2 = (A_1)^2 + (A_2)^2 + 2A_1A_2 \cos(\alpha + \varphi_3) \quad (4.7.20)$$

By using vector geometry, equations (4.7.18) to (4.7.20) gives:

$$\alpha = \tan^{-1} \left( \frac{\cos \varphi_2 - M(\cos \varphi_3 - \cos \varphi_2) - 1}{\sin \varphi_2 - M(\sin \varphi_3 - \sin \varphi_2)} \right) \quad (4.7.21)$$

$$A_2 = \frac{K}{A_1} \quad (4.7.22)$$

$$(A_1)^4 + [2K \cos(\alpha + \varphi_3) - (A'_3)^2](A_1)^2 + (K)^2 = 0 \quad (4.7.23)$$

Where:

$$K = \frac{(A'_2)^2 - (A'_1)^2}{2[\cos(\alpha + \varphi_2) - \cos \alpha]} \quad (4.7.24)$$

$$M = \frac{(A'_2)^2 - (A'_1)^2}{(A'_3)^2 - (A'_2)^2} \quad (4.7.25)$$

Equation (4.7.23) is a quadratic equation in  $(A_1)^2$ , the solution of which provides two independent values. Further attempts to solve for  $A_2$  would result in two dependent values. The two independent values are thus the individual amplitudes of the superimposed waveforms.

In the previous section, a Least-square technique was employed for the solution of the standing wave parameters. This was claimed to be more tolerant of measurement errors. The Least-square method, however, had the disadvantage that it would require data from a greater number of different phase conditions. Due to the complexity of the rig for which this technique was being developed, the additional work required would make this technique impractical. Furthermore, the equation describing wave superposition is much simpler than that for the standing wave equation containing only three unknowns.

## CHAPTER 5 : COMPUTER IMPLEMENTATION

- 5.1 Introduction
- 5.2 Computer System Configuration
- 5.3 Suite of Programs
- 5.4 Datafile Structure
  - 5.4.1 Parameter Datafile
  - 5.4.2 Process Datafile
- 5.5 Program VFLGEN
- 5.6 Program VMODEL
- 5.7 Program VPLOT

## 5.1 Introduction

In chapters 3 & 4, and appendices A & B, the mathematical model for the vane pump was established, together with the techniques for solving the mathematical equations. The fundamental equation describing the various pump processes was shown (chapter 3) to be a non-linear first order differential equation. The solution of such an equation requires the use of time consuming numerical techniques (eg. Runge-Kutta method). It was also shown that under certain conditions, the equation could be approximated to a linear form, while in others a reduced form of the equation could be obtained to which a direct analytical solution was available. The solution of such equations are relatively quick, leading to significant savings in computational time. In order to exploit the time saving advantage, a separate algorithm is required in order to identify the conditions to which the specific equations are applicable, and to select the appropriate solution.

There are two conditions when the application of the time saving solutions are appropriate. The first condition is identified when the port flow effects are dominant over that of leakage, and the second condition for when there is no port flow. Identification of the first condition enables the application of the linearised flow-pressure equation, and the second condition identifies that to which a direct analytical solution exists. In this program, the function of testing for the appropriate conditions and the selecting of the appropriate solution types are implemented by the algorithm Selsol. In addition, the algorithm monitors the validity of the approximation, and the progress of the solution. The details of the various functions of the algorithm are detailed later in the chapter.

In addition to implementing the mentioned solution technique, the

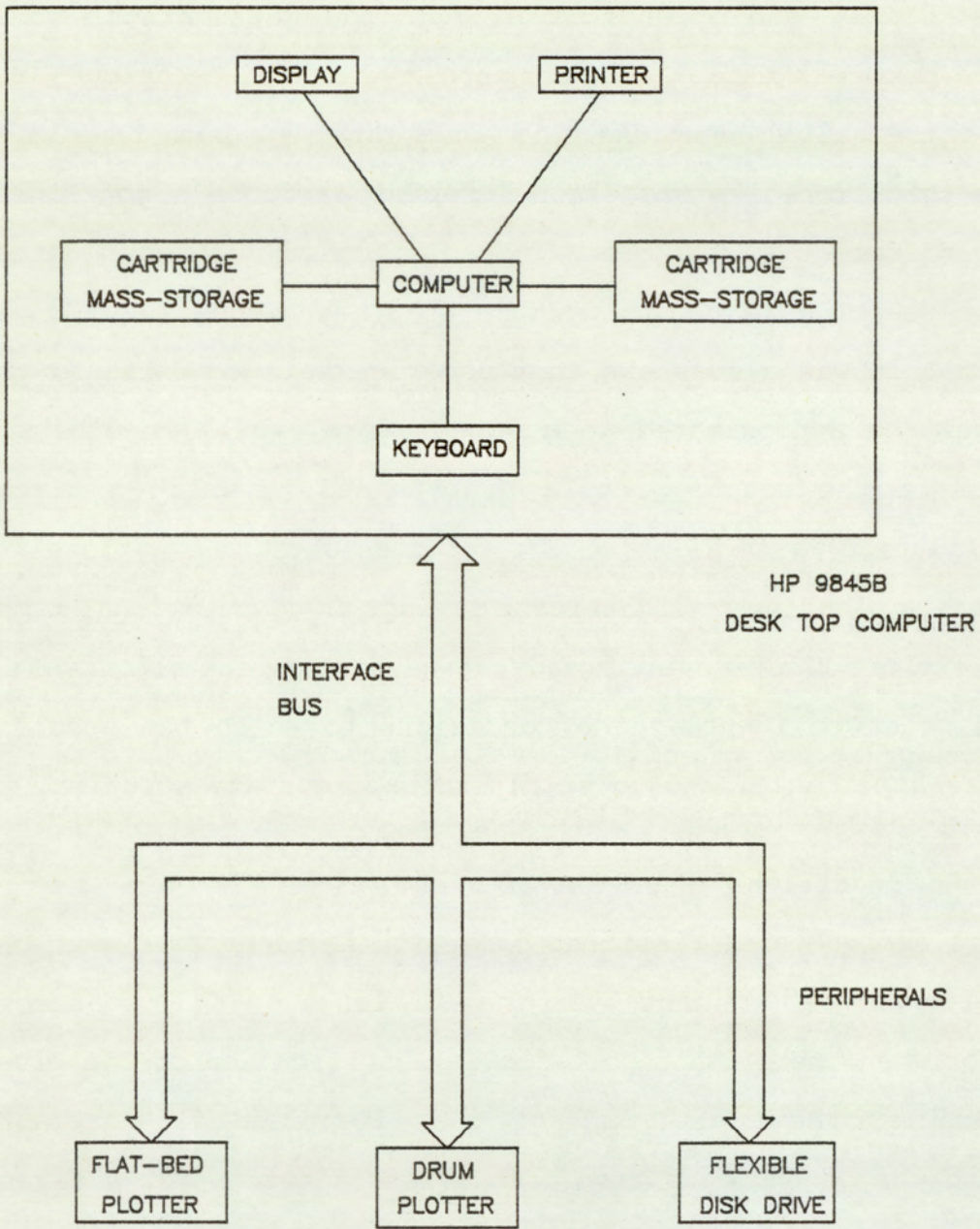


FIG.5.2.1 COMPUTER SYSTEM CONFIGURATION

program incorporates a modular structure which enables the program to be easily modified. The data relating to the physical configuration are defined by a set of arrays. The arrays are generated by appropriate modules which can be easily modified, to take into account changes in pump configuration, whilst maintaining the general solution scheme. This feature is most beneficial in a design application as significant changes are required during the course of development.

This chapter describes the implementation of the model in the form of a structured computer program. The 'top down' approach is applied, both in the documentation and structure of the programs. By this it is implied that the problem will be studied from a global to a particular point of view. In the second section, the computer system around which the programs are structured is described. This is followed by a description of the interconnection of the suite of programs comprising the complete computer implementation. The third to the seventh section provides the details of the individual programs and their algorithms, with the view of emphasising the program structure and not individual routines. These are documented locally in the program listings. To complete the documentation, program listings are provided in appendix C, and a typical simulation run and the associated outputs are presented in appendix D.

## **5.2. Computer System Configuration**

The computer system is the Hewlett-Packard 9845B desk top computer option 204. This incorporates 120k byte of system ROM and 187k byte of available read/write memory for program and data, and an enhanced language processor, which permits execution speeds of three times that

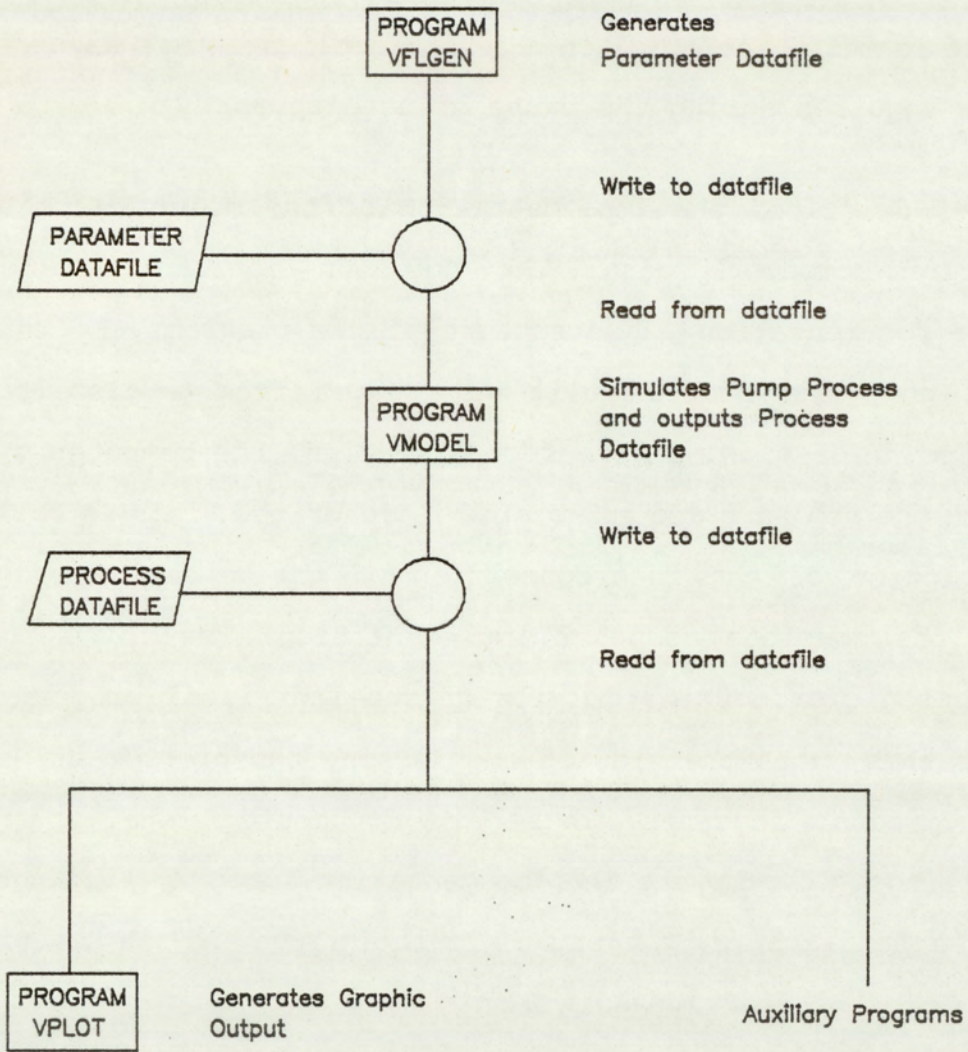


FIG.5.3.1 PROGRAM INTERCONNECTION

of the standard model. The complete system schematic is shown in figure (5.2.1). Integral to the basic system is a graphics display with a 560 x 455 dot resolution, two cartridge mass-storage units of 0.2m byte each, a thermal printer and a QWERTY keyboard. The external peripherals supported were an HP9872A flat-bed plotter, a BENSON drum plotter and a HP9885M flexible disk drive of 0.5m byte storage capacity. The language available on these computers was an enhanced version of interpretive HP BASIC.

### 5.3 Suite of Programs

In this section, the general global structure of the suite of modelling programs for the vane pump is presented. The aim of which is to provide an appreciation of the program interconnections in relation to their processes, and the input and output requirements. In order not to distract the reader from the primary goal of this section, the details are covered separately in the sections that follow. The general structure of the program interaction is presented pictorially in figure (5.3.1).

Three programs constitute the main suite of modelling programs for the vane pump. In addition to these, there is a group of minor programs which deals with further processing of the fundamental simulation data. These are classed under the general heading of auxiliary programs. The programs are divided into three groups, data preparation, simulation and simulation output, these are provided by the programs VFLGEN, VMODEL and VPLOT respectively. Data transfer between programs are via datafiles stored on the mass-storage units and data generated by one program is accessed by another further down the execution tree.

At the head of the flow diagram is the program VFLGEN, this is a highly interactive program which generates and edits the parameter datafile to a format required by the program VMODEL, further down the execution tree. The data is handled by this program in four separate groups, namely pump geometry, operating envelope, inlet groove data and outlet groove data. This enables an efficient data input and editing facility. At exit, the program generates or rewrites a datafile depending on whether the named datafile existed at the start of the program execution.

Further along the execution tree is the main modelling program VMODEL, this program operates in two modes, 'Auto' and 'Manual'. The auto mode permits multiple batch simulations and automatic plotting of the simulated data (via VPLOT), without operator interaction. The manual mode permits only single simulation runs and no automatic plotting facility. Execution stops at the end of the simulation, and if graphical output is required, VPLOT must be manually loaded and run. All the data required for simulation is input via the parameter datafile. This is generally generated by VFLGEN, but can be generated by other means, provided the datafile meets the format requirements. The only required operator interaction is in setting up the auto or manual sequence modes. At the end of the execution, the program outputs the process datafile which contains the results of the simulation.

The final program in the basic series of programs is VPLOT. This program outputs the process data graphically onto one of three plotting devices, a visual display unit (VDU), drum plotter or a flat-bed plotter. As with the previous program VMODEL, this program operates in both auto and manual modes. Auto mode can be entered either manually, by the operator, or automatically as a continuation of the auto

sequence initiated by the program VMODEL. If auto mode is initiated by VMODEL, the plotting device is set to the drum plotter, operator preference is permitted only in the manual mode, and when auto mode is initiated manually.

#### 5.4 Datafile Structure

On the HP9845B system enhanced BASIC there are available two file types and four data types. The available file types are sequential and random. The data types are full precision, short precision, integer precision and string.

A sequential file type is one where data is stored or acquired from the mass-storage device, one data item at a time. In contrast, the random file has the advantage that data items need not be read sequentially from the start of the file. Data can be written to, or read from file in a random sequence of a pre-defined group of data items, called a record. The choice between one file type or another is dependant on application. If quick access to particular data items is required at random, the random file type is required, but this file structure is inefficient in the use of storage medium. As data is stored in records and its size fixed for a particular file, its size must be such as to enable storage of the largest group of data constituting a record. If the other records contain less data, empty spaces are left. Other storage inefficiencies relate to ill correlation between logical and physical record sizes.

The data type relates to the type and required precision of the data to be stored. For numerical data, it can be stored in full, short or integer precision. Full precision provides a twelve significant digit

File Type : Sequential

Data Type : Full Precision

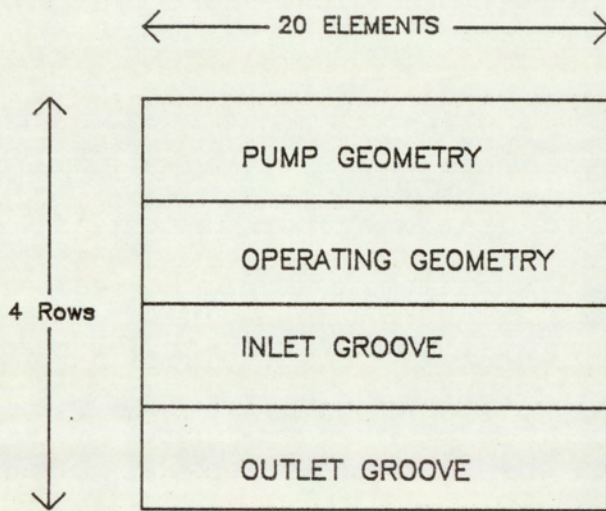


FIG.5.4.1 PARAMETER DATAFILE STRUCTURE

accuracy and an exponent range of -99 through 99. Short precision permits only an accuracy to six significant digits and an exponent range of -63 through 63. With integer precision only integer values in the range -32768 to 32767 are permitted. Besides numeric variables there are string variable. This is for storage of ASCII characters.

Storage requirements are different for the various types of data. For full precision 8 bytes of storage are required due to the higher degree of accuracy required. Short and integer precision requires, 4 bytes of storage per variable. A string character requires 1 byte per character. Where large arrays are involved, it is especially important that a lower precision data type should be defined if the higher precision is not required. This saves both mass-storage space and read/write memory.

#### 5.4.1 Parameter Datafile

The general details of the datafile are presented in figure (5.4.1). The data in this datafile are contained in a single array, Data(\*), of dimension 4 x 20. The symbol '\*' denotes an array variable. The file type is sequential and the data type is full precision. Data is divided into four groups defining, pump geometry, operating envelope, inlet groove and outlet groove. Each data group is assigned one row of the data array.

The list below defines the allocation of the elements of the Data array and the variable represented.

Pump Geometry Parameters:

Data(1,1) : Sdiam - Stator diameter (mm).

Data(1,2) : Rdiam - Rotor diameter (mm).  
 Data(1,3) : L - Rotor length (mm).  
 Data(1,4) : Awdth - Abutment width (mm).  
 Data(1,5) : Aclar - Abutment clearance (mm).  
 Data(1,6) : Vwdth - Vane Width (mm).  
 Data(1,7) : Vclar - Nominal vane tip clearance (mm).  
 Data(1,8) : Pdiam - Inlet/outlet port diameter (mm).  
 Data(1,9) : Pangl - Port angular position from datum (deg).  
 Data(1,10) : Abrad - Cam abutment radius (mm).  
 Data(1,11) : Aarad - Cam actuation radius (mm).  
 Data(1,12) : Aorad - Cam operation radius (mm).  
 Data(1,13) : Aangl - Cam actuation angle (deg).  
 Data(1,14) : Eodiam - End-plate outer diam. (mm).  
 Data(1,15) : Eidiam - End-plate inner diam. (mm).  
 Data(1,16) : Eclar - End-plate clearance (mm).  
 Data(1,17) : Nseg - Number of vane segments per cycle.

\* Elements 15 through 20 of row 1 are undefined.

Operating envelope Parameters:

Data(2,1) : Speed - Rotor speed (rpm).  
 Data(2,2) : Ipsure - Mean input pressure (bar).  
 Data(2,3) : Opsure - Mean outlet pressure (bar).  
 Data(2,4) : Cpsure - Case pressure (bar).  
 Data(2,5) : Rho - Fluid density ( $\text{Kg/m}^3$ ).  
 Data(2,6) : Eta - Fluid viscosity ( $\text{Ns/m}^2$ )  
 Data(2,7) : Beta - Fluid Bulk modulus ( $\text{Ns/m}^2$ )  
 Data(2,8) : Ildiam - Inlet line diameter (mm).  
 Data(2,9) : Oldiam - Outlet line diameter (mm).  
 Data(2,10) : Dcff - Coefficient of discharge.  
 Data(2,11) : Pcav - Cavitation pressure (bar).

\* Elements 11 through 20 of row 2 are undefined.

Inlet Port Parameters:

Data(3,1) : Gdpth(1,1)- Hemispherical groove depth (mm).  
Data(3,2) : Gcdim(1) - Hemispherical groove cutter diam. (mm).  
Data(3,3) : Gastr(1,1)- Hemispherical groove start angle (deg).  
Data(3,4) : Gdpth(1,2)- Square groove depth (mm).  
Data(3,5) : Gcwth2(1) - Square groove width (mm).  
Data(3,6) : Gastr(1,2)- Square groove start angle (deg).  
Data(3,7) : Gdpth(1,3)- Triangular groove depth (mm).  
Data(3,8) : Gcang3(1) - Triangular groove cutter angle (deg).  
Data(3,9) : Gastr(1,3)- Triangular groove start angle (deg).  
Data(3,10) : Gtype(1) - Groove type; 0:no, 1:hemispherical  
2:square; 3:Triangular

\* Elements 11 through 20 of row 3 are undefined.

Outlet Port Parameters:

Data(4,1) : Gdpth(2,1)- Hemispherical groove depth (mm).  
Data(4,2) : Gcdim(2) - Hemispherical groove cutter diam. (mm).  
Data(4,3) : Gastr(2,1)- Hemispherical groove start angle (deg).  
Data(4,4) : Gdpth(2,2)- Square groove depth (mm).  
Data(4,5) : Gcwth2(2) - Square groove width (mm).  
Data(4,6) : Gastr(2,2)- Square groove start angle (deg).  
Data(4,7) : Gdpth(2,3)- Triangular groove depth (mm).  
Data(4,8) : Gcang3(2) - Triangular groove cutter angle (deg).  
Data(4,9) : Gastr(2,3)- Triangular groove start angle (deg).  
Data(4,10) : Gtype(2) - Groove type; 0:no, 1:hemispherical  
2:square; 3:Triangular

\* Elements 11 through 20 of row 4 are undefined.

File Type : Sequential

Data Type : Short Precision

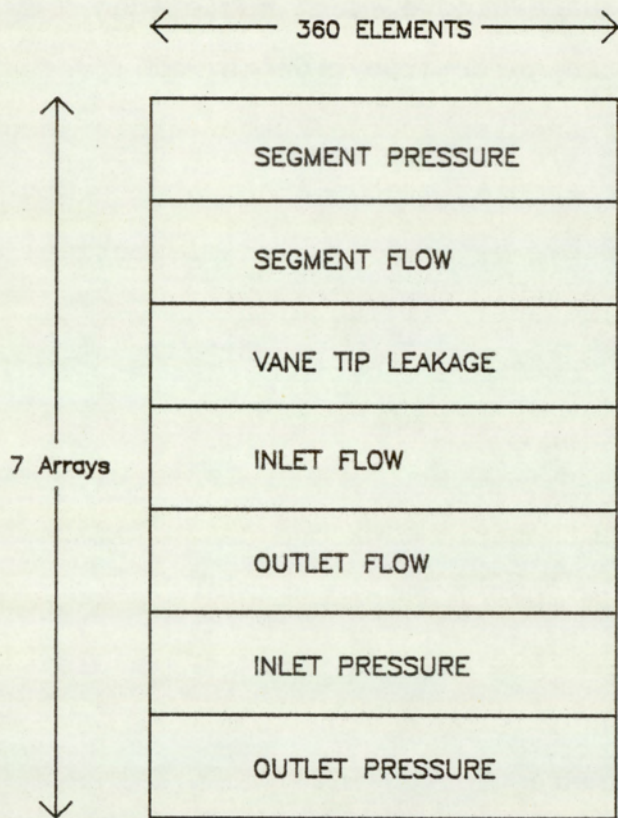


FIG.5.4.2 PROCESS DATAFILE STRUCTURE

### 5.4.2 Process Datafile

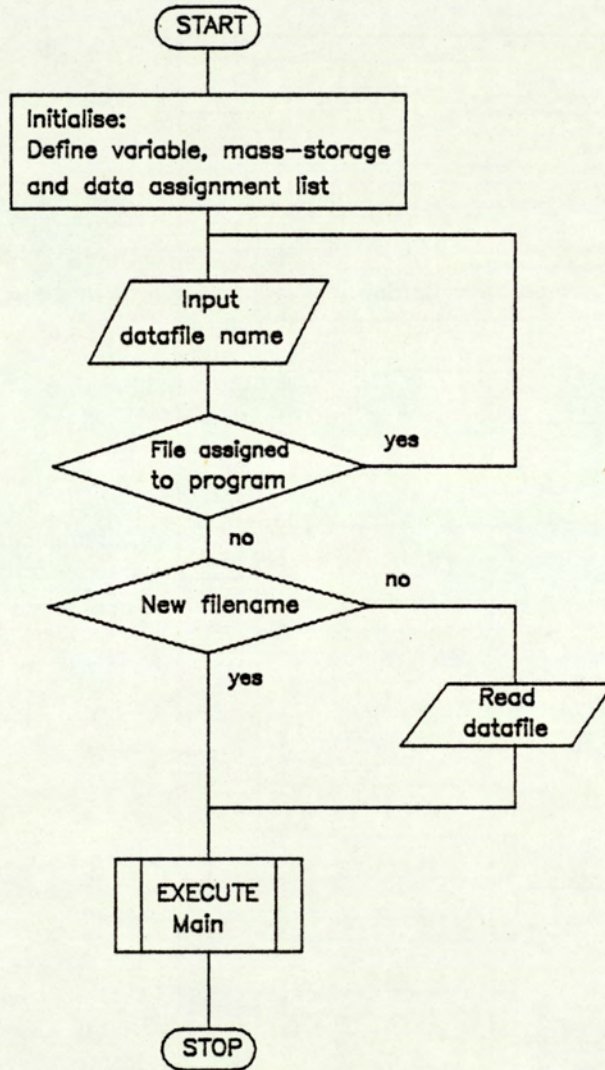
The general details of the process datafile are presented in figure (5.4.2). The datafile contains seven single dimension arrays of 360 elements each. Each array contains data relating to the fundamental pump processes of segment pressure, net segment leakage, net segment flow, and the inlet and outlet port flow and pressure history. The first element from each array corresponds to the rotor position at the rotor angular datum. Due to the symmetry of the pump, the arrays for a rotor rotation of only the first 180 degrees, need be defined. The process for the second half of the rotor cycle is a repetition of the first. The datafile is of the sequential type and the variables are stored in short precision format, in an effort to minimise storage requirements.

The list below defines the allocation of the elements of the Data array and the variable represented.

Process datafile parameters:

- P(\*) - Segment pressure array ( $N/mm^2$ ).
- Ll(\*) - Net total leakage into segment ( $mm^3/s$ ).
- Q(\*) - Net flow from segment ( $mm^3/s$ ).
- Ip(\*) - Input port pressure ( $N/mm^2$ ).
- Op(\*) - Output port pressure ( $N/mm^2$ ).
- If(\*) - Inlet port flow from port ( $mm^3/s$ )
- Of(\*) - Outlet port flow from port ( $mm^3/s$ ).

PROGRAM : VFLGEN  
SEGMENT : MAIN



Permits the display,  
editing, creation,  
and listing of datafiles  
using soft key.  
facility

FIG.5.5.1 FLOW CHART OF PROGRAM VFLGEN : SHEET 1

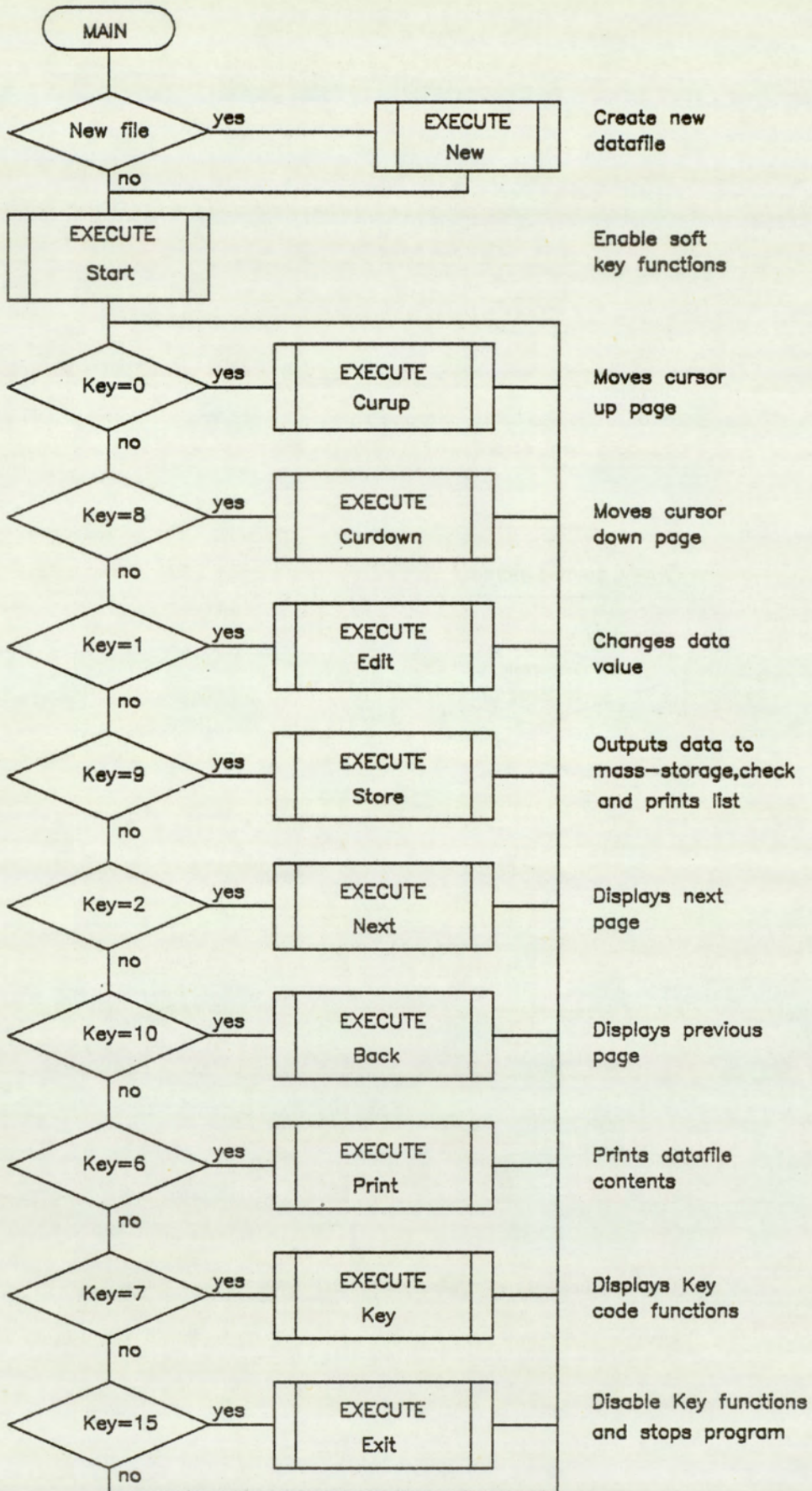


FIG.5.5.2 FLOW CHART OF PROGRAM VFLGEN : SHEET 2

## 5.5 Program VFLGEN

### Description:

This program enables the generation and editing of the datafiles accessed by the main simulation program VMODEL. Program facility is selected by an interaction of the display facility and specially defined key functions. As an aid to data handling, data is handled in pages consisting of data groups describing pump geometry, operating envelope, inlet groove and outlet groove parameters. By means of the specially defined keys, pages are selected for display, parameters identified for input or editing, and outputs selected. In addition, the program performs a limited check for an overlap in groove lengths before outputting the datafile to mass-storage.

### Program Structure:

The flow charts describing the program are shown in figures (5.5.1) and (5.5.2). The first program process is to define the mass-storage unit and to establish the data assignment list. The assignment list defines the association between the elements of the data array and the physical parameter. After this initialisation process, the program prompts for an input datafile name and a check is made of the status of the filename. If the filename has been assigned to a program, another filename is prompted, otherwise execution continues. If the filename is that of an existing datafile, the data is first read before proceeding with the actual data editing and input processes provided by subprogram Main, which is described by figure (5.5.2).

For the case of a new file, execution automatically branches to routine New. This routine prompts for data input and updates the display accordingly. No editing facility is available at this stage. On completion of this initial input process the program displays the first

data page and awaits further execution. Selection of any one of the specially defined keys causes an immediate branching to the appropriate routine. On completion, the program awaits the next function to be selected.

The program permits nine function selection. Four functions are needed to identify any individual parameter. Two functions are required to advance and back step the data pages, and another two to position the cursor within the page. On identifying the parameter, selection of the 'Edit' function permits the replacement of the parameter value. The function 'Store' enables the storing of the edited or new datafile to mass-storage and the outputting of the data list to printer. If an error is encountered during the data check, the routine prints an error message and aborts further execution of this routine. Function 'List' outputs the same data listing and function 'Key', describes the key functions. On selection of 'Exit', key functions are disabled and program execution terminated.

## 5.6 Program VMODEL

### Description:

This is the main program which simulates the flow and pressure states of the vane pump, and operates in two modes 'auto' and 'manual'. In the first mode the program performs batch processing consisting of a series of simulation runs and an optional automatic loading of the Plot program for immediate graphic output, without further operator intervention. In the manual mode the program enables only a single simulation run and termination of the program occurs following the generation of the process datafile. All input and output of data are

PROGRAM : VMODEL  
 SEGMENT : MAIN

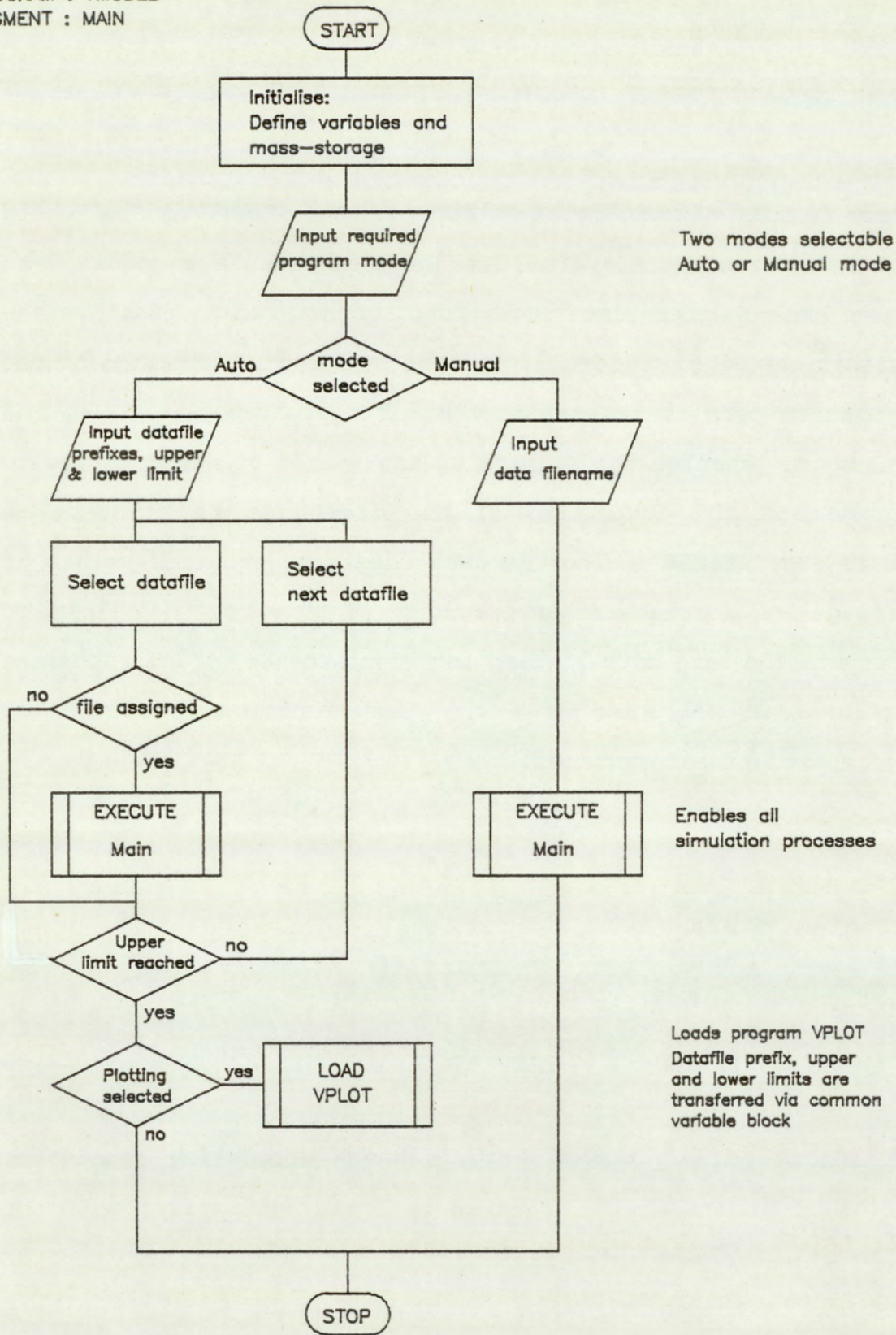


FIG.5.6.1 FLOW CHART OF PROGRAM VMODEL : SHEET 1

via datafiles. The required input data is contained in the parameter datafile and the output data is held in the process datafile. There is a limited operator entry at the start of program initialisation, but these entries are only for the setting of the mode of operation.

#### Program Structure:

##### Control Module - Sheet 1

The figure (5.6.1) shows the main control module which enables the different modes of operation, with the actual simulation processes being handled by the routine Main. The first process is that of program and system initialisation. This involves selecting system operating modes, defining default devices and variables. Following this, there is a prompt for the required operating mode and branching occurs accordingly. If manual mode has been selected, there is a further prompt for the input data filename. On input of a valid data filename the routine Main is called and executed. Program execution terminates at this point.

In auto mode a prompt requests the input and output data filename prefixes, and the upper and lower limits of the file numbers. The file names have a six character format, consisting of four alphanumeric characters followed by two numeric characters. The second to the fourth character of the parameter datafiles are assigned 'DAT' and that for process file 'GDT'. The first character is the filename prefix and is optional. Following the required inputs the program generates the first filename and check the mass-storage directory for availability. If the file exists, the data is read and routine Main is executed. On return, after the completion of routine Main, a check is made of the limit of the current file number. Another pass is performed, if the upper limit has not been attained, and progress if the limit has been reached. If plotting function has been selected, the program VPLOT is loaded and

PROGRAM : VMODEL  
 SEGMENT : MAIN

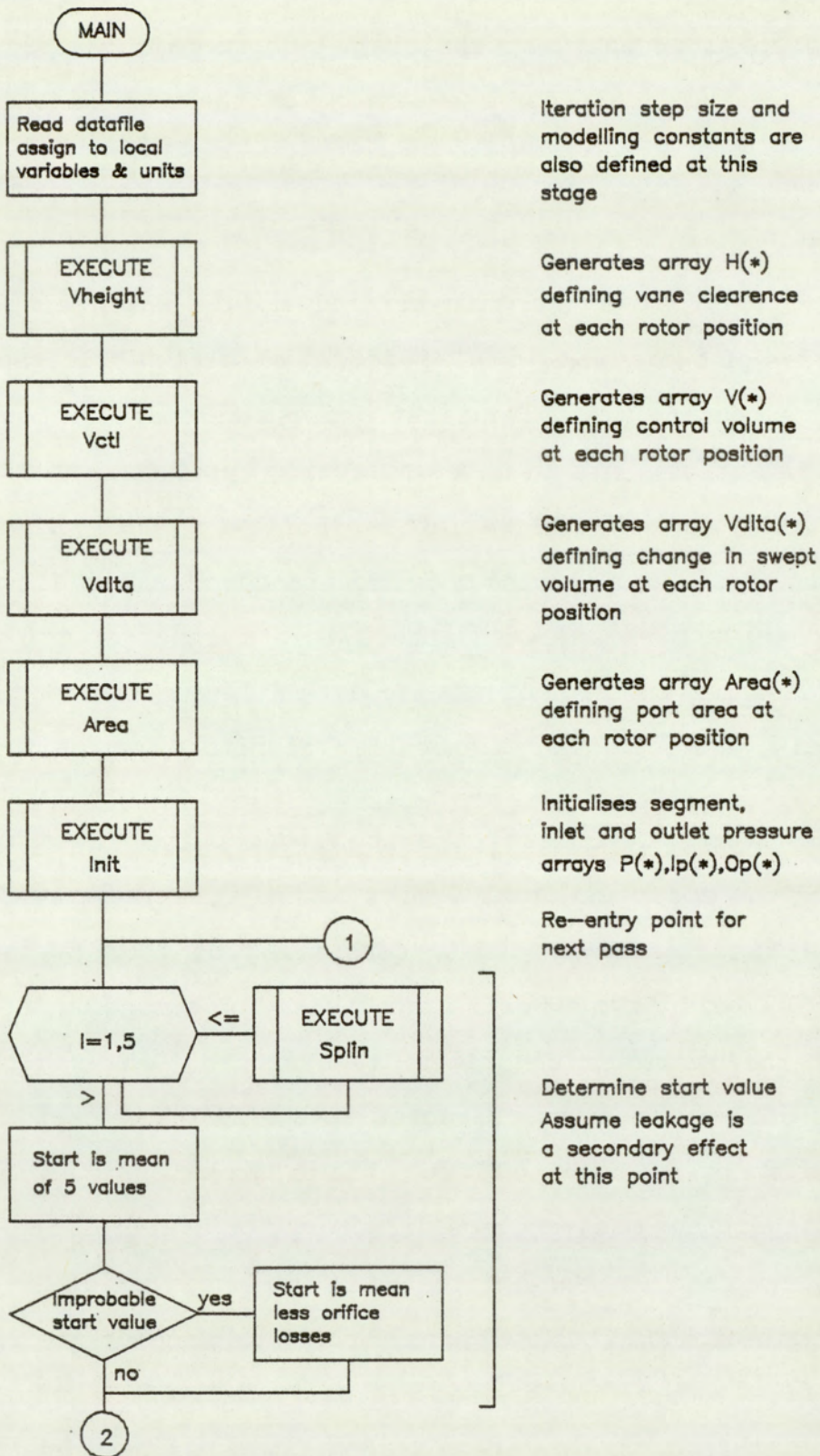


FIG.5.6.2 FLOW CHART OF PROGRAM VMODEL : SHEET 2

PROGRAM : VMODEL  
 SEGMENT : MAIN

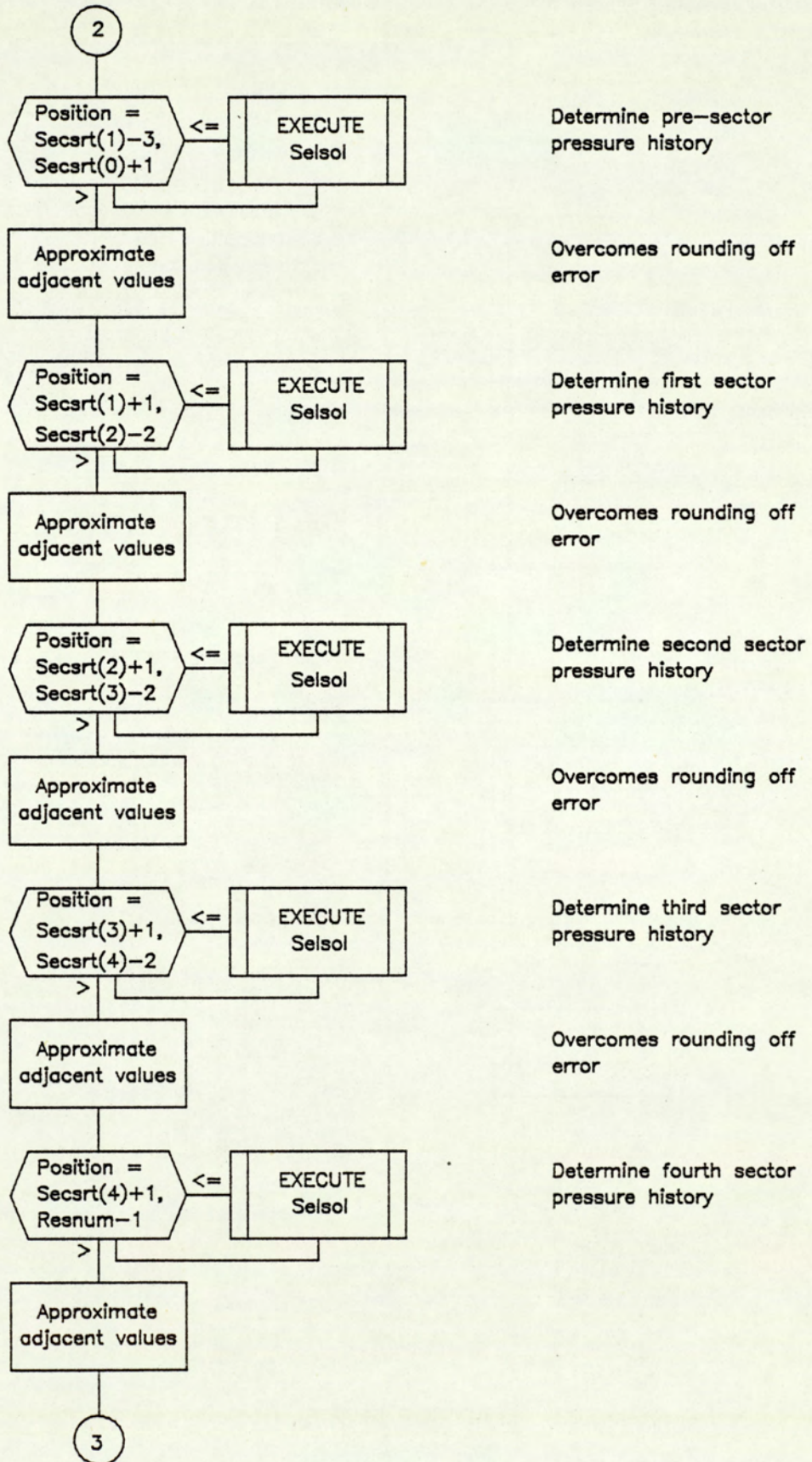


FIG.5.6.3 FLOW CHART OF PROGRAM VMODEL : SHEET 3

PROGRAM : VMODEL  
 SEGMENT : MAIN

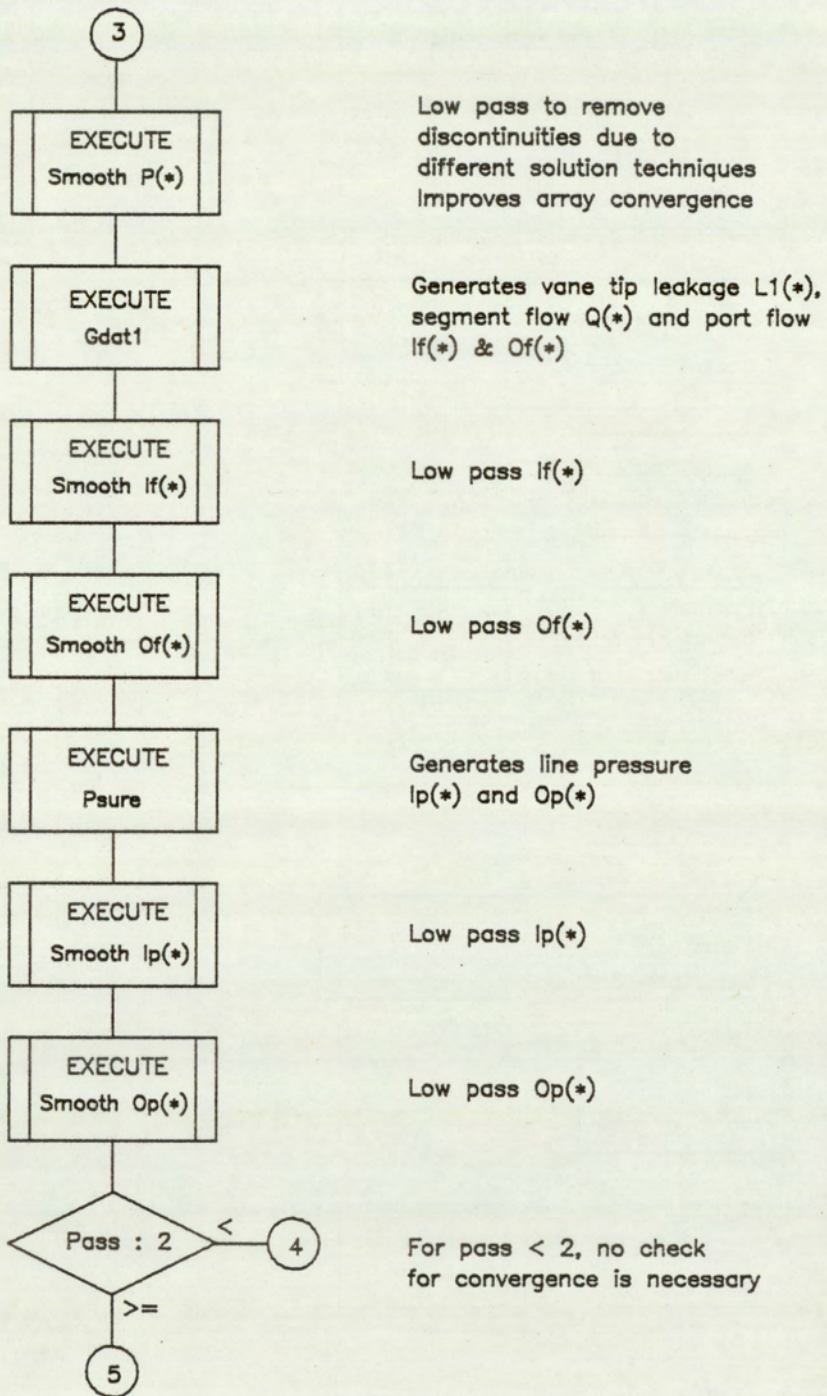
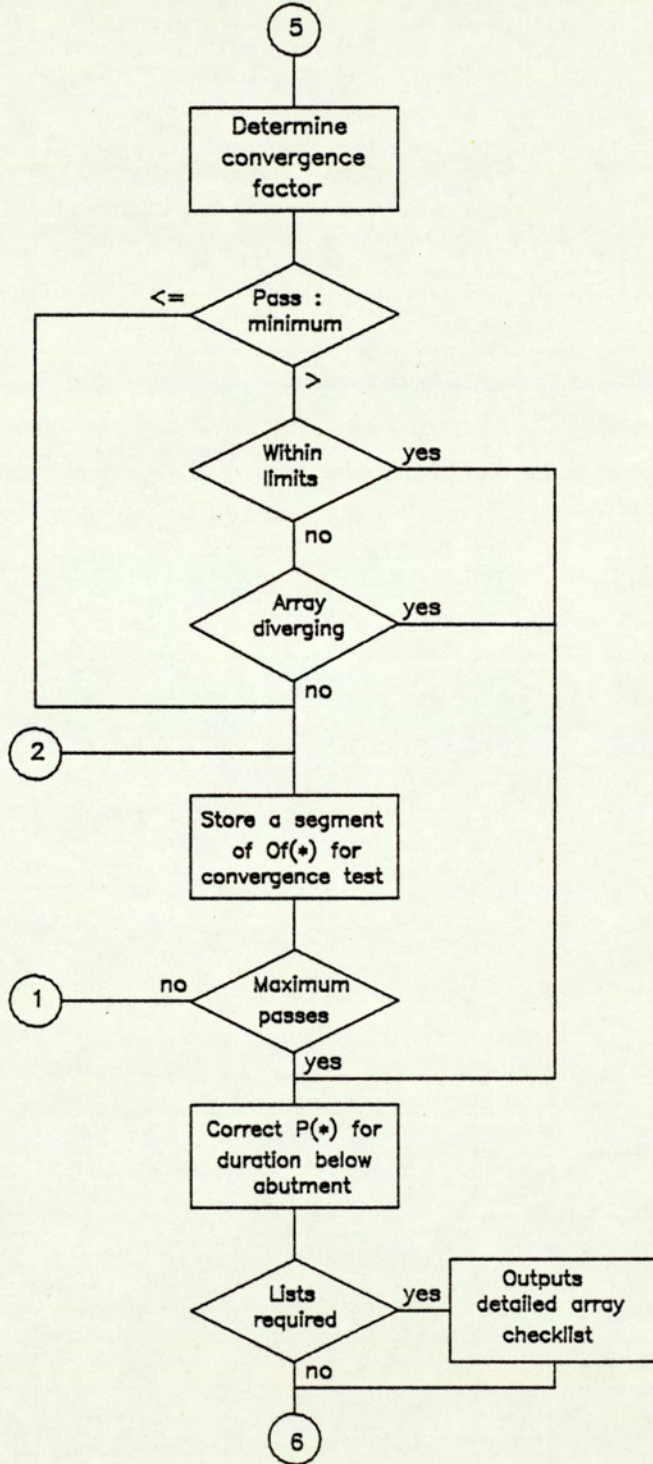


FIG.5.6.4 FLOW CHART OF PROGRAM VMODEL : SHEET 4

PROGRAM : VMODEL  
 SEGMENT : MAIN



The convergence factor indicates the variability between consecutive iterations of  $Of(*)$

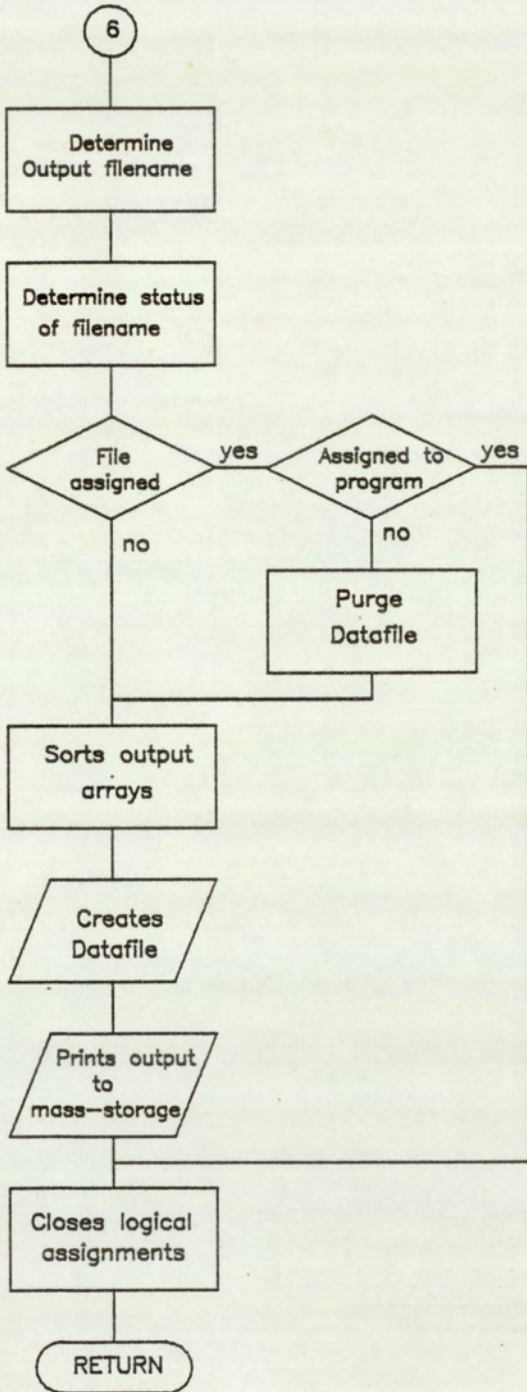
Algorithm requires a minimum number of iterations before executing convergence check

Convergence factor within defined limits

Convergence factor increasing

Branching at 1 for repass  
 No additional pass if maximum number reached

FIG.5.6.5 FLOW CHART PROGRAM OF VMODEL : SHEET 5



Output filename is a derivative of the input filename

No datafile is output if filename is assigned to a program

Reduces output arrays to 360 elements each

Outputs sequentially  
P(\*),L1(\*),Q(\*),  
Ip(\*),Op(\*),If(\*),Of(\*)

FIG.5.6.6 FLOW CHART OF PROGRAM VMODEL : SHEET 6

executed, otherwise program execution is terminated.

#### Simulation Module - Sheet (2-6)

The flow chart of the simulation module are presented by figures (5.6.2) to (5.6.6). This routine is the master routine controlling all the processes of the simulation process, with the bulk of the computation being assigned to minor modules. The routine starts with the reading of the parameter datafile and the execution of five subroutines. The first four routines Vheight, Vctl, Vdlt and Area generates the fundamental geometrical arrays whose values are required repeatedly during the execution of the program. This has the advantage of savings in performing repeated computation and a simpler program structures, but a larger run time memory. The fifth routine Init sets up the initial port and segment pressure arrays. Inlet and outlet pressure arrays are set at their mean pressure levels, and the segment pressure array is set at levels corresponding to a condition relating to incompressible fluid, zero port losses and steady port pressures.

The next process is to determine the start value for computation. As a first approximation, the program assumes a condition where leakage is a secondary effect and attempts the solution under linear condition. The program computes the first five points corresponding to an advance in rotor angular position and assigns the start value to the mean level calculated. Following this, a check is made to test for an improbable condition where the start value is greater than the inlet pressure. If the start value is improbable, an alternative start value is calculated. The start value is taken to be the mean inlet pressure less orifice losses.

Once the start value has been established, the calculation of the segment pressure history can be performed. This is done in blocks

corresponding to sectors. Within each block, routine Selsol is called and the segment pressure is determined at each rotor step. As a precaution against rounding off error, the adjacent points of sectors are approximated. The flow chart is shown in figure (5.6.3).

After the full segment history has been calculated, the routine Smooth is called to process the array P(\*). This routine is effectively a low pass filter which removes discontinuities arising from different solution techniques used in computing the array. The effect of which is to improve the convergency of the arrays. The execution of Gdat1 that follows, calculates the segment flow and leakage arrays together with the port flows. The inlet and outlet flow arrays are similarly smoothed by the subsequent execution of routine Smooth. The next routine to be executed is Psure which calculates the line flow arrays simulating the flow into an anechoic line and termination. The next two executions of Smooth processes the input and output flow arrays. The last process shown on this sheet, figure (5.6.4), is a branching involving the convergence test.

For the first pass, the execution by-passes the convergence test and directly stores a segment of the outlet flow array. This data is required in the calculation of the convergence factor, in subsequent runs when a convergency test is performed. Convergency is defined in terms of the variability in the outlet flow array between consecutive passes. The first test is that of satisfying the minimum pass criteria. If the minimum number of runs has not been performed the test is terminated by a branching and an outlet flow array segment is stored. If the first two conditions are satisfied and the convergence factor is within acceptable limits execution successfully proceeds to the next stage of the simulation. This also occurs should a divergence in

PROGRAM : VMODEL  
 SEGMENT : MAIN

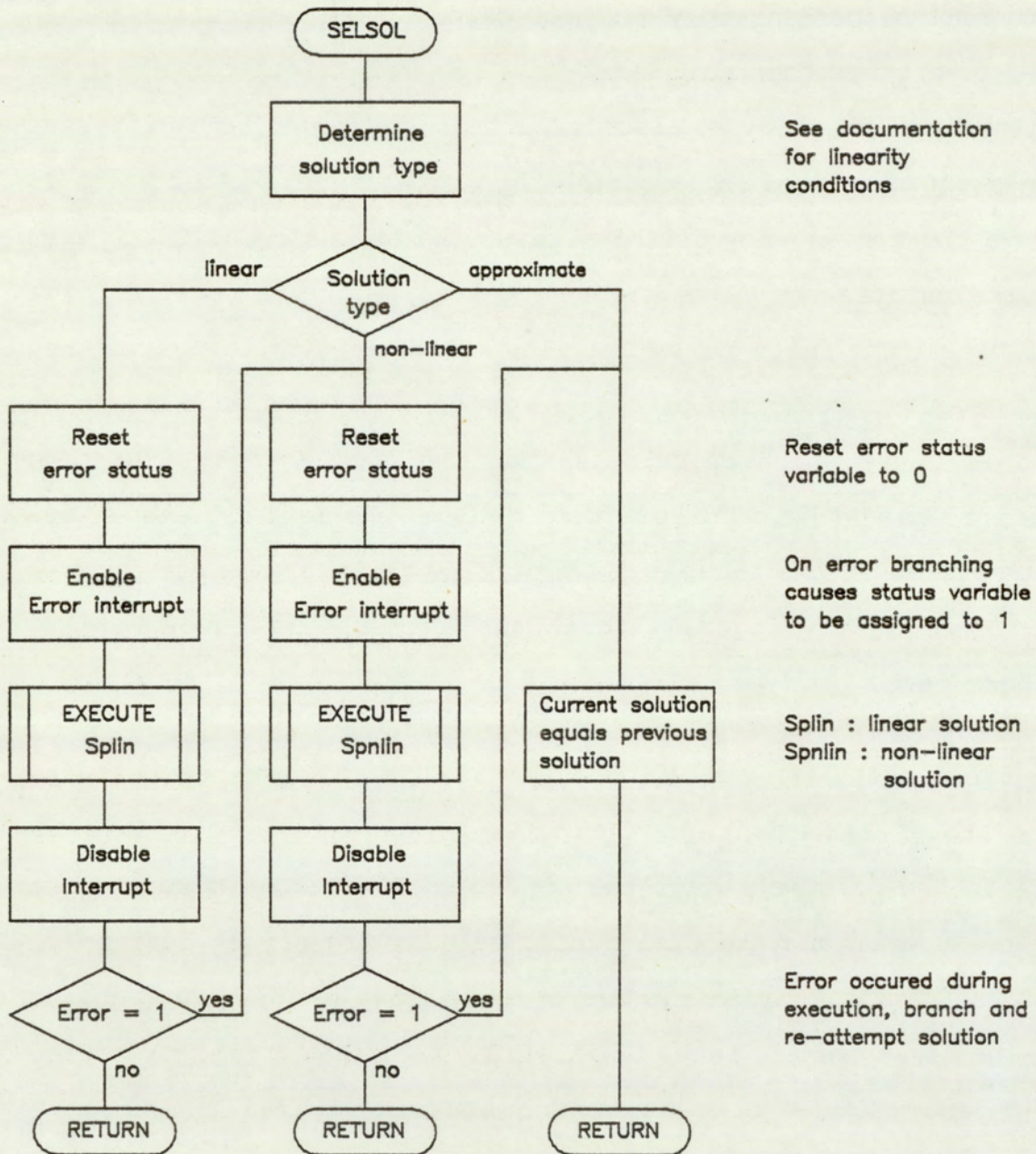


FIG.5.6.7 FLOW CHART FOR PROGRAM VMODEL : SHEET 7

the outlet flow array be detected. For the case where both tests are negative, the outlet array segment is stored and another pass is performed, provided the maximum number of permitted passes has not been exceeded. These flow paths can be seen in figure (5.6.5).

Once convergence has been accepted, the program proceeds with the correction of the segment array for the duration when the vane passes below the abutment. Depending on the checklist variable, a detailed listing is output of the fundamental arrays. The next stage concerns the generation of the output process datafile. The output data filename is first tested for availability. If the filename is unassigned, the program proceeds by reducing the size of the output arrays and writing these out to mass-storage. Following this, logical assignments are closed and the routine returns to the calling control module. If the filename was initially assigned to another datafile, it is purged before a new datafile is generated. For the case where the filename was assigned to a program file, execution is aborted.

#### Select Solution Module - Sheet (7)

This routine identifies the solution type and controls the solution at each iterative point. The general equation defining the process is non-linear and its solutions can be very time consuming. Under particular conditions, the equation can be simplified to a linear condition, for which solutions are more readily available. The linear solution can be applied when there is no port flow and when leakage is a secondary effect. In this algorithm a third technique, the approximate solution, is also used. This solution technique is used on failure of the non-linear solution, and at the end of the final stages of the cycle, when there is little change of segment history and is classed as a non-linear condition. Attempts to solve directly during

PROGRAM : VMODEL  
 SEGMENT : SUBPROGRAM

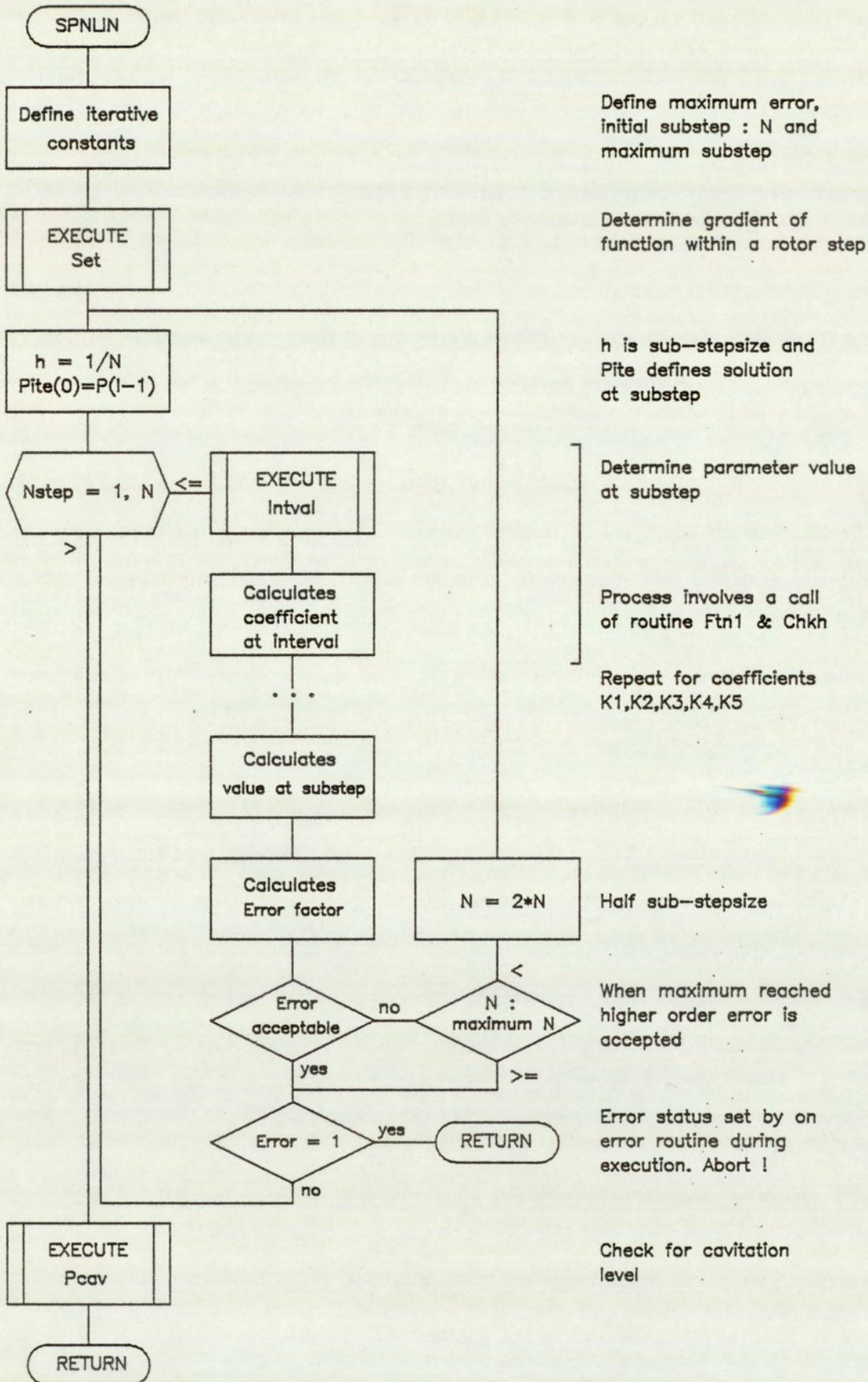


FIG.5.6.8 FLOW CHART OF PROGRAM VMODEL : SHEET 8

this period is time consuming and unnecessary. The approximate solution merely assigns the current solution to that of the previous step.

The algorithm starts by attempting to classify the solution type and branching accordingly, to the appropriate routine and can be seen in figure (5.6.7). Taking the case of an identified linear condition, the routine first initialises the error status variable and enables the on error interrupt. The on error interrupt functions by assigning the error status variable to '1' on encountering a mainframe error, and in this routine, is brought about due to an overflow in the variable specification. Following the initialisation, routine Splin is called and a linear case solution is attempted. On return, the on error facility is disabled and the error status variable is inspected. If no error has occurred, the solution is accepted and execution returns to the calling routine. If an error is detected during the linear solution the non-linear solution is attempted, and failure while executing the non-linear solution results in a branching to the approximate solution.

The case for an initially identified non-linear condition is similar to the linear case, except that the routine Spnlin is called instead of Splin. Failure of this solution results directly in an approximate solution.

#### Non-Linear Solution Module - Sheet (8)

This routine solves the flow-pressure equation for the non-linear condition. The routine is primarily an algorithm performing the Runge-Kutta-Merson method to order four for the solution of differential equations. With this method, there is a danger of partial instability which arises due to an insufficiently small step size being used. Computing throughout at the minimum step size would prove extremely time consuming. A direct variable step size iteration algorithm

cannot be implemented without making the program structure extremely complicated and increasing the computational load. In this algorithm a pseudo-variable step method is employed. Each physical step is sub-divided into sub-steps depending on the error term, and at each sub-step the variables are linearly interpolated and the solution determined using the Runge-Kutta-Merson method. This is repeated till the full physical step is reached.

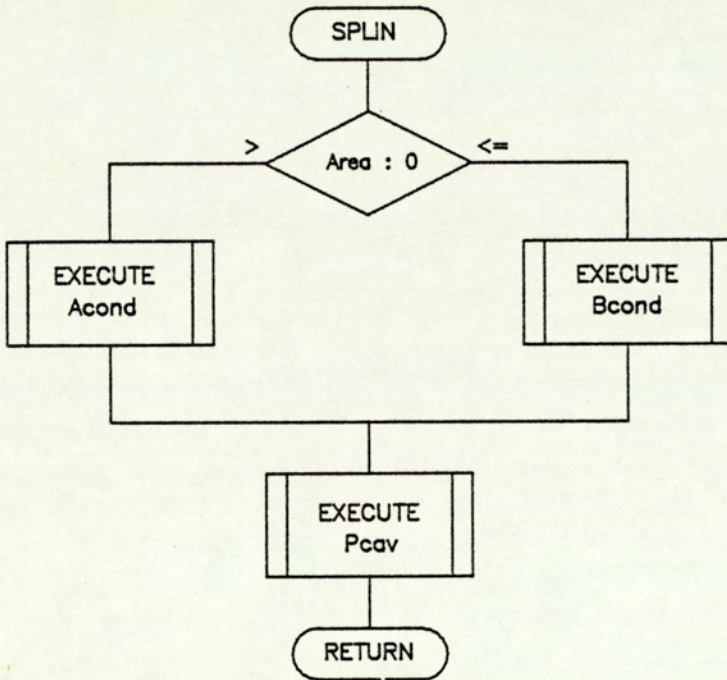
The routine starts with a definition of the iterative constants which indicates the minimum step size, initial step size and acceptable error magnitude. The routine Set that follows determines the gradient of the parameters for which interpolation is required, during the sub-step. The routine next enters a 'For-Next' loop to calculate the solution at each sub-step. Within the loop, the routine Intval calculates the variables at the sub-step and the coefficients of the Runge-Kutta-Merson method and the error term. If the error term is within acceptable limits, execution continues till the end of the physical step. For the case of unacceptable error, the step size is halved, provided the minimum step size has not been reached, and restarts at the new step size. If the minimum step size has been reached, the execution continues at the greater level of error. At the end of each step, a check of the error status variable is performed and the routine aborts if the variable has been set.

At the end of the execution, a check is made of the solution for cavitation level, and is adjusted accordingly.

Linear Solution Module - Sheet (9-10)

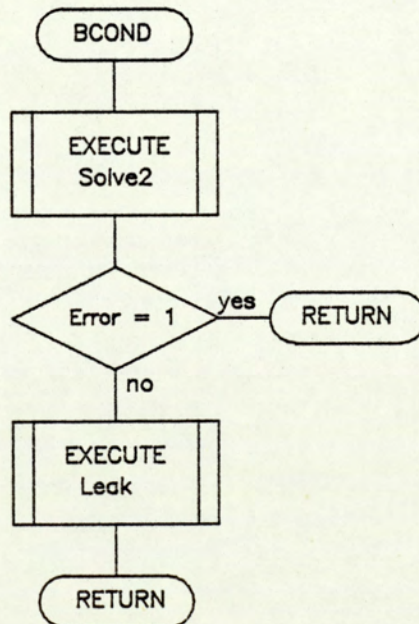
For the linear solution condition there are two possible cases. The first is that for zero port flow and the second that for when leakage flow is a secondary effect. The routine Splin checks for these two

PROGRAM : VMODEL  
SEGMENT : SUBPROGRAM



Acond : Indirect analytical solution  
Bcond : direct analytical solution is available

Check for cavitation pressure condition



Provides direct solution

Computational error occurred  
Abort execution

Calculates vane tip leakage at rotor position

FIG.5.6.9 FLOW CHART OF PROGRAM VMODEL : SHEET 9

PROGRAM : VMODEL  
 SEGMENT : SUBPROGRAM

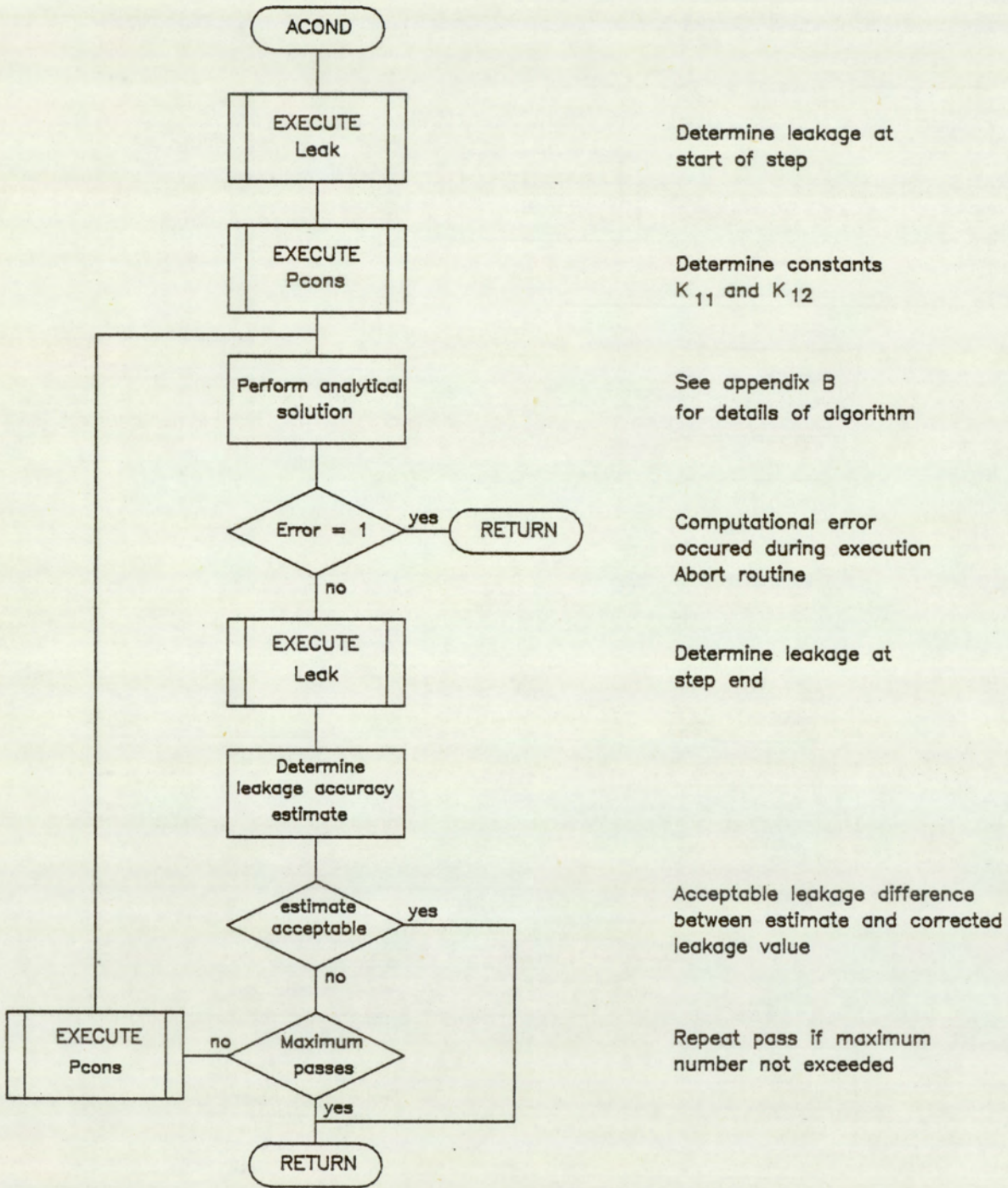


FIG.5.6.10 FLOW CHART OF PROGRAM VMODEL : SHEET 10

conditions and executes the appropriate solution algorithm.

The flow chart of the main driver routine Splin is shown in figure (5.6.9). This routine identifies the port flow condition by checking on the available flow area. For areas greater than zero, routine Acond is selected, and for all other conditions routine Bcond is selected. Following the execution of Acond or Bcond the solution is checked for the cavitation condition and returns to the calling routine.

The routine Bcond is a relatively simple routine. Execution of Solve2 provides the exact analytical solution under the set of conditions. This is followed with a check on the error status and the calculation of leakage at step end. The leakage is required as a basis for testing for the solution condition which, unlike in the other solutions, is not calculated in the intermediate stages of this solution.

The routine Acond begins with an execution of Leak to determine the leakage at the last step. This is used to determine the constants  $K_{11}$  and  $K_{12}$  at the beginning of the step. Execution proceeds with the solution of the equation and returns for an error status check. The detailed algorithms and solution techniques are contained in appendix C. These are presented in the appendices so as not to distract the reader from an appreciation of the fundamental objectives. The routine continues with another execution of Leak which is used to determine the accuracy of the initial estimate of  $K_{11}$  and  $K_{12}$ . If the estimate is acceptable, the routine terminates and returns to the calling routine, otherwise another attempt is made at the new estimates of  $K_{11}$  and  $K_{12}$ . The flow chart is seen in figure (5.6.10).

PROGRAM : VPLOT  
 SEGMENT : MAIN

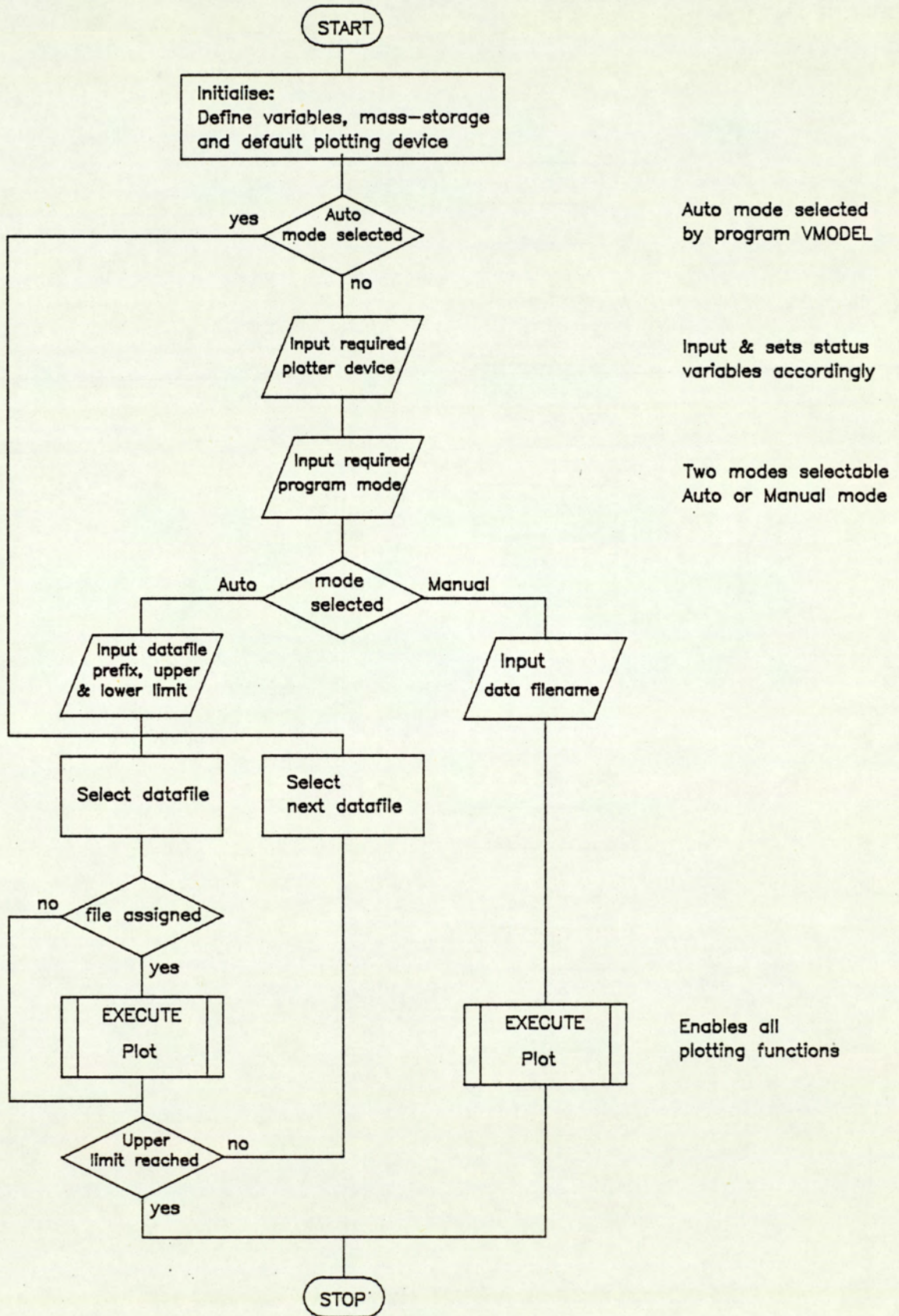


FIG.5.7.1 FLOW CHART OF PROGRAM VPLOT : SHEET 1

PROGRAM : VPLOT  
SEGMENT : MAIN

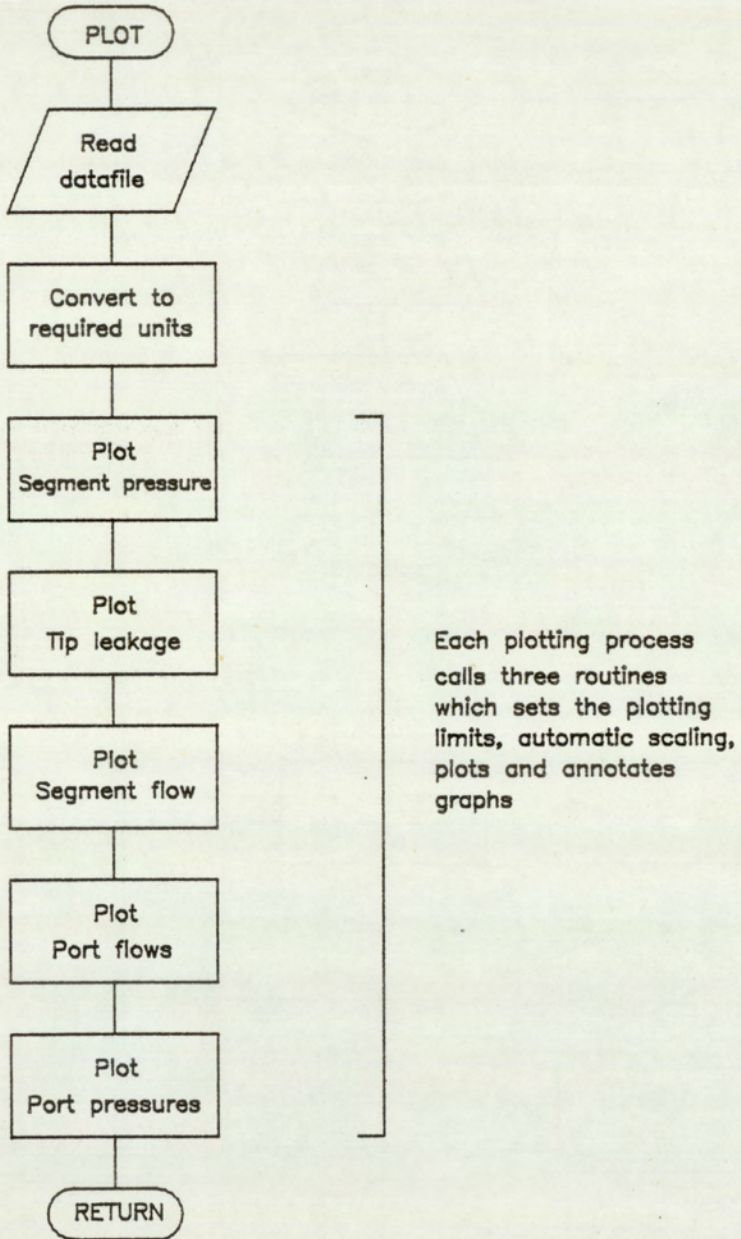


FIG.5.7.2 FLOW CHART OF PROGRAM VPLOT : SHEET 2

## 5.7 Program VPLOT

### Description:

The outline of the program VPLOT is described by flow charts shown by figures (5.7.1) and (5.7.2). This program outputs graphically the process simulation data output by the simulation program VMODEL. This takes the form of five graphs showing the segment pressure history, net segment leakage, net segment flow, port flow ripples and port pressure ripples. A choice of two operating modes and three plotting mediums is available. In auto mode the program can be initiated by program VMODEL or manually by the operator. Auto mode permits batch data processing of the graphical output and with manual mode datafiles are processed individually. The plotting options available are; visual display, drum plotter and a flat bed plotter. In visual display mode a hard copy is available via the internal printer.

### Program Structure:

The first process involves the defining of the mass-storage unit and the default plotting device. If the auto status variable, has already been set by the previous program, execution branches to the auto sequence routine and output is to the default plotting device. For the other cases, the program prompts for the required plotting device and operating mode. Following this, branching takes execution to the auto or manual routines.

In manual mode the program logic is relatively simple. The operator is prompted for the data filename and following a check on the validity of this entry, the routine Plot is called, which performs the reading of the datafile and graphing processes. Failure of the check causes a request for another filename. On completion of the Plot routine the program terminates.

In auto mode, the operator is prompted for the filename prefix and the lower and upper limits of the data filenames. The data filename has a format consisting of four alphanumeric characters followed by two numeric characters (eg. VGDT24). The program scans the mass-storage unit for datafiles with names specified within the upper and lower limits. If a file exists, the routine Plot is executed, otherwise the next filename is inspected. On reaching the upper limit the program execution is terminated.

Routine Plot is the main graphics routine. The routine starts with a reading of the datafile followed by a scaling operation which converts the data to appropriate engineering units. The subsequent stages involves the actual plotting processes which is performed by three different routines. These routines set the appropriate limits, performs automatic scaling of axes and controls the paper feed processes, while taking into account the plotting device and mode selected.

## CHAPTER 6 : STANDARD PUMP SIMULATIONS

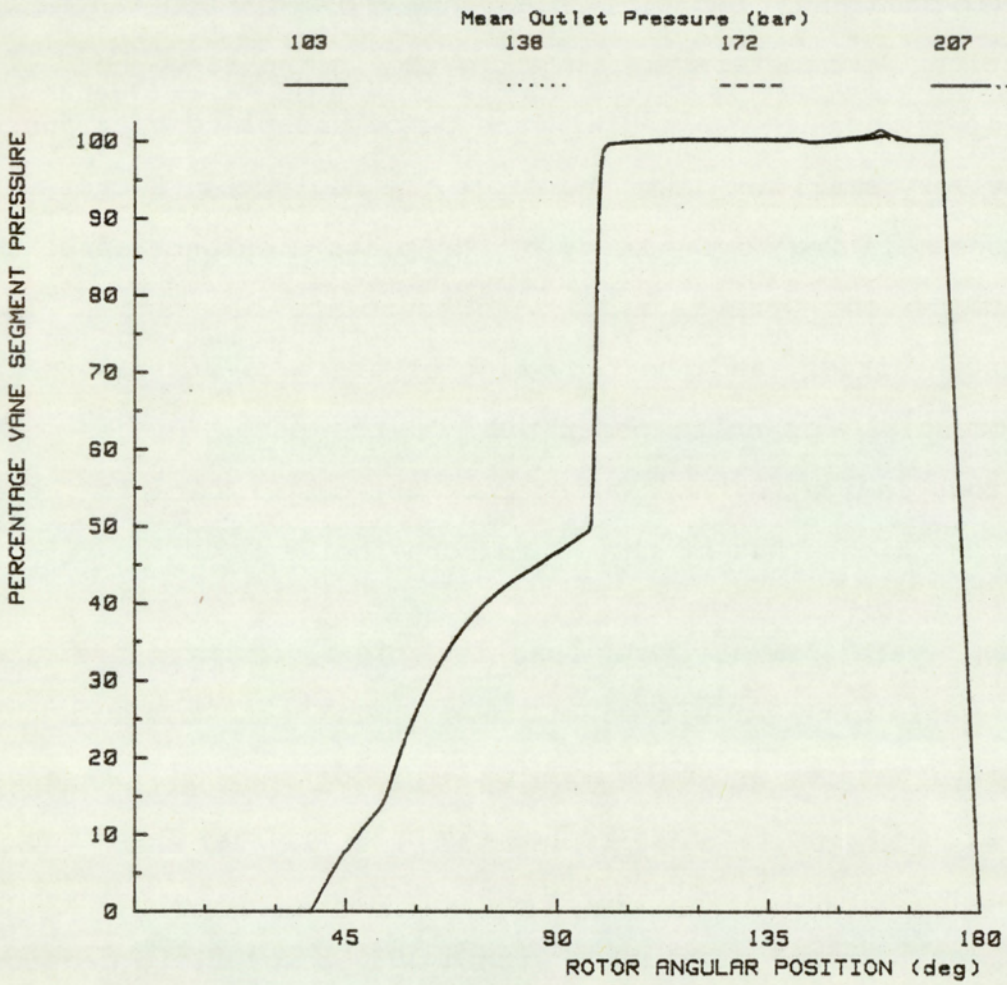
- 6.1 Introduction
- 6.2 Line Pressure Effects
  - 6.2.1 Pressure Effects on Segment History
  - 6.2.2 Pressure Effects on Flow Ripple
- 6.3 Speed Effects
  - 6.3.1 Speed Effects on Segment History
  - 6.3.2 Speed Effects on Flow Ripple
- 6.4 Vane Tip Clearance Effects
  - 6.4.1 Vane Tip Effects on Segment History
  - 6.4.2 Vane Tip Effects on Flow Ripple
- 6.5 Fluid Viscosity Effects
  - 6.5.1 Viscosity Effects on Segment History
  - 6.5.2 Viscosity Effects on Flow Ripple
- 6.6 Fluid Bulk Modulus Effects
  - 6.6.1 Modulus Effects on Segment History
  - 6.6.2 Modulus Effects on Flow Ripple
- 6.7 End-Plate Clearance Effects
  - 6.7.1 End-Plate Effects on Segment History
  - 6.7.2 End-Plate Effects on Flow Ripple
- 6.8 General Conclusions

## 6.1 Introduction

In this chapter the effects of some basic operating parameters are investigated for the standard pump, using the pump model computer program. This study concentrates on the effects of line pressure, shaft speed, vane tip clearance, end-plate clearance and fluid constants. In these simulations, parameters are investigated in the range normally encountered in practice. In a radial vane pump, end-plate clearances are typically very small and can, therefore, be neglected. Except for the simulations relating to the study of end-plate clearance effects, all other simulations were made at zero end-plate clearances. The segment pressure history and the flow ripples are good indicators of the total potential for noise generation of the pump. The segment pressure history indicates the character of the case excitation, and flow ripple variations that of the fluid borne noise.

Fluid constants are primarily a function of fluid pressure and temperature. Variations in either of these parameters affects the fluid viscosity, density and bulk modulus. In addition, the presence of entrained air may significantly reduce the bulk modulus. The effects of fluid density are not investigated. Under conditions of constant operating temperature and pressures, within 3000 bars, fluid density does not change significantly.

The fluid constants used in these simulations are for Tellus 37 at the operating temperature of 45 degrees Centigrade. In these simulations, the fluid constants are varied independantly so as to enable a study of the individual effects. It will, however, be demonstrated that within the limits of the operating conditions, the fluid constants produce only a secondary effect, when compared with those due to operating conditions and pump geometry.



: Mean Inlet Pressure : Shaft Speed :  
 6.3 bar                      2400 rpm

Fig.6.2.1 MEAN LINE PRESSURE EFFECTS ON  
 SEGMENT HISTORY

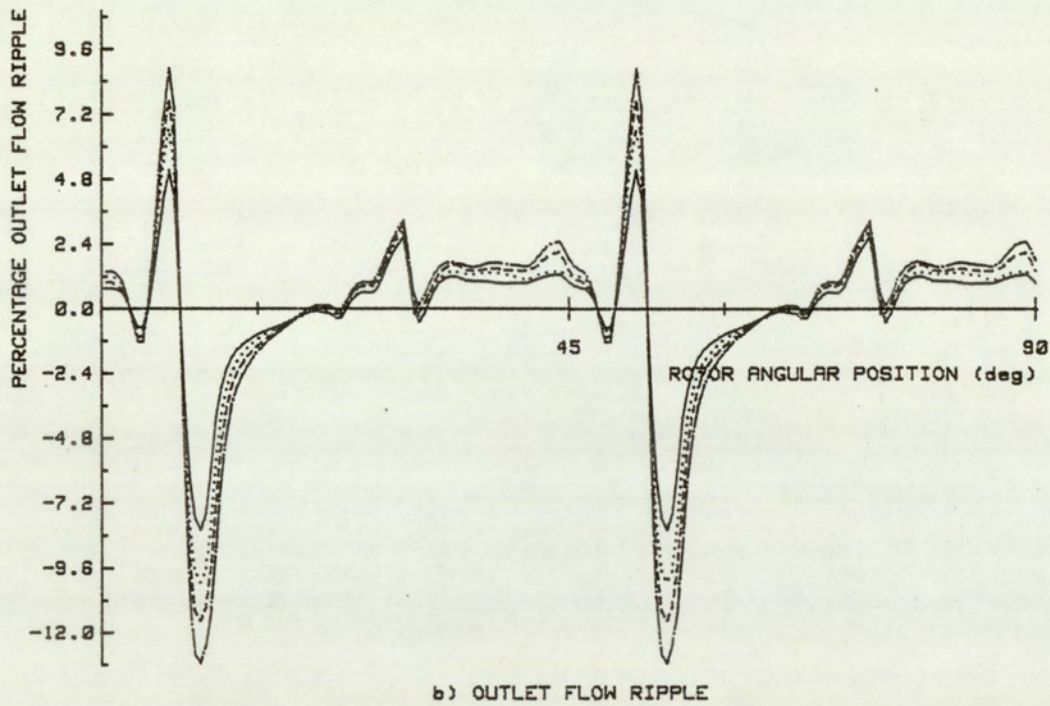
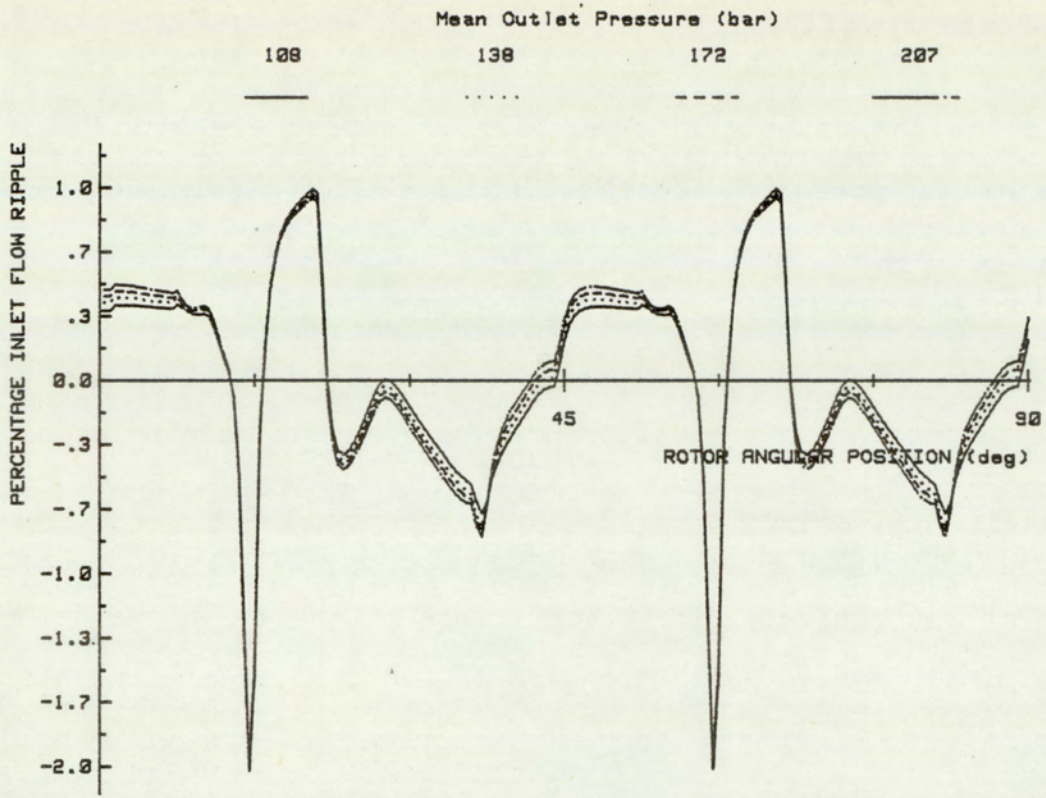
## 6.2 Line Pressure Effects

In this section the effects of mean line pressures are studied in relation to segment pressure history and the port flow ripple. For this study four simulations were made, at mean outlet line pressures of 103, 138, 172 and 207 bars. In a study of the effects of mean line pressures, it is sufficient to vary only one line pressure. The process is primarily dependant on the differences between the mean inlet and outlet levels, at normal operating conditions. The fluid constants for density, viscosity and bulk modulus were  $861 \text{ Kg/m}^3$ ,  $0.025 \text{ Ns/m}^2$  and  $1766 \text{ MN/m}^2$  respectively. These conditions relate to an operating temperature of 45 degrees and a pressure of 138 bars. The mean inlet line pressure was 6.3 bars, and all other parameters were held constant.

### 6.2.1 Pressure Effects on Segment History

The figure (6.2.1) shows the effects of mean outlet line pressure on the segment pressure history. The plots are drawn on a percentage scale where the mean inlet pressure is zero and the mean outlet pressure is one hundred percent.

In the rotor angular position of 0 to 45 degrees, the event relates to that of the first sector (ref. section 3.2). For the greater part of this sector history, the segment communicates directly with the inlet port. At the rotor position of approximately 37 degrees, the trailing vane has almost completely swept pass the port. Due to the net leakage into the segment, the segment pressure begins to rise. This continues completely into the second sector and the initial stages of the third sector. At the position of 97 degrees, the segment pressure is seen to



: Mean Inlet Pressure : Shaft Speed :  
 6.3 bar                      2400 rpm

Fig.6.2.2 MEAN LINE PRESSURE EFFECTS  
 ON FLOW RIPPLE

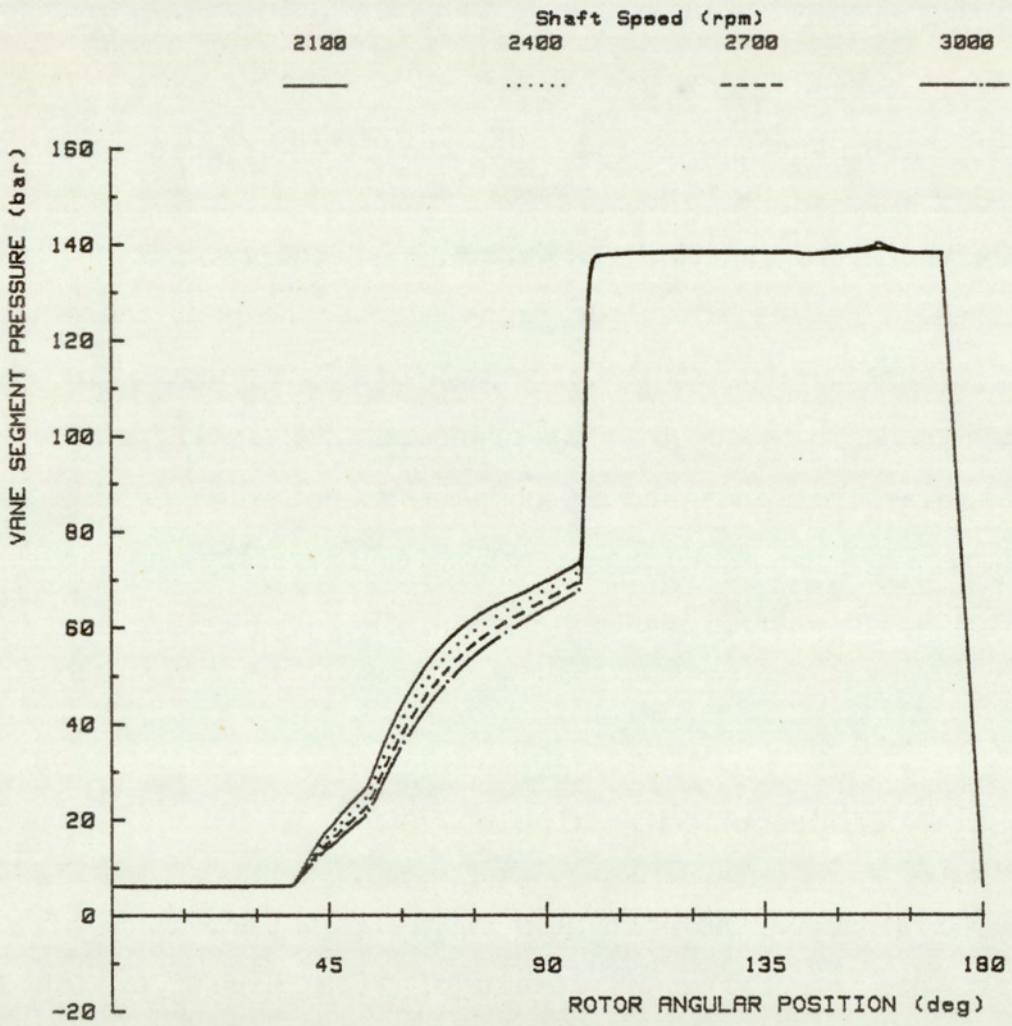
rise very sharply. The pressure differential between the port and segment volume causes a back-flow of fluid, from the outlet port to the segment volume, which is taken up by the compressibility of the fluid. Once the segment volume has attained the full port pressure, the segment pressure remains fairly constant for the rest of the third sector and the majority of the fourth sector. At the angular position 173 degrees the segment cycle effectively ends. The segment is swept pass the outlet abutment and emerges into the inlet of another cycle.

On this scale the plots generally coincide, with the exception of the history at the 157 degree rotor position. Across the port there is a pressure difference due to orifice effects. This is a function of flow rate. At high outlet pressures, this pressure is a small percentage of the total pressure range and in comparison not significant. The effect of increasing the mean line pressure is, therefore, to increase linearly the scale of the pressure history.

### **6.2.2 Pressure Effects on Flow Ripple**

The figure (6.2.2) shows the port flow ripple as a percentage of the mean flow at the four different levels of line pressures. Due to the symmetry of the vane segments, the flow patterns repeat at angular intervals corresponding to a vane pitch. For an eight vane machine the vane pitch is 45 degrees.

At the inlet port the flow variations are dominated by the modelled leakage variations, and at the outlet by the compressibility effects. Inlet variations were small in comparison with the mean flow levels. With the outlet at 103 bars, the inlet peak to peak ripple was 2.95 percent. This rose marginally in equal steps to 2.97 percent at the



: Mean Inlet Pressure : Mean Outlet Pressure :  
 6.3 bar                      . 138 bar

Fig.6.3.1 SHAFT SPEED EFFECTS ON  
 SEGMENT HISTORY

pressure of 207 bars.

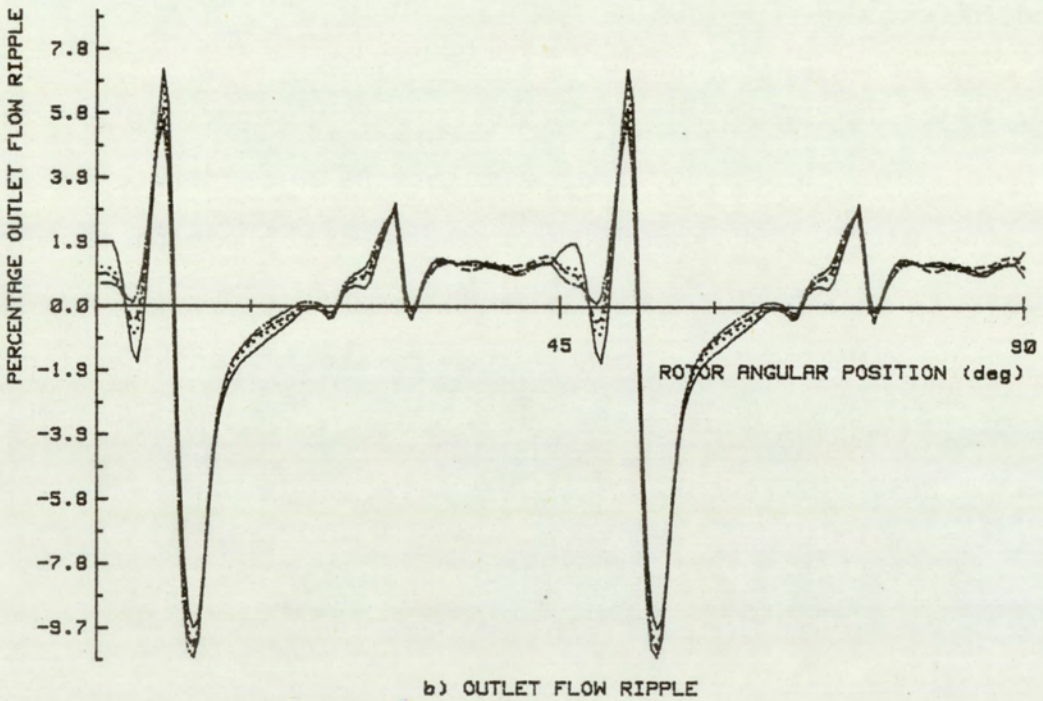
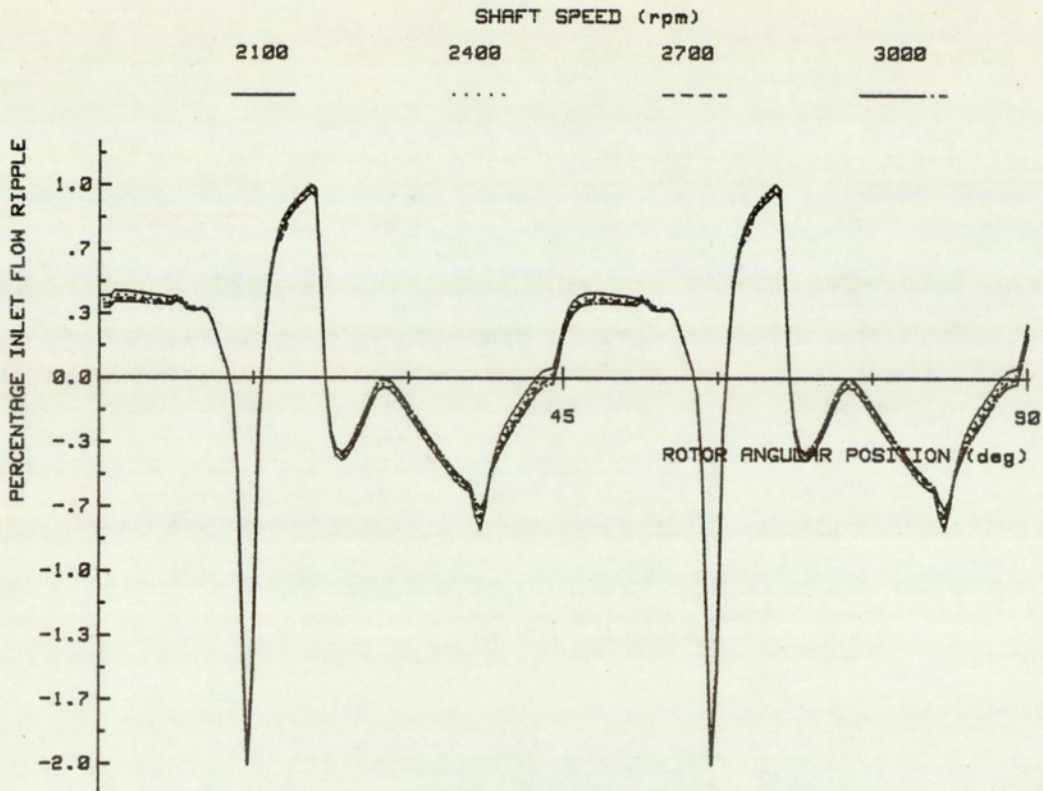
At the outlet, however, flow variations were more significant. At 103 bars, the peak to peak flow ripple was 13.4 percent, rising to 21.9 percent in equal intervals. The dominant flow variations correspond to the period of rapid segment pressure increase. The effects of an increase in line pressure is to increase the level of fluid required to raise the segment pressure to that of the outlet, at the moment of initial port communication, thus resulting in an increase in peak to peak flow ripple. An approximate doubling of pressure levels results in an increase of 0.7 percent for the inlet flow ripple and 63.4 percent for the outlet.

### 6.3 Speed Effects

This section looks at the effects of shaft speed on segment pressure and flow ripple. For this study four simulations were performed at speeds of 2100, 2400, 2700 and 3000 rpm. The fluid constants for density, viscosity and bulk modulus were  $861 \text{ Kg/m}^3$ ,  $0.025 \text{ Ns/m}^2$  and  $1766 \text{ MN/m}^2$  respectively. These conditions relate to an operating temperature of 45 degrees Centigrade and a pressure of 138 bars. The mean inlet line pressure was 6.3 bars, and all other parameters were held constant.

#### 6.3.1 Speed Effects on Segment History

The figure (6.3.1) shows the effects of shaft speed on the segment pressure history. The plots generally coincide except for the region corresponding to the rotor position of 37 to 97 degrees. In this region



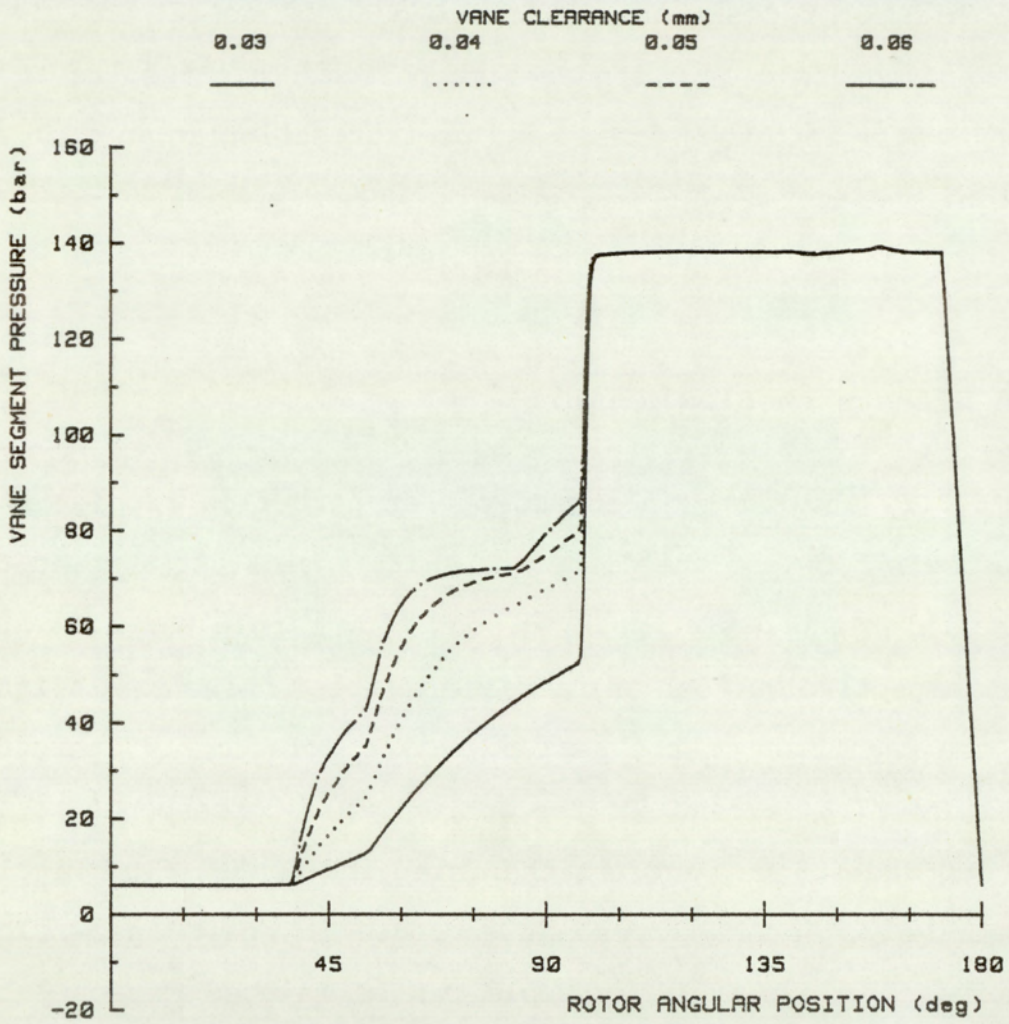
: Mean Inlet Pressure : Mean Outlet Pressure :  
 6.3 bar                      138 bar

Fig.6.3.2 SHAFT SPEED EFFECTS ON  
 FLOW RIPPLE

the segment volume does not communicate directly with either of the ports. The segment is pressurised by the net leakage into the segment, via the leakage paths across the vane tips and end-plate. At lower speeds the segment pressure levels are generally higher, at any given rotor position, than at higher speeds. The net rate of leakage into the segment, in this rotor position, is independent of speed. At lower speeds the event occurs over a longer time period. This results in a greater leakage flow into the segment and pressurisation at an earlier rotor position.

### **6.3.2 Speed Effects on Flow Ripple**

The figure (6.3.2) shows the inlet and outlet port flow ripple as a percentage of mean flow, at the different shaft speeds. At a speed of 2100 rpm, the inlet and outlet peak to peak flow ripple was 2.94 and 16.8 percent respectively. With an increase in speed there is a slight increase in the magnitude of the peak to peak ripple to 2.97 percent for the inlet and 17.6 percent for the outlet. This corresponds to an increase of 1.0 and 4.8 percent, in the inlet and outlet flow ripple levels respectively, for a 43 percent increase in shaft speed. The marginal increase in outlet flow ripple can be related directly to compressibility effects. At the moment of initial port communication, the segment pressures are lower at higher speeds. This requires a greater volume of fluid for segment pressurisation to bring the segment to full port pressure.



: Mean Inlet Pressure : Mean Outlet Pressure : Shaft Speed :  
 6.3 bar                      138 bar                      2400 rpm

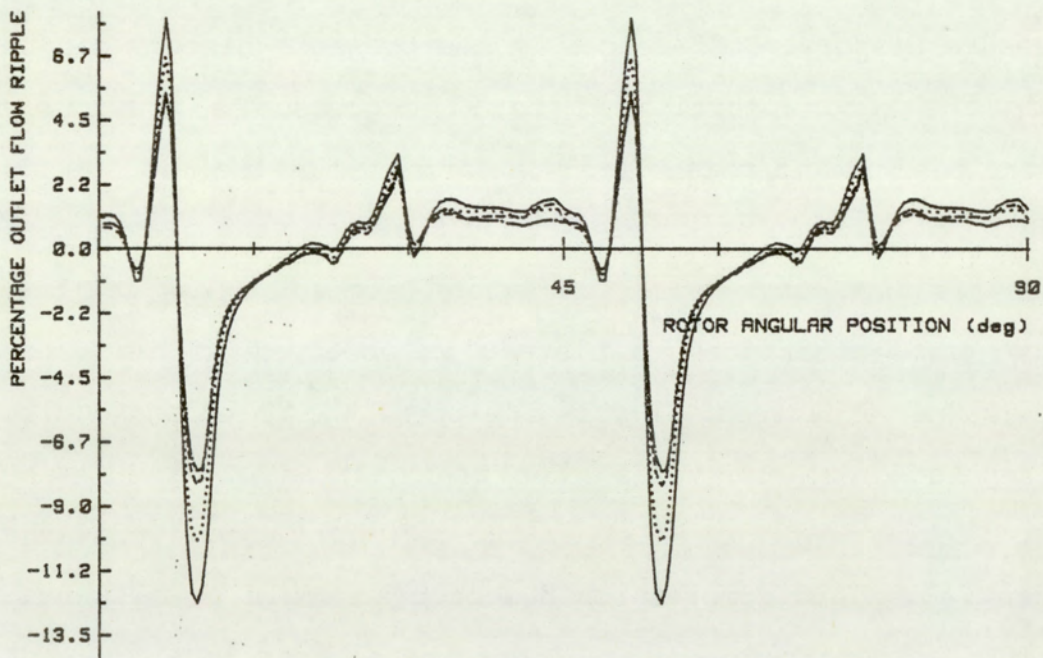
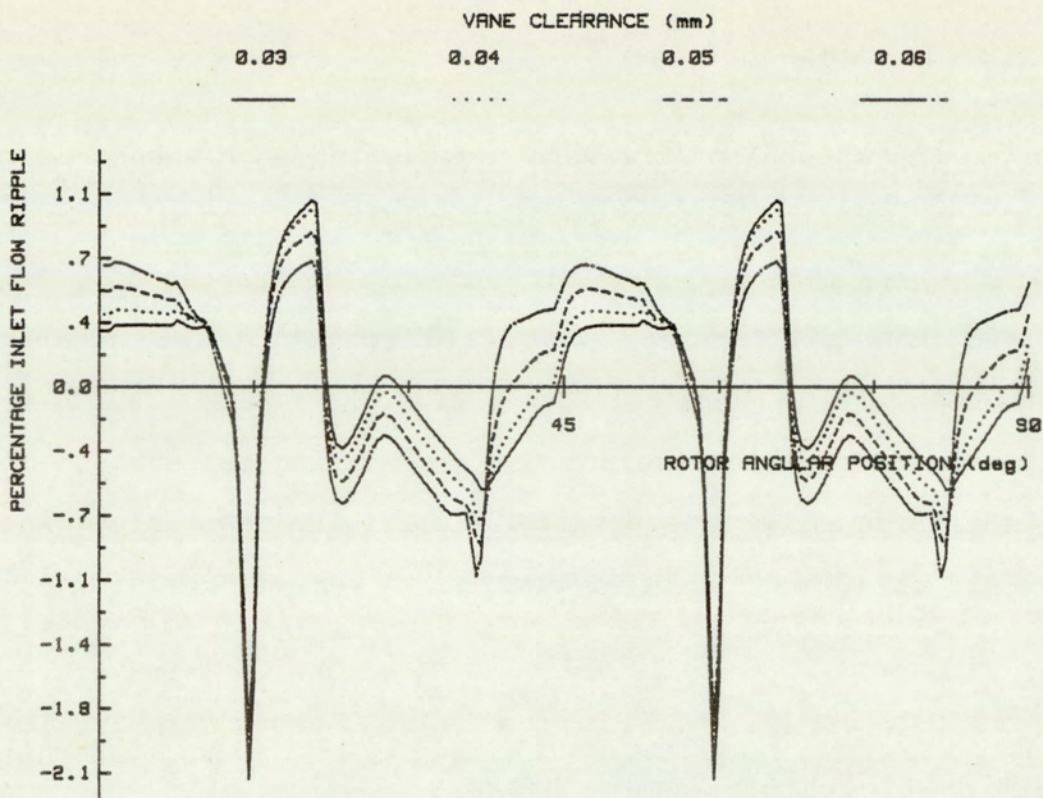
Fig.6.4.1 VANE CLEARANCE EFFECTS ON  
 SEGMENT HISTORY

## 6.4 Vane Tip Clearance Effects

In this section the effects of the vane tip clearance on the segment pressure history and flow ripple are investigated. For this study four simulations were made at increasing vane tip clearances of 0.03, 0.04, 0.05 and 0.06 millimetres. The fluid constants for density viscosity and bulk modulus were  $861 \text{ Kg/m}^3$ ,  $0.025 \text{ Ns/m}^2$  and  $1766 \text{ MN/m}^2$  respectively. These conditions relate to an operating temperature of 45 degrees Centigrade and a pressure of 138 bars. The mean inlet line pressure was 6.3 bars, and all other parameters were held constant.

### 6.4.1 Vane Tip Effects on Segment History

The figure (6.4.1) shows the effects of vane tip clearance on the segment pressure history. Differences in the pressure history can be observed for the rotor position 37 to 97 degrees. As previously described, the behavior in this region is dominated by the net leakage flow available for segment pressurisation. At higher vane clearances, segment pressurisation occurs earlier due to a larger net leakage flow. At the larger vane clearances, a plateau is observed in the rotor position of around 67 degrees. In this position, the inlet and outlet ports are separated by two vanes. For a condition of equal vane clearance and zero end-plate leakage, the maximum segment pressure attained when full fluid compression has occurred would be half that of the combined mean port pressures. Under these conditions, the net flow into the segment is zero. With small vane tip clearances, this plateau is not observed due to insufficient flow being available for full fluid compression to occur.



: Mean Inlet Pressure : Mean Outlet Pressure : : Shaft Speed :  
 6.3 bar                      138 bar                      2400 rpm

Fig.6.4.2 VANE CLEARANCE EFFECTS ON FLOW RIPPLE

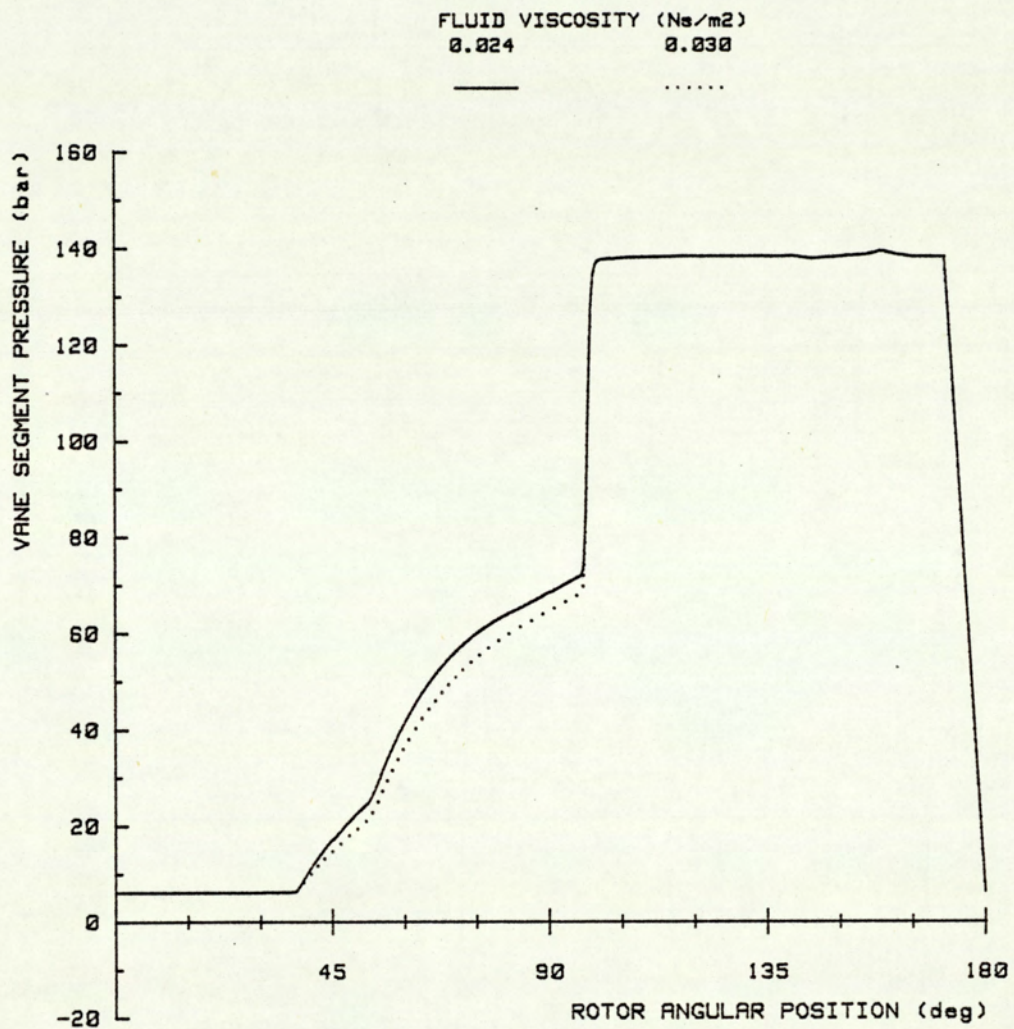
#### 6.4.2 Vane Tip Effects on Flow Ripple

In figure (6.4.2), the effects of vane tip clearance on the flow ripple are presented. At a vane clearance of 0.03 millimetres, the inlet flow ripple was 3.2 percent. This falls to 2.5 percent at the clearance of 0.06 millimetres. A similar effect is observed at the outlet. Flow ripple values were 20.4 and 13.0 percent for the vane clearance of 0.03 and 0.06 millimetres respectively.

At the outlet, the dominant factor affecting the peak to peak ripple is the level of pre-compression before the segment is exposed to the outlet port. With larger vane clearances, the segment achieves a higher level of pre-compression before direct communication is achieved. This reduces the back-flow required to take the segment up to the full line pressure, and thus reduces the outlet flow ripple. The mechanism dominating the inlet flow ripple is leakage. At larger vane clearances, the flow fluctuation is greater, but there is a decrease in the peak to peak values.

#### 6.5. Fluid Viscosity Effects

In this study the effects of fluid viscosity on the segment pressure and flow ripple are investigated. Two simulations were made at levels of 0.024 and 0.03  $\text{Ns/m}^2$ , corresponding to a fluid temperature of 45 degrees Centigrade and pressures of 69 and 207 bars respectively. The other fluid constants of bulk modulus and density were 1766  $\text{MN/m}^2$  and 861  $\text{Kg/m}^3$  respectively were kept constant. The shaft speed, mean inlet pressure and mean outlet pressure were 2400 rpm, 6.3 bars and 138 bars respectively.



: Mean Inlet Pressure : Mean Outlet Pressure : Shaft Speed :  
 6.3 bar                      138 bar                      2400 rpm

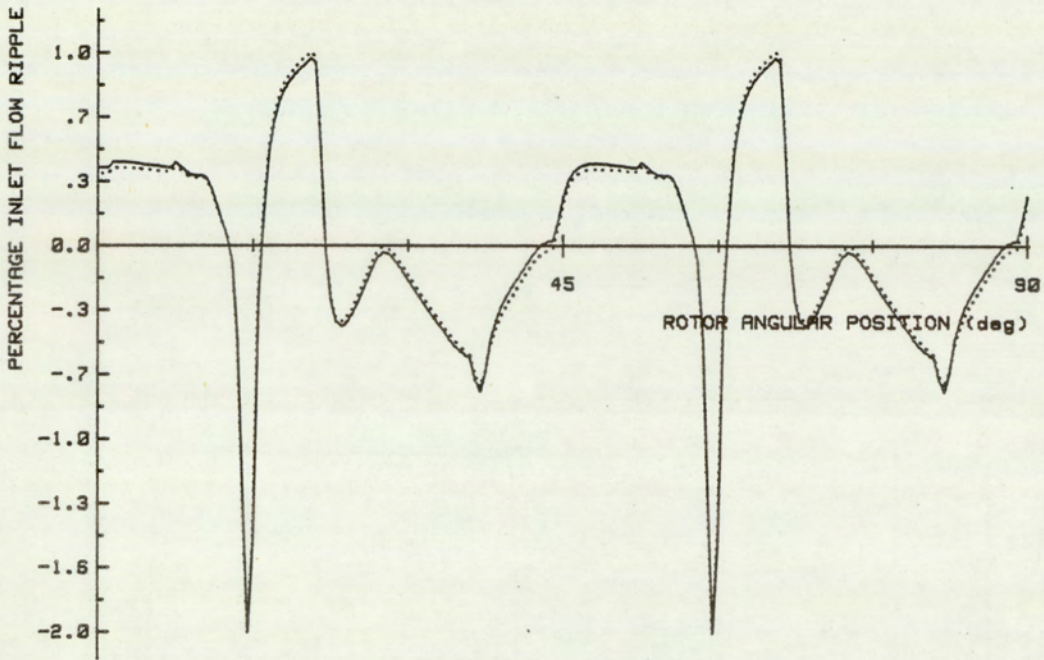
Fig.6.5.1 FLUID VISCOSITY EFFECTS ON SEGMENT HISTORY

FLUID VISCOSITY (Ns/m<sup>2</sup>)

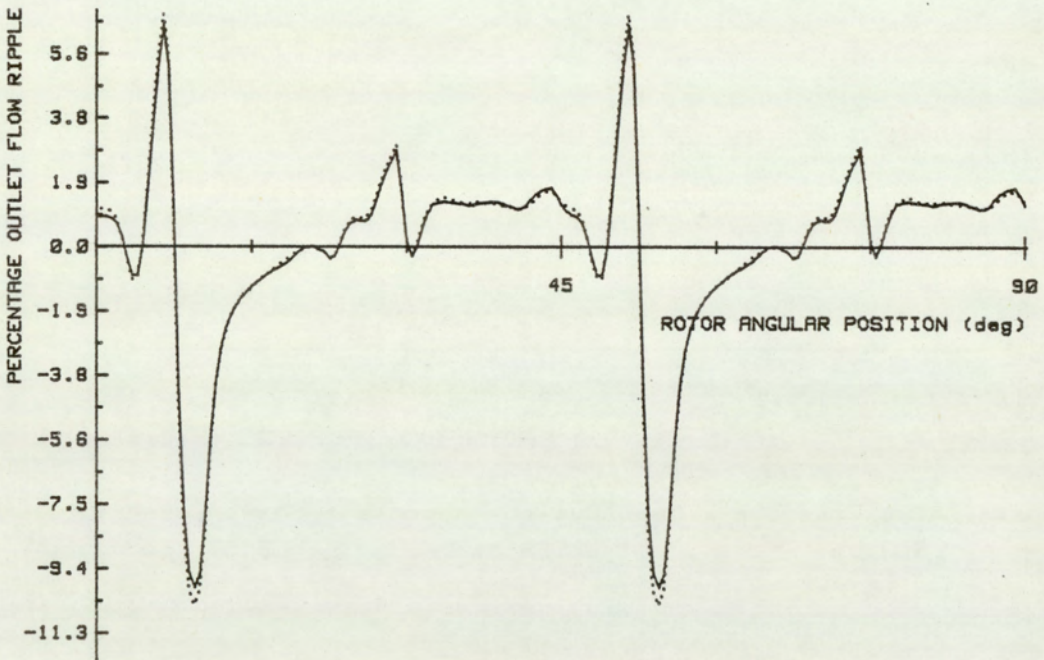
0.024

0.030

—                      ·····



a) INLET FLOW RIPPLE



b) OUTLET FLOW RIPPLE

: Mean Inlet Pressure : Mean Outlet Pressure : Shaft Speed :  
6.3 bar                      138 bar                      2400 rpm

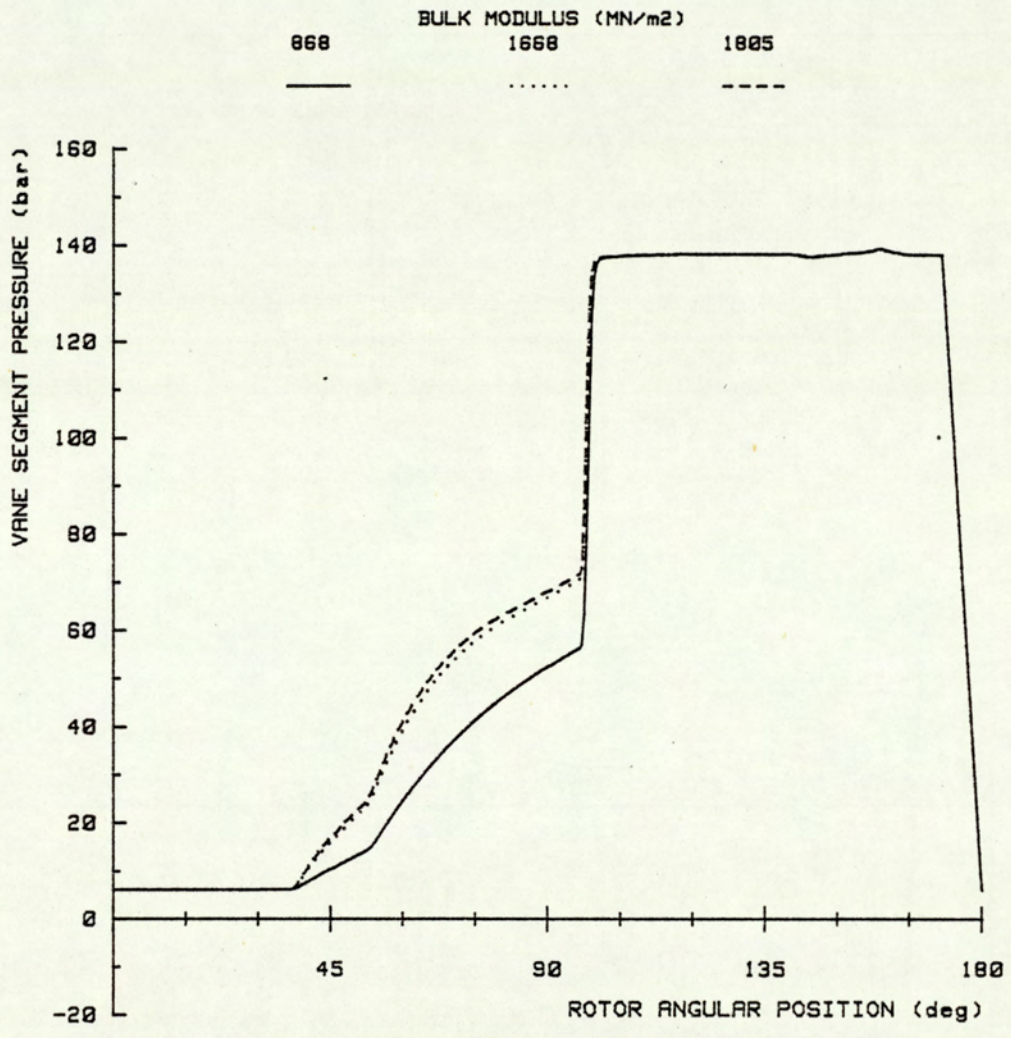
Fig.6.5.2 FLUID VISCOSITY EFFECTS ON  
FLOW RIPPLE

### 6.5.1 Viscosity Effects on Segment History

The figure (6.5.1) shows the effect of fluid viscosity on the segment history. The effect of fluid viscosity changes is similar to that observed due to changes in vane tip clearances. A slight delay in the segment pressurisation is observed at higher viscosity level. A higher viscosity condition corresponds to that of a smaller vane clearance. The greatest effect is seen at the rotor position 37 to 97 degrees. Description of the mechanism affecting segment pressurisation in this region for vane tip effects described in the previous section is appropriate to the effects observed here.

### 6.5.2 Viscosity Effects on Flow Ripple

The figure (6.5.2) shows the effects of fluid viscosity on flow ripple. As with segment pressure, the effects on flow ripple are similar to that due to vane clearance. The increase in fluid viscosity results in a marginal increase in the level of inlet and outlet flow ripple. Again, a description of the mechanism of the effects observed due to vane clearance are appropriate to that of viscosity. As with the effects on segment pressures, viscosity effects in this range are secondary in comparison to those due to changes in operating conditions and vane clearances.



: Mean Inlet Pressure : Mean Outlet Pressure : Shaft Speed :  
 6.3 bar                      138 bar                      2400 rpm

Fig.6.6.1 FLUID BULK MODULUS EFFECTS ON SEGMENT HISTORY

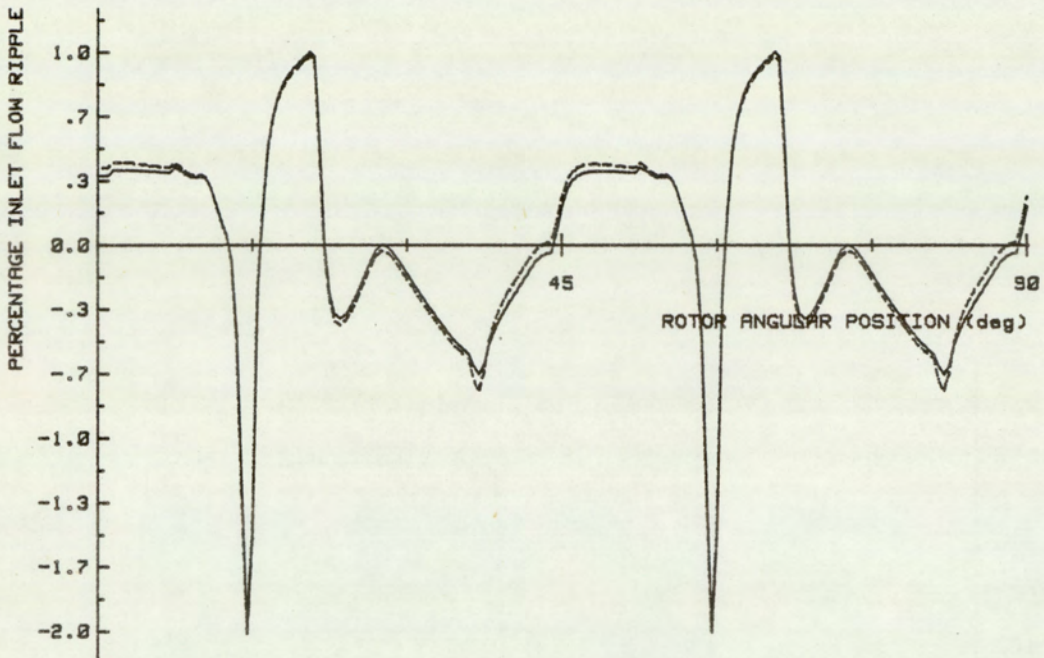
FLUID BULK MODULUS (MN/m<sup>2</sup>)

868

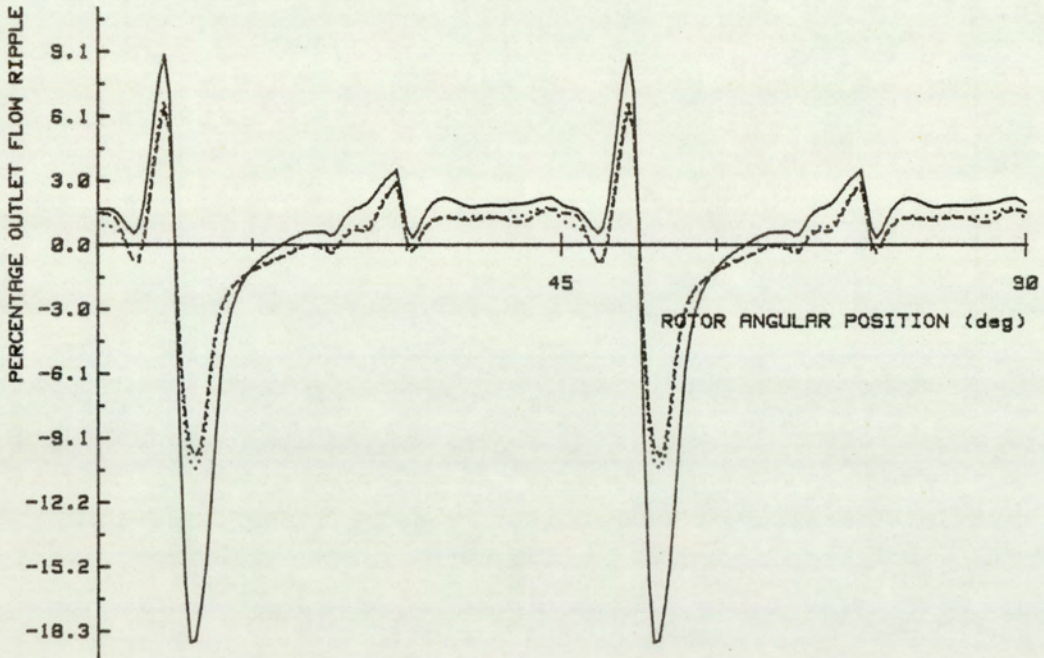
1668

1805

— ····· - - - -



a) INLET FLOW RIPPLE



b) OUTLET FLOW RIPPLE

: Mean Inlet Pressure : Mean Outlet Pressure : Shaft Speed :  
 6.3 bar                      138 bar                      2400 rpm

Fig.6.6.2 FLUID BULK MODULUS EFFECTS ON FLOW RIPPLE

## 6.6. Fluid Bulk Modulus Effects

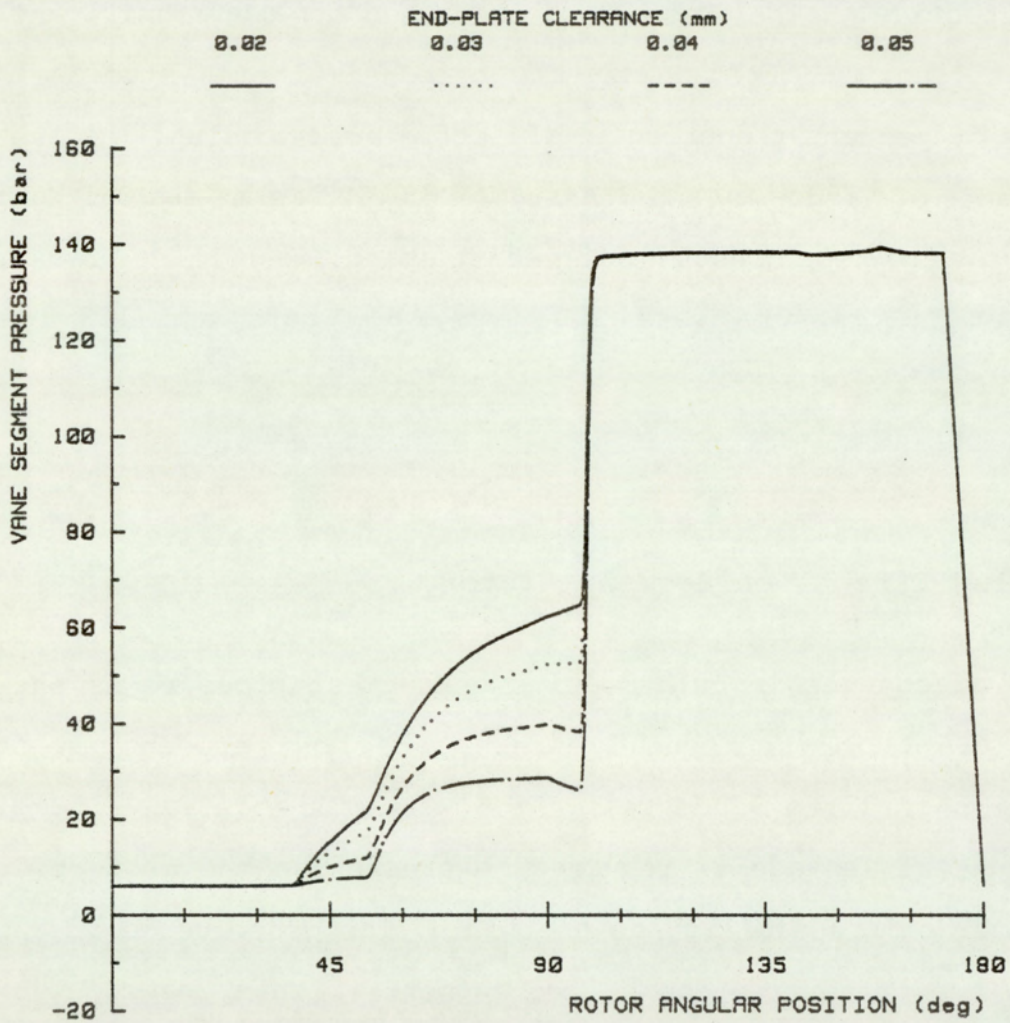
The effects of fluid bulk modulus are shown by three simulations at 1688 and 1805 and 868 MN/m<sup>2</sup>. The first two relate to a fluid temperature of 45 degrees Centigrade and pressures of 69 bars and 207 bars respectively. The presence of entrained air can significantly reduce the effective bulk modulus. The third simulation studies the effects of a 50 percent reduction in effective bulk modulus. The other fluid constants of viscosity and density were 0.025 Ns/m<sup>2</sup> and 861 Kg/m<sup>2</sup> respectively, were kept constant. The shaft speed, mean inlet pressure and mean outlet pressure were 2400 rpm, 6.3 bars and 138 bars respectively.

### 6.6.1 Modulus Effects on Segment History

The effects of changes in bulk modulus on segment pressure is shown in figure (6.6.1). Bulk modulus effects are most evident in the rotor position of 37 to 97 degrees. At lower bulk modulus values, a greater amount of leakage is required to pressurise the segment due to the greater compressibility of the fluid. The consequence of this is to delay the pressurisation of the segment. Within the simulated ideal conditions, the effects are hardly noticeable. At the 50 percent level, however, the segment pressurisation is significantly retarded.

### 6.6.2 Modulus Effects on Flow Ripple

The figure (6.6.2) shows the effects of bulk modulus on flow ripple. From the previous simulations, the main factor affecting the inlet flow ripple levels was leakage. Due to this, little change is visible in



: Mean Inlet Pressure : Mean Outlet Pressure : Shaft Speed :  
 6.3 bar                      138 bar                      2400 rpm

Fig.6.7.1 END-PLATE CLEARANCE EFFECTS ON SEGMENT HISTORY

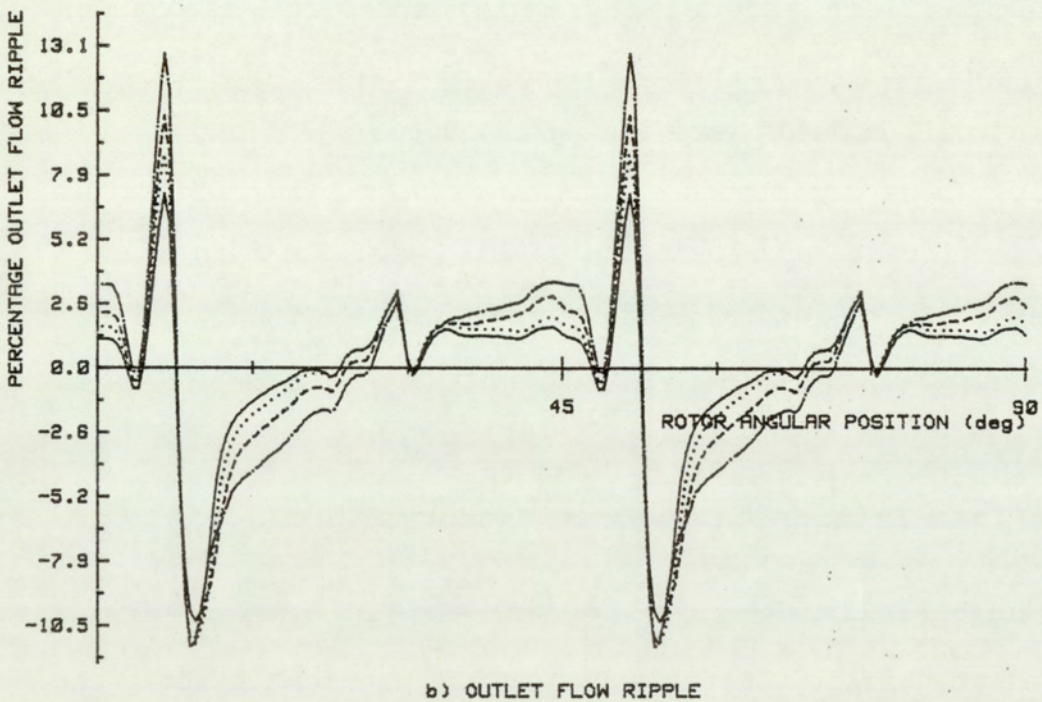
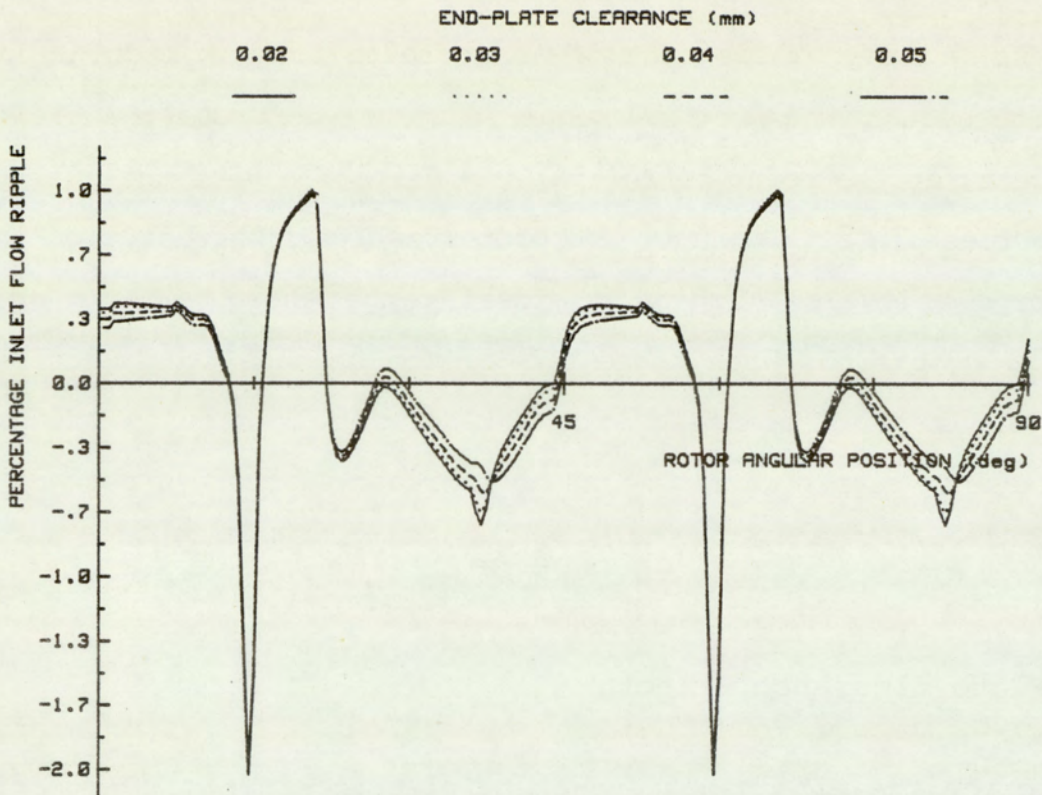
the inlet flow ripple. The effect of an increase in bulk modulus is to reduce the amount of back-flow required to pre-compress the fluid in the segment, at the point of initial communication with the outlet port. An increase in bulk modulus therefore results in a reduction in the flow ripple levels. Within the ideal range these effects are secondary in comparison with those due to the changes in operating conditions and vane clearances. At the reduced bulk modulus value, however, the flow ripple levels shows an increase of over 76 percent.

## **6.7 End-Plate Clearance Effects**

In this section the effects of end-plate clearances on the segment pressure history and flow ripple are investigated. For this study four simulations were made at increasing end-plate clearances of 0.02, 0.03, 0.04 and 0.05 millimetres. The fluid constants for density, viscosity and bulk modulus were 861 Kg/m<sup>3</sup>, 0.025 Ns/m<sup>2</sup> and 1766 MN/m<sup>2</sup> respectively. These conditions relate to an operating temperature of 45 degrees Centigrade and a pressure of 138 bars. The mean inlet line pressure was 6.3 bars, and all other parameters were held constant.

### **6.7.1 End-Plate Effects on Segment History**

The figure (6.7.1) shows the effects of end-plate clearances on the segment pressure history. Differences in the pressure history can be observed for the rotor position 37 to 97 degrees. The presence of end-plate leakage reduces the net leakage into the segment available for segment pressurisation. With high end-plate clearances, it is possible for the net leakage to approach zero. This is especially so



: Mean Inlet Pressure : Mean Outlet Pressure : : Shaft Speed :  
 6.3 bar                      138 bar                      2400 rpm

Fig.6.7.2 END-PLATE CLEARANCE EFFECTS ON FLOW RIPPLE

when the vane tip clearance is small. The effect of end-plate clearance is therefore to delay the pressurisation of the segment volume and thus increase the level of pressure mis-match at the point of initial port communication.

### **6.7.2 End-Plate Effects on Flow Ripple**

In figure (6.7.2), the effects of end-plate clearances on the flow ripple are presented. At a vane clearance of 0.03 millimetres, the inlet flow ripple was 2.95 percent. This rises marginally to 2.98 percent at a 0.06 millimetre clearance. A similar effect is observed at the outlet. Flow ripple values were 17.4 and 23.8 percent for the clearance of 0.03 and 0.06 millimetre respectively. The general effect of an increase in end-plate clearance is to increase the inlet and outlet flow ripple. In comparison, the effects on the inlet ripple is negligible.

As explained in the previous studies, the increase in the level of mis-match between segment and port pressures leads to an increase in outlet flow ripple.

### **6.8 General Conclusions**

The purpose of the first three and the sixth simulations involving speed, pressure, vane clearances and end-plate clearance was to study qualitatively the effects of those parameters on the pump output. The two additional simulations, looking at the effects of fluid viscosity and bulk modulus were to demonstrate the secondary effects of these parameters, within the conditions of interest.

The behavior under the effects of speed and pressure are widely known for hydraulic pumps in general. The correlation with the computer model serves as an initial confirmation of the validity of the model.

In normal applications, it is an accepted practice to increase line pressures in preference to increasing the shaft speed, when a greater power output is required. This has been shown to be more beneficial in terms of a lower noise potential, Wusthof et al.(58). This effect has been quantified in the earlier simulations. Power output from a hydraulic pump is a product of line pressure and flow. It has been shown that for a doubling of line pressures, there was an increase in outlet flow ripple of 63.4 percent. The doubling of shaft speed, corresponding to a doubling of flow rate and, at least, a doubling of flow ripple magnitudes. There is therefore an advantage in increasing pressure over speed as a means of increasing power output, in the interest of a lower noise potential.

## CHAPTER 7 : RELIEF GROOVES

- 7.1 Introduction
- 7.2 Groove Profiles
- 7.3 Groove Profile Effects
  - 7.3.1 Profile Effects on Segment History
  - 7.3.2 Profile Effects on Flow Ripple
- 7.4 Groove Length Effects
  - 7.4.1 Length Effects on Segment History
  - 7.4.2 Length Effects on Flow Ripple
- 7.5 Inlet Groove Effects
  - 7.5.1 Inlet Effects on Segment History
  - 7.5.2 Inlet Effects on Flow Ripple
- 7.6 Speed Effects
  - 7.6.1 Speed Effects on Segment History
  - 7.6.2 Speed Effects on Flow Ripple
- 7.7 Line Pressure Effects
  - 7.7.1 Pressure Effects on Segment History
  - 7.7.2 Pressure Effects on Flow Ripple
- 7.8 End-Plate Effects
  - 7.8.1 End-Plate Effects on Segment History
  - 7.8.2 End-Plate Effects on Flow Ripple
- 7.9 Optimum Groove Criteria

## 7.1 Introduction

Relief grooves are resistive flow paths which communicate between the segment volume and the inlet or outlet port area. It has been shown by Taylor (59) and Kelsey et al.(60) that by the application of correctly designed relief grooves, significant reduction in output flow ripple can accrue. Relief grooves permit the segment pressure history to be profiled, enabling the removal of any sudden increases in segment pressures due to pre-compression mis-match between segment and port pressures. The effect of this is to reduce the fluid flow ripple which is a major source of fluid borne noise (FBN).

In this chapter, three different groove profiles are investigated in relation to their effect on the segment pressure history and the flow ripple. The effects of speed, line pressures and end-plate leakage on optimum groove performance are investigated.

## 7.2 Groove Profiles

In practice there are three commonly used groove types. These are all sloping, and hemispherical, triangular or square in cross-section. These are assumed to possess a linear relationship for groove depth to groove length. This is readily achieved in manufacture. Details of the groove parameter definitions and their geometrical relationships are provided in appendix (A.2).

The figure (7.2.1) shows the cross-sectional area available for flow and figure (7.2.2) the change in cross-sectional area, for the three groove profiles plotted as a function of groove position. The graphs were generated for a condition of unit groove width at the position

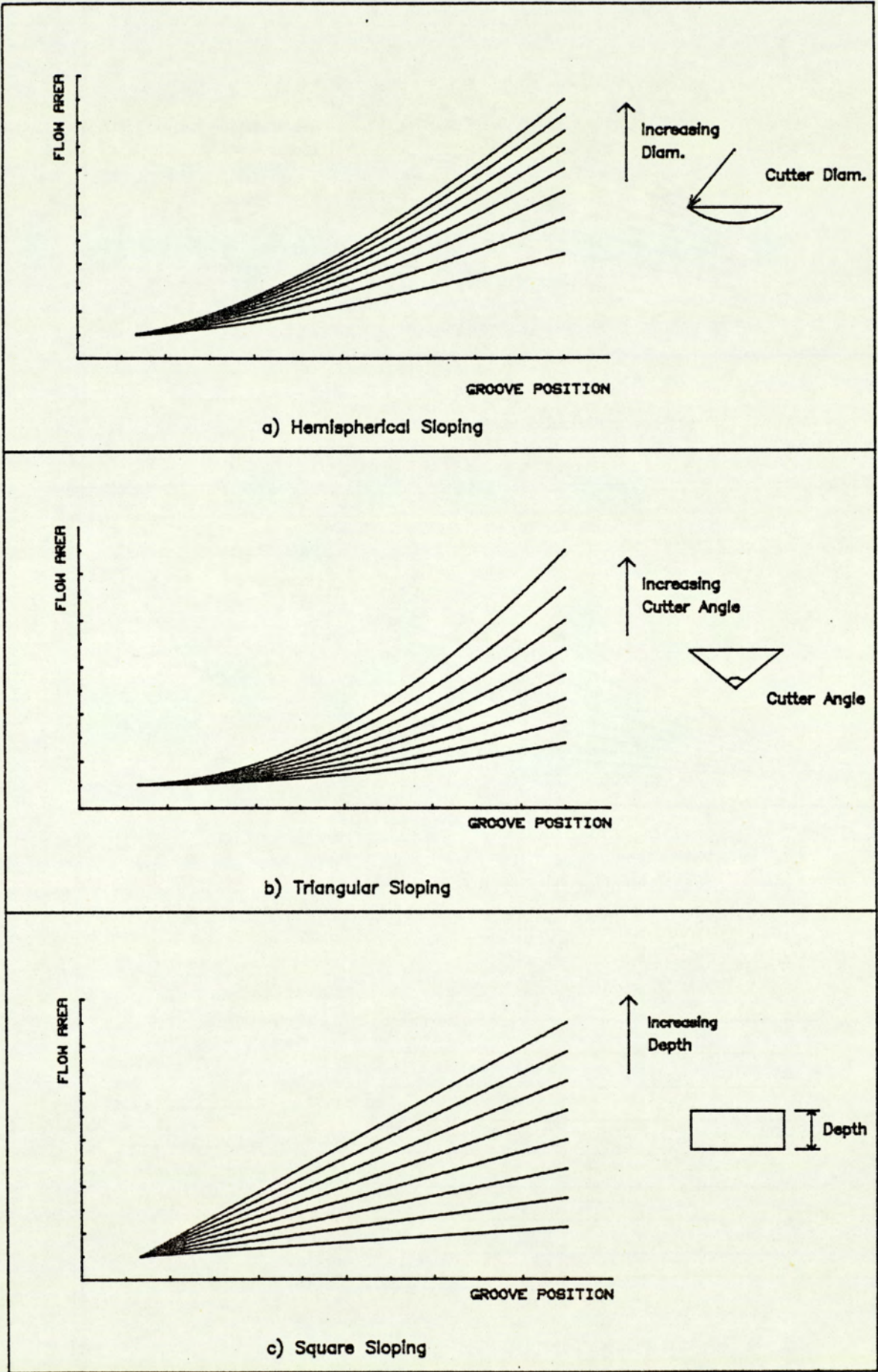


FIG.7.2.1 GROOVE FLOW AREA VS GROOVE POSITION

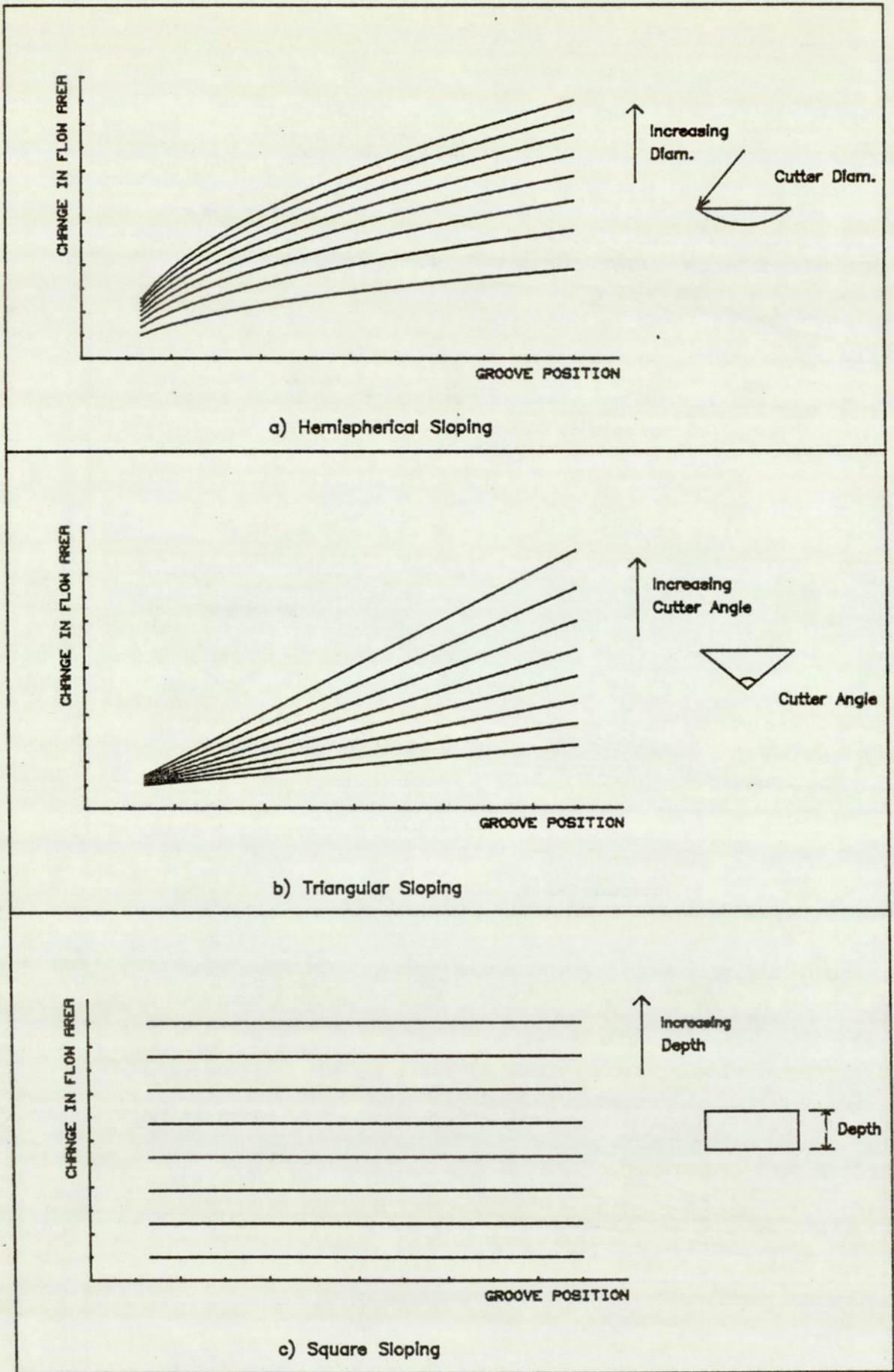


FIG.7.2.2 CHANGE IN GROOVE FLOW AREA VS GROOVE POSITION

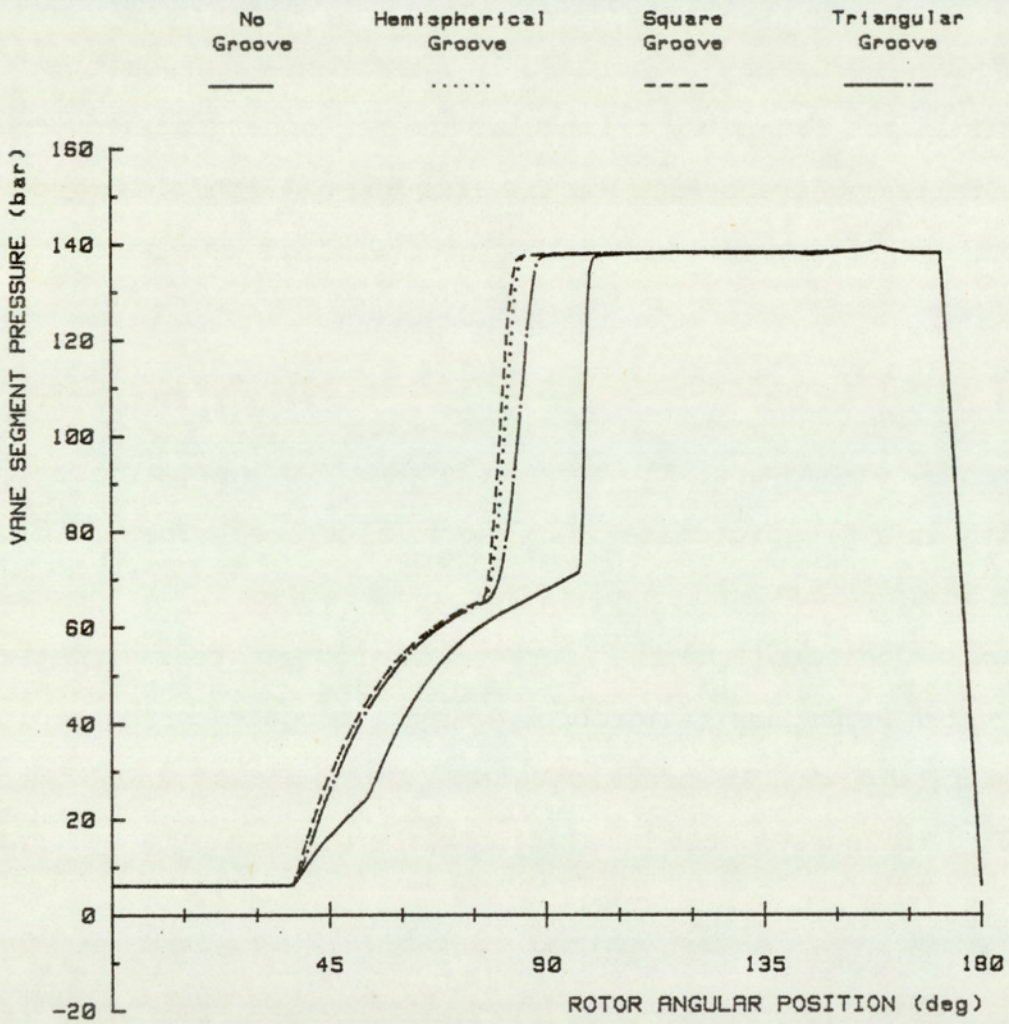
of maximum flow area. These reveal a fundamental difference in the groove profile characteristics which must be considered when specifying a profile type.

The primary differences in the three profiles lies in the way the flow area changes with groove position. In the case of the square sectioned groove, the rate of increase in flow area with position is constant. This is not so for the triangular and hemispherical sectioned grooves. The initial increase in flow area for the hemispherical groove is greater than that for the triangular groove. This can be seen in figure (7.2.2).

Further differences occur in the way increases in flow area relate to their fundamental parameters. An increase in depth of a square section groove results in a proportionate increase in flow area. The increase in flow area with groove cutter angle for a given depth, in the case of the triangular section, and the increase in groove cutter diameter, in the case of the hemispherical groove, does not produce corresponding increases in flow area. In practice when cutter angles are in the region of 30 to 60 degrees, the behavior for the triangular section is approximately linear in this respect.

### **7.3 Groove Profile Effects**

In this section the effects of groove profile is studied in relation to segment pressure history and the port flow ripple. The data for this study consists of data from four simulations. The first is for the original pump without any relief groove, and the others are for the same pump but incorporating an outlet groove for each of the three groove type studied. The four simulations were made at the same



: Mean Inlet Pressure : Mean Outlet Pressure : Shaft Speed :  
 6.3 bar                      138 bar                      2400 rpm

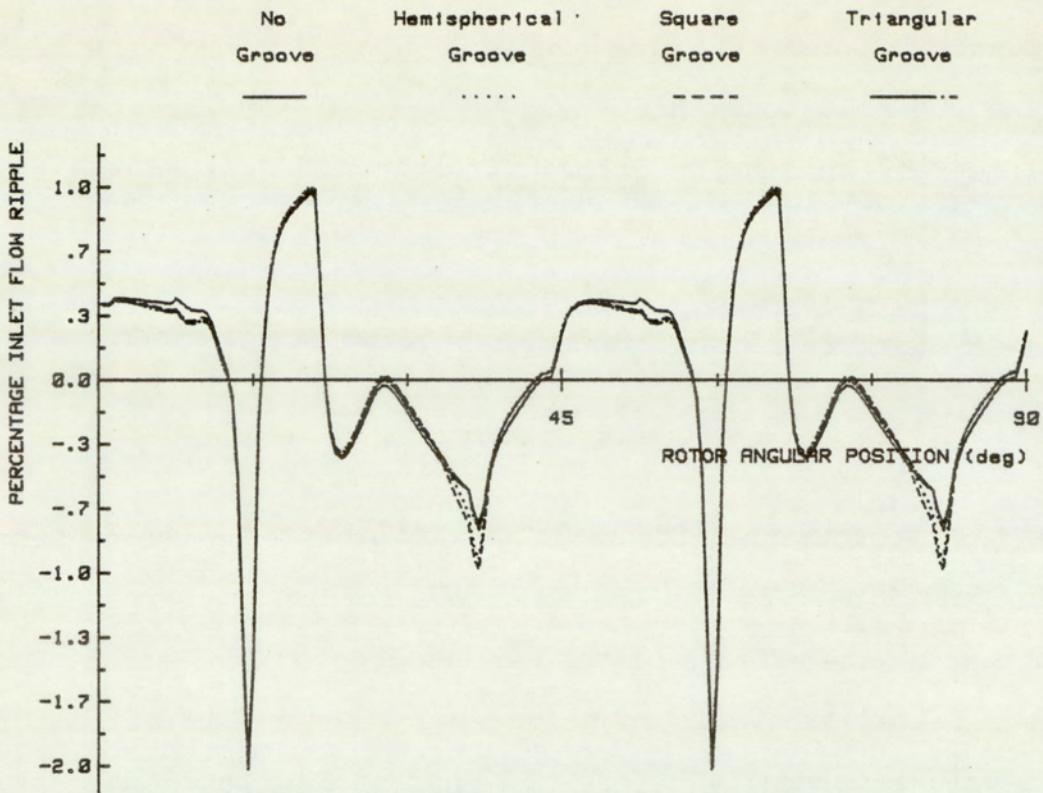
Fig.7.3.1 OUTLET GROOVE PROFILE EFFECTS ON SEGMENT HISTORY

operating conditions and all other unspecified parameters were kept constant. The outlet grooves had the same maximum flow area of 7.5 square millimetres, an angular groove length of 20 degrees and the same maximum groove width.

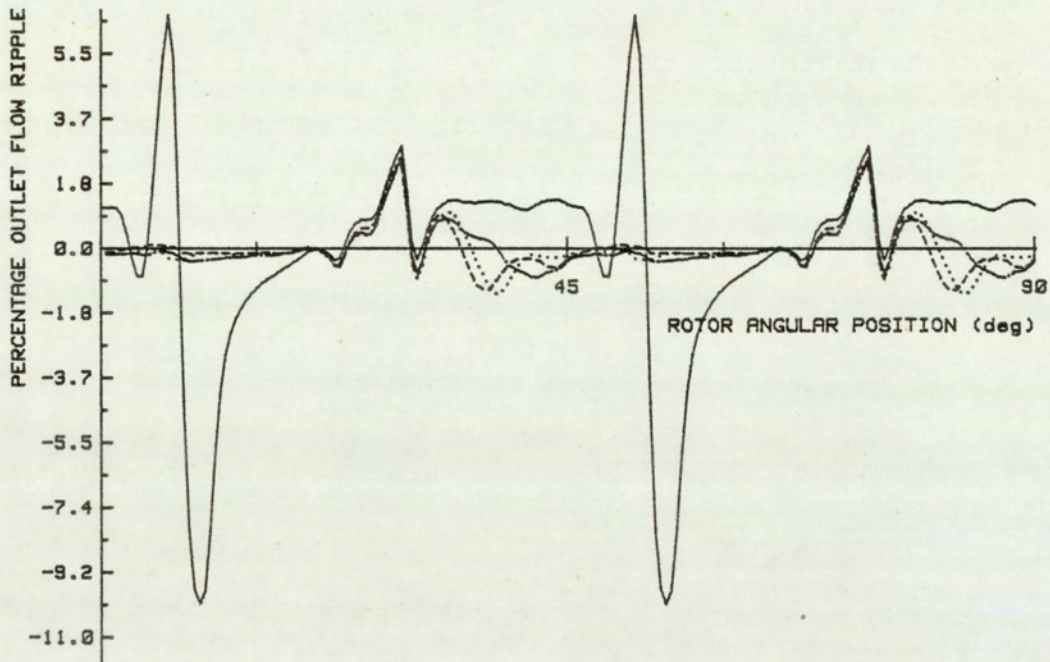
### **7.3.1 Profile Effects on Segment History**

The figure (7.3.1) shows the effects of groove profile on the segment history. The full line plot for the no groove condition, serves as a datum for comparing the effects of the various grooved conditions. The effect of the relief groove is to bring about the pressurisation of the segment volume gradually before the segment is opened directly to port. This can be seen in the less steep increase in the segment pressure history, at the angular position of around the 90 degree position. The segment pressure can also be seen to attain full outlet line pressure at an earlier stage. By profiling the segment pressure in this way the back-flow of fluid which is usually needed to pressurise the segment, as it starts to communicate with the outlet port, is substantially reduced. This is achieved by spreading the flow over a longer period.

The difference in groove profile behavior can be seen in the way the segment pressurisation has occurred. The pressure rise occurs later in the cycle with the triangular groove. This is due to the very slow initial rate of increase in flow area. The square and hemispherical grooves appear to provide the segment with full line pressures at the same time. The initial increase in segment pressure is marginally more gradual for the hemispherical groove. This effect correlates well with the rate of increase in flow area relationships of the grooves.



a) INLET FLOW RIPPLE



b) OUTLET FLOW RIPPLE

: Mean Inlet Pressure : Mean Outlet Pressure : Shaft Speed :  
 6.3 bar                      138 bar                      2400 rpm

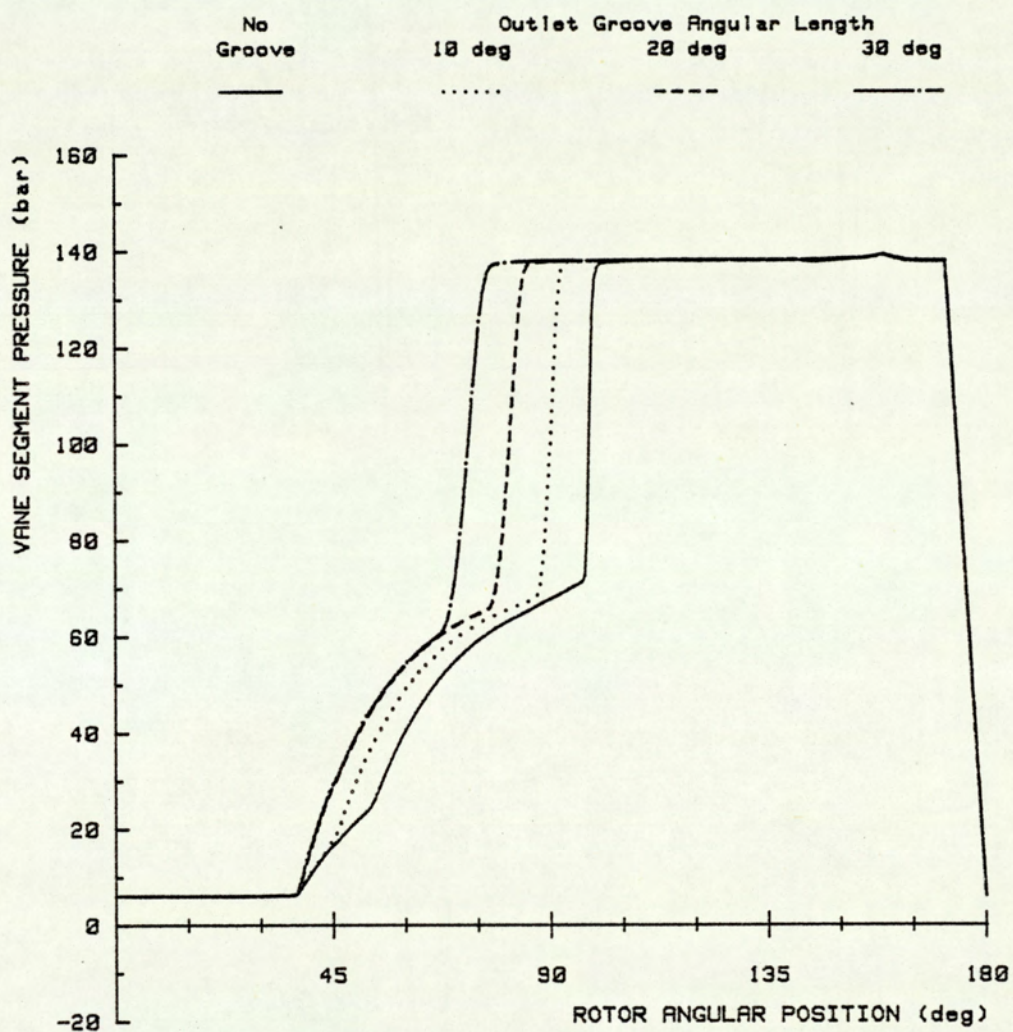
Fig.7.3.2 OUTLET GROOVE PROFILE EFFECTS ON FLOW RIPPLE

In general the hemispherical groove appears to be the more advantageous groove profile, it provides a more gradual increase in segment pressure at the start of the cycle and a quicker attainment of line pressures. This is especially beneficial when it is not possible to implement long groove lengths. Long groove lengths would unnecessarily increase the unwanted leakage and lead to a loss in mechanical efficiency. The final choice must, however, relate to the particular pump (motor) geometry.

### 7.3.2 Profile Effects on Flow Ripple

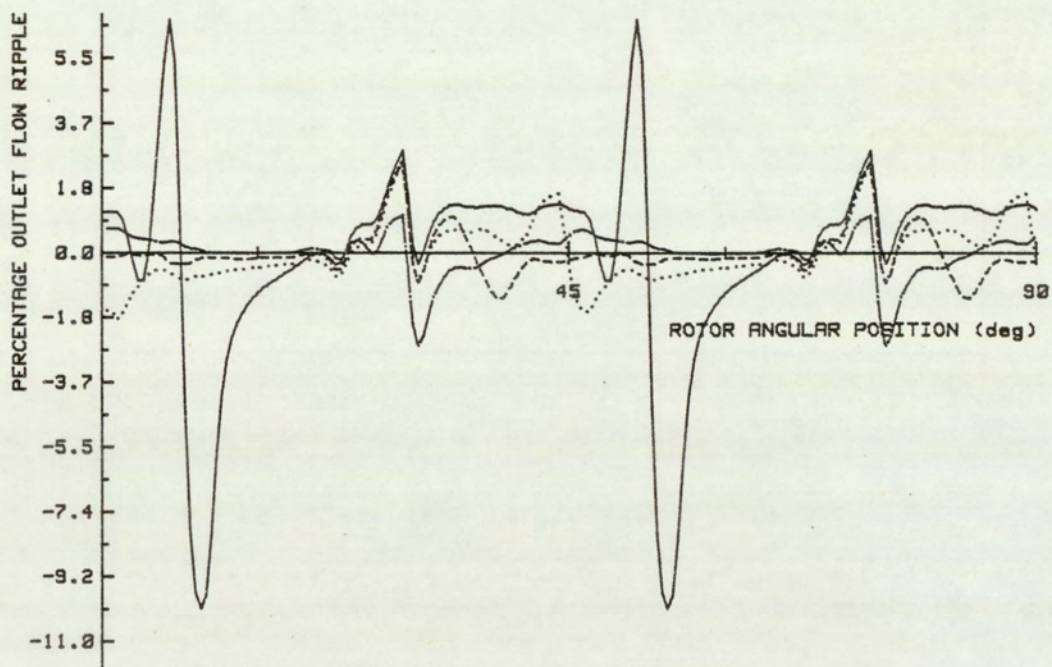
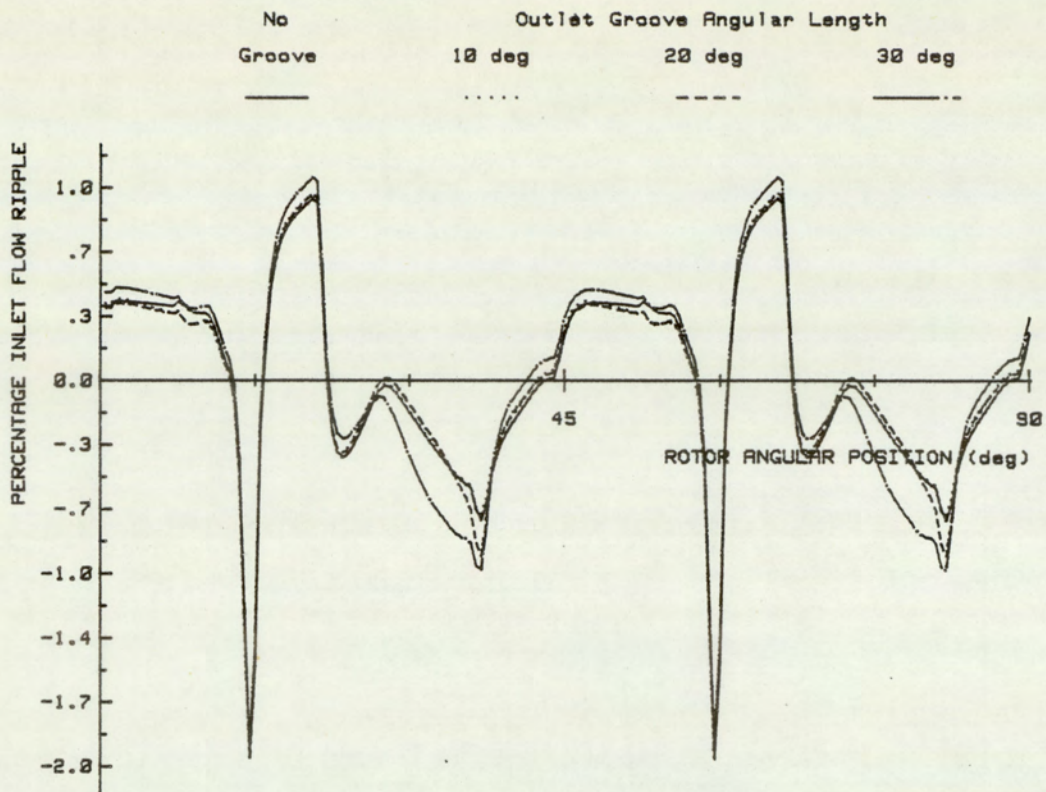
The figure (7.3.2) shows the port flow ripple as a percentage of the mean flow for the three different groove profiles simulated. A no groove simulation is provided as a datum for comparison.

There appears to be no significant differences in the magnitudes of the peak to peak ripple, for the three grooved conditions. At the inlet, the flow ripple variations were insignificant, varying from 2.98 to 2.97 percent, against the no groove level of 2.94 percent. The corresponding outlet flow ripple levels were 3.58, 3.45 and 3.03 percent, against the no groove value of 16.71 percent. This represents a typical increase of 1.25 percent, in the inlet peak to peak flow ripple levels, against a 79.9 percent reduction in the outlet flow levels. Expressed in terms of the total RMS ripple, a similar trend is observed. The levels were typically 0.20 and 0.21 percent for the inlet and outlet respectively, against the no groove values of 0.19 and 0.89 percent. The hemispherical groove shows a marginally lower RMS value at the outlet.



: Mean Inlet Pressure : Mean Outlet Pressure : Shaft Speed :  
 6.3 bar                      138 bar                      2400 rpm

Fig.7.4.1 OUTLET GROOVE LENGTH EFFECTS  
 ON SEGMENT HISTORY



: Mean Inlet Pressure : Mean Outlet Pressure : Shaft Speed :  
 6.3 bar                      138 bar                      2400 rpm

Fig.7.4.2 OUTLET GROOVE LENGTH EFFECTS ON FLOW RIPPLE

## **7.4 Groove Length Effects**

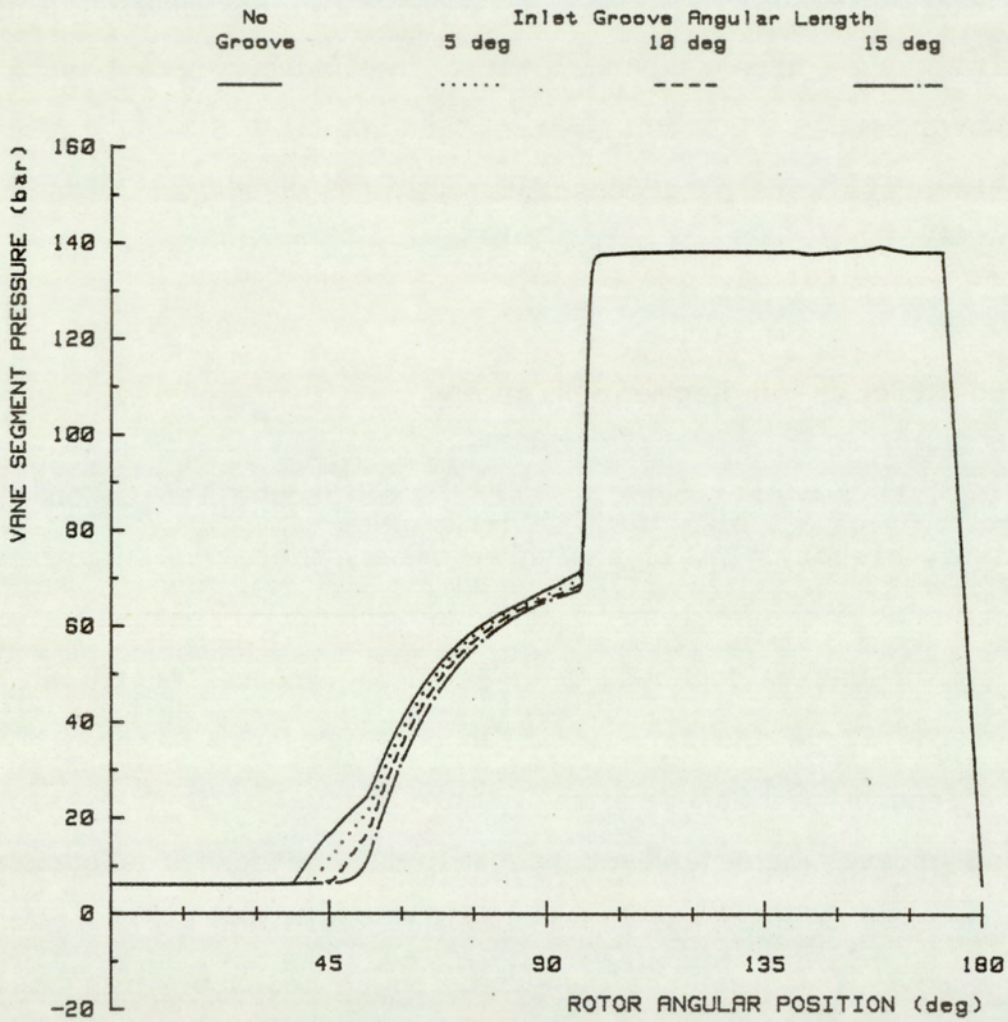
This section looks at the effects of groove length on segment pressure and flow ripple. For this study four simulations are presented. The first provides the datum no groove condition, and the other three incorporate outlet grooves of different angular lengths of 10, 20 and 30 degrees. All three grooves incorporated the hemispherical section with a cutter diameter of 6 millimetres and depth 1.5 millimetres. All other parameters were held constant.

### **7.4.1 Length Effects on Segment History**

The figure (7.4.1) demonstrates the effects of groove length on the segment pressure history. In all the three cases, there was sufficient groove flow to enable the segment to achieve full port pressure before direct port communication occurred. Changes in the groove length can be seen to alter the stage and rate at which port pressure was reached. Longer groove lengths permit a marginally more gradual segment pressure profile. Long grooves can, however, be seen to increase the general leakage levels and thus decrease the mechanical efficiency of the pump. The optimum groove length is the shortest length possible which could provide the required pre-compression of the segment to occur.

### **7.4.2 Length Effects on Flow Ripple**

The figure (7.4.2) shows the corresponding effects on flow ripple as a percentage of mean flow, for the conditions simulated. The effects at the inlet are minimal with levels of 2.96, 2.97 and 2.97 percent for the 10, 20 and 30 degree groove lengths respectively. The



: Mean Inlet Pressure : Mean Outlet Pressure : Shaft Speed :  
 6.3 bar                      138 bar                      2400 rpm

Fig.7.5.1 INLET GROOVE EFFECTS ON  
 SEGMENT HISTORY

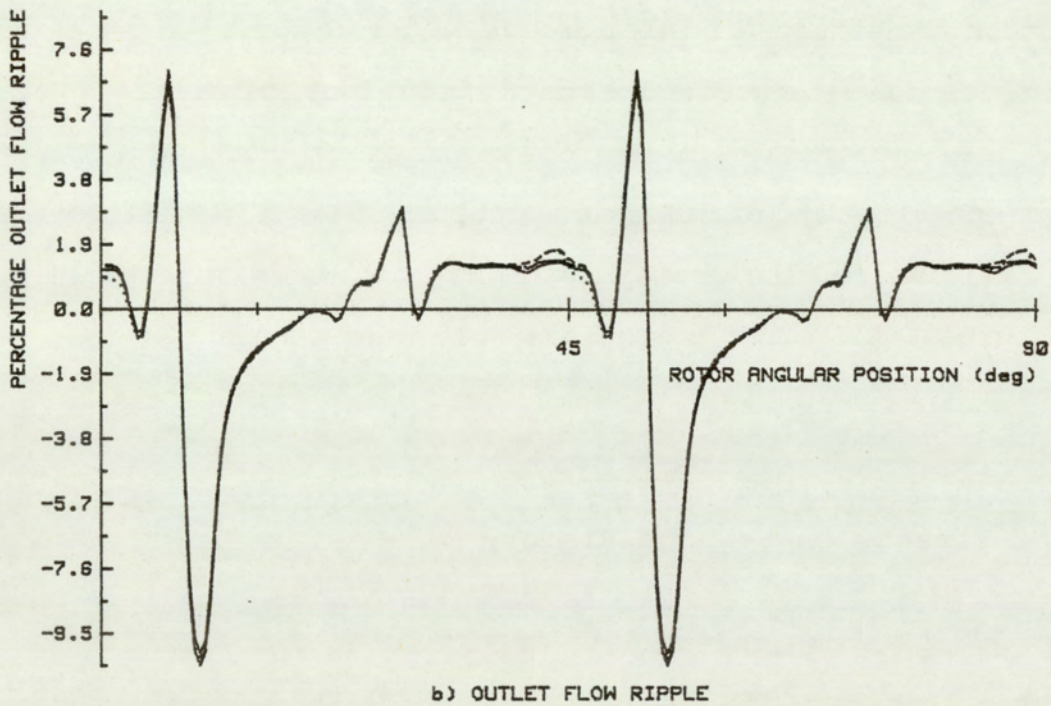
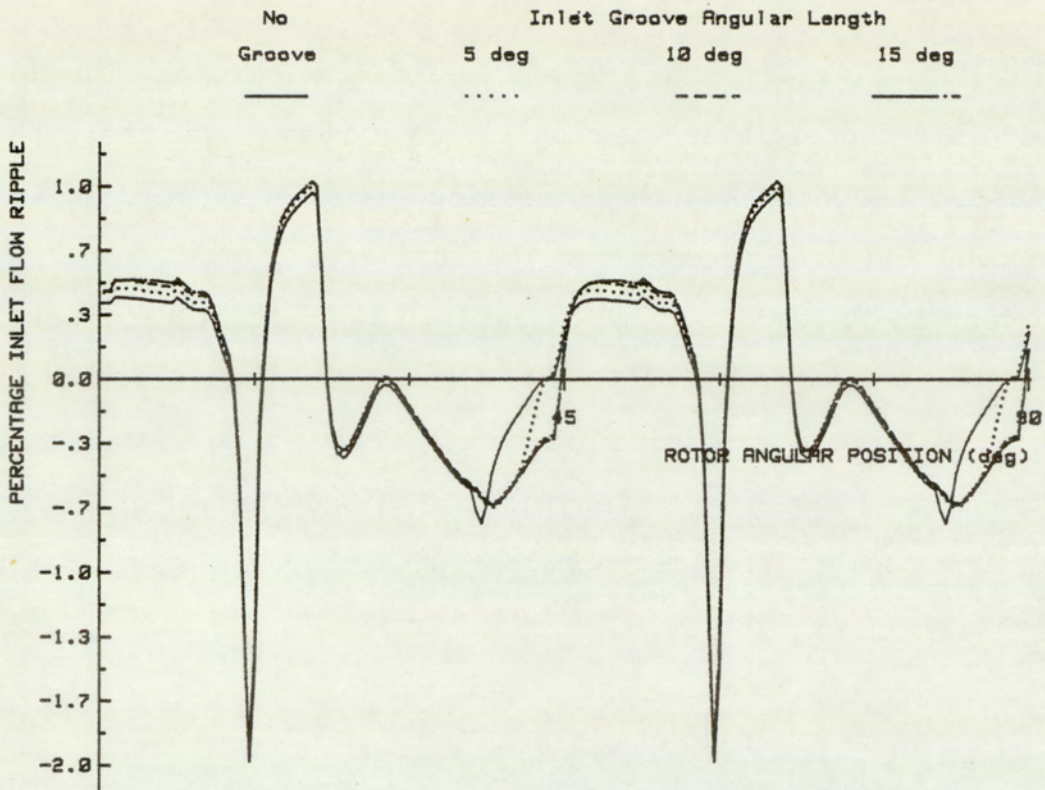
corresponding outlet values were 4.11, 3.59 and 3.64 percent. The RMS values provide additional data. The ripple levels increase at the inlet but decreases at the outlet with increasing groove length. The RMS levels were 0.20 and 0.34 percent for the 10 degree groove, and 0.25 and 0.17 percent at 30 degrees, for the inlet and outlet respectively. Provided the groove removes the effects of the abrupt pressurisation of the segment, due to pre-compression mis-match, there is no significant advantage in increasing groove length. The disadvantage of using excessively long grooves are most apparent when there is significant end-plate leakage.

## **7.5 Inlet Groove Effects**

In this section the effects of inlet groove on the segment pressure and flow ripple are investigated. The data from four simulations are presented. Three incorporate inlet grooves and one without. The groove type was hemispherical and of dimensions; cutter diameter 4 millimetres and depth 1 millimetre. The groove angular length was simulated at 5, 10 and 15 degrees. All other parameters were held constant.

### **7.5.1 Inlet Effects on Segment History**

The figure (7.5.1) shows the effects of the inlet groove on segment pressure. When compared with the no groove condition, it can be seen that the groove introduces a delay into the pressurisation of the segment which increases with increasing inlet groove length. The controlled leakage provided by the groove results in a more gently changing pressure profile at the inlet sections. The outlet stage of



: Mean Inlet Pressure : Mean Outlet Pressure : Shaft Speed :  
 6.3 bar                      138 bar                      2400 rpm

Fig.7.5.2 INLET GROOVE EFFECTS ON FLOW RIPPLE

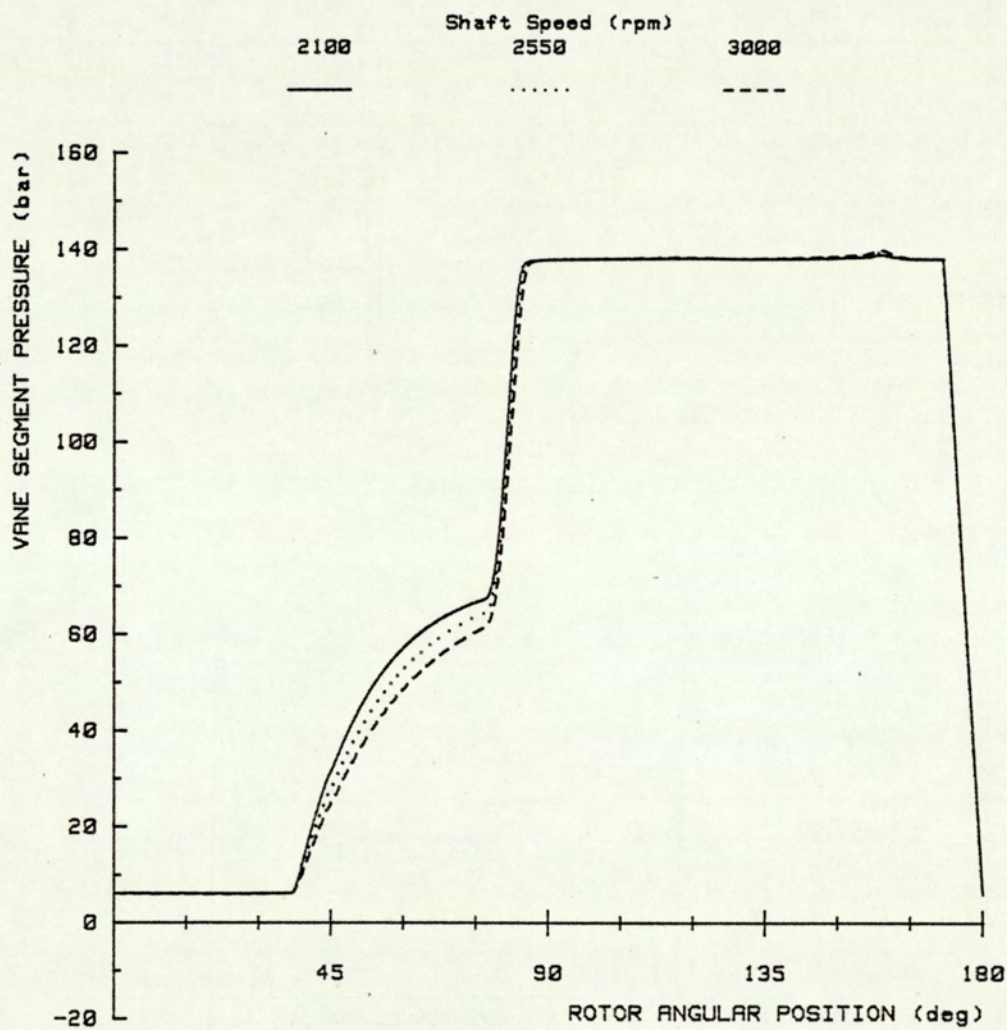
the cycle, beyond 100 degrees, remain unaffected by the inlet groove.

### **7.5.2 Inlet Effects on Flow Ripple**

In figure (7.5.2) the effects of the inlet groove on the flow ripple are presented. The inlet groove does not appear to be of significant benefit in reducing the peak to peak flow ripple. The inlet levels were 2.94, 2.94 and 2.93 percent for the groove length of 5, 10 and 15 degrees respectively. At the outlet there is a marginal increase in the flow ripple. These levels were 16.9, 17.0 and 17.3 percent. The datum no groove values were 2.94 and 16.7 percent, for the inlet and outlet flows respectively. Observations of the RMS levels indicates a trend of similar magnitude. The increase in outlet ripple levels is due to the delaying effects on segment pressures of the inlet groove. Under the conditions simulated there is no significant benefit to be obtained from an inlet groove. An inlet groove can, however, be of advantage in reducing the risk of cavitation at high speeds.

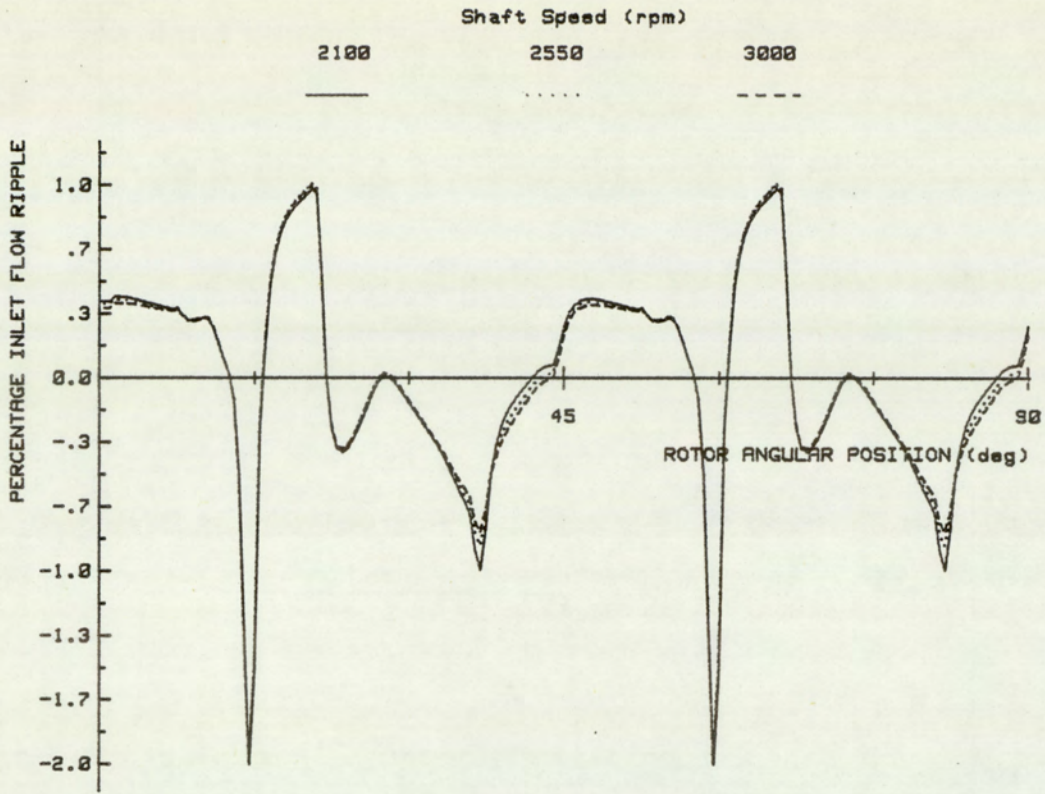
### **7.6 Speed Effects**

In this study of the effects of speed on the segment pressure and flow ripple, data from three simulations are presented. Simulations were made at three shaft speeds of 2100, 2550, and 3000 rpm for a grooved condition. Only an outlet groove was simulated. The groove type was hemispherical and of length 20 degrees. The other groove dimensions were, depth 1.5 millimetres and groove cutter diameter 6 millimetres. All other parameters were held constant.

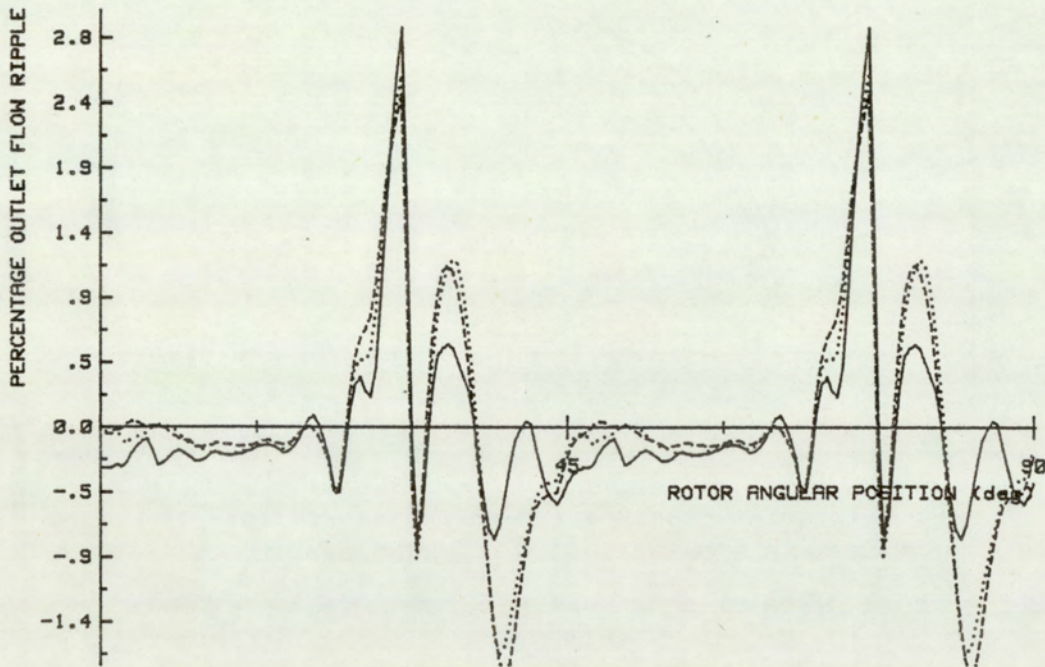


: Mean Inlet Pressure : Mean Outlet Pressure :  
 6.3 bar                                      138 bar

Fig.7.6.1 SPEED EFFECT ON SEGMENT HISTORY  
 OF SILENCED PUMP



a) INLET FLOW RIPPLE



b) OUTLET FLOW RIPPLE

: Mean Inlet Pressure : Mean Outlet Pressure :  
 6.3 bar                      138 bar

Fig.7.6.2 SPEED EFFECTS ON FLOW RIPPLE  
 OF SILENCED PUMP

### **7.6.1 Speed Effects on Segment History**

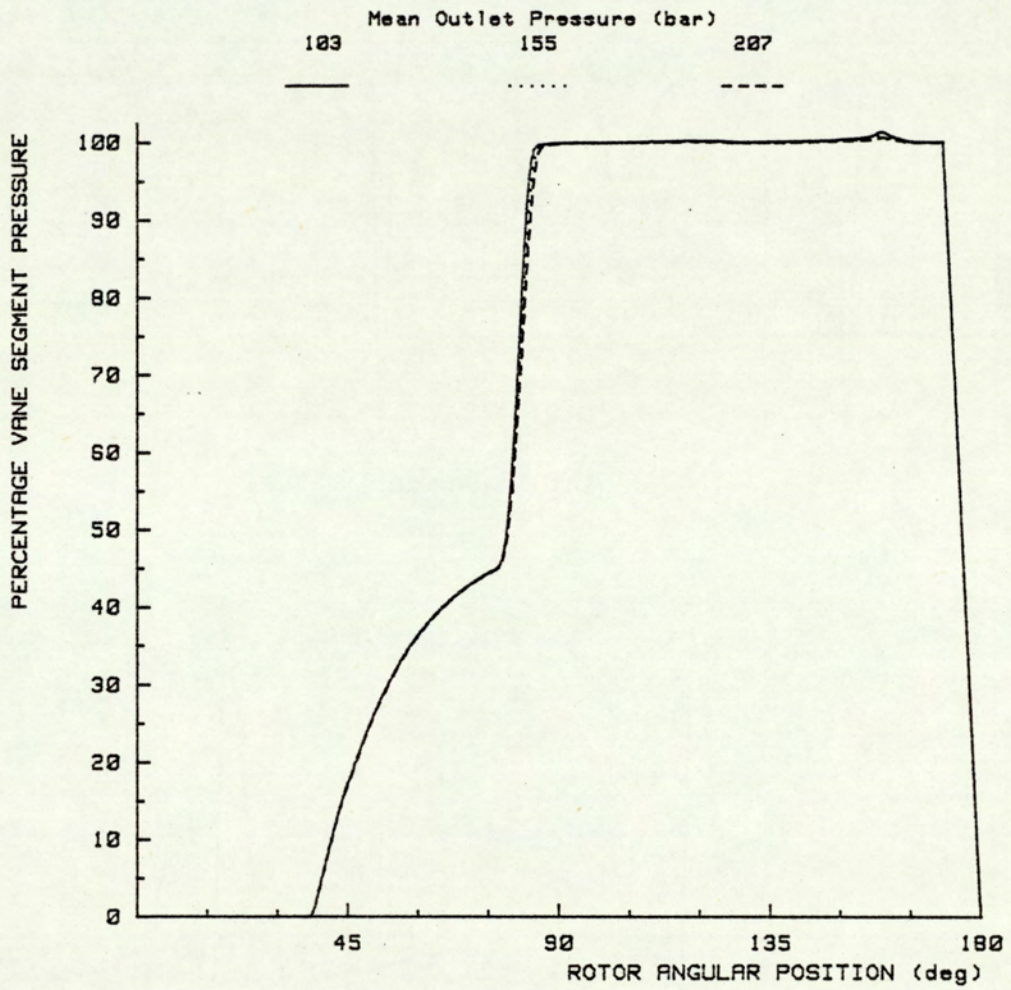
The figure (7.6.1) shows the effect of speed on the segment pressure history. The segment pressure can be seen to achieve the same levels at a much later angular position. In the angular position of approximately 37 to 83 degrees, the segment pressurisation occurs primarily due to leakage via the regular paths or the groove flows. At lower speeds, the net flow which is operative over a finite rotational distance, occurs over a longer period of time. The consequence of this effect is that a greater amount of fluid can enter into the segment to pressurise it, than when operating at higher speeds. At low speeds, therefore, smaller groove dimensions are required.

### **7.6.2 Speed Effects on Flow Ripple**

The figure (7.6.2) shows the effects of speed on the flow ripple. At the lower speed of 2100 rpm, the inlet flow peak to peak ripple was 2.98 percent and the outlet level was 3.37 percent. At 3000 rpm the levels were 2.98 and 3.98. The corresponding RMS values of the flow ripple was 0.19 for both the inlet and outlet at 2100 rpm, and 0.19 and 0.25 at 3000 rpm. Although speed has a significant effect on groove performance, there is a wide range of effective operation.

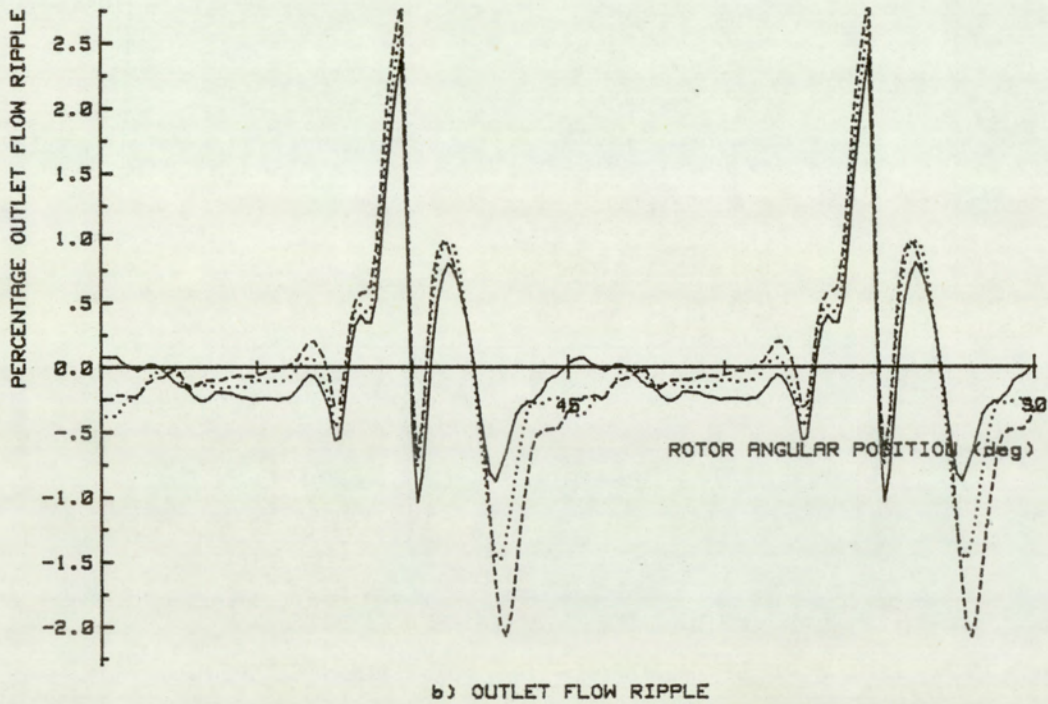
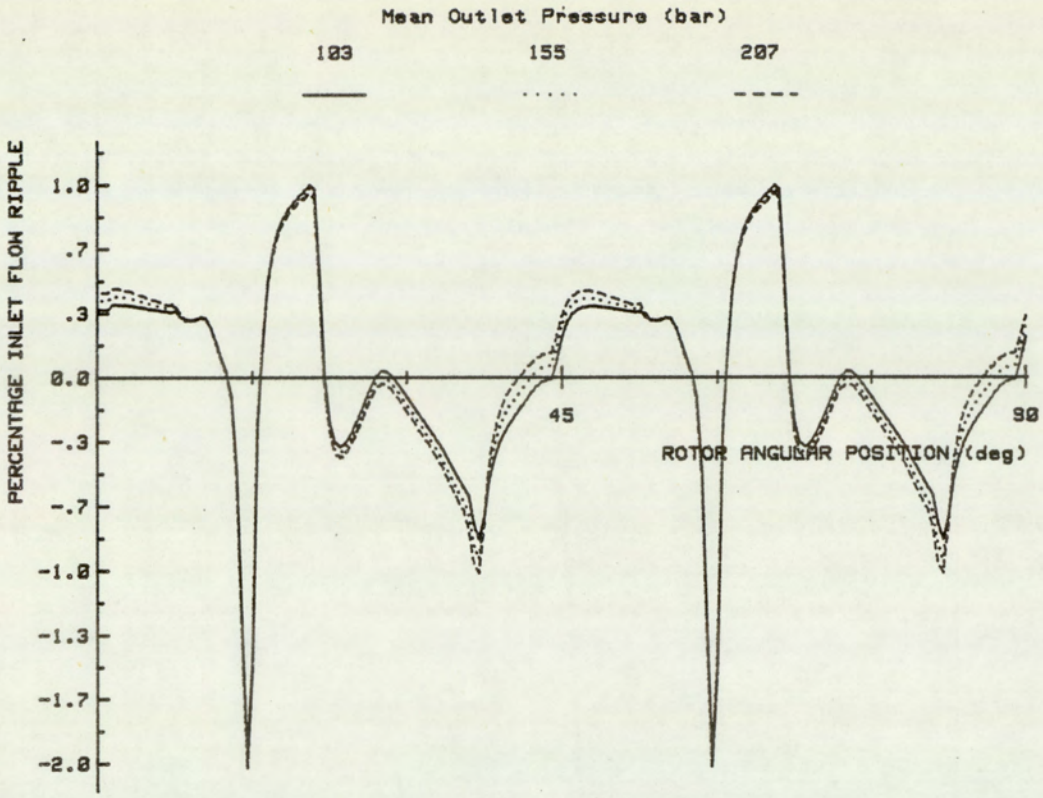
## **7.7 Line Pressure Effects**

Three simulations were performed to study the effects of the mean line pressure. The data relates to three different mean outlet pressures of 103, 155 and 207 bars. The simulations were made with a hemispherical type outlet groove. The dimensions of the groove were angular length 20



: Mean Inlet Pressure : Shaft Speed :  
 6.3 bar                      2400 rpm

Fig.7.7.1 MEAN LINE PRESSURE EFFECTS ON  
 SEGMENT HISTORY OF SILENCED PUMP



: Mean Inlet Pressure : Shaft Speed :  
6.3 bar                      2400 rpm

Fig.7.7.2 MEAN LINE PRESSURE EFFECTS ON  
FLOW RIPPLE OF SILENCED PUMP

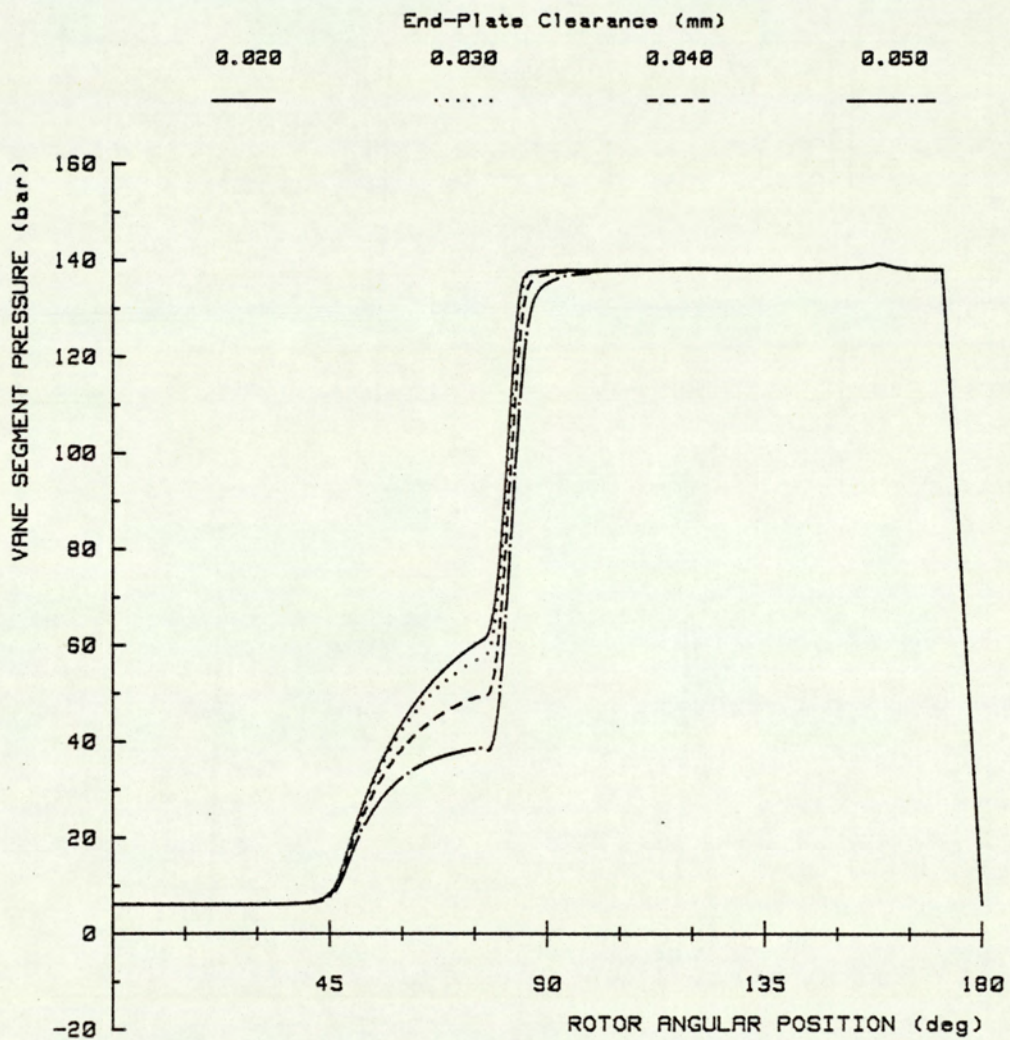
degrees, cutter diameter 6 millimetres and depth 1.5 millimetres. All other parameters were kept constant.

### **7.7.1 Pressure Effects on Segment History**

The figure (7.7.1) shows the effects of outlet line pressure on the segment pressure. The various plots are drawn on a percentage scale where mean inlet is zero and the mean outlet is one hundred percent. On this scaling basis, the plots generally coincide except for the regions corresponding to the rotor position of 75 to 90 degrees, and the position of 157 degrees. The first region corresponds to the period when the outlet groove is operative. The effects of an increase in line pressure is to increase both the general leakage levels and the level of fluid required to enable segment pre-compression. These effects are seen as a slower pressurisation of the segment. The discrepancies observed in the second region are due to orifice and scaling effects. These effects have been described in section (6.2.1).

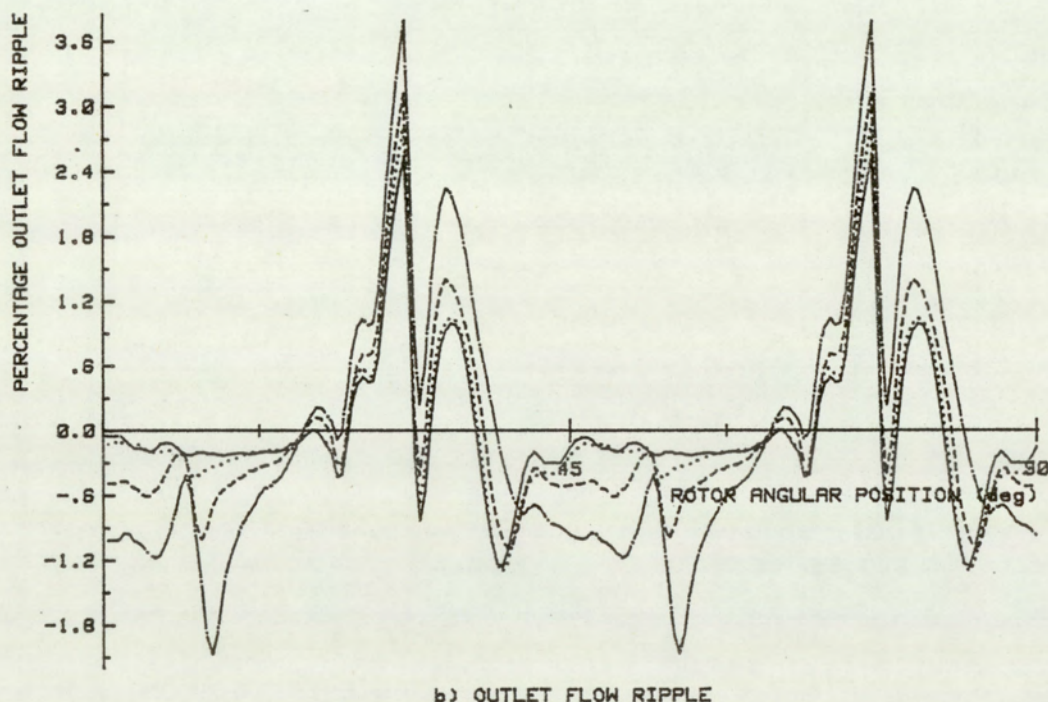
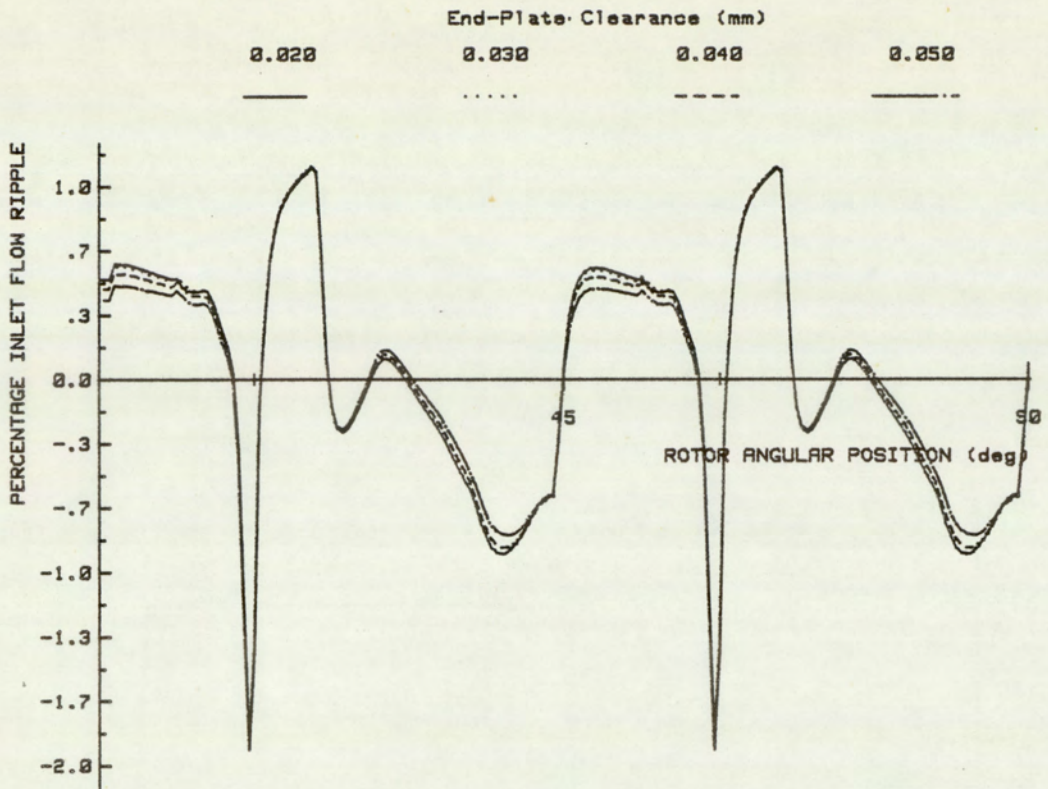
### **7.7.2 Pressure Effects on Flow Ripple**

The figure (7.7.2) shows the effects of mean line pressure on the flow ripple. The inlet peak to peak flow ripple was 2.98 at the line pressure of 103 bars. This fell to 2.96 percent at 207 bars. At the outlet, ripple levels were 3.19 and 4.52 percent. The corresponding RMS values were 0.19 for both the inlet and outlet at 103 bars, and 0.20 and 0.25 at 207 bars, for the inlet and outlet respectively. These effects can be explained in terms of an increase in leakage flow levels due to the increase in line pressures.



: Mean Inlet Pressure : Mean Outlet Pressure : Shaft Speed :  
 6.3 bar                      138 bar                      2400 rpm

Fig.7.8.1 END-PLATE CLEARANCE EFFECTS ON SEGMENT HISTORY OF SILENCED PUMP



: Mean Inlet Pressure : Mean Outlet Pressure : Shaft Speed :  
 6.3 bar                      138 bar                      2400 rpm

Fig.7.8.2 END-PLATE CLEARANCE EFFECTS ON FLOW RIPPLE OF SILENCED PUMP

## **7.8 End-Plate Clearance Effects**

Three simulations were performed to study the effects of the end-plate clearance. The data relates to four different clearances of 0.02, 0.03, 0.04 and 0.05 millimetres. The simulations incorporated a hemispherical type groove at both the inlet and outlet. The dimensions of the groove at the inlet were angular length 10 degrees, depth 1 millimetre and cutter diameter 4 millimetres. The outlet groove was of angular length 20 degrees, cutter diameter 6 millimetres and depth 1.5 millimetres. The vane tip clearance was 0.04 millimetres. All other parameters were kept constant.

### **7.8.1 End-Plate Effects on Segment History**

The figure (7.8.1) shows the effects of end-plate clearances on segment pressure. It can be seen that the effect of increasing the end-plate clearance is to delay the segment pressurisation. This is most evident at the angular region of 37 to 97 degrees. Increasing the clearance causes a corresponding leakage out of the segment, thus resulting in a decrease in the fluid available for pressurisation of the segment. The outlet groove can, however, be seen to provide a gradual transition of the segment to full port pressures.

### **7.8.2 End-Plate Effects on Flow Ripple**

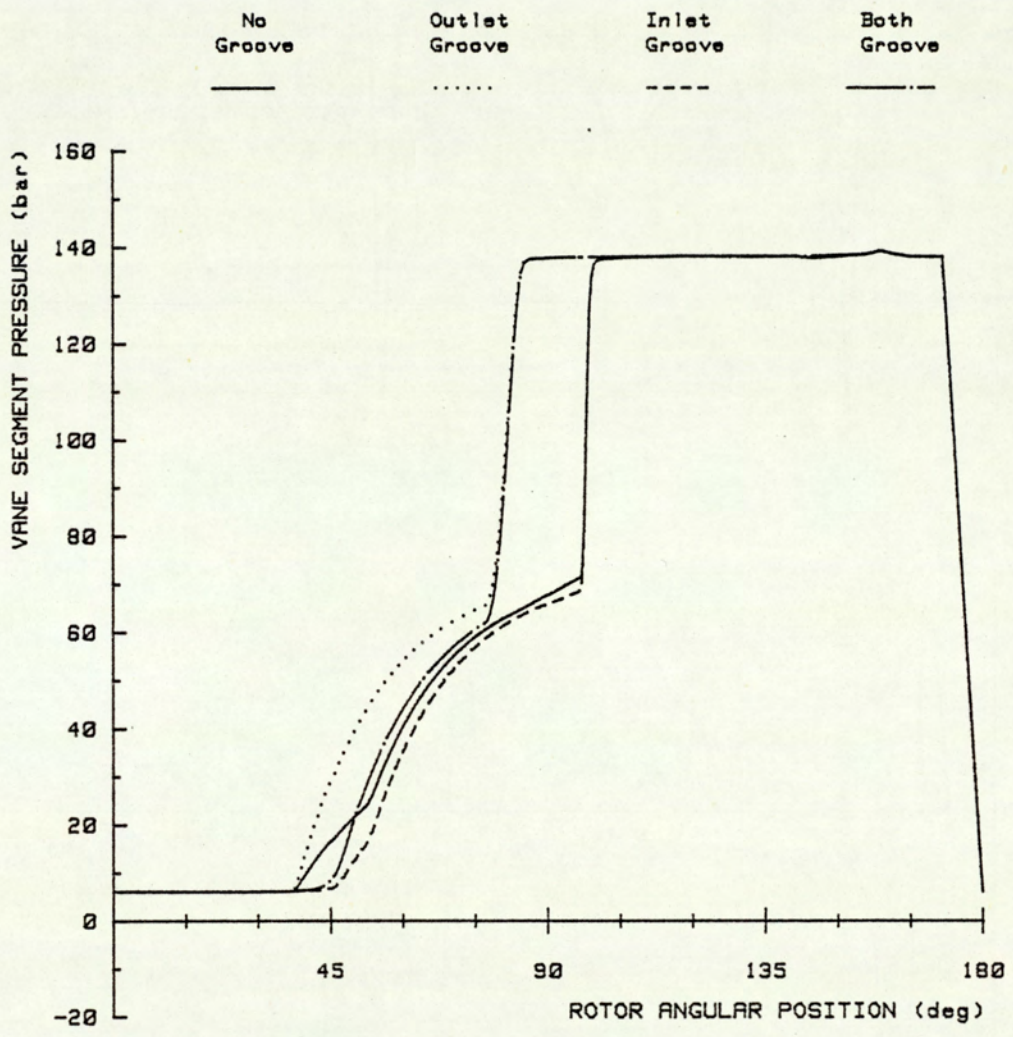
The figure (7.8.2) shows the effects of end-plate clearance on the flow ripple. Without silencing grooves (ref. section 6.7), the peak to

peak values were between 2.95 and 2.98 for the inlet, and 17.5 and 23.8 percent for the outlet, for the condition of increasing clearances from 0.02 to 0.05 millimetres. With silencing grooves, these values were reduced to 2.95 and 2.99 percent for the inlet, and 3.6 to 5.5 percent for the outlet. Within the range of end-plate clearances, the reduction of outlet flow ripple was greater than 76.8 percent. This further demonstrates the wide operating range of silencing grooves.

### 7.9 Optimum Groove Criteria

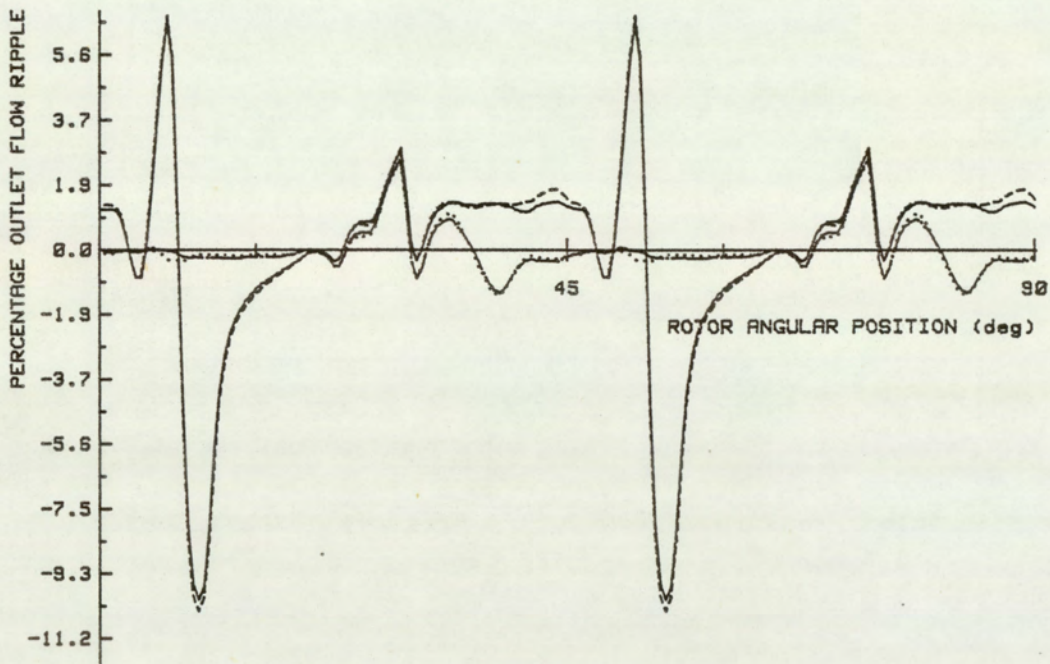
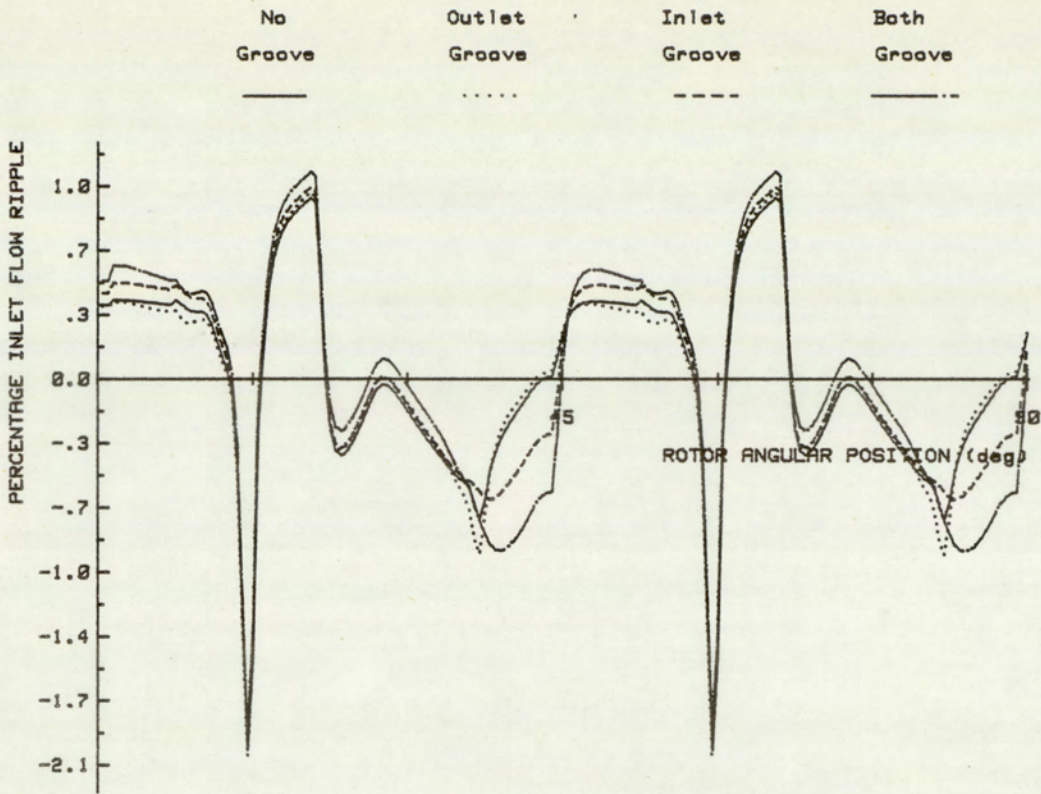
In the preceding sections, the various factors affecting the segment pressure profile and the subsequent inlet and outlet flow ripple have been demonstrated. There appears to be no simple criteria on which to base the design of silencing grooves. For any given pump (motor), the factors affecting the flow ripple are too numerous to enable the derivation of a particular optimum solution. The key to the problem is the availability of a suitable simulation program. With this tool many different groove types can be modelled and their effects ascertained. At the risk of over simplifying the problem, the silencing of a pump is a compromise between minimising groove leakage and removing the effects of pre-compression mis-match.

A methodical approach is of particular importance in the route towards a quick solution. In the previous sections, it has been shown that the groove performance was affected by both line pressures and speed. The first stage is therefore to decide on the operating conditions at which to optimise the groove performance. The most logical condition for this, in most applications, is the normal operating condition. This would give optimum silencing under normal conditions and a slight loss



: Mean Inlet Pressure : Mean Outlet Pressure : Shaft Speed :  
 6.3 bar                      138 bar                      2400 rpm

Fig.7.9.1 SEGMENT HISTORY OF THE SILENCED PUMP



: Mean Inlet Pressure : Mean Outlet Pressure : Shaft Speed :  
 6.3 bar                      138 bar                      2400 rpm

Fig.7.9.2 FLOW RIPPLE OF THE SILENCED PUMP

in groove performance outside these conditions.

The first simulation to be performed has to be that at the chosen optimum condition for the original pump (motor). This would provide a datum on which to base silencing improvements, and an insight into the existence of potentially noisy conditions. In the figures (7.9.1) and (7.9.2), a simulation under such a condition exists. The optimum condition was chosen to be 2400 rpm at 138 bar. For the original no groove condition there is observed a very abrupt increase in segment pressure at about the 97 degree angular position. This corresponds to when the segment at low pressure first communicates directly with the outlet port. At this point there is a sudden backflow of high pressure fluid, and is a main source of fluid and structural borne noise. This point corresponds to the angular position of 7 degrees and subsequent positions at 45 degree increments, in the flow ripple plots. Another position where the segment pressure rises sharply is at 37 degree, when the segment is just beginning to be pressurised. The changes are, however, not as abrupt as for the outlet stages.

In this solution of silencing the pump, sloping hemispherical section grooves are incorporated in both the inlet and outlet ports. The outlet has a 20 degree long groove of 6 millimetres cutter diameter, and a maximum depth of 1.5 millimetres. The groove at the inlet port is 10 degrees long with a cutter diameter of 3 millimetres and depth 1.0 millimetres.

Hemispherically sectioned grooves are chosen for their combined initial slow area changes and faster full flow characteristics. The slow change provided by the triangular section requires a longer groove length. The square section does not have the benefit of slow initial area change. In this particular pump configuration where the segment is only closed

to both inlet and outlet for slightly over 45 degrees, it is important to minimise total groove lengths. Excessively long grooves would unnecessarily increase the general leakage levels.

At the outlet, a long groove was introduced to remove the effects of the abrupt segment pressurisation, at initial port communication. A smooth segment pressure history reduces case excitation. The total effect of the outlet groove is a reduction in both the structural and fluid borne noise levels.

A short inlet groove is used primarily for the purpose of smoothing out the initial pressure rise, at the 37 degree position. This is provided as a refinement of the silencing process. The inlet groove has the unwanted effect of increasing leakage and flow ripple. At the designed speed condition this groove is not absolutely essential. Inlet grooves would be more advantages at higher speeds when large port flows or low inlet pressures would increase the risk of cavitation.

## CHAPTER 8 : EXPERIMENTAL WORK

- 8.1 Introduction
  - 8.1.1 Data Acquisition and Analysis System
  - 8.1.2 Pump System Schematic
  - 8.1.3 Transmission Line System Schematic
- 8.2 Pump Model Correlation
  - 8.2.1 Harmonic Analysis of Pump Data
  - 8.2.2 Time Average Analysis of Pump Data
- 8.3 Correlation of Pump Performance Data
  - 8.3.1 Performance of Standard Pump
  - 8.3.2 Performance of Silenced Pump
- 8.4 Conclusion on Pump Model
- 8.5 Acquiring Transmission Line Data
  - 8.5.1 Standing Wave Data
- 8.6 Conclusion on Transmission Line Model
- 8.7 Procedure for the Deconvolution of Pressure Ripples

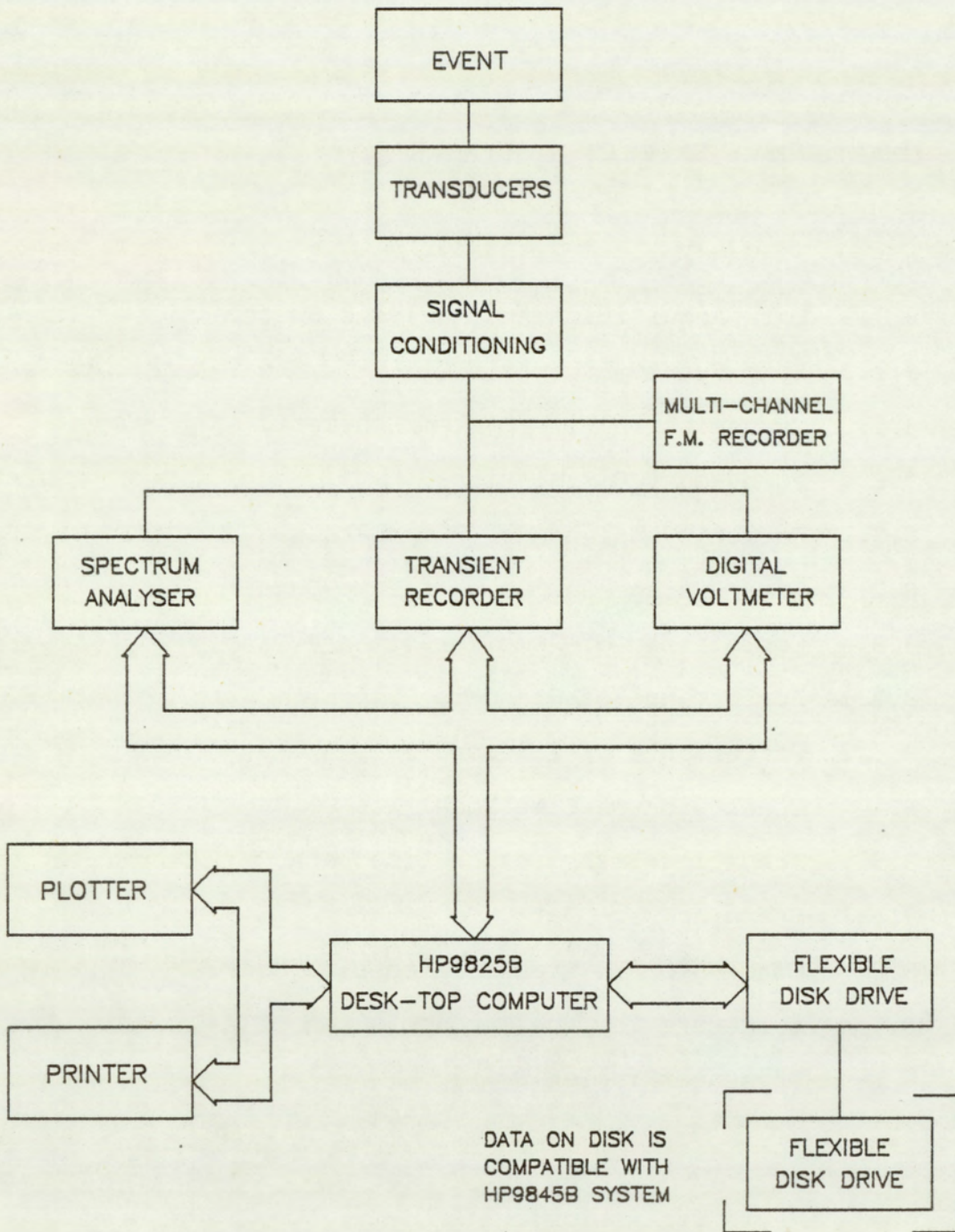


FIG.8.1.1 DATA ACQUISITION AND ANALYSIS SYSTEM

## **8.1 Introduction**

In the earlier chapters two analytical models were developed, one for a vane pump and the other for a transmission line. This chapter deals with the work relating to the experimental verification of these models. In the first section is described the data acquisition and analysis system developed for this work. In addition, a brief schematic of the system is presented with particular emphasis on instrumentation. This section is followed by details of the method of data acquisition and analysis, used to obtain the data for correlating the mathematical model to experimental data. The work relating to the pump and transmission line models are handled separately. In sections two, three and four, the data relating to the vane pump is presented. This is followed in sections five and six with the data relating to the transmission line work.

### **8.1.1 Acquisition and Analysis Systems**

The figure (8.1.1) shows the general schematic of the data acquisition and analysis system. The system is based around a desk-top computer, the HP9825B computer with 64k of random access memory. Supporting the computer is a number of peripherals consisting of a plotter, thermal printer, and both cartridge and flexible mass-storage devices. Within this system, the computer serves primarily as a controller for the Spectrum analyser, Transient recorder and Digital voltmeter, and enables the storage of data onto the flexible disk drive. Analysis at this stage is limited. This is performed by the HP9845B system (described in chapter 5). Data is transferred from one system to the other via the data compatible flexible disks.

The related experimental work is essentially based on the measurement of the dynamic pressure fluctuations. For the purpose of detecting the pressure fluctuations, piezo-electric and strain gauge pressure transducers were used. The former operates utilising the piezo-electric effect. A charge is produced which is proportional to the applied force on the transducer diaphragm. These transducers possess an extremely high frequency response. The strain gauge pressure transducer exploits the strain gauge effect. A stress on the transducer diaphragm is transferred to the strain gauge and results in a change in its resistance. This type of transducer has a lower dynamic range. Unlike the piezo-electric transducer, however, the strain gauge transducer provides both mean and dynamic pressure data.

Prior to measurement, the signal is required to be conditioned by an appropriate amplifier. A charge amplifier is required to convert the output charge from a piezo-electric pressure transducer to voltage, and a strain gauge amplifier is required for the strain gauge pressure transducer. Following conditioning, a voltage proportional to total pressure is obtained from the strain-gauge transducer, and a voltage proportional to dynamic pressure is obtained from the piezo-electric transducer.

In addition, a proximity switch located on the pump shaft, provides a synchronization signal. This is used to correlate the measurements and provide the signal required for time average analysis.

Following signal conditioning, the data can be directly analysed or stored on a multi-channel recorder. Recording enables a detailed analysis of available data as the same block of data can be analysed repeatedly by a variety of methods. This significantly reduces the experimental work relating to multiple channel analysis.

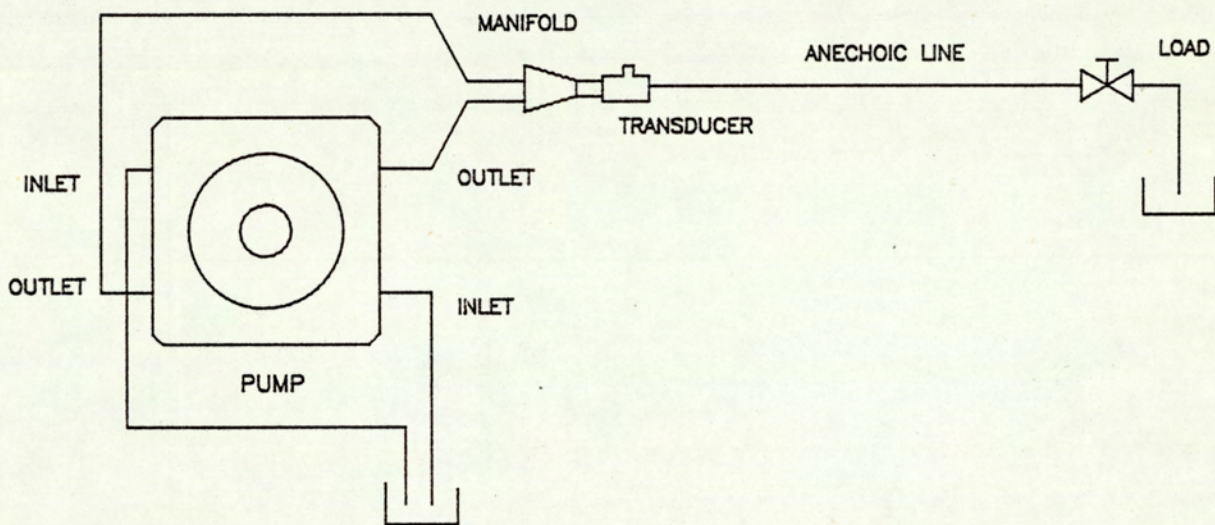


FIG.8.1.2 PUMP SYSTEM SCHEMATIC

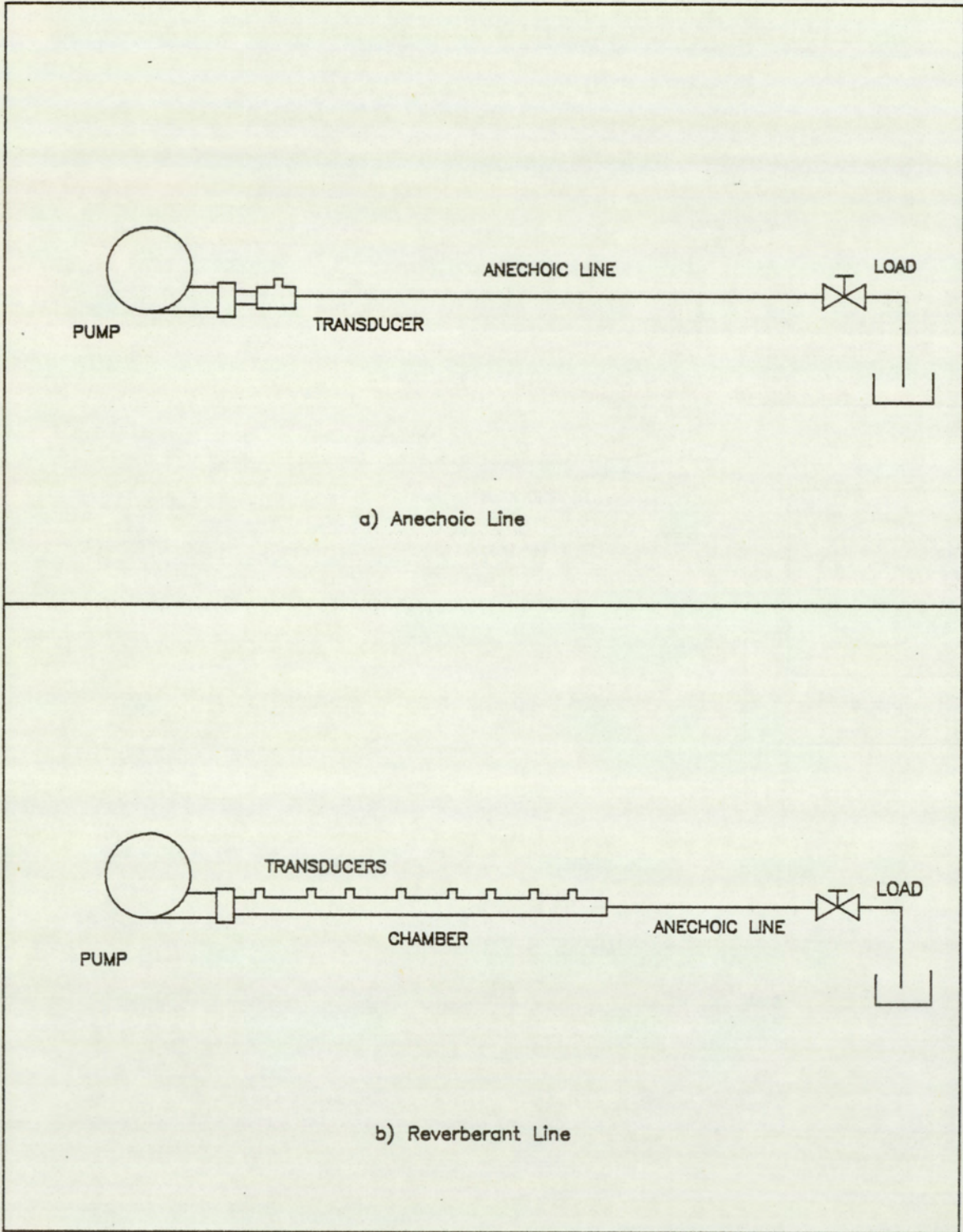


FIG.8.1.3 TRANSMISSION LINE SCHEMATIC

### 8.1.2 Pump System Schematic

The figure (8.1.2) shows the essential elements of the pump system. The two pump outlets are joined at the manifold which feeds into a 30 millimetre bore transducer housing containing a piezo-electric pressure transducer. The housing is in turn connected to a 20 metre long anechoic line of 31.8mm. nominal bore which terminates into a load valve. At the pump end a proximity switch, suitably mounted on the drive shaft, provides a synchronization pulse. In addition a strain gauge pressure transducer, mounted in the pump, measures the pressure of the vane segment. This transducer is located in the vane passage and actually provides the pressure at the base of the vane. Due to the presence of a low resistance pathway, running up the vane and terminating into the segment volume, the segment pressure history is provided by this transducer. The pump is driven by a speed controlled electric motor which maintains a constant operating speed. A cooling circuit maintains a steady operating temperature, and a boost pump and accumulator provides a constant inlet supply pressure.

### 8.1.3 Transmission Line System Schematic

The figure (8.1.3) shows the schematic of the systems used to verify the transmission model. The essential elements in both the systems is a seven piston axial pump connected to an anechoic, and a reverberant termination. The function of the pump is basically that of a flow ripple source. A piston pump was used as the flow ripple exhibits strong harmonic contents. The pump is instrumented with a proximity switch which provides a synchronization signal, and is driven by a

speed controlled hydraulic motor.

In the first system, the pump is directly connected to a piezo-electric pressure transducer and a 30 metre long anechoic line which terminates at a load valve. The transducer housing has a 30 millimetre bore, and the anechoic line has a 1.25 inch nominal bore. The pressure transducer measures the anechoic pump output.

In the second system, a reverberant chamber possessing an internal bore of 88.9 millimetres and of length 1.95 metres, is connected in place of the transducer housing. Located evenly spaced along this chamber is a set of eight pressure transducers which measures the pressure variations along the length of the chamber.

## **8.2 Pump Model Correlation**

For the purpose of theoretical and experimental correlation, two sets of data are presented. The first relates to the pump operating without silencing grooves, and the other operating with the grooves. For each set, data is presented at the three different operating speed of 700, 1050 and 1400 rpm. The mean inlet and outlet pressures were held constant during these tests at 6.9 bars and 68.9 bars respectively. The fluid temperature was maintained in the range of between 20 to 25 degrees Centigrade. At each of these conditions, dynamic recordings of the pump outlet flow and segment pressure history were made. In addition, measurements were made of the mean outlet flow rate.

In an effort to minimise the system effects, measurements of the pump outlet flow ripple were made whilst connected to an anechoic line. With this pump configuration, it is not possible to completely remove these

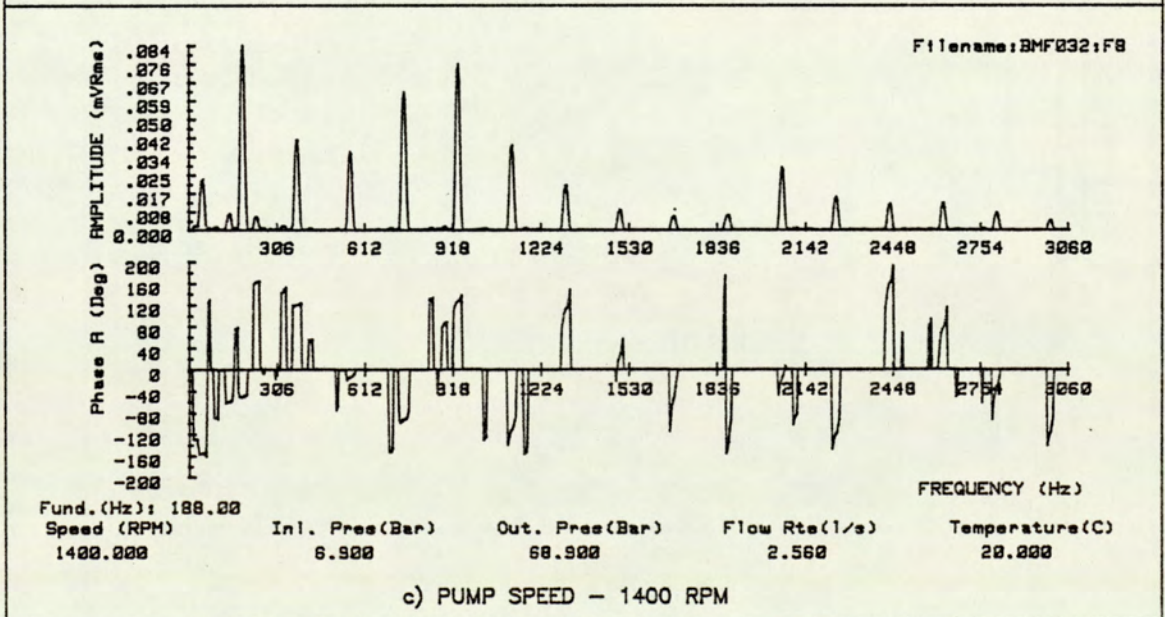
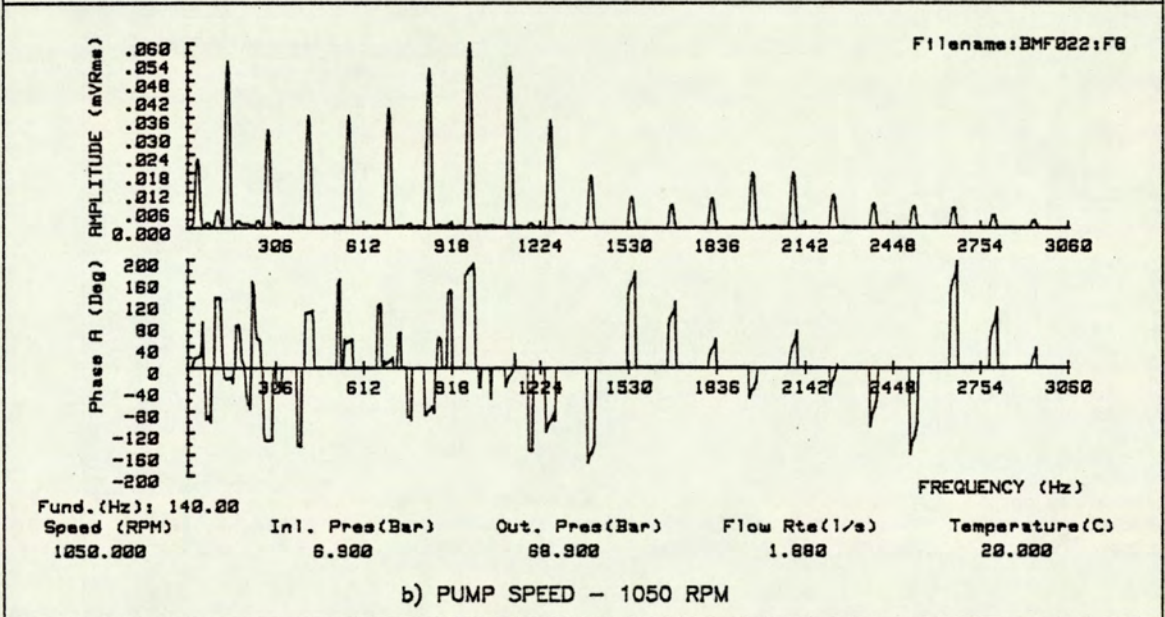
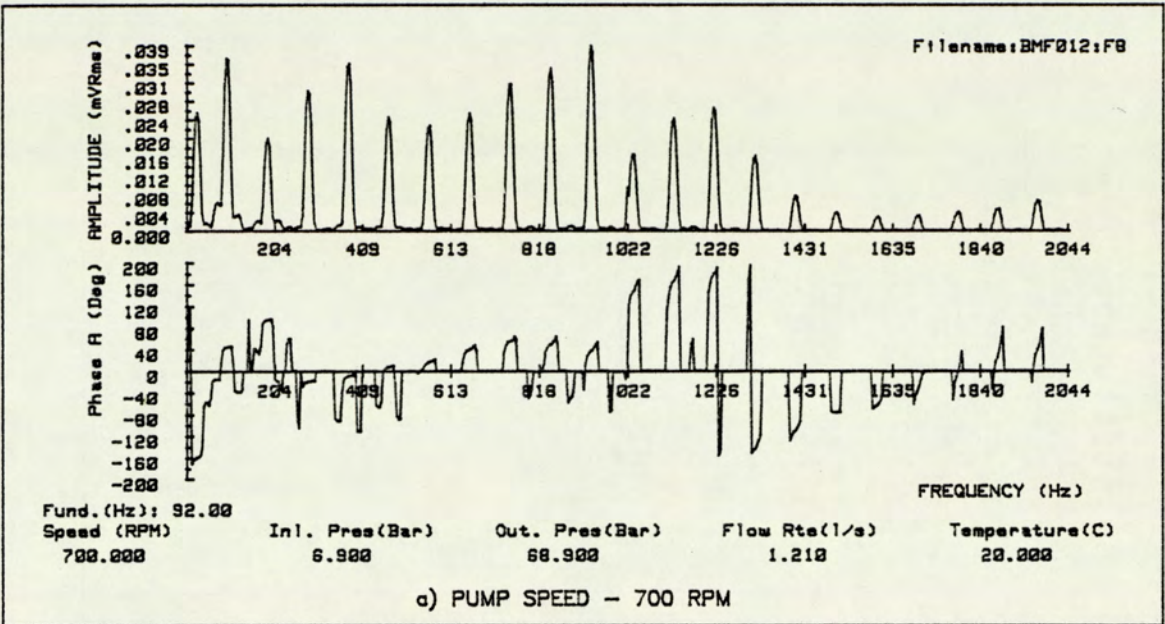


Fig.8.2.1 OUTLET SPECTRUM OF UNSILENCED PUMP

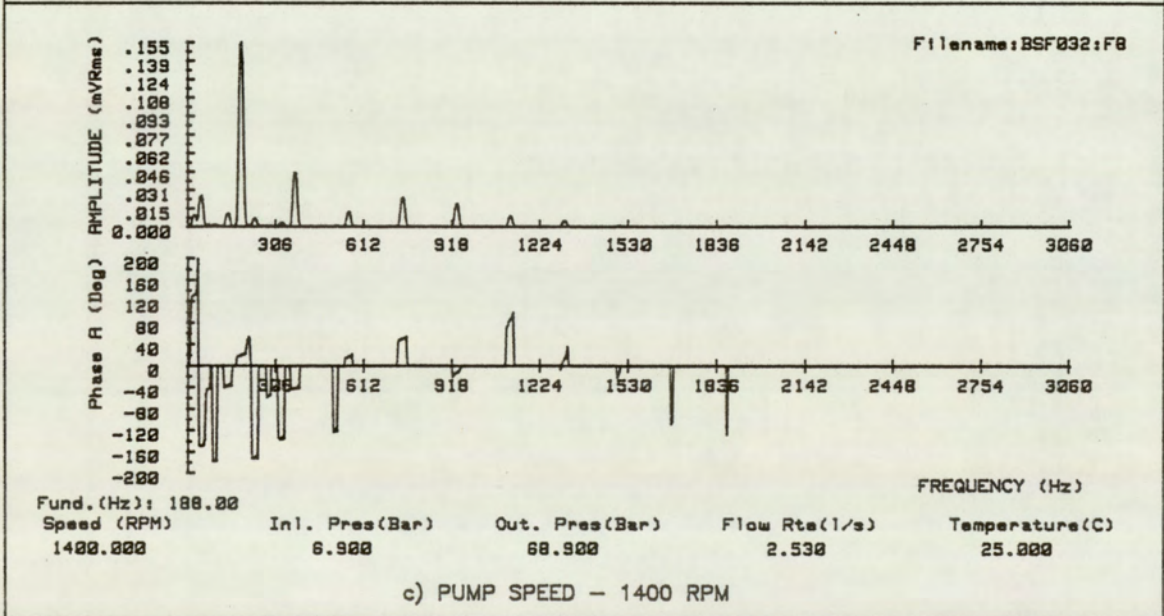
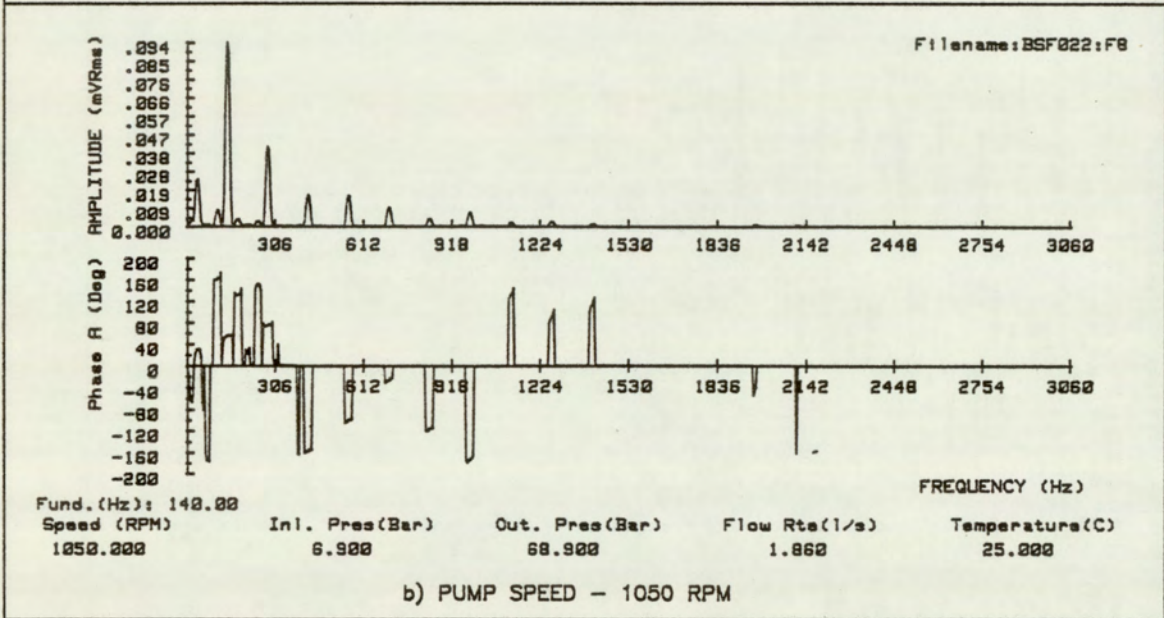
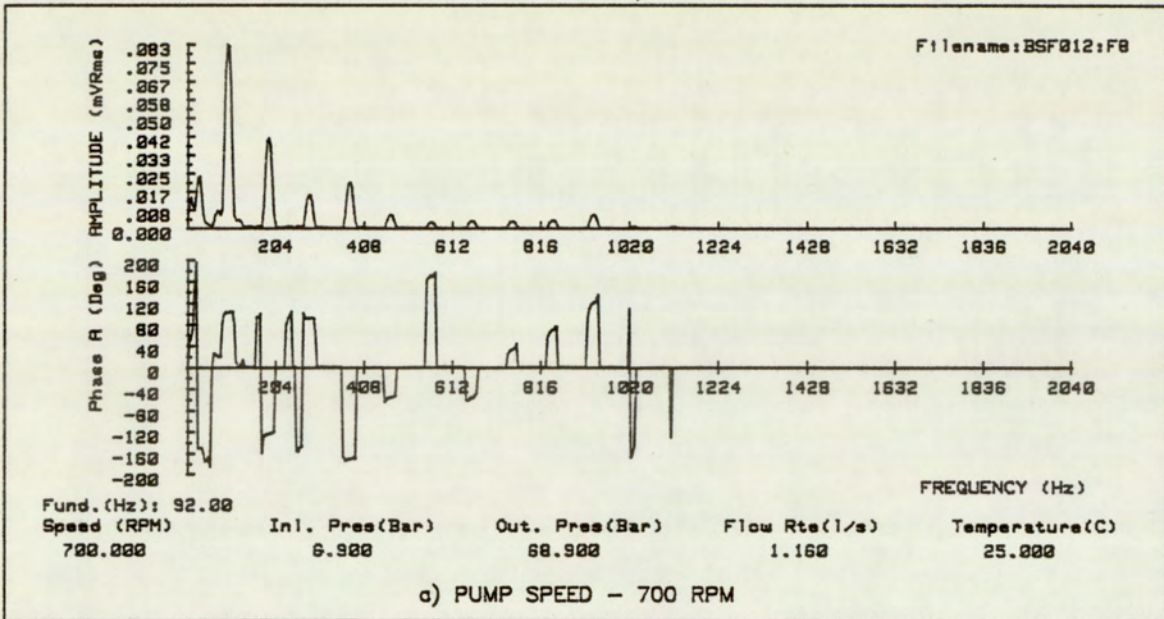


Fig.8.2.2 OUTLET SPECTRUM OF SILENCED PUMP

unwanted effects. The pump is required to operate with balanced port pressures and thus necessitates the ports to be connected externally. Introduction of the manifold into the flow stream results in a mis-match of the upstream and downstream admittance at the manifold. This results in wave reflection and a standing wave being created upstream of the manifold.

When measuring the segment pressure, the system effects can be ignored. These effects operate at frequencies much higher than those of the event under study.

### **8.2.1 Harmonic Analysis of Pump Data**

When correlating the experimental data to the theoretical simulations, it is inevitable that system effects are included in the comparison. It is, however, necessary to minimise these system effects to enable the best possible comparisons to be made. Although both the flow and segment correlation will be made in the time domain, preparation of the flow data starts with a spectral analysis. From this spectral data, the significant components are extracted and the corresponding time series re-synthesized. Observations of the data in the frequency domain also aids in the appreciation of the contributions from system effects.

The figures (8.2.1) and (8.2.2) provides the full spectrum and shows the harmonic signatures of the pump at the three speed conditions. This represents the time averaged spectral data of the outlet flow. With a rotating machine, the spectral components can only occur at harmonic intervals of the fundamental frequencies. With a geometrically perfect machine, the fundamental frequency would be that of the vane. In applying this assumption, the sub-harmonic components of the vane

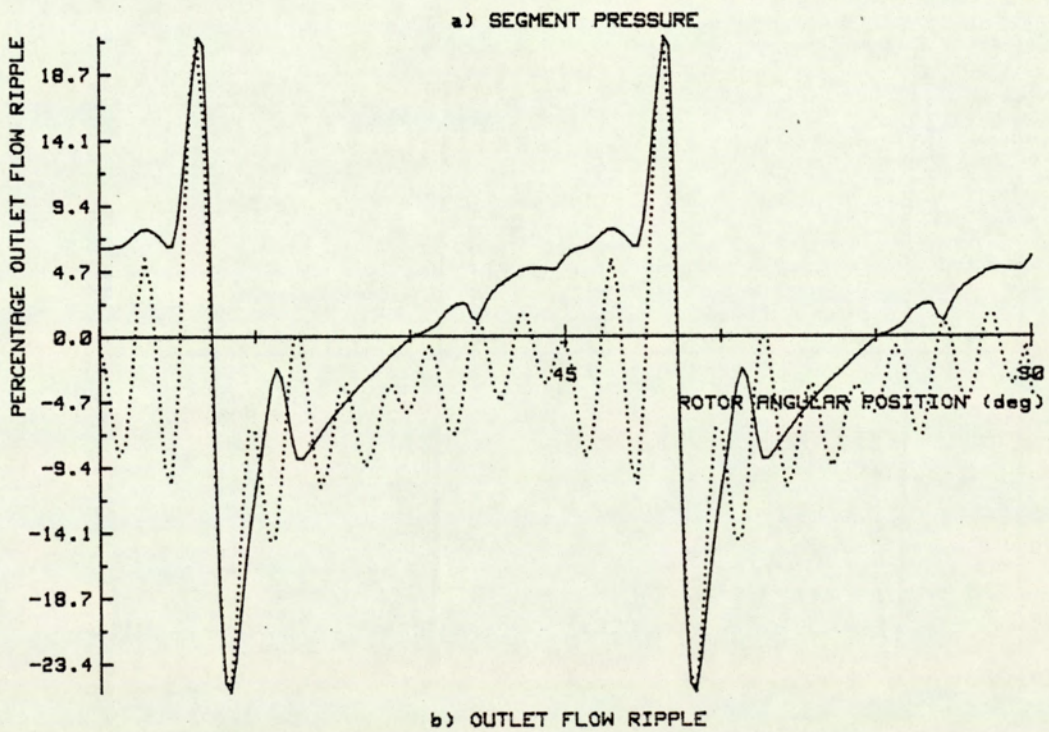
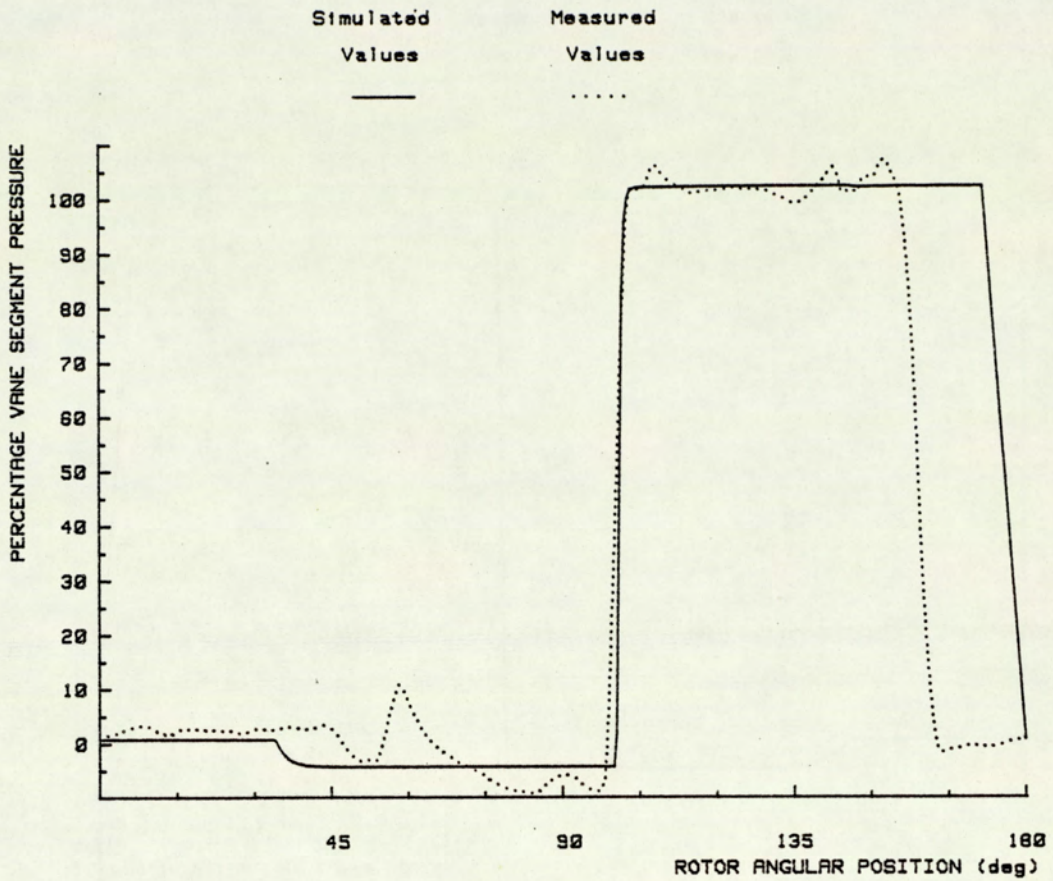
frequency can be neglected. The significance of the relative nature of the standard and silenced spectrums are discussed later in the chapter.

### **8.2.2 Time Average Analysis of Pump Data**

Although the segment pressure measurements, were not affected by the system effects, the strain gauge pressure transducer signal had a significant noise component. This problem was effectively removed by applying 'Time Series Averaging'. This is achieved by taking blocks of consecutive and synchronized time data, and calculating the average time series. Synchronization was provided by the pulse from the proximity switch. When a sufficiently large number of averages are taken, the random noise components are removed leaving a clean pressure history which was used in the subsequent presentation.

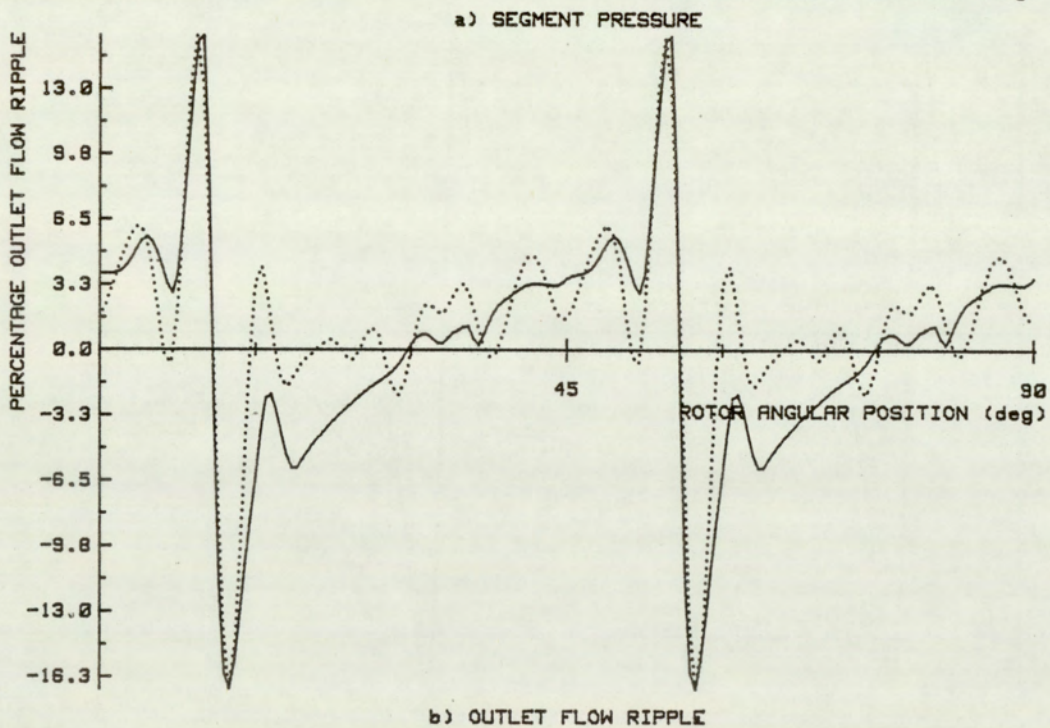
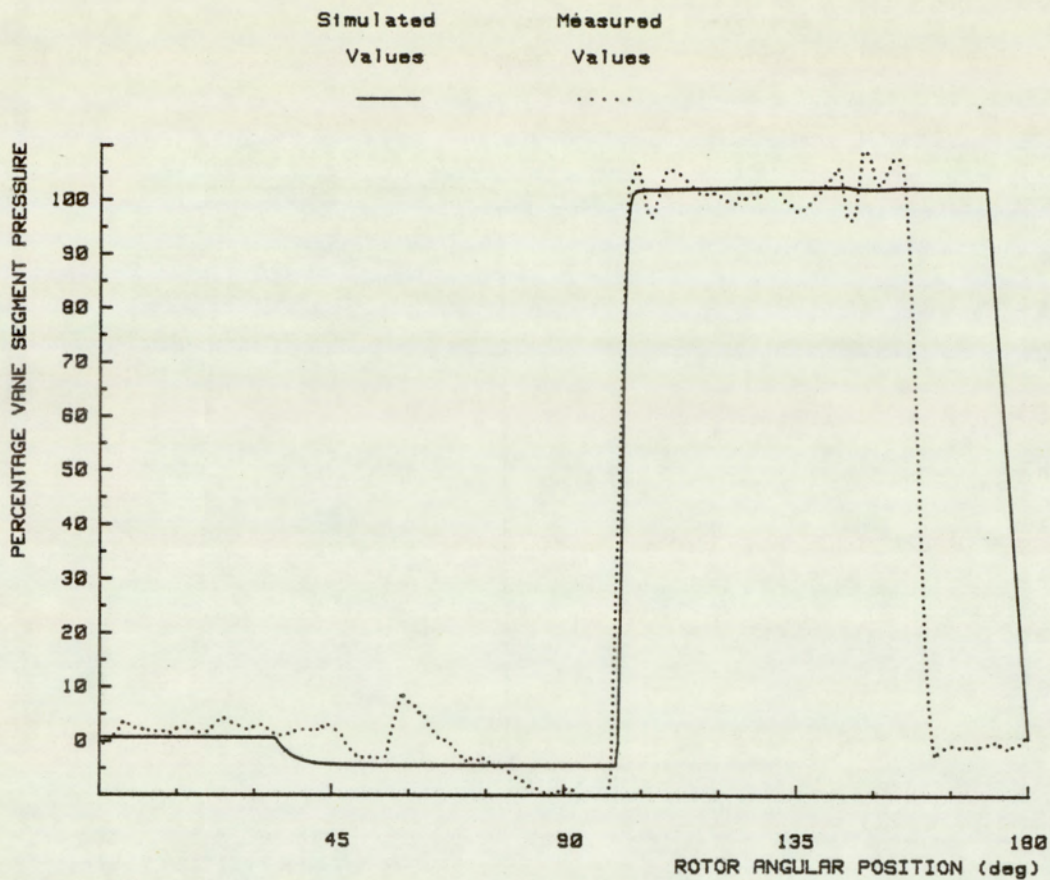
### **8.3 Correlation of Pump Performance Data**

The data is presented for correlation by superimposing the theoretical and experimental results. With the segment history study, the data is presented as a percentage of the port pressure range. The difference in mean port pressures represents 100 percent. The pressure measurement obtained by the transducer is effectively the segment pressure, as defined in the pump model. There is, however, a discrepancy which occurs at the later stages of the cycle. The experimental data shows a fall in the pressure at approximately 15 degrees earlier to that simulated. The transducer accesses the segment pressure via a low resistance channel running up the vane. The entrance to this channel



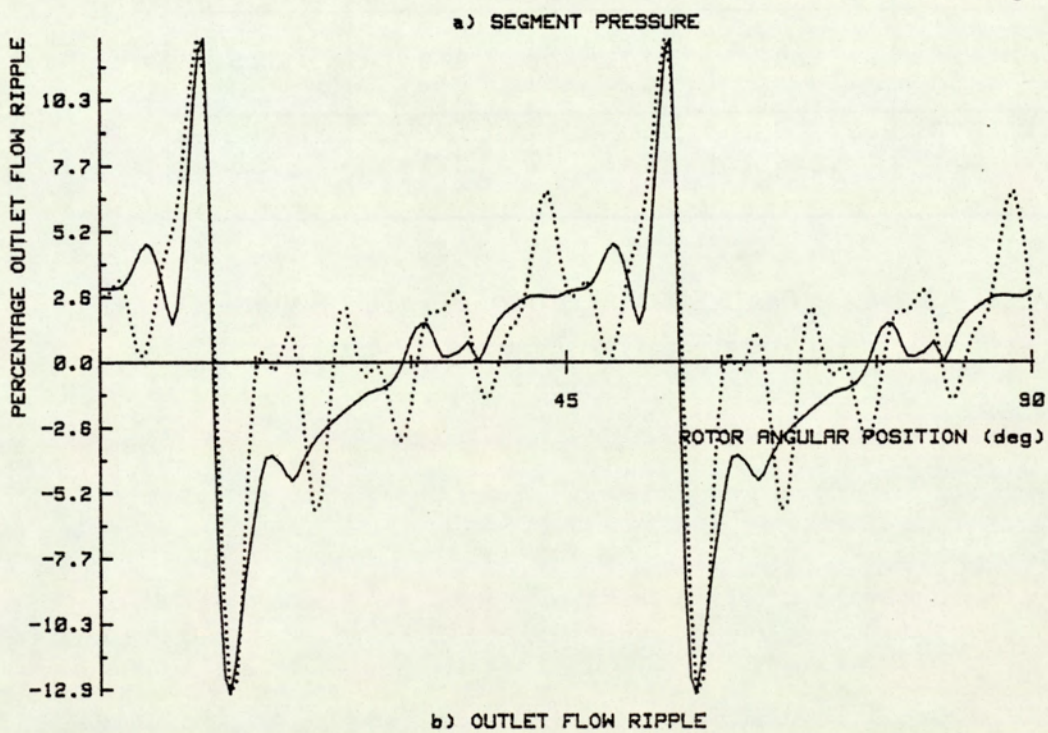
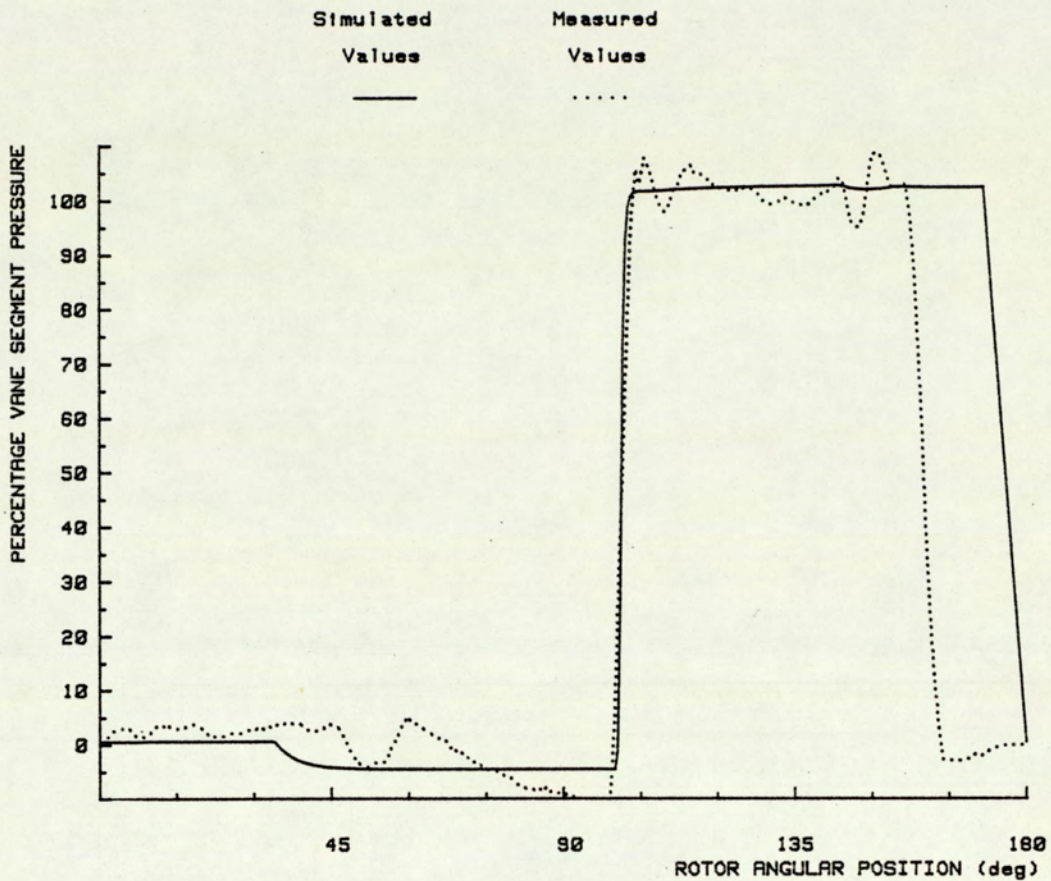
: Mean Inlet Pressure : Mean Outlet Pressure : Shaft Speed :  
 6.3 bar                      68.9 bar                      700 rpm

Fig.8.3.1 PERFORMANCE CORRELATION OF  
 STANDARD PUMP AT 700 RPM



: Mean Inlet Pressure : Mean Outlet Pressure : Shaft Speed :  
 6.3 bar                      68.9 bar                      1050 rpm

Fig.8.3.2 PERFORMANCE CORRELATION OF  
 STANDARD PUMP AT 1050 RPM



: Mean Inlet Pressure : Mean Outlet Pressure : Shaft Speed :  
 6.3 bar                      68.9 bar                      1400 rpm

Fig.8.3.3 PERFORMANCE CORRELATION OF  
 STANDARD PUMP AT 1400 RPM

NO GROOVE DATA

SPEED (RPM)	MEAN FLOW (l/s)		PEAK TO PEAK FLOW (%)	
	EXPERIMENTAL	SIMULATED	EXPERIMENTAL	SIMULATED
700	1.21	1.11	44.1	46.9
1050	1.88	1.79	29.9	32.5
1400	2.56	2.47	24.1	25.8

TABLE 8.3.1 QUANTITATIVE CORRELATION BETWEEN SIMULATED  
AND MEASURED FLOW RIPPLE – STANDARD

is, however, only completely exposed to the segment when the vane is fully extended. At the end of the cycle, the vane is retracted and results in the premature isolation of the transducer from the segment.

The flow ripple comparison is similarly presented by superimposing the theoretical and experimental data. The theoretical data is shown as a percentage of the mean flow. The experimental data is drawn suitable scaled following re-synthesis from the harmonic data. The scaling results in a forced correlation of the peak to peak values of the theoretical and experimental data. For a quantitative correlation, two comparisons are made, one of the absolute time domain peak to peak flow fluctuations, and the other of the mean flow levels. The flow levels are determined using the equation (4.5.8) for an anechoic termination of characteristic line impedance, and negligible  $Z_0/Z_S$  ratio. The constants used are bore diameter 30 mm., fluid density 861 Kg/m<sup>3</sup> and effective bulk modulus 883 MN/m<sup>2</sup>. The subsequent peak to peak levels determined were compared quantitatively with the levels predicted theoretically.

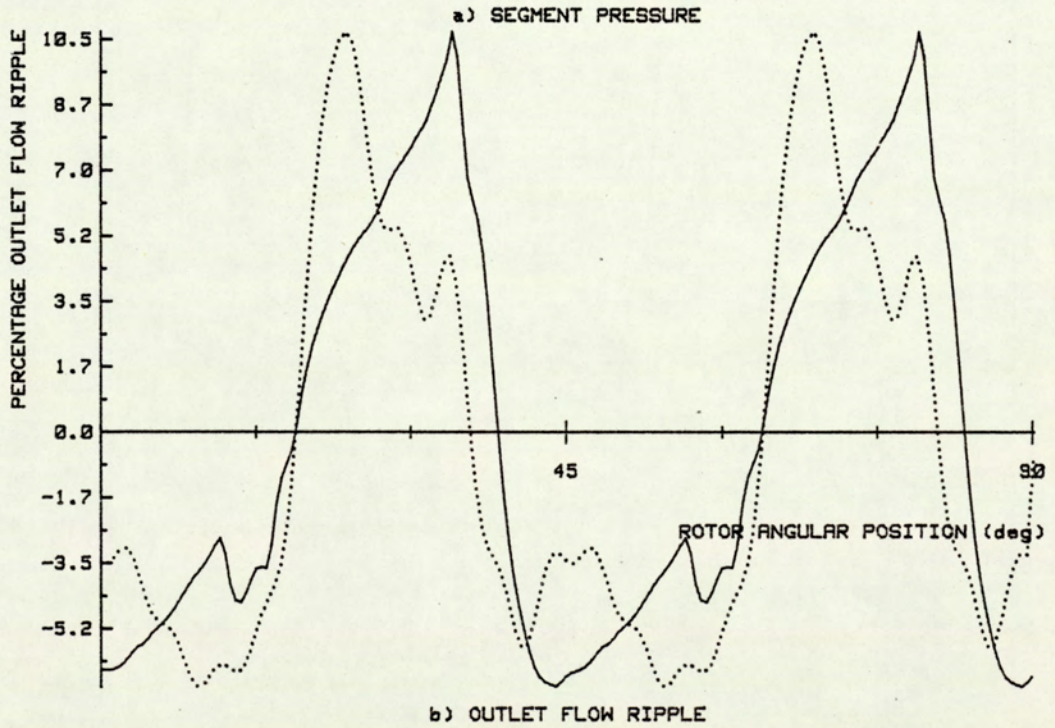
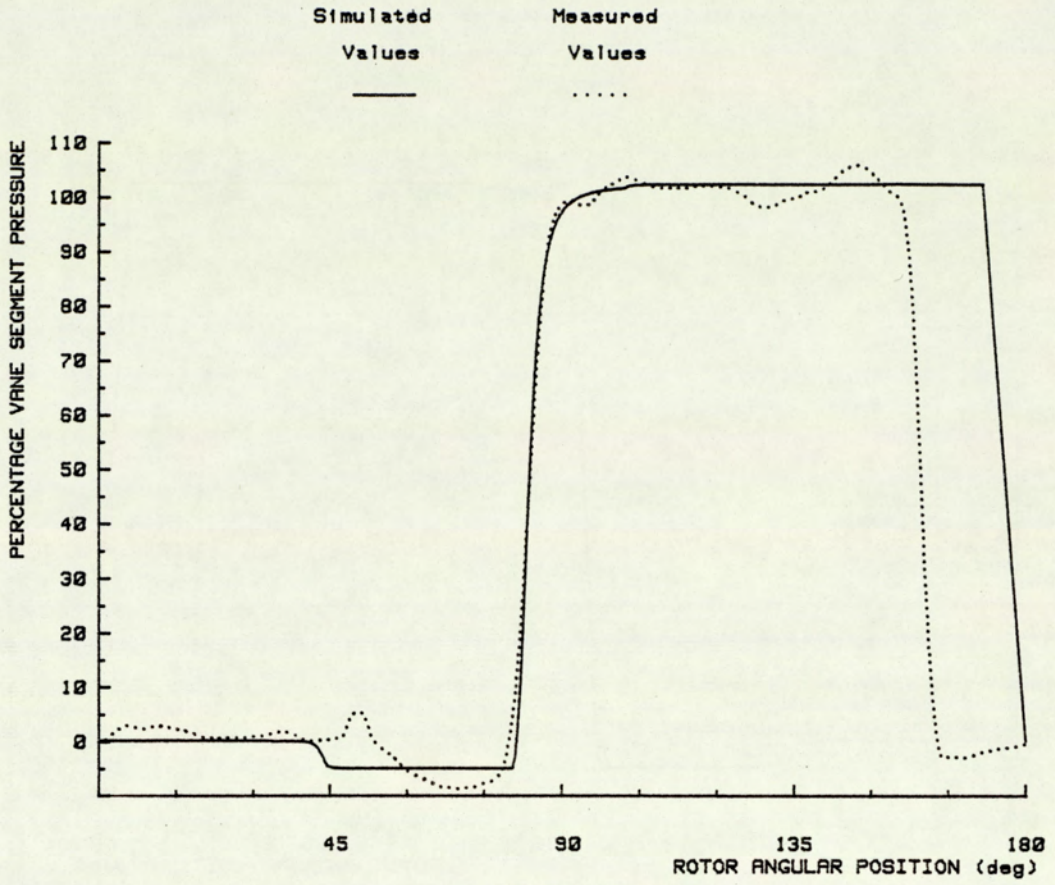
### 8.3.1 Performance of Standard Pump

The figures (8.3.1) to (8.3.3) and table (8.3.1) shows the correlation data for the standard pump. In practice the harmonic content of pumps are generally defined up to the tenth harmonic. Within this range, the significant components are found to be fully represented. In order to minimise the higher frequency system effects, the flow ripple has been subsequently re-synthesized from the first ten harmonic.

The figures demonstrate a high degree of qualitative correlation at the three speed conditions. In addition to the previously explained

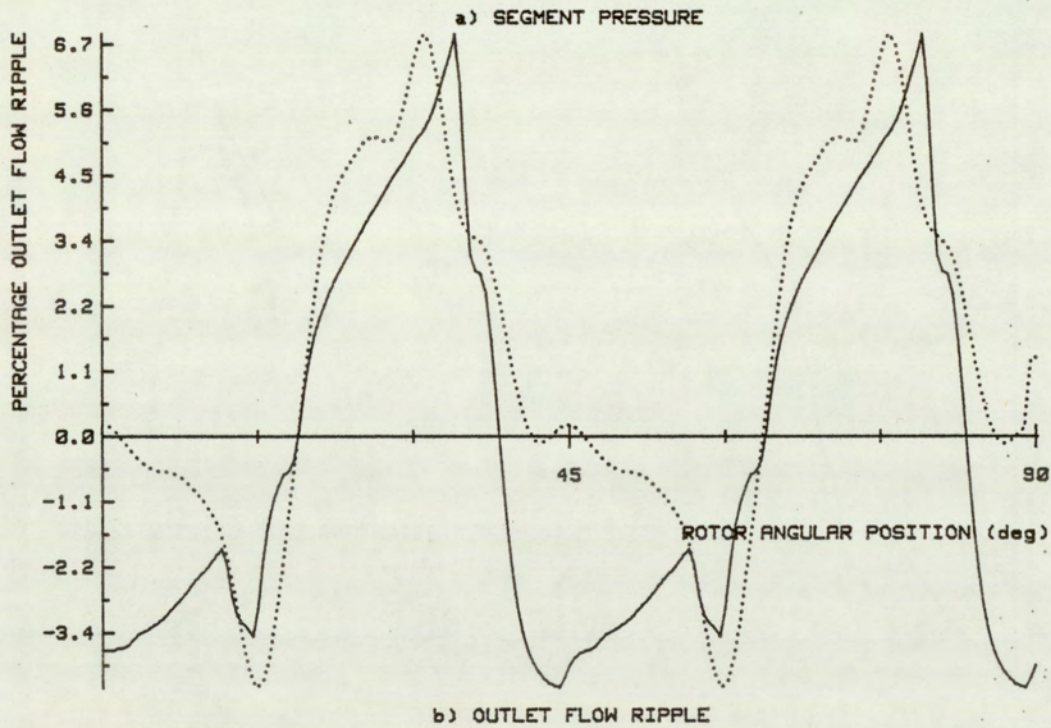
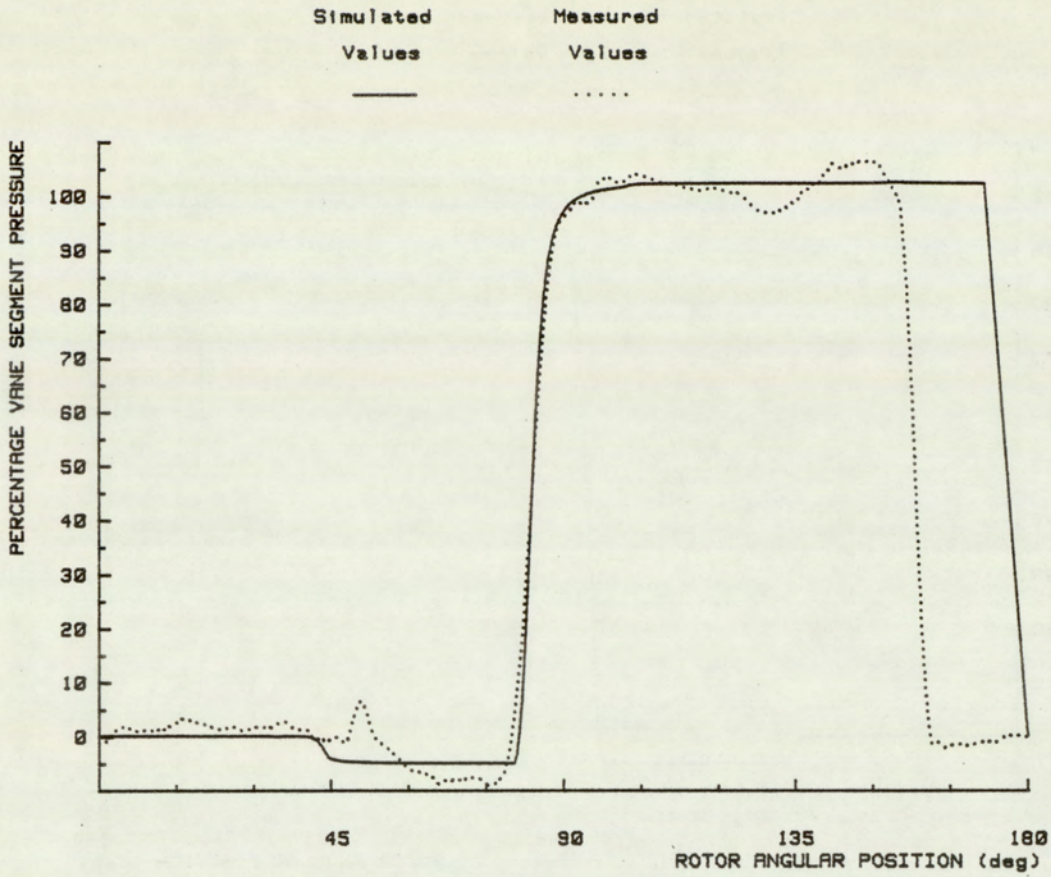
discrepancy at the end of the cycle, there are additional differences at the 30 to 60 degree rotor position. At the 35 degree position, the simulation shows the segment pressure falling. This event is observed later in the experimental observations. This discrepancy is easily explained due to the difference between the actual and modelled port geometry. The ports of the tested pump contains a geometrically complex scalloped section. This effectively provides a much greater flow area, up till the instant the vane sweeps past the port, thus delaying the fall in the segment pressure. The rise in the measured segment pressure at the 60 degree rotor position can be attributed to geometrical imperfections in the actual pump. In this region, the only flow into the segment is due to leakage. As there are also no geometrical changes occurring, the only cause of pressure rise must be due to a net change in leakage levels. This can occur due to both changes in vane tip and end-plate clearances. These variations are observed in geometrical measurements made of the pump.

The flow ripple is seen to correlate equally well with the theoretical predictions. The qualitative comparison provided by the re-synthesized harmonic data shows a good overlap in the theoretical and experimental data. A strong harmonic component, independant of speed, is visible in all the three speed conditions. This component is in the frequency range of 920 to 1000 Hz. With the aid of the full spectral data, this effect can be confidently attributed to a system resonance at this frequency. The table (8.3.1) provides the basis of the quantitative correlation. A comparison is presented between the experimental and simulated peak to peak levels. Within the range studied, a discrepancy of only between 6.3 to 8.7 percent is observed between the simulated and the experimental values.



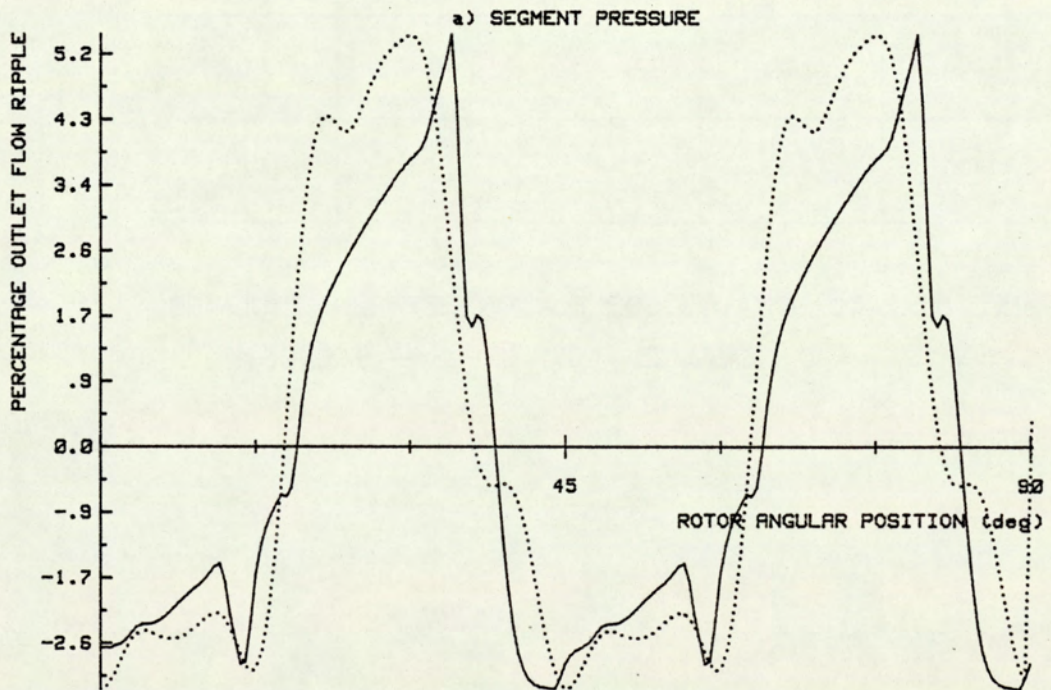
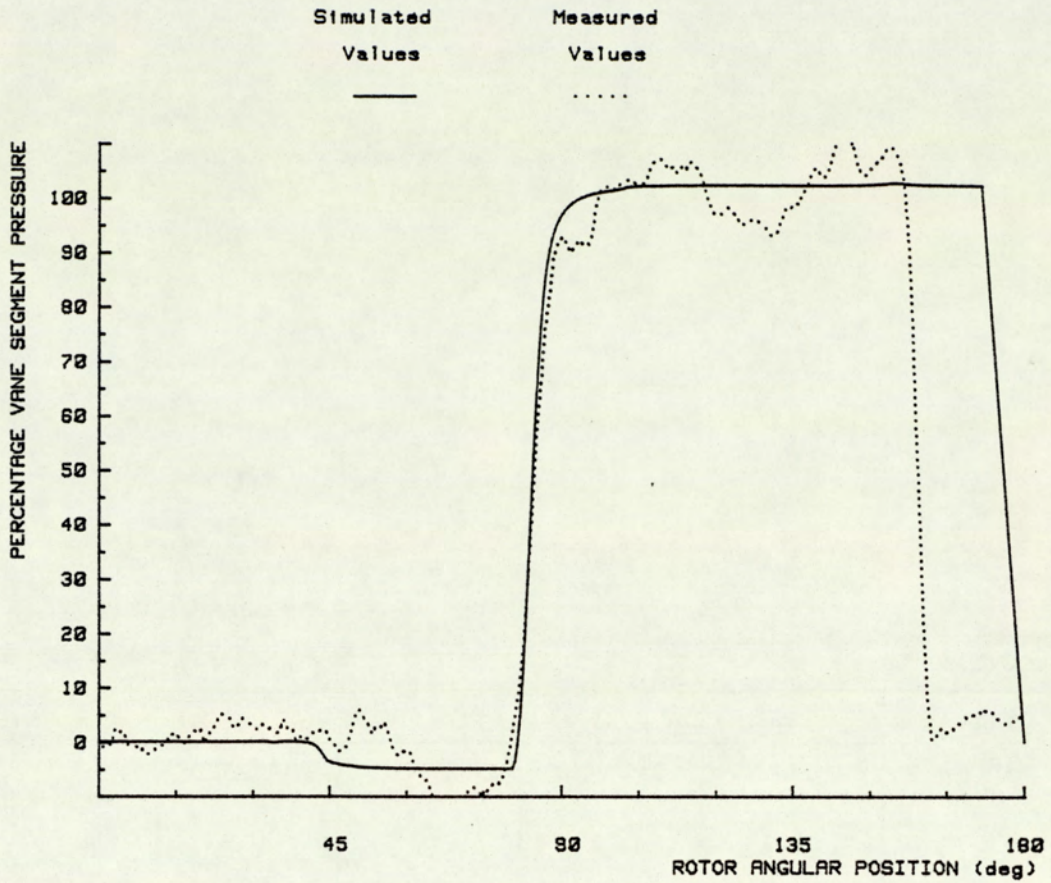
: Mean Inlet Pressure : Mean Outlet Pressure : Shaft Speed :  
 6.3 bar                      68.9 bar                      700 rpm

Fig.8.3.4 PERFORMANCE CORRELATION OF SILENCED PUMP AT 700 RPM



: Mean Inlet Pressure : Mean Outlet Pressure : Shaft Speed :  
6.3 bar 68.9 bar 1050 rpm

Fig.8.3.5 PERFORMANCE CORRELATION OF SILENCED PUMP AT 1050 RPM



: Mean Inlet Pressure : Mean Outlet Pressure : Shaft Speed :  
 6.3 bar : 68.9 bar : 1400 rpm

Fig.8.3.6 PERFORMANCE CORRELATION OF SILENCED PUMP AT 1400 RPM

GROOVED DATA

SPEED (RPM)	MEAN FLOW (l/s)		PEAK TO PEAK FLOW (%)	
	EXPERIMENTAL	SIMULATED	EXPERIMENTAL	SIMULATED
700	1.16	1.06	21.1	17.5
1050	1.85	1.75	16.4	11.2
1400	2.53	2.44	14.1	8.61

TABLE 8.3.2 QUANTITATIVE CORRELATION BETWEEN SIMULATED AND MEASURED FLOW RIPPLE – SILENCED

### 8.3.2 Performance of Silenced Pump

The correlation data for the silenced pump is presented by the figures (8.3.4) to (8.3.6) and table (8.3.2). A similar correlation technique is applied for the silenced pump as for the earlier standard pump data. The segment pressure history, and the flow ripple are drawn with the experimental data suitable scaled and superimposed on the theoretical data. The experimentally derived flow ripple is, as previously, re-synthesised from the first ten harmonics of the time averaged spectrums.

A good correlation can be seen for the segment pressure history at the three speed conditions. The two discrepancies (explained in the earlier section), is again apparent. This is at the 40 to 60 degree and the 150 degree rotor position. The effects of the silencing grooves are seen to correlate well, both at the inlet and the outlet. The effects of the outlet groove are more apparent, with the resulting earlier and more gradual pressurisation of the segment. At the inlet, the effect of the groove is to delay the fall of the segment pressure in the 40 to 60 degree rotor position. The groove enables a limited pathway between the port and segment, even after the trailing vane has swept past the inlet port. The result of which is to delay the fall in segment pressure for the duration of the effectiveness of the inlet groove. This is seen in both the theoretical and experimental data.

The flow ripple simulations are qualitatively well correlated. The trends in the variability of the simulated flow are reflected in the experimental data. There is observed, however, a significant difference between the experimentally and theoretically predicted ripple levels.

In the region studied, the flow ripples were experimentally determined to be 21.1, 16.4 and 14.1 percent. In comparison, the simulated levels were 17.5, 11.2, and 8.61 percent respectively. This reflects a mean underestimation in the percentage flow ripple of 5.49 percent of the mean flow. The trend of reduction in percentage flow ripple with speed can be seen to be consistent in both the experimental and theoretical data.

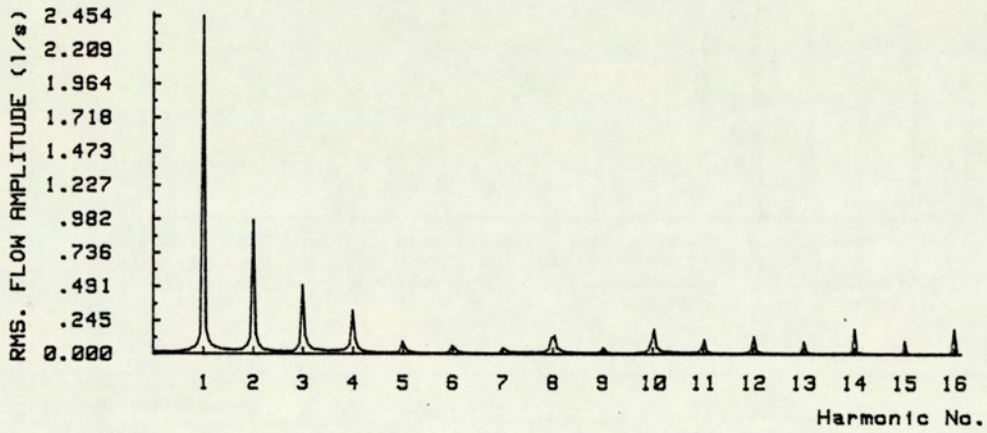
#### **8.4 Conclusion on Pump Model**

The data provided indicates a good correlation between the theoretical and experimental values. In the case of the standard pump, correlation was achieved within 6.3 to 8.7 percent of the experimental levels. The amplitude levels for the silenced pump was less well correlated, with discrepancies of 17.1, 31.7, and 38.9 percent of the experimental levels, for the speed condition of 700, 1050 and 1400 rpm.

With most pumps, operating under realistic conditions, leakage forms only a small percentage of the total flow of the pump. The pump was tested under non-typical condition of extremely high end-plate and small vane tip clearances, resulting in an exaggerated leakage fluctuation and changes in segment pressure variations. Under these conditions the leakage levels were typically 12.3, 9.61 and 7.56 percent of the swept volume at 700, 1050 and 1400 rpm respectively. The pump model adopts a theoretical estimation of leakage levels based on optimum design values. Local variations in geometry can lead to significant increases in the fluctuation levels.

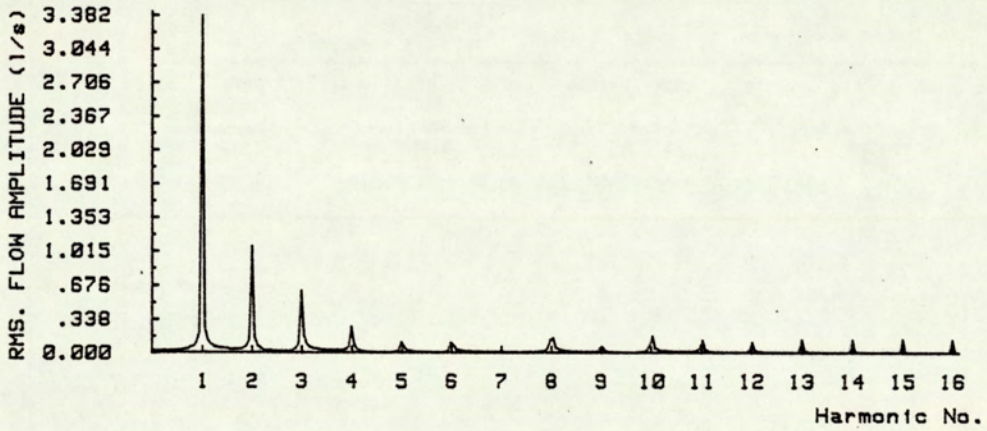
While operating under the standard pump configuration, the dominant mechanism of flow fluctuation is that due to fluid compressibility

Filename:FGDT00:T14



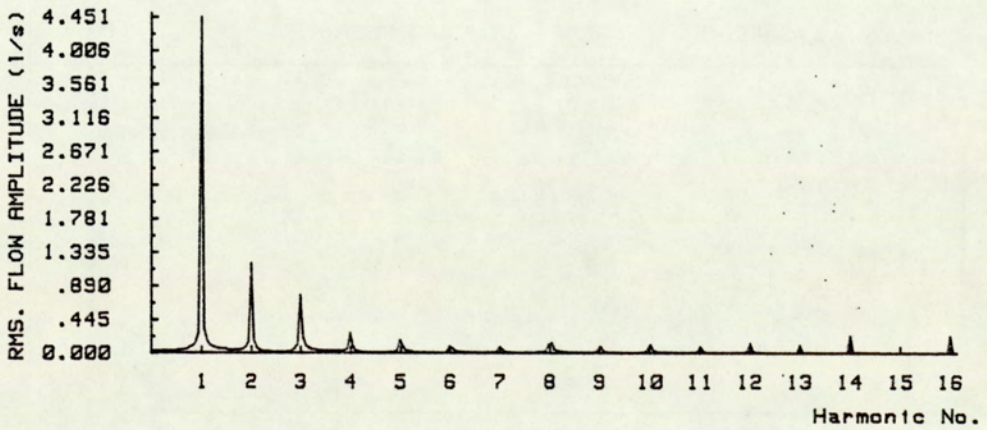
a) END-PLATE CLEARANCE : 0.0525 mm.

Filename:FGDT02:T14



b) END-PLATE CLEARANCE : 0.0600 mm.

Filename:FGDT04:T14



c) END-PLATE CLEARANCE : 0.0675 mm.

Fig.8.4.1 END-PLATE CLEARANCE EFFECTS ON OUTLET SPECTRUM

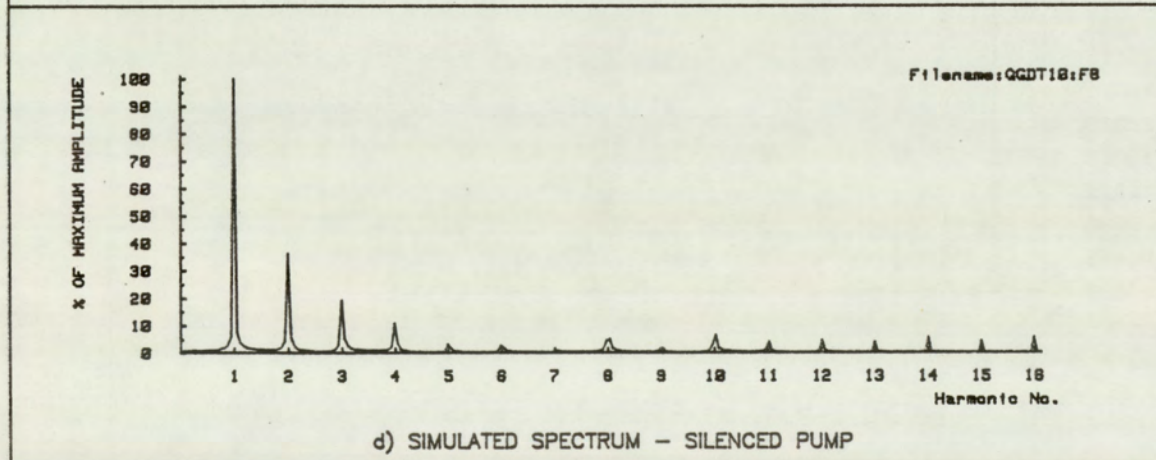
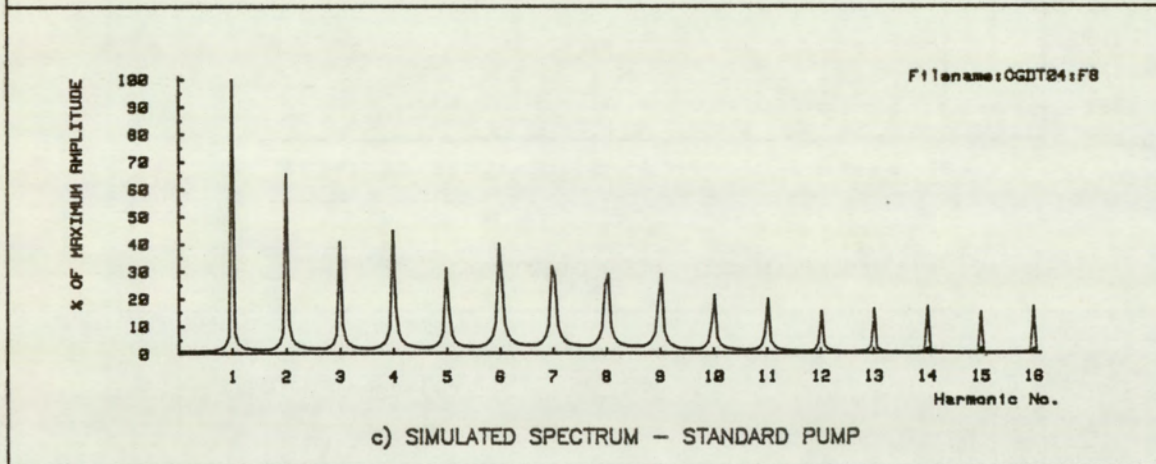
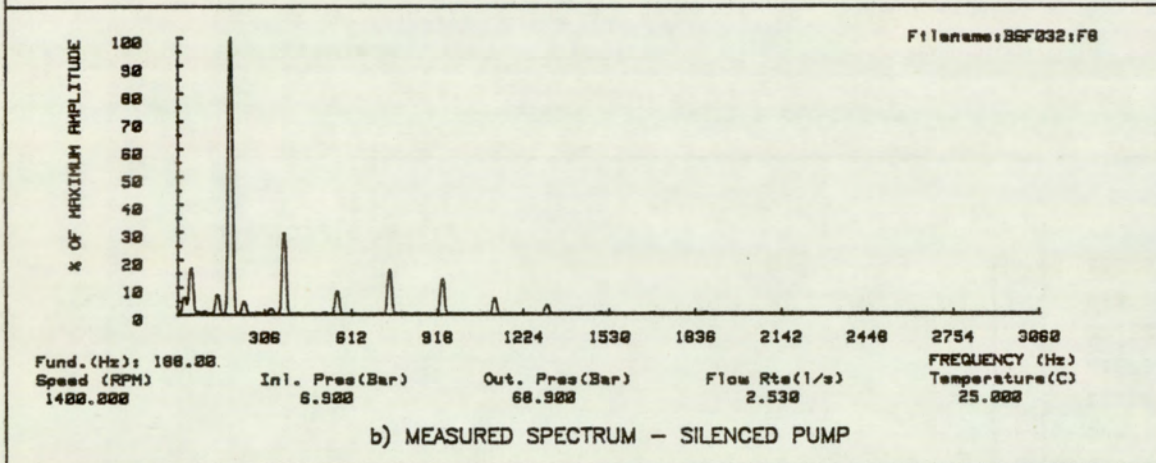
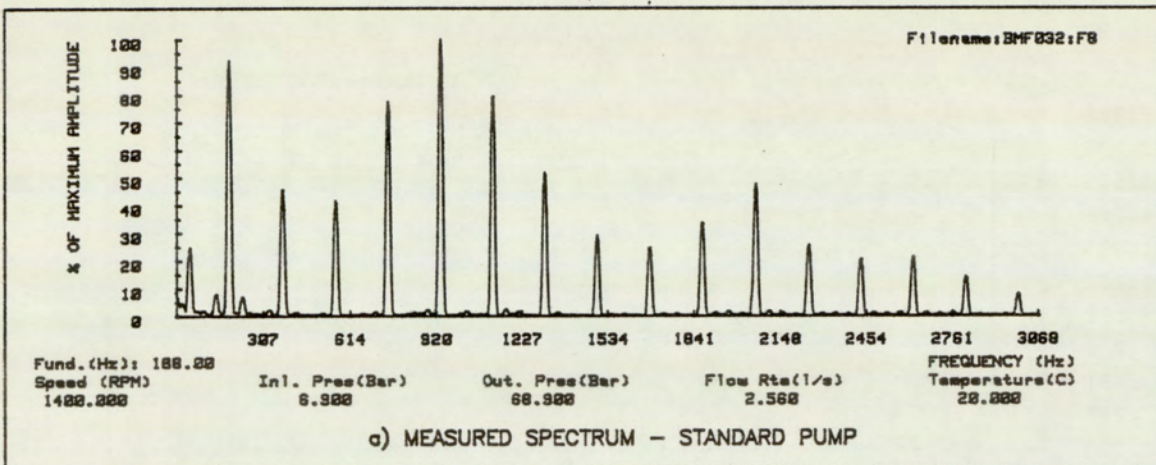


Fig.8.4.2 OUTLET SPECTRUM OF STANDARD AND SILENCED PUMP

and the back-flow of fluid into the segment volume at the moment of initial port communication. Under these conditions, any discrepancy between the simulated and actual leakage variations results in only a minimal effect on the simulated flow levels. With the case of the silenced pump, very little (if any) of the flow fluctuation due to the back-flow and compressibility effects remains. The flow fluctuations are based almost completely on leakage effects. Under these conditions accurate estimation of the leakage flow fluctuations is essential to enable precise simulation of flow fluctuation. A small discrepancy between the actual and estimated levels would result in a large percentage error between simulated and measured values.

In an earlier section, two figures (8.2.1) and (8.2.2) were presented, as being the spectrum of the outlet flow for the standard and silenced pump. Following from the theoretical observations made in chapters 7 and 8, the increase in amplitude of the lower harmonics are not to be expected in practice. The simulations of figure (8.4.1) shows the effects of changes in end-plate clearances on the spectral output of the outlet flow. Three simulations were made at end-plate clearances of 0.0525, 0.06 and 0.0675 millimetres. The mean value of 0.06 millimetres was that used in the correlation studies. The increase in end-plate clearance, in the range presented, resulted in a comparable increase in the amplitude of the fundamental component to that observed in the experimental spectra. The variations cited in the simulations are within the range expected, due to measurement errors and re-assembly variations.

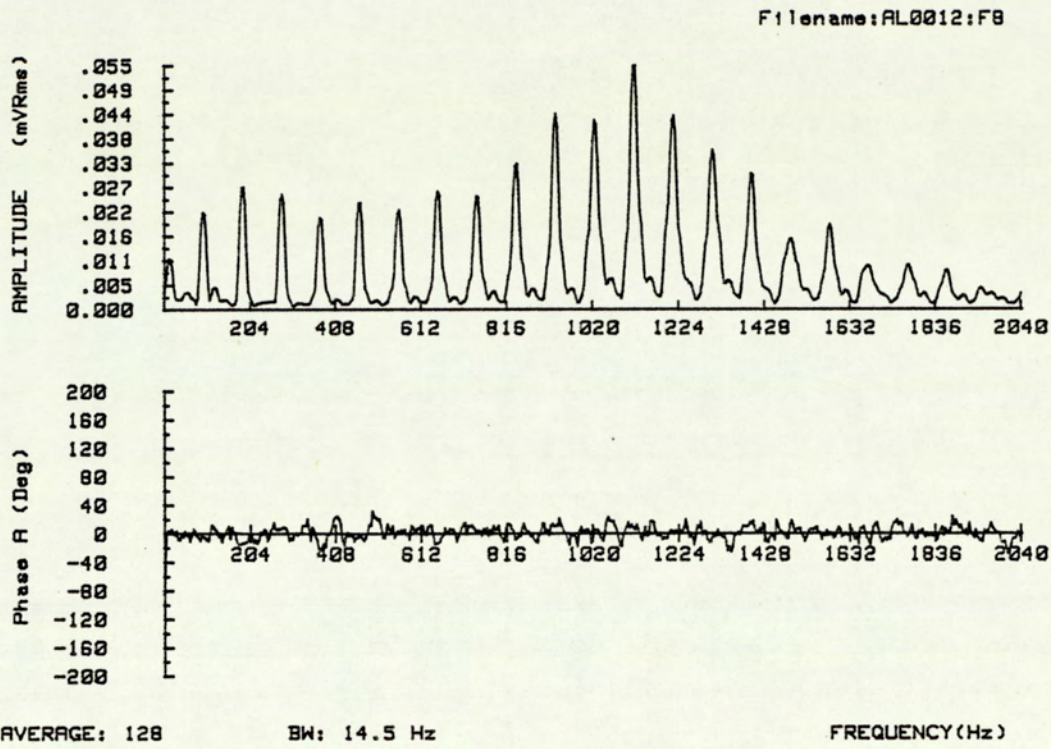
The effectiveness of the model is re-affirmed by figure (8.4.2) which provides and compares the spectral content of the pump outlet flow ripple, derived from both theoretical simulations and experimental

measurements. Figures (8.4.2a) and (8.4.2b) provides the experimental data and figures (8.4.2c) and (8.4.2d) the simulated data for the standard and silenced pump respectively. As indicated in the earlier section (8.3.1), there is a significant broad band system effect at the frequency of 1000 and 2000 Hz. Accounting for this effect, which manifest itself as an accentuation of the spectra at these frequencies, the diagrams shows a good correlation of the frequency spectra of both the standard and silenced pump. The effectiveness of the silencing grooves in reducing the higher frequency harmonics is clearly shown.

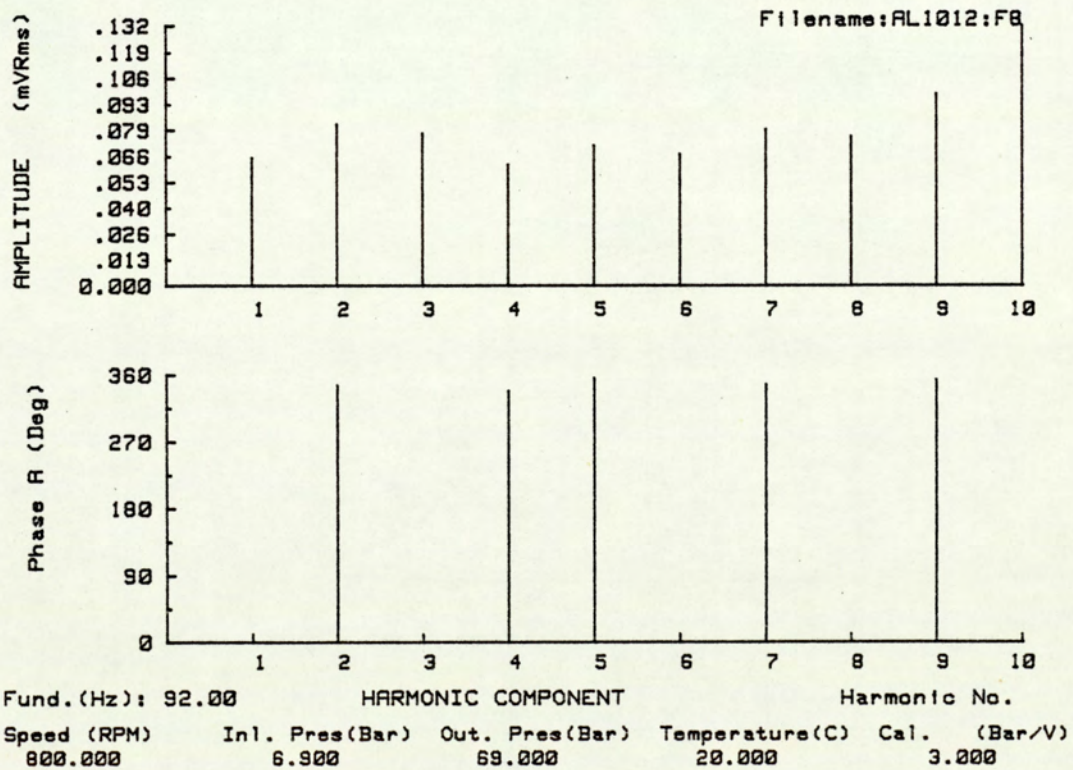
The pump model has been shown to be an effective tool for design and verification. The model has been used effectively to design silencing grooves which has significantly reduced the flow fluctuations. Over the speed range, the flow ripple has been reduced to a typical value of 53.7 percent of the original levels, representing a 5.4 dB reduction in the fluid borne noise output at the expense of a marginal decrease in efficiency. The silencing grooves resulted in a mean decrease in efficiency of 2.29 percent, over the speed condition studied. The loss in efficiency results primarily from an increase in end-plate leakage. In practice end-plate clearances are typically much smaller and thus a lower loss in efficiency can be expected.

## **8.5 Acquiring Transmission Line Data**

The aim of the experiment was to investigate the method of unravelling the standing wave effects (described in chapter 4). The first step was to determine the pump signature under supposedly anechoic conditions at a chosen datum of operating speed 800 rpm., inlet pressure 6.9 bars, outlet pressure 69.0 bars and fluid temperature 20 degrees Centigrade.



a) Full Spectrum



b) Harmonic Content

Fig.8.5.1 ANECHOIC DATA

Amplitude:Lin

DIRCH1:F8

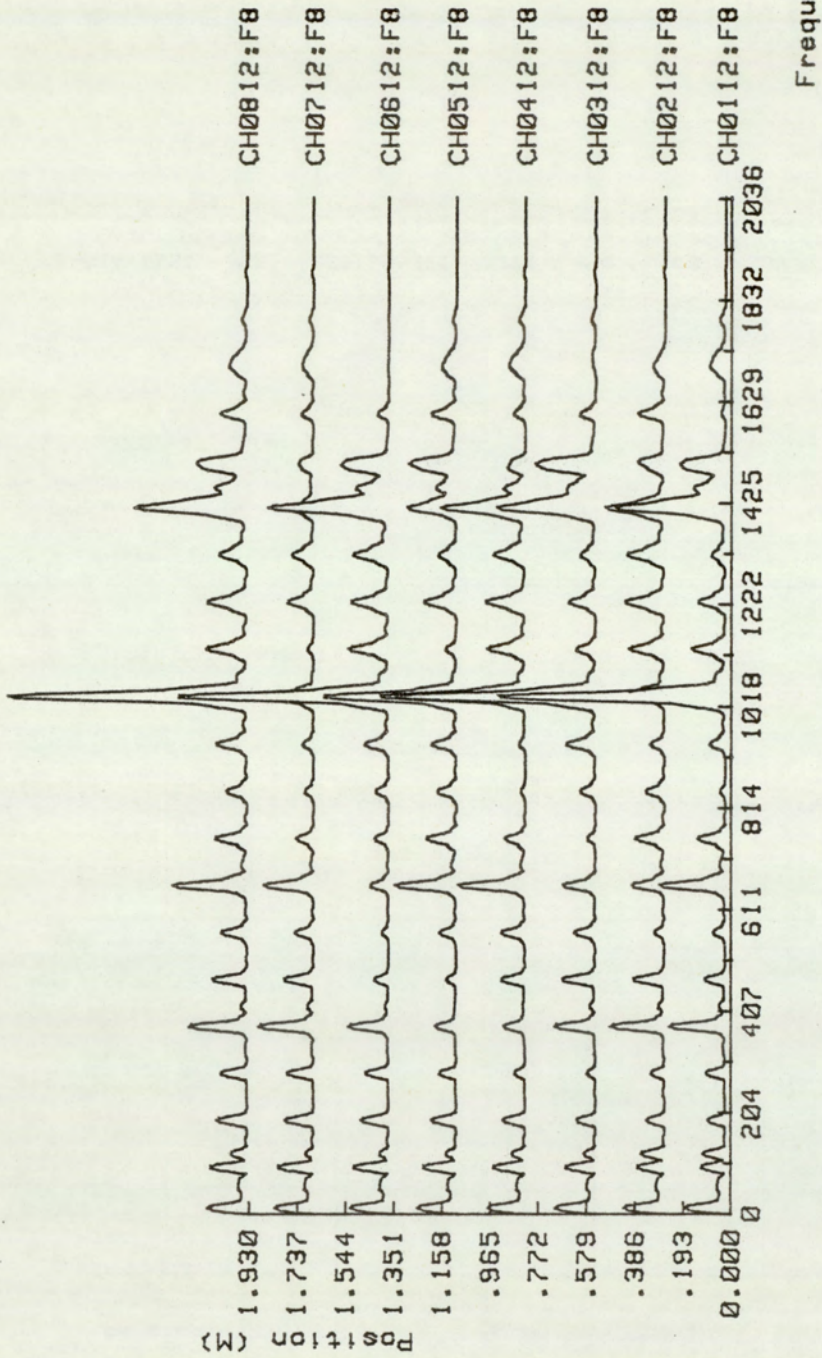


Fig. 8.5.2 SPECTRAL MAP OF REVERBERANT CHAMBER

The full and the harmonic spectrum at the outlet of the pump under this condition, is shown in figure (8.5.1). The spectrum represents a 256 point averaged spectrum of the pump output. In this study the frequency bandwidth of interest is restricted to within the first and the tenth harmonic, thus giving a frequency range of 93.3 to 933 Hertz.

On establishing the pump signature, the test was repeated with the chamber connected inline. While running at the datum condition, simultaneous recordings were made of the pressure transducer readings. Similar to the anechoic data analysis, the spectral content at the eight transducer points were determined. The figure (8.5.2) shows the full spectrum distribution measured along the chamber. This type of presentation is known as a 'Waterfall Diagram'. The spectrums are drawn on an offset Y-axis, determined by the transducer position, and the amplitudes are represented by the distance from the mean offset.

This diagram highlights the problem encountered in measuring the pump performance under the influence of standing wave effects. The spectrums were measured simultaneously, under the same operating conditions. The amplitudes are, however, seen to vary considerably depending on the position of the transducer.

Prior to unravelling the anechoic data from the standing wave effects, the amplitudes of the harmonic component along the chamber was first determined for each of the ten harmonic components of interest.

#### **8.5.1 Standing Wave Data**

Given the amplitudes of the various components along the line, the standing wave equation was solved using the 'Least-squares' method

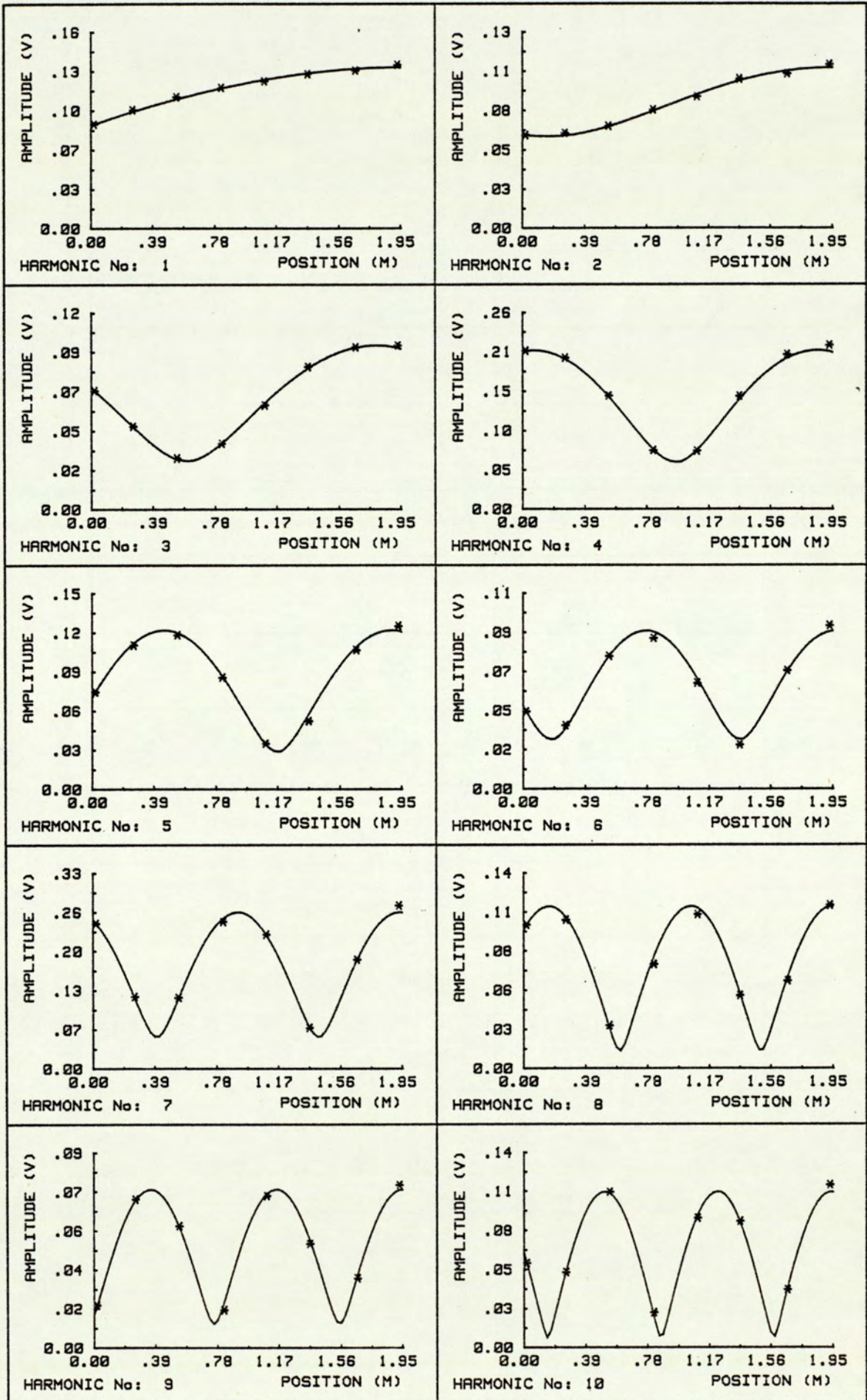


FIG.8.5.3 STANDING WAVE IN REVERBERANT CHAMBER

HARMONIC NUMBER	FREQUENCY (Hz)	HARMONIC AMPLITUDES (V)			PERCENTAGE ERROR
		BASIC	SCALED	ANECHOIC	
1	93.3	0.077	0.066	0.066	-
2	186.7	0.102	0.087	0.083	4.8
3	280.0	0.082	0.069	0.078	11.5
4	373.3	0.076	0.065	0.062	4.8
5	466.7	0.088	0.075	0.072	4.2
6	560.0	0.072	0.062	0.067	7.5
7	653.3	0.101	0.086	0.080	7.5
8	746.7	0.080	0.068	0.070	2.9
9	840.0	0.068	0.058	0.098	40.8
10	933.3	0.080	0.068	0.133	48.8

TABLE 8.5.1 QUANTITATIVE CORRELATION BETWEEN ANECHOIC AND DERIVED PRESSURE AMPLITUDES

developed in chapter 4. As described earlier (chapter 4), the solution proceeds with the determination of the wave propagation constant and the termination constant. With a knowledge of these unknowns, the solution proceeds to determine the values of the source reflection constant and the effective anechoic amplitude of the particular harmonic component. The procedure is repeated for each of the other components.

The figure (8.5.3) summarises the solution obtained for each of the harmonic components and the obtained fit. The symbol '\*' marks the magnitude of the measured harmonic component at the particular position along the chamber, and the full line describes the solved standing wave function.

In attempting to solve a multi-degree of freedom problem, there exists a number of mathematical solutions. Some of these, however, lead to non-physical solutions and must be rejected. In the search for a real solution, the values of the reflection constants are constrained to a modulus of less than or equal to 1. A value greater than 1 infers a reflected wave of greater amplitude than the incident wave, thus resulting in a non-physical solution. The solution was obtained using a computer program developed to implement the solution technique.

The table (8.5.1) shows the correlation between the directly obtained and the derived anechoic levels. The table expresses the amplitudes in volts and can be directly related to pressure levels. The tabled anechoic levels expresses that measured for a 30 millimetre bore, and the chamber had a 88.9 millimetre bore. Before comparing the amplitude levels, the derived anechoic levels have to be related to the same bore size. Using the equations (4.5.1) and (4.5.7), we obtain a scaling factor of 8.51. Combined with a calibration factor of 0.1 reduces

this to 0.851. The scaling factor of 10 was introduced into the data to avoid the calculation errors relating to the processing of small values. The table shows a variation in error of between 0 to 48.8 percent. When the two highest frequency harmonics are excluded, the error is reduced to a maximum of 11.5 percent, and a mean of 5.4 percent.

### **8.6 Conclusion on Transmission Line Model**

The good correlation between the anechoic data and the data derived from the reverberant chamber suggests the validity of the analysis. The method has also been shown to be relatively simple to operate and provides good correlation over a wide range of frequencies, given only a relatively small number of transducers. The poor correlation at the nine and tenth harmonic reflects the fundamental problem relating to the optimising of the transducer position, for a given number of transducers.

The standing wave function is cyclic and repeats itself at a wavelength along the line. To define the function effectively, the transducer must provide mutually exclusive data points. At the lower frequencies up to that whose wavelength is greater than the line length, an evenly spaced transducer layout provides the necessary conditions for a good fit. As the frequency increases, and the wavelength decreases, the mutually exclusive condition cannot be guaranteed. A worst case is possible where the only exclusive transducer readings exists within the first cycle, and subsequent data are but a cycle along and in phase. The situation existing with the nine and tenth harmonic are tending towards this condition.

For a given frequency range, a solution is to provide a greater number of transducers. This, however, increases both analysis problems and cost. An alternative method would be to distribute a given number of transducers more effectively. This can be achieved by positioning the transducers such that two-thirds of the transducers are located at one half of the line and the remaining third at the other half. Within these groups, the transducers should be distributed evenly. This distribution would improve the mutually exclusive condition of the data at the higher frequencies and not compromise unduly the conditions at the lower frequency end.

### **8.7 Procedure for the Deconvolution of Pressure Ripples**

Due to a change in the project schedule, the technique awaits the implementation on the 'back to back' test rig. This section, however, outlines the rig schematic and details the procedures to be adopted in applying the techniques developed for the deconvolution of the pump, motor pressure ripples from the unwanted system effects.

The rig comprises of two hydraulic propulsion motors coupled together. The motors are identical except that one is operated as a pump. The main fluid supply is from the pump into the high pressure line, through the motor and returns back to the pump via an oil cooler. The leakage that occurs is made up by external make-up pumps, and the pump-motor combination is driven by another motor. In addition to the standard mean pressure gauges, a set of eight piezo-electric dynamic pressure transducers and a proximity switch are installed to provide the necessary dynamic pressure measurements and synchronization signal. The dynamic pressure transducers are distributed evenly, where

possible, around the steel high pressure line. The proximity switch is located on the pump-motor coupling shaft. Prior to data acquisition, the signal from the pressure transducers and proximity switch require the appropriate signal conditioning. The signal from the piezo-electric transducers are converted from a charge to a voltage proportional to the dynamic pressure variations, and the proximity switch signal is processed by a Schmitt trigger to produce a clean square pulse.

The technique for the deconvolution of the individual pump, motor involves two stages. The first stage involves the unravelling of the superimposed pump and motor pressure ripples from the standing wave effects, and the second stage that of separating the individual pump and motor ripples. Although the standing wave effects can be obtained from the eight pressure measurements at one run, the decoupling of the individual pressure ripple effects require data at different phase settings. This is required to provide the necessary data for the solution of the equation (4.7.21) to (4.7.25) which contains three unknowns. If the initial phase setting of the pump and motor are known, only two runs are required to determine the two unknowns of individual pressure ripple amplitudes. As it is difficult to determine accurately the initial phase setting, the alternative scheme of adopting the the initial setting as a datum, and obtaining two further runs at known phase variations is preferred. This, however, requires the additional third run.

At each run, data is simultaneously acquired and stored on a tape recorder possessing the required dynamic range. The data is then available for processing at a later date. Data processing begins with the Fourier analysis of the pressure ripples measured at the eight transducer positions for the three runs, at different phase settings.

From this spectral data, the harmonic components are extracted for unravelling. The individual harmonic component are observed to vary in amplitude along the transmission line. This is due to the standing wave effects. The standing wave effects are removed using the numerical analysis techniques detailed in section (4.7.1) and demonstrated in section (8.5). When the standing wave effects are removed, three amplitudes at each harmonic components are left. Using the equations, derived in section (4.7.2), the individual pump and motor pressure ripple components are derived. The procedure is repeated for each of the harmonic components of interest.

## **CHAPTER 9 : CONCLUSION**

9.1 Conclusion

9.1.1 Conclusion on Pump Model

9.1.2 Conclusion on Transmission Model

9.2 Recommendation for Further Work

## **9.1 Conclusion**

This thesis describes the work undertaken, by the author, in part fulfilment of the responsibilities of the University of Aston towards the research and development programme described earlier (chapter 1). The work identified at the start of the project was that of developing a radial vane pump model. A model was required which could enable the assessment of the original fluid borne noise potential, and to study the effects of various parameters and relief grooves, for the purpose of reducing the identified noise level. In addition, a transmission model and technique was required which could be applied to unravel the effects of the standing wave in a transmission line.

In the preceding chapter (chapter 8), results were presented to enable a correlation between actual measurements and the theoretical model developed. For both these models, good correlation was achieved between theoretical and experimental results.

### **9.1.1 Conclusion on Pump Model**

The resources required to develop a new hydraulic pump is costly in terms of both money and time. With the aid of computer simulation, the development cost and time can be significantly reduced. Taking the particular case of this radial vane pump, there were many development problems to be tackled before the actual noise potential could be ascertained. At the initial stages of development, the fluid borne noise measurements were not necessarily indicative of the true noise levels of a fully developed pump. Through simulations, the computer model would provide an insight into the factors affecting the noise level and indicate the levels to be expected.

At the early stages of development, the vane tips were not extended out to the required clearance. This resulted in a condition which was beneficial in terms of the fluid borne noise levels, and measurements taken at this stage underestimated the true noise potential. During another period of the development, the vane tip clearance was over corrected leading to untypically small clearances. In addition, the effect of a larger than designed end-plate leakage resulted in an accentuated noise level.

In an attempt to improve the computation time required for each simulation, a semi-analytical technique (chapter 3) was implemented for the solution of the 'flow-pressure' equation. This technique has been shown to be significantly faster and less prone to numerical instability in comparison to the standard 'Runge-Kutta' or 'Gear' method, for the solution of the non-linear first order differential equation (3.5.8). The method assumes that leakage is a secondary component within an iterative step. As mentioned earlier (chapter 3), no significant loss in solution accuracy will result if sufficiently small iterative steps are taken. The good qualitative and quantitative correlation presented in chapter 8, indicates that the 'approximation' does not affect the accuracy of the solution, to any discernible extent.

The application of the program for the purpose of designing silencing grooves has also been demonstrate. A significant reduction in fluid flow ripple was obtained at the expense of a minimal reduction in efficiency. The most significant reduction in the percentage flow ripple was observed at the lower speed. At 700 rpm, the percentage flow ripple was reduced from 44.1 to 21.1 percent of its mean flow. This was achieved with a 4.1 percent reduction in efficiency, thus representing

a 6.4 dB reduction in the ripple values. The typical reduction over the speed range of 700 to 1400 rpm was 5.4 dB with a corresponding loss in efficiency of 2.29 percent. With typical end-plate clearances, the losses in efficiency can be expected to be reduced.

The results of the simulation studies indicate that there is a very broad range of operation for which the silencing grooves are effective. This has been verified by the experimental measurements made of the pump operating under a wide range of line pressures and speed.

Although the problem of structural borne noise has not been studied, measurements were made of the structural vibration on the casing of the pump. The reduction in structural noise has been significant. As a consequence of the implementation of the silencing grooves the typical case vibration was reduced by 20 dB.

### **9.1.2 Conclusion on Transmission Model**

The data presented in chapter 8, demonstrates the 'Least-squares' method, developed in chapter 4, for unravelling the effects of standing waves. The good correlation obtained between the datum anechoic data and the unravelled amplitude confirms the validity of the technique. Excluding data at the two highest frequencies, correlation was achieved with an error of less than 11.5 percent and a typical error of 5.4 percent.

The 40.8 and 48.8 percent discrepancy at the ninth and tenth harmonic respectively, is attributed to the poor positioning of the transducers in relation to the standing wave pattern. An alternative transducer distribution has been suggested which would improve the mutually

exclusive condition of the data at the higher frequencies, without compromising the conditions at the low frequency end. The recommended layout is such that two thirds of the available transducers are evenly distributed at one half of the line and the remaining transducers at the other.

The technique was primarily developed to enable the derivation of the equivalent anechoic data from measurements along the transmission line under the influence of standing wave effects. Although the experimental work described in chapter 8 demonstrates the ability of the technique developed for this application, the method is not intended to be used as a general means of deriving anechoic data. This is due to the amount of intermediate data processing required to obtain the data. The method is, however, applicable when it is not possible or impractical to implement a test under normal anechoic conditions. The work is also beneficial as it further demonstrates the usefulness of the transmission line theory in the modelling of hydraulic transmission systems.

The problem of numerical instability was encountered while seeking a direct solution of the full standing wave equation. This problem was effectively overcome by approaching the solution in two stages. When the pressure is expressed in terms of a datum, the number of unknowns are reduced. This decreases the number of unknowns at each stage of the solution and significantly improves the stability of the solution technique, thus resulting in a successful solution.

## 9.2 Recommendation for Further Work

The radial vane pump program has successfully progressed through the 'author validation' stage of development, and has been demonstrated to be useful to the designer. It is recommended that the program be further tested and developed for an industrial design environment. In some less demanding design applications, it is possible to further optimise the program for quicker simulation.

The program has been designed and developed encompassing structured programming techniques. This results in software which is highly modular. Modularity implies independent program segments which can be identified to perform specific tasks. The modular nature of the program lends itself to further development, to include pumps of a different physical configuration.

The program was developed using a simplified theoretical estimation of leakage levels. Under 'silenced' conditions where leakage is dominant, it was observed that there was a significant discrepancy between the measured and simulated leakage values. By employing a more complex theoretical model for leakage or by using an experimentally based leakage model, the leakage estimates may be improved. This is, however, not necessary for the intended application of designing quieter pumps.

The testing of pumps using anechoic terminations is an accepted means of obtaining fluid borne noise data, as it is obtained while operating under conditions representative of normal operations. The implementing of anechoic terminations can, however, at times prove to be expensive and difficult to implement. Due to the effects of standing wave, direct measurement of the pressure wave is not possible.

The application of frequency response techniques are widely applied in

other engineering fields, particularly in structural vibration. If a transfer function can be defined for the reverberant termination, relating the anechoic to the measured pressure levels, pump testing could be simplified. The single measurement at the pump output could be directly transformed to give the required results. In hydraulic applications, there are specific problems which have to be solved before the techniques can be applied.

## APPENDIX A : GEOMETRICAL RELATIONSHIPS

- A.1 Cam Actuation Profile
- A.2 Silencing Groove Geometry
- A.3 Port Geometry
- A.4 Segment Geometry

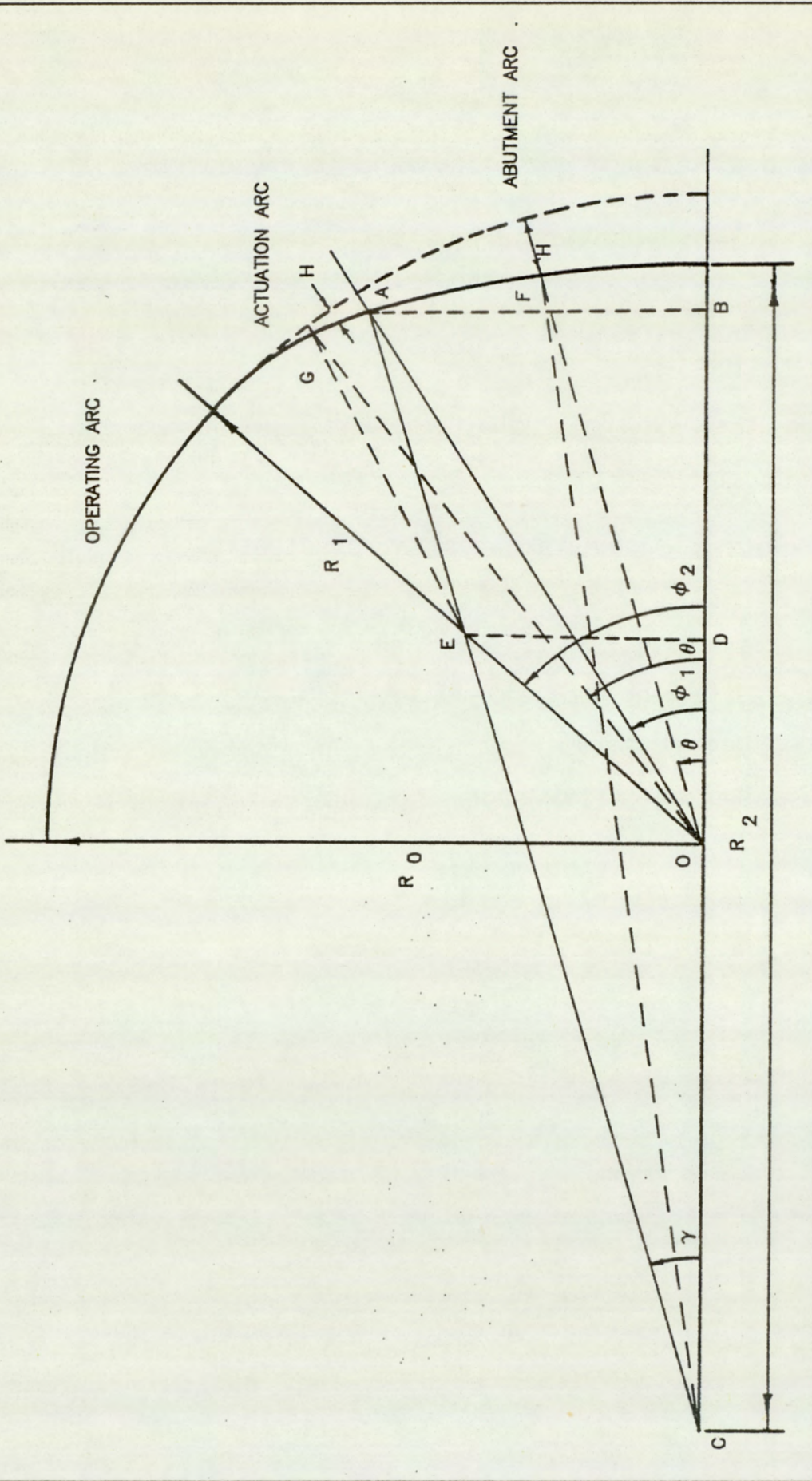


FIG.A.1.1 CAM PROFILE GEOMETRY

## A.1 Cam Actuation Profile

The cam profile defines the vane tip clearance at different rotor positions and consists of three different basic radii. During this cycle, the vane tip is gradually actuated so as to take it from the operating to abutment clearance. A well defined profile is required to minimise cam track stresses during operation. Details of the cam profile analysis can be found in the thesis by Wuerzer(3). In this section the cam profile is re-defined in terms of the three basic radii and the cam actuation angle. These are the parameters used to define the cam profile for manufacture.

With reference to the figure A.1.1, the parameters defining the cam geometry are:

- 1)  $R_0$  : operating radius
- 2)  $R_1$  : actuation radius
- 3)  $R_2$  : abutment radius
- 4)  $\phi_2$  : actuation angle

$$\tan \phi_1 = \frac{AB}{OB}$$

Where:

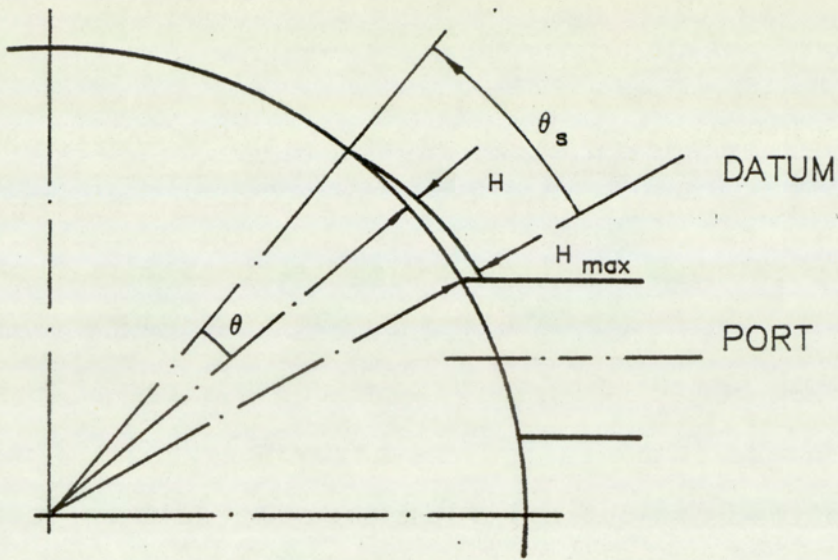
$$AB = R_2 \sin \gamma$$

$$OB = R_2 \cos \gamma - CO$$

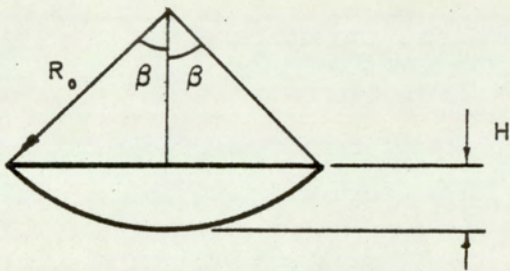
$$CO = (R_2 - R_1) \cos \gamma - OD$$

$$OD = (R_0 - R_1) \cos \phi_2$$

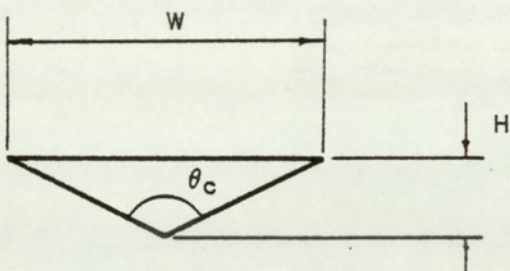
$$\gamma = \sin^{-1} \left( \frac{(R_0 - R_1) \sin \phi_2}{(R_2 - R_1)} \right)$$



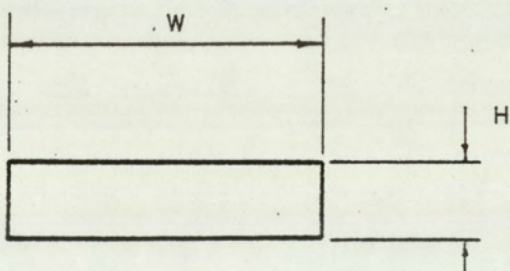
a) General Geometry



b) Hemispherical Sloping



c) Triangular Sloping



d) Square Sloping

FIG.A.2.1 Groove Geometry

Therefore:

$$\tan \phi_1 = \frac{R_2 \sin \gamma}{R_1 \cos \gamma + (R_0 - R_1) \cos \phi_2}$$

When:  $0 \leq \theta \leq \phi_1$

$$H = R_0 - OF$$

Where:

$$OF^2 + (2 \cdot OC \cdot \cos \theta) OF + OC^2 - (R_2)^2 = 0$$

When:  $\phi_1 \leq \theta \leq \phi_2$

$$H = R_0 - OG$$

Where:

$$OG^2 - [2(R_0 - R_1) \cos(\phi_2 - \theta)] OG + [(R_0)^2 - 2R_0R_1] = 0$$

and OF and OG are the roots of the quadratic equation.

## A.2 Silencing Groove Geometry

The silencing groove provides a controlled resistive path between the segment volume and the port. The resistance to flow is dependant on the available flow area offered by the groove. In this section is developed the relationship between rotor angular position, relative to a datum, and the groove cross-sectional area. Relationships for three different profiles; hemispherical, triangle and square are derived.

The figure A.2.1a defines the general groove parameters, which are common to all three profiles.

$\theta_s$  : groove start angle

$\theta$  : groove reference angle

H : groove depth at angle  $\theta$

$H_{\max}$  : groove depth at angular datum

The groove depth is defined by:

$$H = \left( \frac{H_{\max}}{\theta_s} \right) \theta \quad (\text{A.2.1})$$

Using trigonometry relationships, the following equations are derived, for conditions when the groove depth is less than the groove width.

Hemispherical Groove:

With reference to figure A.2.1b.

$R_0$  : cutter radius

$A_h$  : groove area for hemispherical groove

$$\beta = \text{Cos}^{-1}[1 - (H/R_0)] \quad (\text{A.2.2})$$

$$A_h = 2\beta/[\pi(R_0)^2] - (R_0)^2 \text{Sin}\beta \text{Cos}\beta \quad (\text{A.2.3})$$

Triangular Groove:

With reference to figure A.2.1c,

$\theta_c$  : cutter angle

$\theta_t$  : groove area for triangular groove

W : groove width

$$W = 2H \cdot \text{Tan}(\theta_c/2) \quad (\text{A.2.4})$$

$$A_t = H^2 \text{Tan}(\theta_c/2) \quad (\text{A.2.5})$$

Square Sloping:

With reference to figure A.2.1d,

W : cutter width

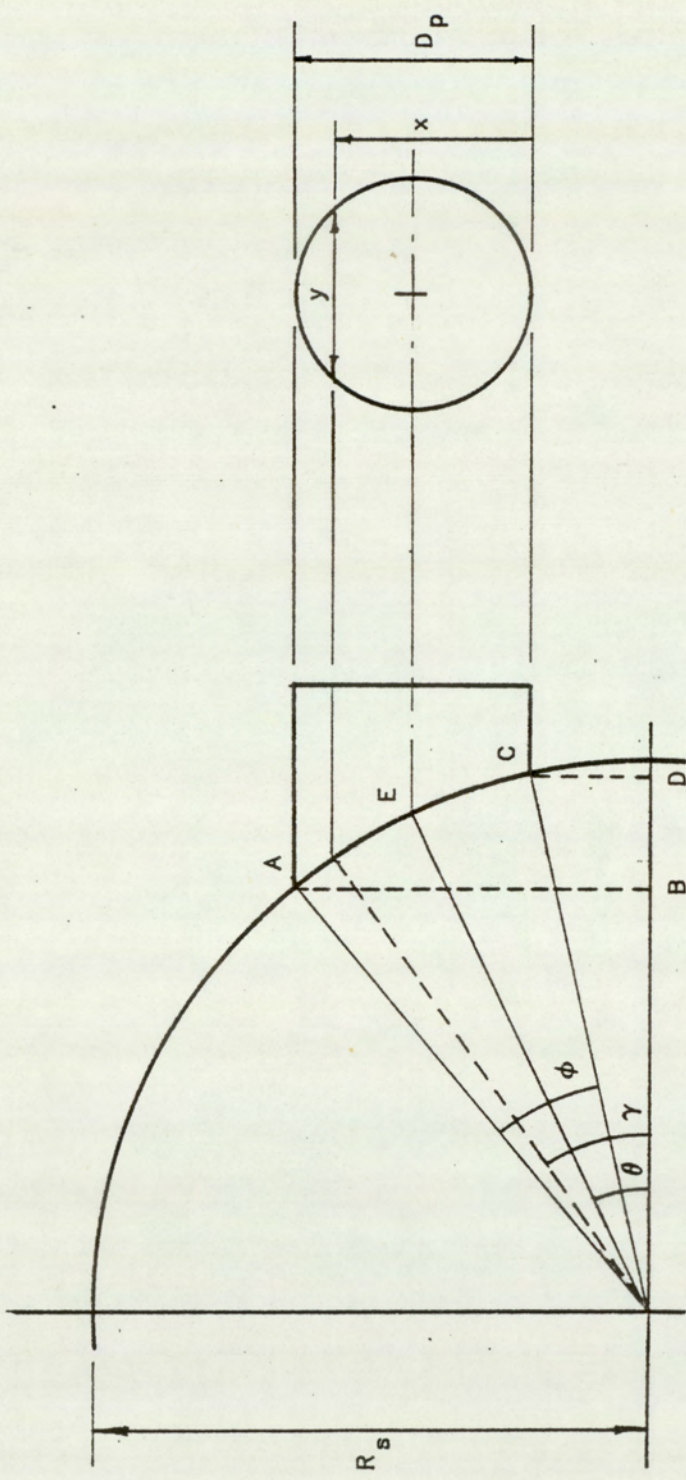


FIG.A.3.1 PORT GEOMETRY

$A_S$  : groove area for square groove

$$A_S = H.W$$

(A.2.6)

### A.3 Port Geometry

In this section, the geometrical relationship for the port and stator parameters are defined. These equations permit the port to be located, and its area to be defined, in terms of the stator angular position.

With reference to figure A.3.1, which defines the port parameters,

$$D_p = AB - CD \quad (A.3.1)$$

$$AB = R_S \sin[\theta + (\phi/2)] \quad (A.3.2)$$

$$CD = R_S \sin[\theta - (\phi/2)] \quad (A.3.3)$$

Where  $R_S$  is the stator radius.

Solving equation (A.3.1), (A.3.2) and (A.3.3) gives:

$$D_p = R_S [2 \cos \theta \sin(\phi/2)] \quad (A.3.4)$$

and

$$\phi = 2 \sin^{-1} \left( \frac{D_p}{D_S \cos \theta} \right) \quad (A.3.5)$$

Where:

$$D_S = 2R_S$$

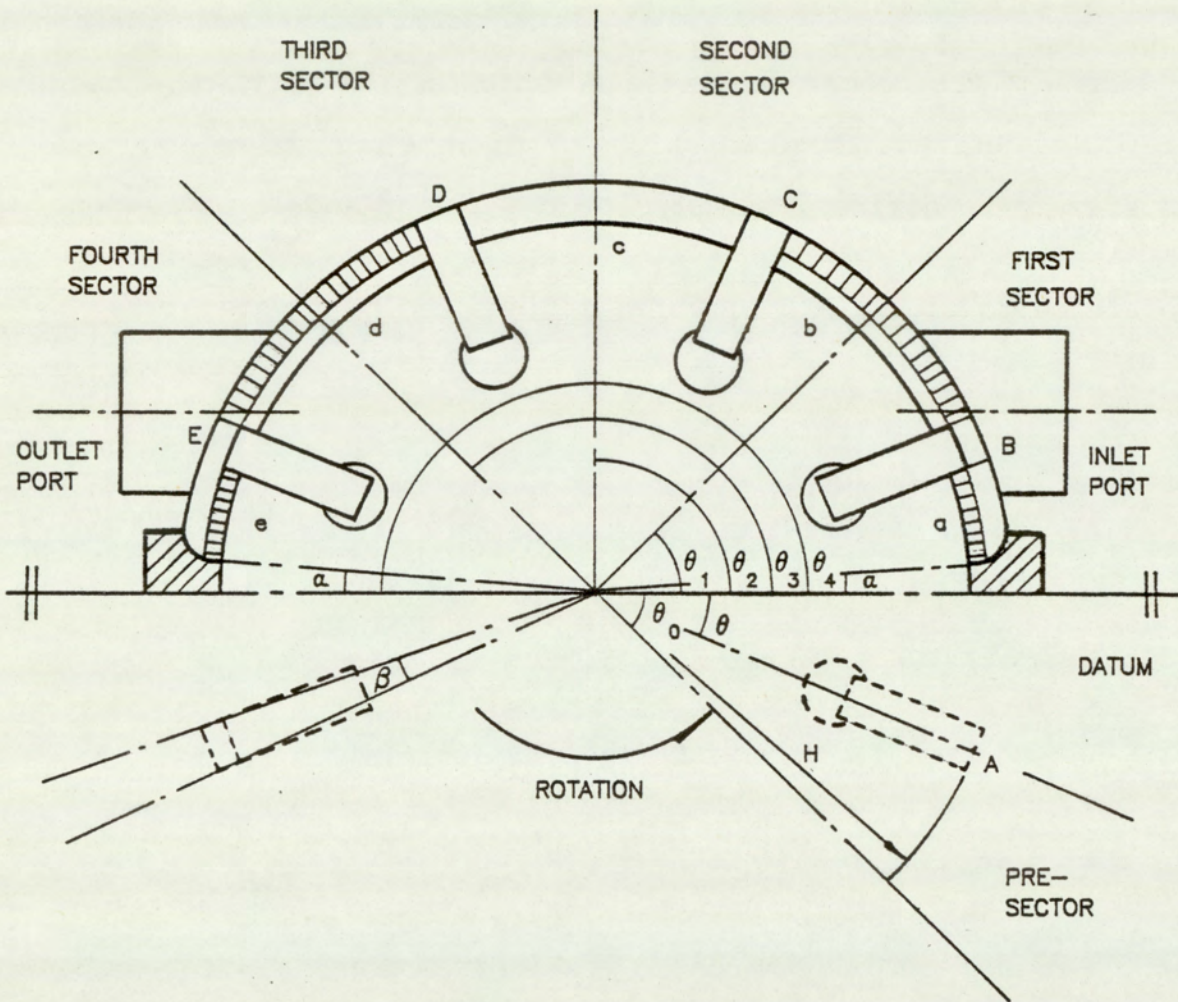


FIG.A.4.1 SEGMENT GEOMETRY

Also:

$$\left(\frac{D_p}{2}\right)^2 = \left(\frac{y}{2}\right)^2 + \left(x - \frac{D_p}{2}\right)^2$$

Giving:

$$y = 2\sqrt{x(D_p - x)} \quad (\text{A.3.6})$$

But

$$x = R_s \sin \gamma - CD \quad (\text{A.3.7})$$

The port area  $A_p$ , is thus defined:

$$A_p = \int_0^x y \, dx \quad (\text{A.3.8})$$

#### A.4 Segment Geometry

In this section the segment volume and the effective swept volume are defined with respect to the rotor angular position. The figure A.4.1 shows five vanes indicated by letters A to E. Corresponding to each vane is a volume which is referred to as the segment volume. The associated segment volume is indicated by the lowercase of the character defining the segment reference vane. The equations are derived for a general number of vanes. The geometrical symmetries assumed in section 3.2 are applied.

With reference to figure A.4.1

L : vane length

$\beta$  : angle subtended at centre by vane thickness at stator radius

- $\alpha$  : half the angle subtended by abutment width at centre  
 $H_1, H_r$  : vane tip extension for the leading and trailing vanes respectively  
 $\theta$  : reference vane angular position  
 $N$  : number of vanes  
 $D_s, D_r$  : stator and rotor diameters respectively

The sector limits are defined:

$$\theta_0 = -\gamma \quad (\text{A.4.1})$$

Where  $\theta_0$  is the start of pre-sector and  $\gamma$  is the vane pitch, defined by:

$$\gamma = 2\pi/N \quad (\text{A.4.2})$$

$$\theta_1 = \gamma \quad (\text{A.4.3})$$

Where  $\theta_1$  is the end of first sector

$$\theta_2 = 2\gamma \quad (\text{A.4.4})$$

Where  $\theta_2$  is the end of second sector

$$\theta_3 = (\pi - \gamma) \quad (\text{A.4.5})$$

Where  $\theta_3$  is the end of third sector

$$\theta_4 = \pi \quad (\text{A.4.6})$$

Where  $\theta_4$  is the end of fourth sector

The segment volume  $V$  is defined:

For  $-\gamma \leq \theta \leq [-\gamma + (\beta/2) + \alpha]$

$$V = 0 \quad (\text{A.4.7})$$

For  $[-\gamma + (\beta/2) + \alpha] \leq \theta \leq [\alpha - (\beta/2)]$

$$V = \frac{(D_S)^2 - (D_R)^2}{8} [\theta + \gamma - \alpha - (\beta/2)] \quad (\text{A.4.8})$$

For  $[\alpha - (\beta/2)] \leq \theta \leq [\pi - \gamma - \alpha + (\beta/2)]$

$$V = \frac{(D_S)^2 - (D_R)^2}{8} (\gamma - \beta) \quad (\text{A.4.9})$$

For  $[\pi - \gamma - \alpha + \beta] \leq \theta \leq [\pi - \alpha - (\beta/2)]$

$$V = \frac{(D_S)^2 - (D_R)^2}{8} [\pi - (\beta/2) - \alpha - \theta] \quad (\text{A.4.10})$$

For  $[\pi - \alpha - (\beta/2)] \leq \theta \leq \pi$

$$V = 0 \quad (\text{A.4.11})$$

The swept volume  $V_S$  is defined:

For  $-\alpha \leq \theta \leq [-\gamma + (\beta/2) + \alpha]$

$$V_S = 0 \quad (\text{A.4.12})$$

For  $[-\gamma + (\beta/2) + \alpha] \leq \theta \leq [\alpha + (\beta/2)]$

$$V_S = \frac{(2H_1)^2 - (D_R)^2}{8} L \quad (\text{A.4.13})$$

For  $[\alpha + (\beta/2)] \leq \theta \leq \gamma$

$$V_S = \frac{(D_S)^2 - (2H_R)^2}{8} L \quad (\text{A.4.14})$$

For  $\gamma \leq \theta \leq [\pi - 2\gamma]$

$$V_S = 0 \quad (\text{A.4.15})$$

For  $[\pi - 2\gamma] \leq \theta \leq [\pi - \gamma - \alpha - (\beta/2)]$

$$V_S = \frac{(D_S)^2 - (2H_1)^2}{8} L \quad (\text{A.4.16})$$

For  $[\pi - \gamma - \alpha - (\beta/2)] \leq \theta \leq [(\pi - \alpha - (\beta/2))]$

$$V_S = \frac{(2H_R)^2 - (D_R)^2}{8} L \quad (\text{A.4.17})$$

For  $[\pi - \alpha - (\beta/2)] \leq \theta \leq \pi$

$$V_S = 0 \quad (\text{A.4.18})$$

**APPENDIX B : SOLVING FOR THE ROOTS OF  
EQUATIONS (3.6.13) AND (3.6.19)**

- B.1 Introduction
- B.2 Algorithm 1
- B.3 Algorithm 2
  - B.3.1 Starting Point For  
Equation (3.6.13) At Branch (A.2.1)
  - B.3.2 Starting Point For  
Equation (3.6.19) At Branch (A.2.3)
- B.4 Algorithm 3
- B.5 Algorithm 4
  - B.5.1 Starting Point For  
Equation (3.6.13) At Branch (A.4.1)
  - B.5.2 Starting Point For  
Equation (3.6.13) At Branch (A.4.3)
- B.6.1 Solving for the roots of a  
non-linear equation
- B.6.2 Modified Regula-Falsi Method
- B.6.3 Newton-Raphson Method
- B.6.4 Algorithm for the solution of the root  
of the equation

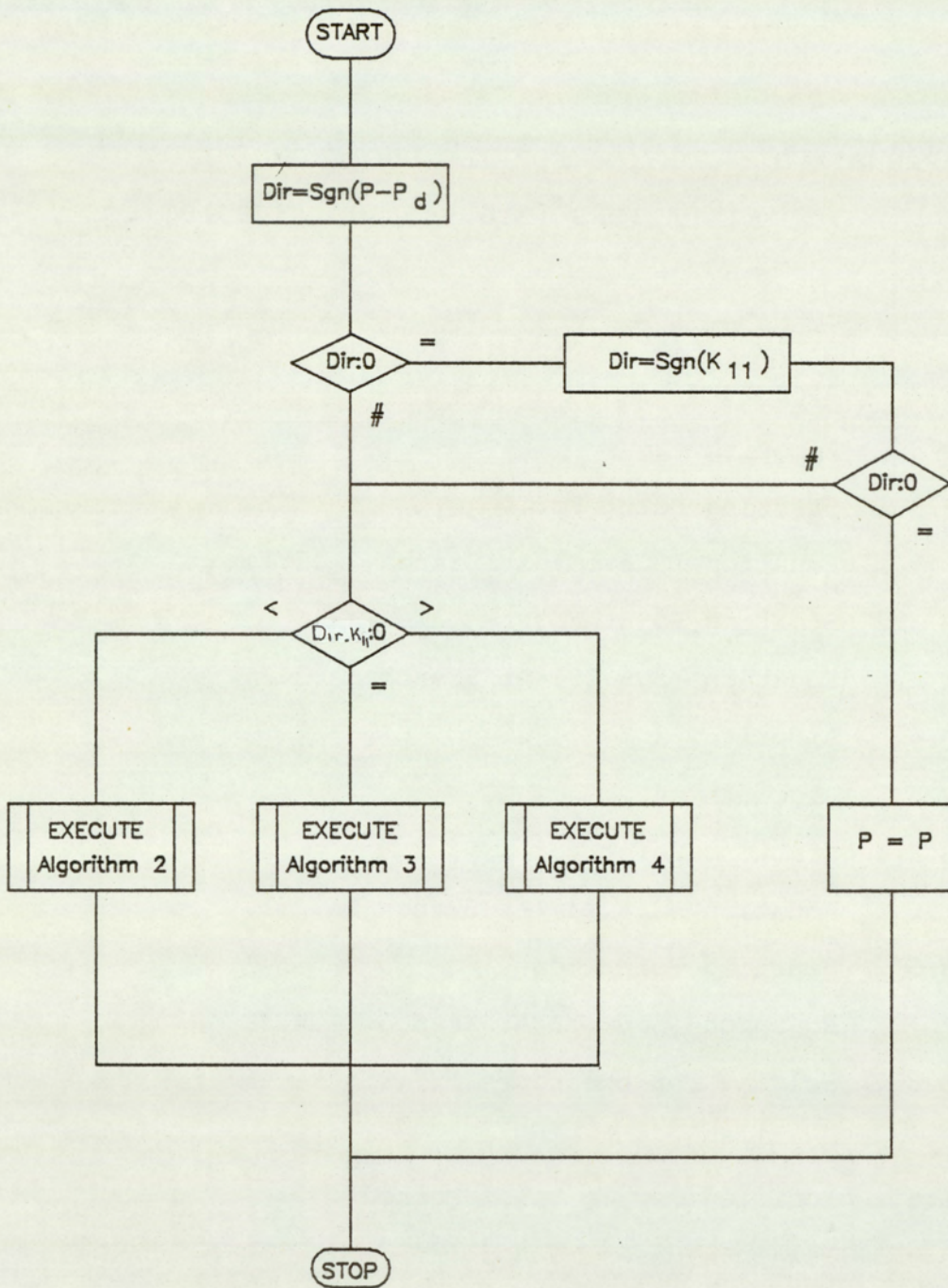


FIG.B.1.1 ALGORITHM 1

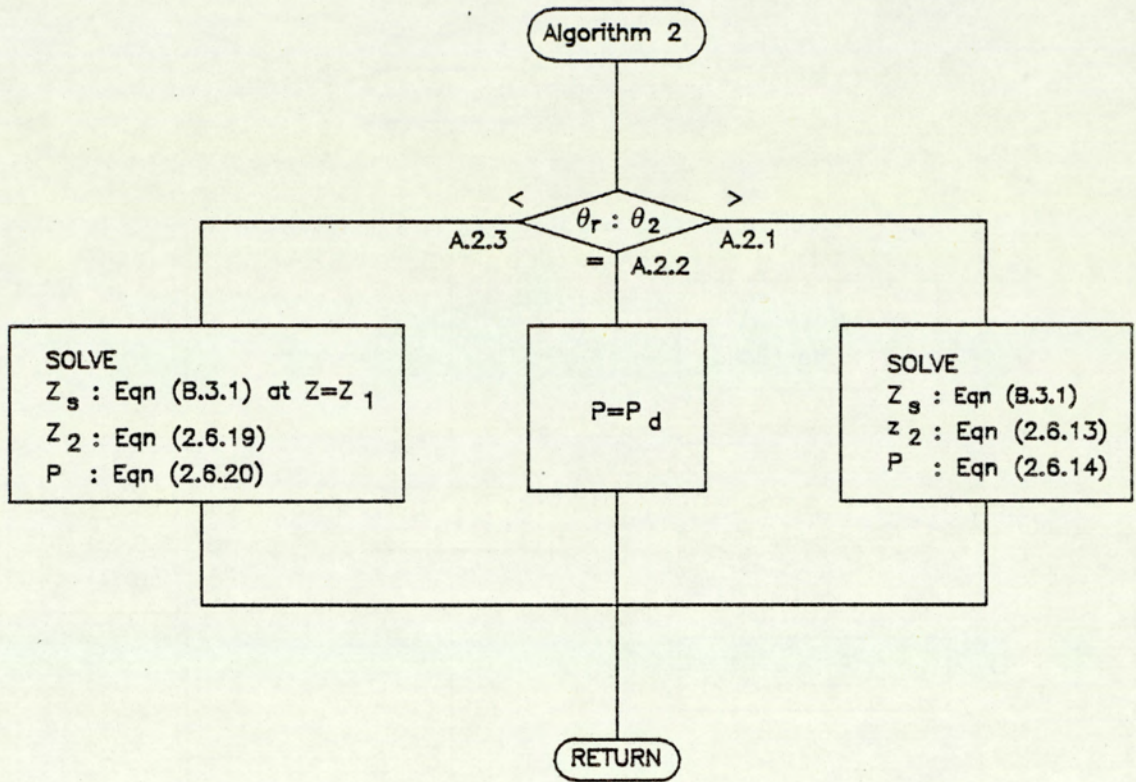


FIG.B.1.2 ALGORITHM 2

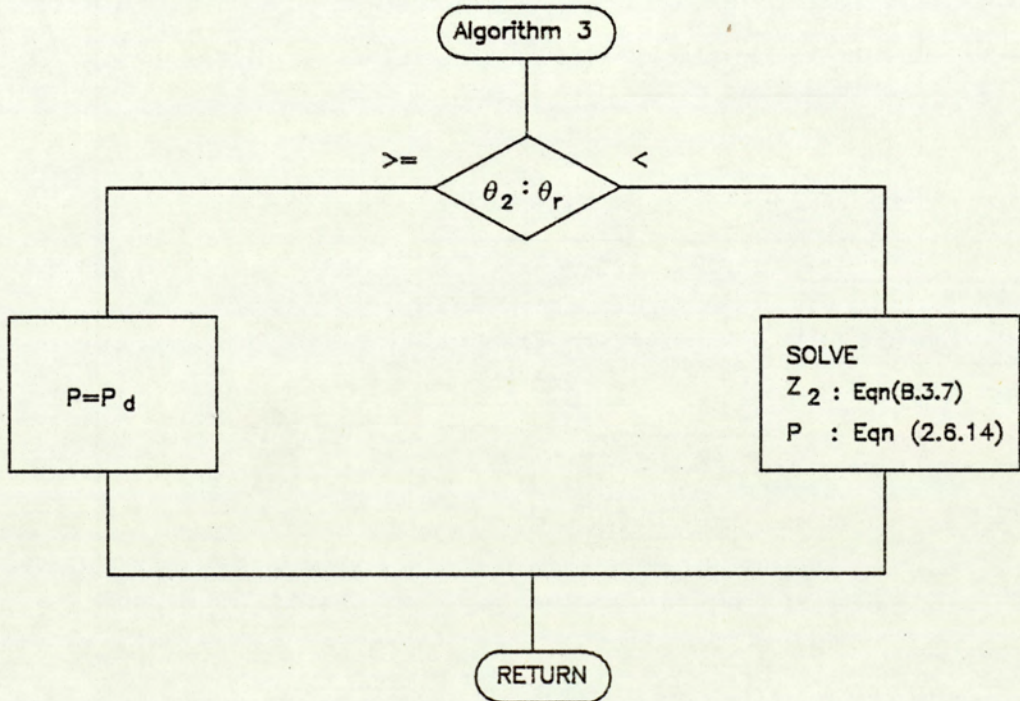


FIG.B.1.3 ALGORITHM 3

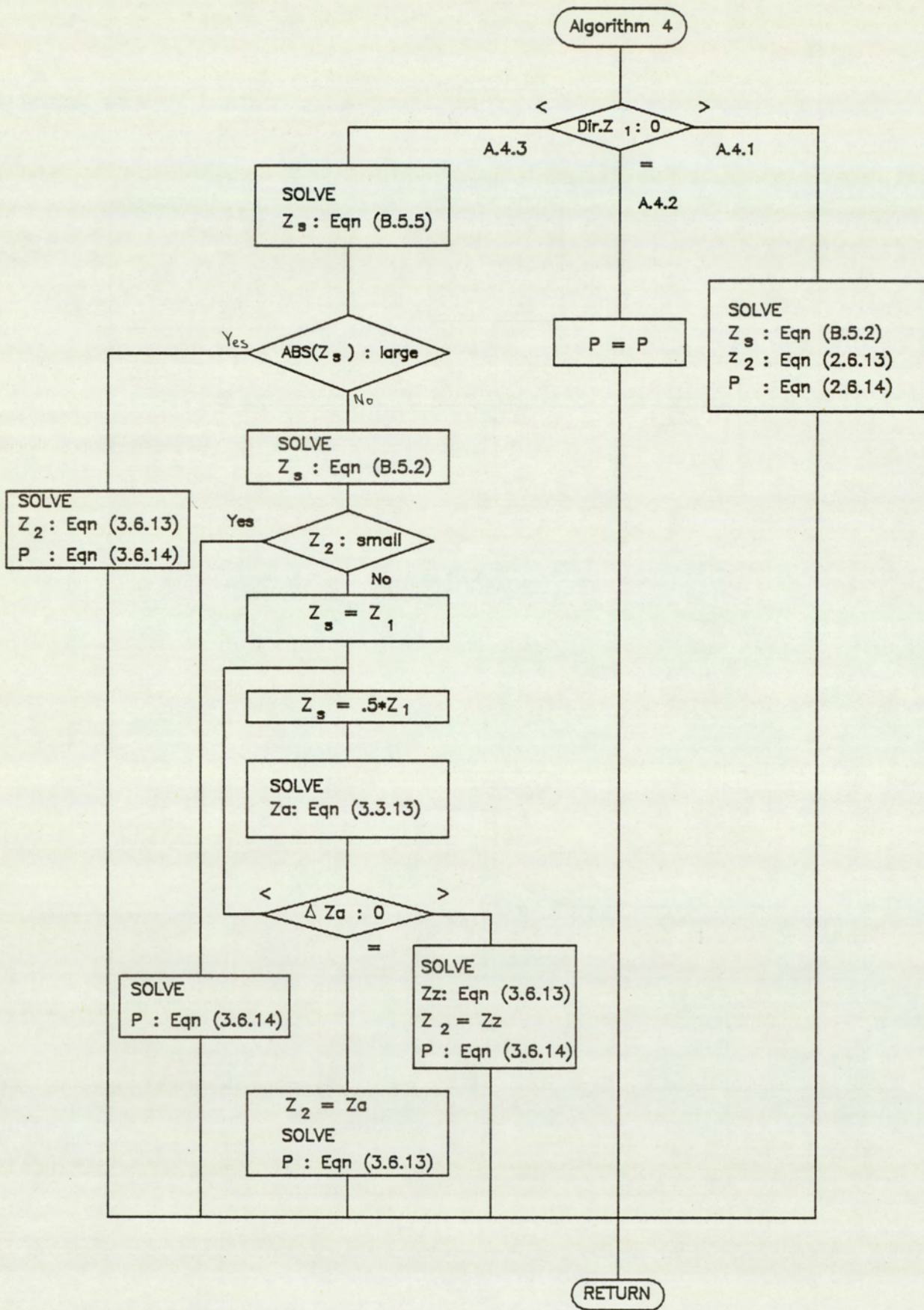


FIG.B.1.4 ALGORITHM 4

## B.1 Introduction

The roots of the equation (3.6.13) and (3.6.19) can be found using a reiterative numerical method. A suitable method being the Newton-Raphson method, which exhibits rapid convergence when a good starting point is chosen., William (61). A further saving in computation can accrue if checks are made on the constants Dir,  $K_{11}$  and  $Z_1$ , as under certain conditions the roots can be obtained analytically, without the need to resort to a numerical solution. The algorithm that follows is in principal similar to that employed in the piston pump model by Hannan (30), The version documented here has been refined to take into account the symmetry that exist in the original algorithm. This results in a more compact algorithm which permits for a more efficient computer implementation. The algorithms are shown in figures (B.1.1) to (B.1.4).

The relevant equations, from chapter 3, are listed below:

a) Without flow reversal:

$$\frac{\text{Dir}.2(Z_2 - Z_1)}{(K_{12})^2} - \frac{\text{Dir}.2K_{11}}{K_{12}} \ln \left( \frac{Z_2}{Z_1} \right) - (\theta_2 - \theta_1) = 0 \quad (3.6.13)$$

$$P_2 = P_d + \text{Dir} \left( \frac{K_{11} - Z_2}{\text{Dir}.K_{12}} \right)^2 \quad (3.6.14)$$

b) With flow reversal:

$$\theta_r = \theta_1 + \frac{\text{Dir}.2}{(K_{12})^2} (K_{11} - Z_1) - \frac{\text{Dir}.2K_{11}}{(K_{12})^2} \ln \left( \frac{K_{11}}{Z_1} \right) \quad (3.6.16)$$

$$- \frac{\text{Dir}.2}{(K_{12})^2} \left[ Z_1 + Z_2 - 2K_{11} + K_{11} \ln \left( \frac{(K_{11})^2}{Z_1 Z_2} \right) \right] - (\theta_2 - \theta_1) = 0 \quad (3.6.19)$$

$$P_2 = P_d - \text{Dir} \left( \frac{Z_2 - K_{11}}{\text{Dir} \cdot K_{12}} \right)^2 \quad (3.6.20)$$

c) Common equations:

From equations (3.6.10) and (3.6.12) is obtained:

$$Z_1 = K_{11} - \text{Dir} \cdot K_{12} \sqrt{P_1 - P_d} \quad (B.1.1)$$

$$Z_2 = K_{11} - \text{Dir} \cdot K_{12} \sqrt{P_2 - P_d} \quad (B.1.2)$$

Where:

$$\text{Dir} = \text{Sgn}(P - P_d) \quad (B.1.3)$$

The algorithms used for the solution of the roots of the above equations (3.6.13) and (3.6.19) are shown in figures (B.1.1) to (B.1.4). The subsequent sections discuss the structure and processes of the various algorithms.

## B.2 Algorithm 1

This is the main algorithm which identifies the direction of the dominant port flow at the start of the step, using equation (B.1.3). For the case of  $\text{Dir} = 0$ ,  $\text{Dir}$  is assigned the value of  $\text{Sgn}(K_{11})$ . This defines the dominant port flow after a small angular displacement. If  $K_{11} = 0$ , then from equations (B.1.1) and (B.1.2),  $P = P$ . This implies that the pressure at the end of the step is equal to that at the start of the step.

When  $\text{Dir} \neq 0$ , then there are three possible branches that the solution

can progress along. The branching is dependant on the sign of the constant  $K_{11}$  and the value of Dir. When  $\text{Dir.Sgn}(K_{11}) > 0$ , there is no mechanism for flow reversal within the step, and branching progresses along to algorithm 2. For  $K_{11} = 0$ , equation (3.6.13) can be further simplified and for this condition algorithm 3 handles the solution. The final branch goes to algorithm 4 and this is for the case when  $\text{Dir.Sgn}(K_{11}) < 0$ . Under this condition there is a possibility of flow reversal and the algorithm has to check for this eventuality.

### B.3 Algorithm 2

Within this branch there is a possibility of flow reversal within the step, the first task is therefore to determine the angular position at which flow reversal occurs, using equation (3.6.16) A check can produce one of three possibilities; flow reversal after the end of the step, flow reversal within the step and flow reversal at the end of the step. If flow reversal occurs after the the end of the step, then the equation (3.6.13) can be used, for the condition of no flow reversal. If flow reversal occurs at the end of the step then the pressure  $P = P_d$ , the port pressure at the start of the step. For the case of flow reversal within the step, equation (3.6.19) is used.

As mentioned earlier, rapid convergence when employing the Newton-Raphson method is dependant on a good starting point. The following sub-sections deals with the problem of determining a good starting point for equation (3.3.13) and (3.6.16) at branches (A.2.1) and (A.2.3) respectively.

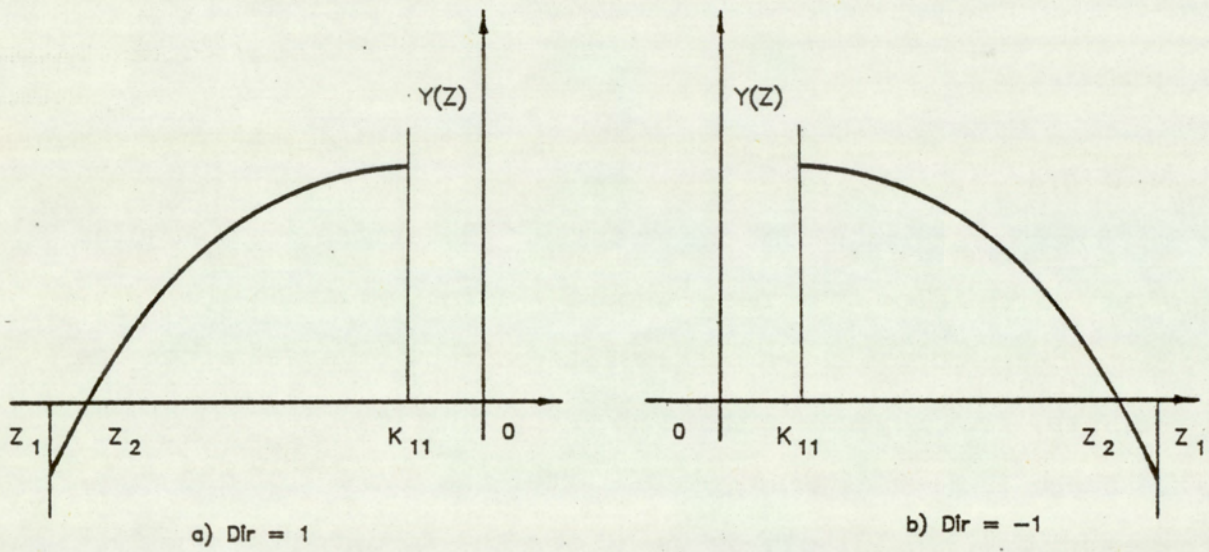


FIG.B.3.1 STARTING VALUES FOR BRANCH (A.2.1)

### B.3.1 Starting point for equation (3.6.13) at branch (A.2.1)

The equation (3.6.13) can be written as:

$$Y(Z) = \frac{\text{Dir}.2(Z_2 - Z_1)}{(K_{12})^2} - \frac{\text{Dir}.2K_{11}}{K_{12}} \ln\left(\frac{Z}{Z_1}\right) - (\theta - \theta_1) \quad (\text{B.3.1})$$

The figure (B.3.1) shows the function  $Y(Z)$ , defined above for the two cases of  $\text{Dir} = 1$  and  $\text{Dir} = -1$ .

From the figures (B.3.1a) and (B.3.1b) it can be seen that  $Z_1$  is a good starting point for the equation (3.6.13). The limits of the root  $Z_2$  at this branch is  $Z_1$  and  $K_{11}$ . For values of  $Z$  beyond  $K_{11}$ , the condition of flow reversal applies.

### B.3.2 Starting point for equation (3.6.19) at branch (A.2.3)

The equation (3.6.19) can be written as:

$$F(Z) = - \frac{\text{Dir}.2}{(K_{12})^2} \left[ Z_1 + 2K_{11} + K_{11} \ln\left(\frac{(K_{11})^2}{Z_1 \cdot Z}\right) \right] - (\theta - \theta_1) \quad (\text{B.3.2})$$

A function  $F(Z)$  can be defined as:

$$F(Z) = Y(Z) + \frac{\text{Dir}.2Z}{(K_{12})^2} \quad (\text{B.3.3})$$

The function  $F(Z)$  and  $Y(Z)$  are shown in figures (B.3.2a) and (B.3.2b) for the condition  $\text{Dir} = 1$  and  $\text{Dir} = -1$  respectively. The function  $Y(Z)$  is shown in full line whilst  $F(Z)$  is shown chain dotted.

From figure (B.3.1) it can be seen that  $Z_S$  provides a good starting point for solving the root of equation (3.6.19).

(S - fS)

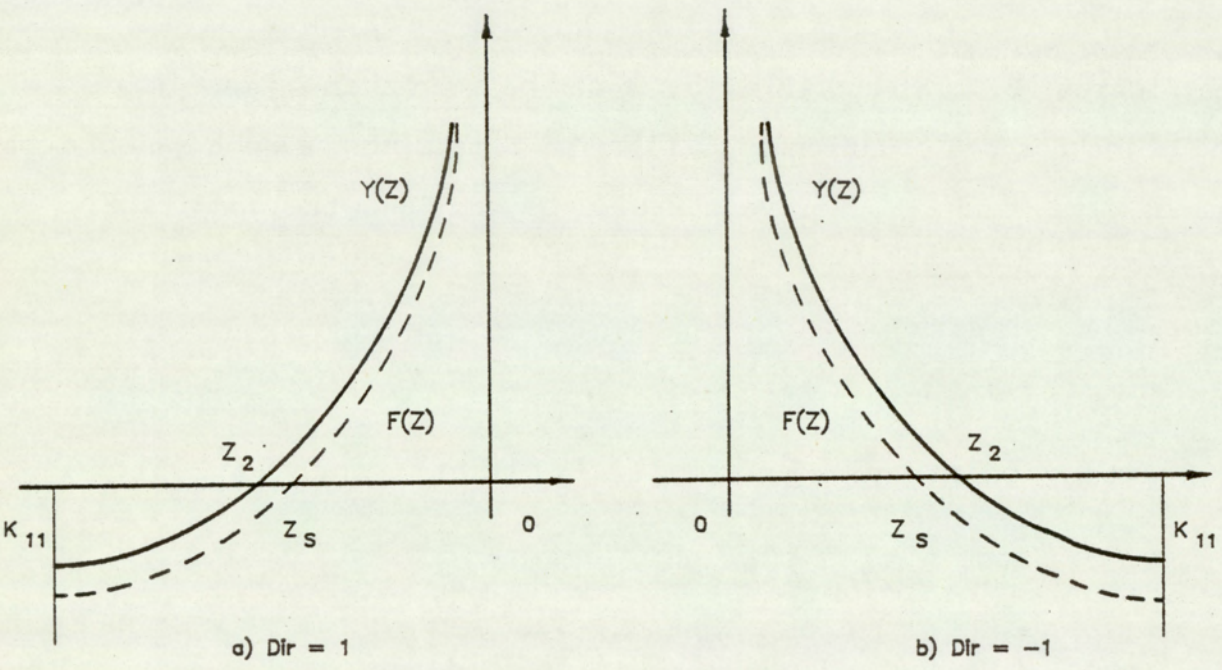


FIG.B.3.2 STARTING VALUES FOR BRANCH (A.2.3)

The point  $Z_S$  can be found by substituting equation (B.3.2) into (B.3.3) for the condition  $F(Z_S) = 0$  :

$$Z_S = \frac{(K_{11})^2}{Z_1} e^K \quad (B.3.4)$$

Where:

$$K = -2 + \frac{Z_1}{K_{11}} + \frac{(\theta_2 - \theta_1)}{\text{Dir.}2K_{11}} (K_{12})^2 \quad (B.3.5)$$

#### B.4 Algorithm 3

With the substitution of  $K_{11} = 0$ , the equation (3.6.13) reduces to:

$$\frac{\text{Dir.}2(Z_2 - Z_1)}{(K_{12})^2} - (\theta_2 - \theta_1) = 0 \quad (B.4.1)$$

Re-arranging gives:

$$Z_2 = Z_1 + \frac{(K_{12})^2}{\text{Dir.}2} (\theta_2 - \theta_1) \quad (B.4.2)$$

With  $K_{11} = 0$ , there is no mechanism for flow reversal. The above equation is valid only for the angular limits  $\theta_1$  to  $\theta_r$ . Where  $\theta_r$  is the equilibrium point. At equilibrium  $Z_2 = 0$ , substitution into equation (B.4.1) and re-arranging gives:

$$\theta_r = \theta_1 + \frac{2.\text{Dir}}{(K_{11})^2} Z_1 \quad (B.4.3)$$

Substitution of  $Z_2 = 0$  into equation (B.1.2) gives:

$$P = P_d$$

For  $\theta_2 > \theta_r$ .

### B.5 Algorithm 4

This algorithm solves for the condition when  $K_{11}$  and Dir are of the same sign, there is therefore no possibility of flow reversal at this branch. The initial check on the sign of  $Z_1$  and the sign of Dir identifies one of three possibilities. Branching to (A.4.1), (A.4.2) or (A.4.3) occurs for  $\text{Dir.Sgn}(Z_1)$  being greater than, equal to, or less than zero respectively. When  $Z_1$  equals zero, the values of  $Z_2$  and P at the end of the step can be obtained analytically. As  $K_{11}$  is assumed constant over the step, the pressure P at the end of the step must be the same as that at the start of the step. For the two other branch conditions, the value of  $Z_2$  must be solved numerically. The subsequent sub-sections deals with the problem of choosing a good starting point.

#### B.5.1 Starting Point For Equation (3.6.13) At Branch (A.4.1)

The equation (3.6.13) can be presented as equation (B.3.1) :

$$Y(Z) = \frac{\text{Dir}.2(Z - Z_1)}{(K_{12})^2} - \frac{\text{Dir}.2K_{11}}{K_{12}} \ln \left( \frac{Z}{Z_1} \right) - (\theta - \theta_1)$$

A function F(Z) is defined as:

$$F(Z) = Y(Z) - \frac{\text{Dir}.2Z}{(K_{12})^2} = -\frac{\text{Dir}.2Z_1}{(K_{12})^2} - \frac{\text{Dir}.2K_{11}}{K_{12}} \ln \left( \frac{Z}{Z_1} \right) - (\theta - \theta_1)$$

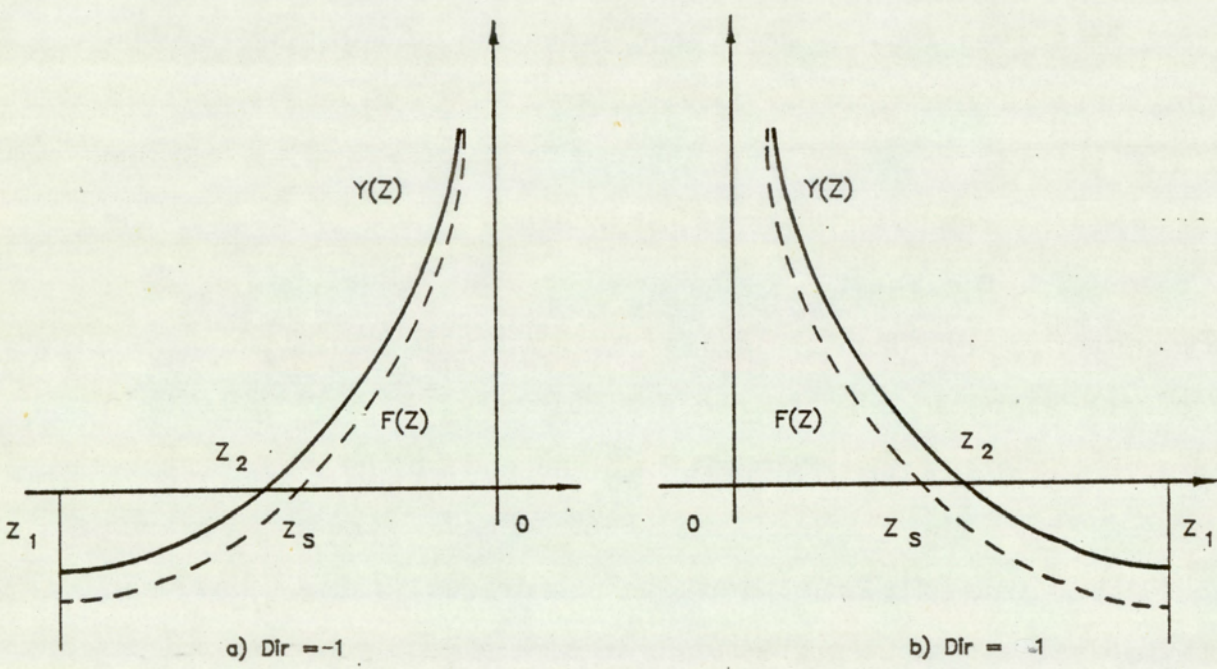


FIG.B.5.1 STARTING VALUES FOR BRANCH (A.4.1)

The function  $F(Z)$  and  $Y(Z)$  are shown in figures (B.5.1a) and (B.5.1b) for  $\text{Dir} = 1$  and  $\text{Dir} = -1$  respectively. The function  $Y(Z)$  is shown in full line whilst the function  $F(Z)$  is shown chain dotted.

From figure (B.5.1) it can be seen that  $Z_S$  provides a good starting point for the equation (3.6.13).

Solving the equation above for  $F(Z_S) = 0$  gives:

$$Z_S = Z_1 e^K \quad (\text{B.5.2})$$

Where:

$$K = - \left( \frac{(\theta_2 - \theta_1)(K_{12})^2}{\text{Dir} \cdot 2K_{11}} + \frac{Z_1}{K_{12}} \right) \quad (\text{B.5.3})$$

From equation (B.5.1) it can be seen that for small values of  $Z_S$ ,  $F(Z_S) = Y(Z_S)$  and thus  $Z_2 = 0$ .

### B.5.2 Starting Point For Equation (3.6.13) At Branch (A.4.3)

A function  $F(Z)$  can be defined as:

$$F(Z) = Y(Z) - \frac{\text{Dir} \cdot 2}{(K_{12})^2} (Z - Z_1) = - \frac{\text{Dir} \cdot 2K_{11}}{(K_{12})^2} \ln \left( \frac{Z}{Z_1} \right) - (\theta - \theta_1) \quad (\text{B.5.4})$$

The function  $F(Z)$  and  $Y(Z)$  as defined by equations (B.5.4) and (B.5.1) are shown in figure (B.5.2a) and (B.5.2b) for  $\text{Dir} = 1$  and  $\text{Dir} = -1$  respectively. The function  $Y(Z)$  is shown in full line and  $F(Z)$  is shown chain dotted.

From figure (B.5.2) it can be seen that  $Z_S$  provides a good starting point for the equation (3.6.13).

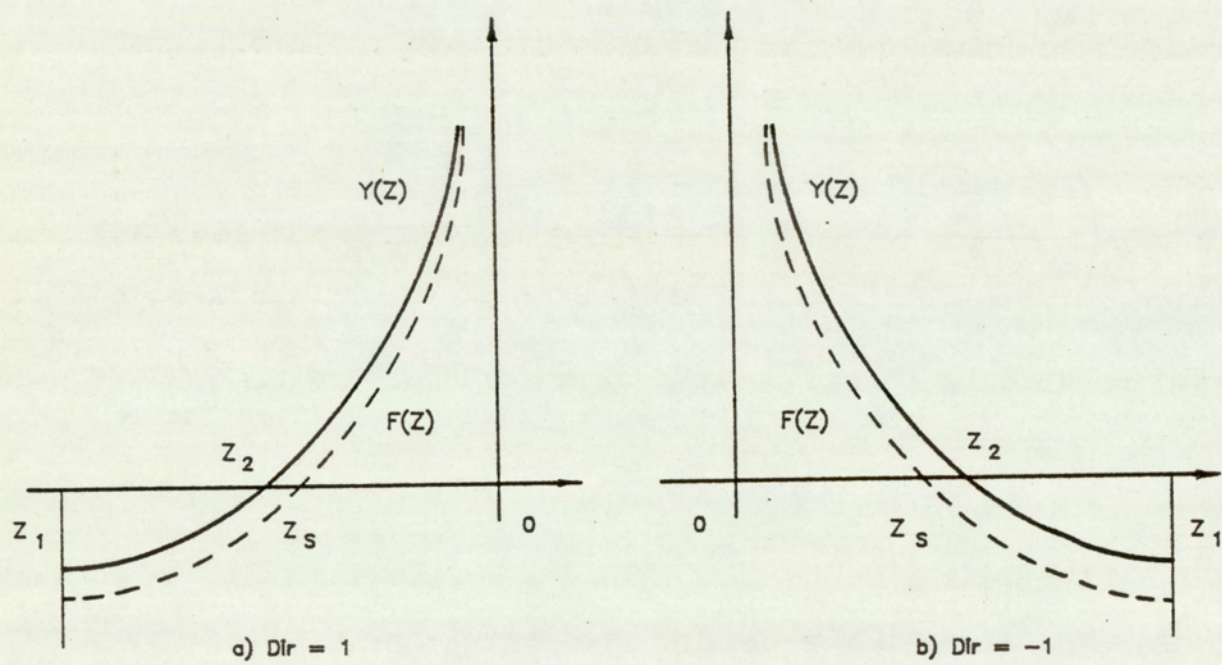


FIG.B.5.2 STARTING VALUES FOR BRANCH (A.4.3)

Solving the equation above for  $F(Z_S) = 0$  gives:

$$Z_S = Z_1 e^K \quad (B.5.5)$$

Where:

$$K = - \frac{(\theta_2 - \theta_1)(K_{12})^2}{\text{Dir.}2K_{11}} \quad (B.5.6)$$

The starting value given by equation (B.5.5) has a disadvantage in that for small values of  $Z_S$ , there is a problem of computer 'overflow' (value outside the range of representation). This problem can be overcome by first making a check before attempting to proceed with the solution. If  $Z_S$  is small, an alternative starting point can be used, as defined by equation (B.5.2). Also from equation (B.5.1) it can be seen that for small values of  $Z_S$ , the root of the equation  $Z_2 = Z_S$ . If both of these branches do not resolve a solution, the value of  $Z_1$  is halved until the function  $Y(Z_1)$  changes sign. The value of  $Z_1$  at this point is used as the starting point for equation (3.6.13)

### **B.6.1 Algorithm for Solving for Root of Non-linear Equation**

In the preceding sections the algorithm for the solution of the differential equations were presented. Integral to this algorithm is one which solves for the roots of the resulting non-linear equation. The algorithm described here, is the one used in the computer implementation of the analytical solution and is an implementation of the Modified Regula-Falsi and Newton-Raphson method for the solution of non-linear equation. The Regula-Falsi is a modified bisection method which has the advantage of always converging and simple to operate. The disadvantage is that convergence is slow. The Newton-Raphson method

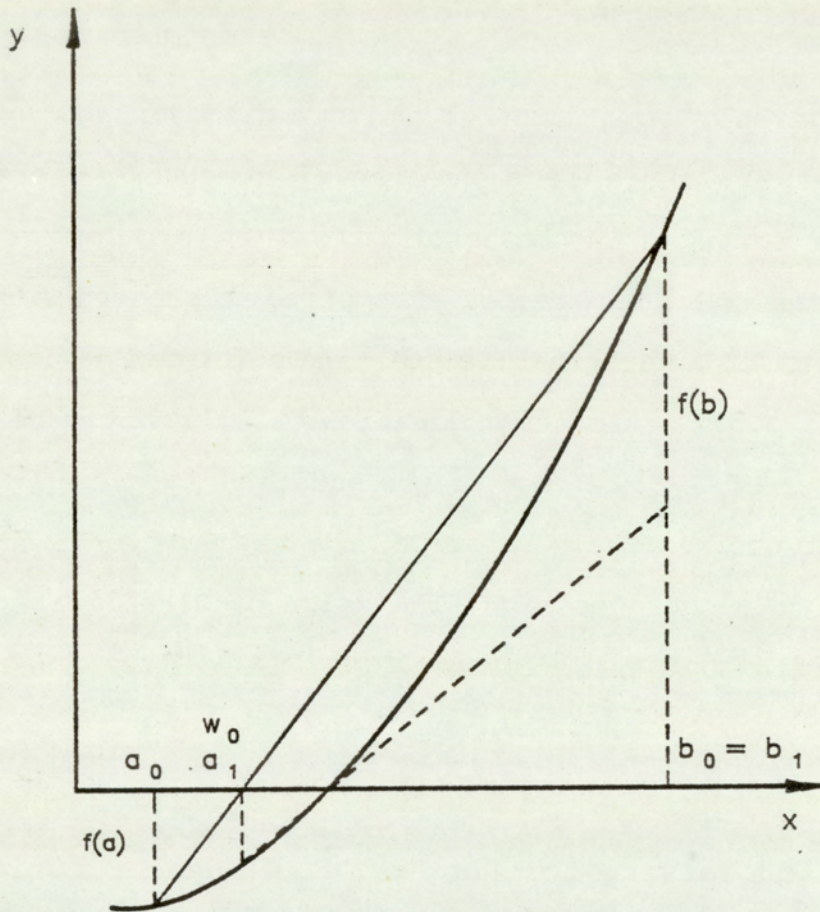


FIG.B.6.1 MODIFIED REGULA-FALSI METHOD

on the other hand results in a quick convergence, provided the first approximation is sufficiently close, but is, however, prone to failure due to instability. For a discussion of the numerical techniques mentioned above, references should be made to Williams (61). In this section the implementation of the methods are highlighted, while providing a description of the numerical methods involved.

### **B.6.2 Modified Regula-Falsi Method**

The method of Modified Regula-Falsi is best described with reference to figure (B.6.1). The method begins with a root bounded by the limits  $a$  and  $b$ . The necessary condition for the presence of a root is for the function value to change sign between the limits. The first process begins with the determination of the intercept of the line  $y = 0$  and the line joining the function at the limits  $a$  and  $b$ . This intercept point,  $w$ , defined by equation (B.6.1) below, is next determined and used as one of the next set of limits. The other point is determined on the function sign at the previous limits. If the sign of the function at  $w$  and  $a$  are the same, then the value of  $w$  is assigned to  $a$ , and  $w$  is assigned to  $b$  for when the sign of the function at  $w$  and  $b$  are the same. The next stage involves a reiteration of the above procedure, but with a slight modification. The function value at the replaced limit is calculated from the function equation, but the function value at the other limit is arbitrarily taken as half that at the previous step. Repeated reiterations converges the limits about the root and terminates when sufficient convergence is achieved.

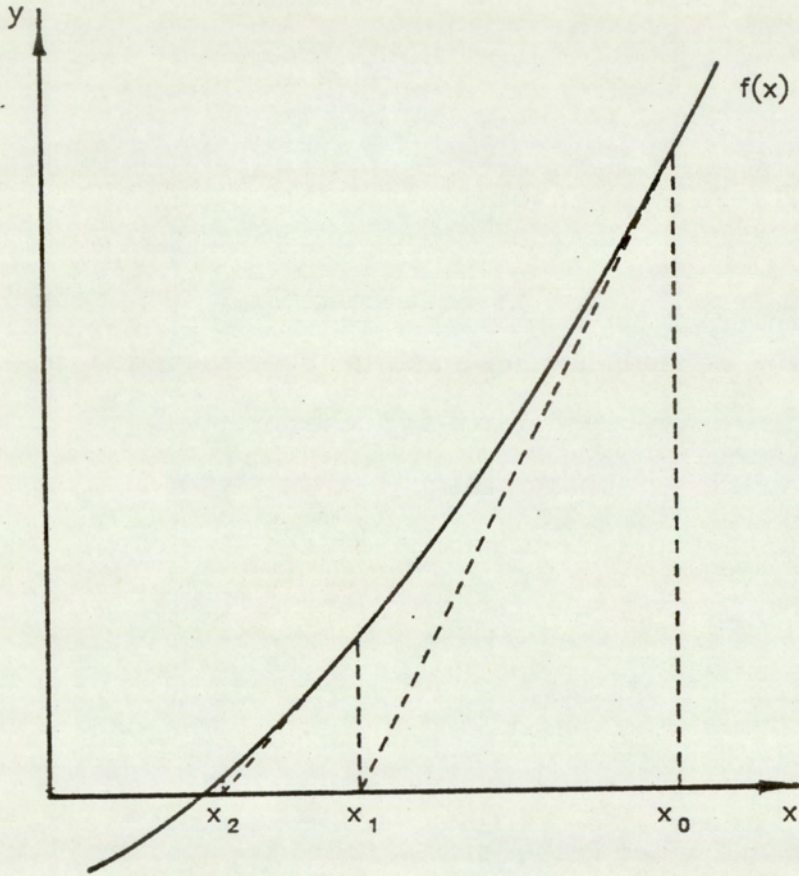


FIG.B.6.2 NEWTON-RAPHSON METHOD

The position of  $w$  is defined by:

$$w_{n+1} = \frac{(G_{an} - F_{bn})}{(G - F)} \quad (\text{B.6.1})$$

Where  $n$  is the  $n$ th iteration, and  $F$  and  $G$  are the assumed function values at  $a_n$  and  $b_n$  respectively.

### B.6.3 Newton-Raphson Method

The method, in brief, attempts to fit a tangent to the curve of the function at the point of the current estimate of the root of the function. The point of intersection of the tangent with the line  $y = 0$  provides the next estimate of the root. This procedure is repeated till a sufficiently close estimate is obtained. This procedure is shown in figure (B.6.2).

The equation defining the Newton-Raphson method is:

$$x_{n+1} = x_n - \frac{f(x_n)}{f'(x_n)} \quad (\text{B.6.2})$$

Where  $n$  is the  $n$ th iteration.

### B.6.4 Algorithm For The Solution Of The Root Of The Equation

The algorithm shown in figure (B.6.3) and (B.6.4) starts with a definition of the iterative constants, these constants define the maximum permitted error tolerances and the maximum iteration count. The first check is of the function value at the start value. If the value is within the acceptable limits, the routine branches to the

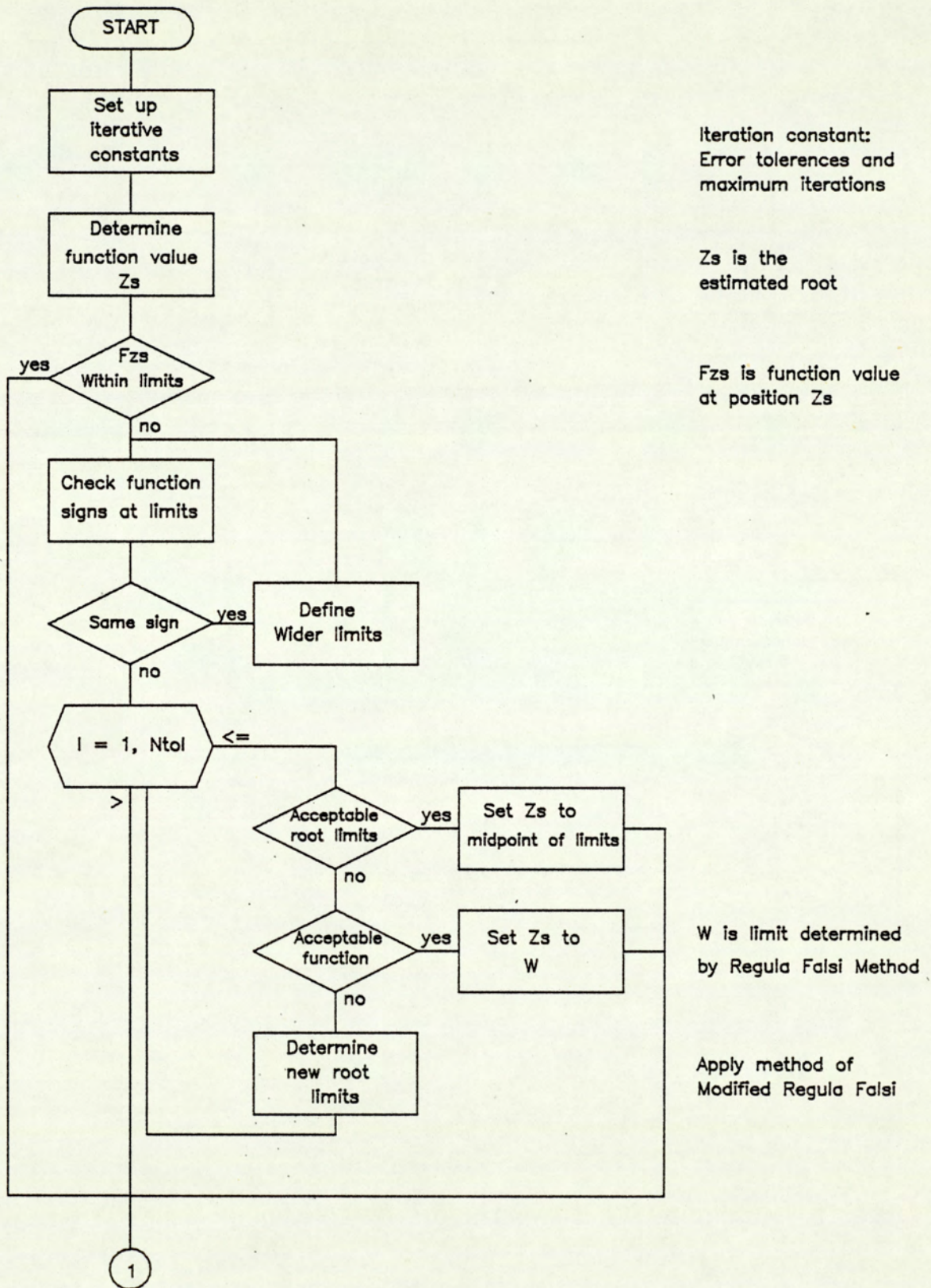


FIG.B.6.3 ALGORITHM FOR SOLVING ROOTS OF EQUATION – SHEET 1

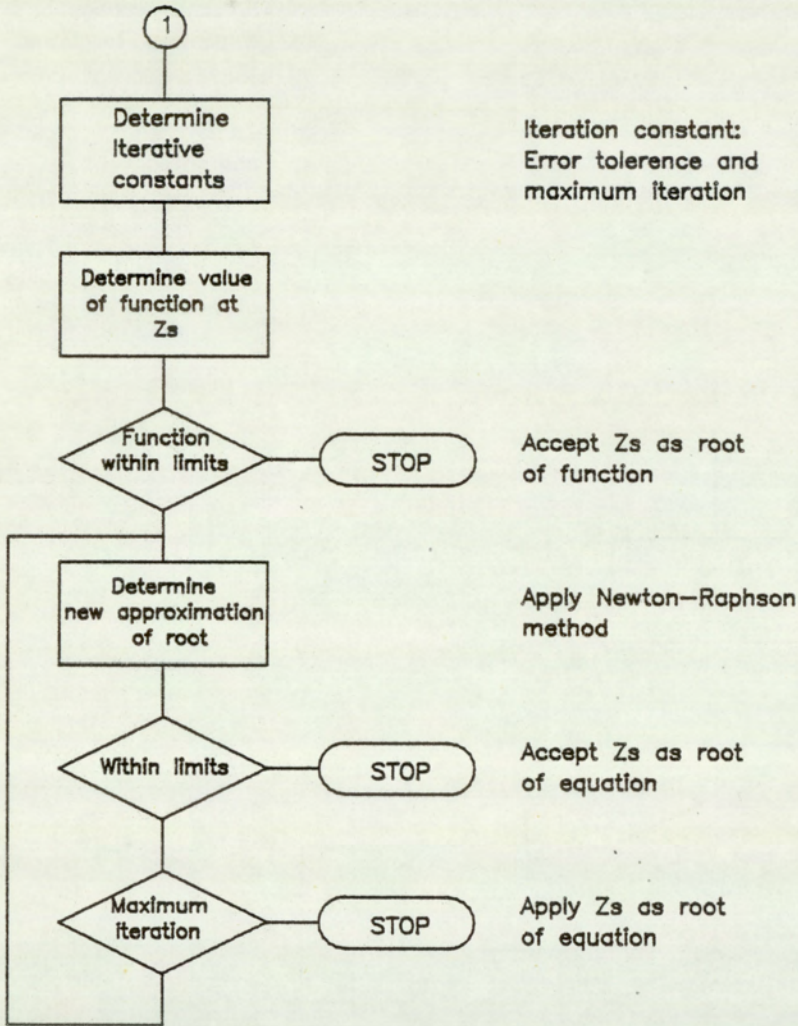


FIG.B.6.4 ALGORITHM FOR SOLVING ROOTS OF EQUATIONS – SHEET 2

Newton-Raphson solution for a closer estimate of the root, otherwise, another check is made to determine the sign of the function at the limits of the root. The condition for the existence of a root between the limits is for the function to be of different signs at these points. For the condition where the function is of the same sign, the limits are doubled until a root is located within the limits. Execution then proceeds to narrow the limits, whilst containing the root of the equation. Within the constraints of a maximum number of reiterations, the Regula-Falsi method is applied. At each stage, a check is made on the size of the limits, and on achieving an acceptable limit, the routine branches to the Newton-Raphson method. For other conditions new limits are defined as determined by the Regula-Falsi method.

The section of this routine which performs the Newton-Raphson method begins, as previously, with a definition of the iterative constants. Prior to processing the Newton-Raphson method, a check is performed to determine the value of the function at the first estimate point. If the value is within the accepted error tolerance, the routine ends with  $Z_s$  as the root of the equation, and proceeds otherwise. With the first estimate, the correction is processed until the required level of convergence is achieved, or the maximum number of reiterations is reached. Termination then occurs taking the current value of  $Z_s$  as the root of the equation.

**APPENDIX C : LISTING OF PUMP MODEL PROGRAMS**

- C.1 Program VPLOT
- C.2 Program VMODEL
- C.3 Program VPLOT

C.1 PROGRAM VFLGEN

```

10  ! RE-STORE"VFLGEN:F8"
20  ! ***** PROGRAM VFLGEN *****
30  ! *
40  ! * THE PROGRAM GENERATES THE DATAFILE FOR THE VANE MACHINE *
50  ! * PARAMETERS.
60  ! *
70  ! * Data is input and edited in groups consisting of ;
80  ! * M/C GEOMETRY, OPERATING ENVELOPE, INLET GROOVE and
90  ! * OUTLET GROOVE parameters.
100 ! *
110 ! * Functions are controlled by the use of special function *
120 ! * keys.
130 ! *
140 ! *
150 ! * Revision#1:18:JUL:83
160 ! *      Included inlet groove data
170 ! *
180 ! * ORIGIN: G.SEET  MECH.ENG. ASTON VARSITY
190 ! * DATE: 15 MARCH 83
200 ! *
210 ! *****
220 DIM Y$(0)
230 COM Label$(4,20)[35],Data(1:4,1:20),Name$[10],Z
240 PRINTER IS 16
250 Mstore$=":F8 " ! Define mass_storage unit
260 EXIT GRAPHICS
270 PRINT "ABC"&CHR$(12)
280 PRINT " PROGRAM VFLGEN EXECUTING "
290 ! Assign label arrays.
300 Label$(1,0)="      PUMP GEOMETRY      "
310 Label$(1,1)="      1  STATOR DIAMETER (mm) : "
320 Label$(1,2)="      2  ROTOR  DIAMETER (mm) : "
330 Label$(1,3)="      3  ASSEMBLY LENGTH (mm) : "
340 Label$(1,4)="      4  ABUTMENT WIDTH (mm) : "
350 Label$(1,5)="      5  ABUT. CLEARANCE (mm) : "
360 Label$(1,6)="      6  VANE    WIDTH (mm) : "
370 Label$(1,7)="      7  VANE  CLEARANCE (mm) : "
380 Label$(1,8)="      8  PORT   DIAMETER (mm) : "
390 Label$(1,9)="      9  PORT    ANGLE(deg) : "
400 Label$(1,10)="     10  CAM ABUT.  RAD. (mm) : "
410 Label$(1,11)="     11  CAM ACT.   RAD. (mm) : "
420 Label$(1,12)="     12  CAM OP.   RAD. (mm) : "
430 Label$(1,13)="     13  CAM ACT.  ANGLE(deg) : "
440 Label$(1,14)="     14  NUMBER OF SEGMENTS : "
450 Label$(2,0)="     OPERATING ENVELOPE  "
460 Label$(2,1)="     1  SHAFT SPEED   (RPM): "
470 Label$(2,2)="     2  INLET PRESSURE (bar): "
480 Label$(2,3)="     3  OUTLET PRESSURE (bar): "
490 Label$(2,4)="     4  FLUID DENSITY (Kg/m3): "
500 Label$(2,5)="     5  FLUID VISCOSITY(NS/m2): "
510 Label$(2,6)="     6  BULK MODULUS  (MN/m2): "
520 Label$(2,7)="     7  INPUT LINE DIAM. (mm): "
530 Label$(2,8)="     8  OUTPUT LINE DIAM. (mm): "
540 Label$(2,9)="     9  DISCHARGE COEFF. : "
550 Label$(2,10)="    10  CAVITATION PRESS.(bar): "
560 Label$(3,0)=" INLET GROOVE PARAMETERS "
570 Label$(3,1)=" 1)Hemisphere:Groove depth (mm): "
580 Label$(3,2)="      Cutter diam. (mm): "
590 Label$(3,3)="      Start angle (deg): "
600 Label$(3,4)=" 2)Square :Groove depth (mm): "

```

```

610 Label$(3,5)="          Groove width (mm):"
620 Label$(3,6)="          Start angle (deg):"
630 Label$(3,7)="3)Triangular:Groove depth (mm):"
640 Label$(3,8)="          Cutter angle(deg):"
650 Label$(3,9)="          Start angle (deg):"
660 Label$(3,10)="INLET GROOVE TYPE  (0-3)  :"
670 Label$(4,0)=" OUTLET GROOVE PARAMETERS "
680 Label$(4,1)="1)Hemisphere:Groove depth (mm):"
690 Label$(4,2)="          Cutter diam. (mm):"
700 Label$(4,3)="          Start angle (deg):"
710 Label$(4,4)="2)Square      :Groove depth (mm):"
720 Label$(4,5)="          Groove width (mm):"
730 Label$(4,6)="          Start angle (deg):"
740 Label$(4,7)="3)Triangular:Groove depth (mm):"
750 Label$(4,8)="          Cutter angle(deg):"
760 Label$(4,9)="          Start angle (deg):"
770 Label$(4,10)="OUTLET GROOVE TYPE  (0-3)  :"
780 !
790 Input1:LINPUT "INPUT DATA FILENAME (%DAT%):",Name#[1,6]
800 Name#[7,10]=Mstore$
810 ASSIGN Name$ TO #1,Z
820 IF Z<>2 THEN Start
830 PRINT "ABC"&CHR$(12)
840 PRINT USING "#,K";CHR$(27)&"&a23r0C"
850 PRINT " WRONG FILE TYPE :";Name$
860 Input2:LINPUT " OVERWRITE FILE (Y/N) ",Y$
870 IF Y$="Y" THEN Start
880 IF Y$="N" THEN Input1
890 GOTO Input2
900 Start:ON Z+1 GOTO Oldfile,Newfile,Newfile
910 Oldfile:Newfile=0
920 MAT READ #1;Data
930 GOTO Mainseg
940 Newfile:Newfile=1
950 Mainseg:CALL Main(Label$(*),Data(*),Name$,Mstore$,Newfile)
960 END
970 !
980 ! ++++++ SUBROUTINE MAIN ++++++
990 ! +
1000 ! + Special key functions and subfunctions
1010 ! +
1020 ! ++++++
1030 SUB Main(Label$(*),Data(*),Name$,Mstore$,Newfile)
1040 IF Newfile=1 THEN GOSUB New
1050 GOSUB Start
1060 Disp: DISP "SELECT "
1070 WAIT 200
1080 DISP "          FUNCTION"
1090 WAIT 200
1100 GOTO Disp
1101 !
1102 ! ***** Library of Subroutine *****
1110 Start:! Initialise and define soft keys.
1120 Menu=1
1130 GOSUB Menu1
1140 GOSUB Menu
1150 ON KEY #0 GOSUB Curup
1160 ON KEY #8 GOSUB Curdown
1170 ON KEY #1 GOSUB Edit
1180 ON KEY #9 GOSUB Store

```

```
1190     ON KEY #2 GOSUB Next
1200     ON KEY #10 GOSUB Back
1210     ON KEY #6 GOSUB Print
1220     ON KEY #7 GOSUB Key
1230     ON KEY #15 GOSUB Exit
1240     RETURN
1250 Curup: ! Moves cursor up
1260     IF Cursor<2 THEN RETURN
1270     GOSUB Cursor2
1280     Cursor=Cursor-1
1290     GOSUB Cursor1
1300     RETURN
1310 Curdown: ! Moves cursor down
1320     IF Cursor>Curmax-1 THEN RETURN
1330     GOSUB Cursor2
1340     Cursor=Cursor+1
1350     GOSUB Cursor1
1360     RETURN
1370 Cursor1: ! Mark Down cursor
1380     PRINT USING "#,A";CHR$(128)
1390     PRINT USING "#,K";CHR$(27)&"&a"&VAL$(Cursor+Rofset)&"r"&
50C"
1400     PRINT USING " #,3A";CHR$(130)&"*"&CHR$(128)
1410     RETURN
1420 Cursor2: ! Mark Up cursor
1430     PRINT USING "#,A";CHR$(128)
1440     PRINT USING "#,K";CHR$(27)&"&a"&VAL$(Cursor+Rofset)&"r"&
50C"
1450     PRINT USING " #,3A";CHR$(128)&" "
1460     RETURN
1470 Menu: ! Prints Menu on to Display
1480     PRINT CHR$(128)
1490     PRINT "ABC"&CHR$(12)
1500     Rofset=INT((19-Curmax)/2)
1510     IF Ofset<0 THEN Ofset=0
1520     PRINT USING "#,K";CHR$(27)&"&a"&VAL$(Rofset)&"R"
1530     PRINT USING "#,20X,K";CHR$(129)&Label$(Menu,0)&CHR$(128)
1540     PRINT
1550     FOR I=1 TO Curmax
1560     PRINT USING "15X,35A,5D.4D";Label$(Menu,I);Data(Menu,I)
1570     NEXT I
1580     Cursor=1
1590     GOSUB Cursor1
1600     RETURN
1610 Edit: ! Requests variable value
1620     BEEP
1630     Data$=""
1640     INPUT " INPUT VARIABLE VALUE :",Data$
1650     IF LEN(Data$)<>0 THEN Data(Menu,Cursor)=VAL(Data$)
1660     DISP " "
1670     PRINT USING "#,K";CHR$(27)&"&a"&VAL$(Cursor+Rofset)&"r"&
50C"
1680     PRINT USING "#,5D.4D";Data(Menu,Cursor)
1690     GOSUB Curdown
1700     RETURN
1710 Store: ! Stores datafile
1720     Error=0
1730     GOSUB Check ! Check for non-permitted dimensions.
1740     IF Error=1 THEN RETURN
1750     Y$=""
```

```
1760 INPUT " SAME FILENAME (DEFAULT:Y) : ",Y$
1770 IF LEN(Y$)=0 THEN Store3
1780 Store2:LINPUT " INPUT NEW FILENAME : ",Name$
1790 IF LEN(Name$)=0 THEN Store2
1800 Name$[7,10]=Mstore$
1810 ASSIGN Name$ TO #1,Z
1820 IF Z=1 THEN Store3
1830 BEEP
1840 DISP "FILE ASSIGNED ",Name$
1850 WAIT 1000
1860 INPUT "Overwrite File : ",Y$
1870 IF Y$="Y" THEN GOTO Store3
1880 GOTO Store2
1890 Store3:Name$[7,10]=Mstore$
1900 ASSIGN Name$ TO #1,Z
1910 IF Z=0 THEN PURGE Name$
1920 CREATE Name$,3
1930 ASSIGN Name$ TO #1,Z
1940 MAT PRINT #1;Data,END
1950 ASSIGN * TO #1
1960 GOSUB Print
1970 RETURN
1980 Next: Select next menu
1990 IF Menu>3 THEN RETURN
2000 Menu=Menu+1
2010 ON Menu GOSUB Menu1,Menu2,Menu3,Menu4
2020 GOSUB Menu
2030 RETURN
2040 Back: Previous menu
2050 IF Menu<2 THEN RETURN
2060 Menu=Menu-1
2070 ON Menu GOSUB Menu1,Menu2,Menu3,Menu4
2080 GOSUB Menu
2090 RETURN
2100 Menu1:Curmax=14
2110 RETURN
2120 Menu2:Curmax=10
2130 RETURN
2140 Menu3:Curmax=10
2150 RETURN
2160 Menu4:Curmax=10
2170 RETURN
2180 Key: Prints Key
2190 PRINT CHR$(128)
2200 PRINT "ABC"&CHR$(12)
2210 PRINT "Curup "; "Edit "; "Next "; TAB(59); "Print "; "Key
"
2220 PRINT "Cdown "; "Store "; "Back "; TAB(65); "EXIT"
2230 WAIT 1000
2240 GOSUB Menu
2250 RETURN
2260 Print: Prints data table
2270 PRINTER IS 0
2280 IMAGE /,21X,33A,/
2290 IMAGE 21X,33A,5D.4D
2300 PRINT LIN(3)
2310 PRINT TAB(14); "DATA FILENAME : ";Name$
2320 PRINT
2330 GOSUB Menu1
2340 PRINT USING 2280;Label$(1,0)
```

```

2350     FOR I=1 TO Curmax
2360     PRINT USING 2290;Label$(1,I);Data(1,I)
2370     NEXT I
2380     PRINT LIN(1)
2390     GOSUB Menu2
2400     PRINT USING 2280;Label$(2,0)
2410     FOR I=1 TO Curmax
2420     PRINT USING 2290;Label$(2,I);Data(2,I)
2430     NEXT I
2440     PRINT LIN(1)
2450     GOSUB Menu3
2460     PRINT USING 2280;Label$(3,0)
2470     FOR I=1 TO Curmax
2480     PRINT USING 2290;Label$(3,I);Data(3,I)
2490     NEXT I
2500     PRINT
2510     GOSUB Menu4
2520     PRINT USING 2280;Label$(4,0)
2530     FOR I=1 TO Curmax
2540     PRINT USING 2290;Label$(4,I);Data(4,I)
2550     NEXT I
2560     PRINT LIN(8)
2570     PRINTER IS 16
2580     RETURN
2590 New: ! New data file
2600     FOR Menu=1 TO 4
2610     ON Menu GOSUB Menu1,Menu2,Menu3,Menu4
2620     GOSUB Menu
2630     Cursor=1
2640 Next_pt:GOSUB Edit
2650     IF Cursor<Curmax THEN Next_pt
2660     GOSUB Edit ! Overcomes auto check in SUB Edit
2670     NEXT Menu
2680     Newfile=0
2690     RETURN
2700 Check: ! Check for Inlet/Outlet groove overlap
2710     DEG
2720     In_groove=Out_groove=0
2730 In_gv: IF Data(3,10)=0 THEN Out_gv
2740     In_groove=Data(3,3*Data(3,10))
2750 Out_gv: IF Data(4,10)=0 THEN Sum_ang
2760     Out_groove=Data(4,3*Data(4,10))
2770 Sum_ang: Total_angle=In_groove+Out_groove
2780     Phi=2*ASN(Data(1,8)/(Data(1,1)*COS(Data(1,9))))
2790     Max_angle=180-2*(.5*Phi+Data(1,9))
2800     IF Total_angle<Max_angle THEN RETURN
2810     BEEP
2820     PRINT "ABC"&CHR$(12)
2830     DISP " "
2840     PRINT " DATA ERROR DETECTED "
2850     PRINT LIN(1);"OVERLAP OF INLET AND OUTLET GROOVE and/or"
2860     PRINT "GROOVE TOO LONG"
2870     PRINT LIN(1);"<cont>"
2880     PAUSE
2890     Menu=(Data(3,10)>Data(4,10))*3+(Data(3,10)<Data(4,10))*4
2900     GOSUB Menu
2910     Data_pt=(Data(3,10)<>0)*(Data(3,10)*3)+(Data(3,10)=0)*(Da
2920     ta(4,10)*3)
2920     FOR Point=1 TO Data_pt-1
2930     GOSUB Curdown

```

```
2940     NEXT Point
2950     Error=1
2960     RETURN
2970 Exit:!! Exits from routine
2980     OFF KEY #0
2990     OFF KEY #8
3000     OFF KEY #1
3010     OFF KEY #9
3020     OFF KEY #2
3030     OFF KEY #10
3040     OFF KEY #6
3050     OFF KEY #7
3060     OFF KEY #15
3070     PRINT CHR$(128)
3080     PRINT "ABC"&CHR$(12)
3090     DISP " "
3100     SUBEXIT
3110 SUBEND
```

C.2 PROGRAM VMODEL

```

10 | RE-STORE "VMODEL:F8 "
20 | ***** PROGRAM VMODEL *****
30 | * THE PROGRAM COMPUTES THE GEOMETRIC VARIABLES OF CONTROL *
40 | * VOLUME, SEGMENT PARAMETERS OF; LEAKAGE, FLOW AND PRESSURE, *
50 | * AND THE INPUT AND OUTPUT PARAMETERS OF FLOW AND PRESSURE *
60 | * FOR THE VANE M/C , AT THE VARIOUS ROTOR POSITIONS. *
70 | *
80 | * The model considers the interaction of leakage, fluid *
90 | * compressibility, fluid flow and change in segment volume. *
100 | *
110 | * Revision Notes: *
120 | * Revision# 1:28:OCT:81 initial model developed. *
130 | * # 2:24:NOV;81 outlet model change *
140 | * # 3:20:JAN;82 inlet model incl and re-structured *
150 | * # 4:11:FEB:82 inc. motor modelling. *
160 | * # 5:24:MAY:82 anal sol inc removed inlet model *
170 | * # 6: 8:SEP:82 extended anal. sol & re-structured *
180 | * # 7:20:OCT:82 restructured with mod sub 'Selsol' *
190 | * # 8:13:NOV:82 mod. Sol technique. *
200 | * # 9: 2:FEB:83 dev. inlet and improved conv. chk *
210 | * #10: 1:APR:83 Mod Solve2 and data structure. *
220 | * #11:10:MAY:83 Include inlet groove *
230 | * #12: 6:JUN:83 Mod SUB Area *
240 | * #13:28:FEB:84 End-plate leakage *
250 | * This version performs 1440 point resolution computation *
260 | *
270 | * A smaller step size can be invoked by redefining Resftr *
280 | * (Resftr:Resolution 1:360,2:720,3:1080,4:1440) *
290 | * This may be suitable for operating speeds above 2000 RPM. *
300 | * Below this there is a risk of computational instability *
310 | * and/or inaccurate solutions. *
320 | *
330 | * The program operates in two modes; AUTO and MANUAL. *
340 | * AUTO : Automatic control permitting 'BATCH' operation *
350 | * with plot option. *
360 | * MANUAL: Manual input for single runs. *
370 | *
380 | * ORIGIN: G. SEET Mech. Eng. ASTON VARSITY *
390 | * DATE: 30 JUNE 81 *
400 | *****
410 | DIM Data(1:4,1:20), Y$(0), Name1$(10), Conv2(10), Iname$(4)
420 | DIM Oname$(4), Mstore$(4), Name$(10), Pite(150), Secart(4)
430 | DIM Gdpth(1:2,1:3), Gcdim1(1:2), Gastr(1:2,1:3), Gcwth2(1:3)
440 | DIM Gtype(2)
450 | COM Auto(1:3), Aprefix$(1), Err_stat
460 | COM SHORT Ip(-360:1440), Op(-360:1440), If(-360:1440), Of(-360:14
40)
470 | COM SHORT L1(-360:1440), P(-360:1440), Q(-360:1440)
480 | COM SHORT Qi0(360), Qi1(360), Qo1(360), Qo2(360), Qo3(360)
490 | COM SHORT Vdlt(-360:1440), V(-360:1440), Area(-360:1440), H(1440
)
500 | COM Beta, Dcff, Eta, Pcau, Rho
510 | RAD
520 | MAT Auto=(0) ! Init. 'AUTO' facility array.
530 | Mstore$=":T14" ! Defines mass storage device.
540 | OVERLAP
550 | EXIT GRAPHICS
560 | PRINTER IS 16
570 | PRINT "ABC"&CHR$(12)&" PROGRAM VMODEL EXECUTING "
580 | !

```

```

590 ! Select mode
600 Input:LINPUT "IS AUTO SEQUENCE REQUIRED (Y/N):",Y$
610 IF Y$="N" THEN Manual
620 IF Y$="Y" THEN Auto
630 GOTO Input
640 !
650 ! #####
660 ! AUTO SEQUENCE ROUTINE
670 ! The routine permits batch processing of VDAT%% and the
680 ! batch running of "V PLOT". Datafiles residing on the
690 ! specified mass-storage media are accessed sequentially
700 ! between the specified upper and lower limits.
710 !
720 Auto: Iname$="VDAT"
730 LINPUT "INPUT FILENAME PREFIX: Default (V)DAT :",Dummy$
740 IF LEN(Dummy$)<>0 THEN Iname$[1,1]=Dummy$[1,1]
750 Oname$="VGDT"
760 LINPUT "OUTPUT FILENAME PREFIX: Default (V)GDT :",Dummy$
770 IF LEN(Dummy$)<>0 THEN Oname$[1,1]=Dummy$[1,1]
780 Aprefix$=Oname$[1,1] ! Auto mode data prefix
790 Auto1:INPUT "INPUT LOWEST DATAFILE NO. (>=0):",Auto(2)
800 IF (Auto(2)<0) OR (Auto(2)>99) THEN Auto1
810 Auto2:INPUT "INPUT HIGHEST DATAFILE NO. (<=99):",Auto(3)
820 IF (Auto(2)<0) OR (Auto(2)>99) THEN Auto2
830 Auto3:LINPUT "IS PLOT REQUIRED (Y/N):",Y$
840 IF Y$="N" THEN Auto(1)=2 ! Auto without plot
850 IF Y$="Y" THEN Auto(1)=1 ! Auto with plot
860 IF (Y$<>"Y") AND (Y$<>"N") THEN Auto3
870 Count=Auto(2)
880 Name$[1,4]=Iname$
890 Auto4:T=Count DIV 10
900 I=Count MOD 10
910 Name$[5]=CHR$(48+T)
920 Name$[6]=CHR$(48+I)
930 Name$[7,10]=Mstore$
940 ASSIGN Name$ TO #1,Z
950 IF Z=0 THEN Auto5
960 Count=Count+1
970 IF Count>Auto(3) THEN Rend
980 GOTO Auto4
990 Auto5: GOSUB Main
1000 Count=Count+1
1010 IF Count>Auto(3) THEN GOTO Rend
1020 GOTO Auto4
1030 Rend:IF Auto(1)=1 THEN LOAD "V PLOT"&Mstore$,330
1040 Auto(1)=0
1050 GOSUB Exit
1060 STOP
1070 !
1080 ! #####
1090 ! MANUAL SEQUENCE ROUTINE
1100 ! The routine requires individual input of data filenames
1110 Manual:Auto(1)=0 ! 'Manual' mode assigned.
1120 LINPUT " ENTER DATA FILENAME (VDAT%%): ",Name$[1,6]
1130 Oname$=Name$[1,1]&"GDT"
1140 PRINT "ABC"&CHR$(12)&" PROGRAM VMODEL EXECUTING "
1150 PRINT USING "#,K";CHR$(27)&"&a23r0C"
1160 Name$[7,10]=Mstore$
1170 PRINT " OUTPUT DATAFILE IS : ";Oname$&Name$[5,10]
1180 ASSIGN Name$ TO #1,Z

```

```

1190 IF Z=0 THEN Msrt
1200 BEEP
1210 PRINT "ABC"&CHR$(12)
1220 PRINT USING "#,K";CHR$(27)&"&a23r0C"
1230 IF Z=1 THEN PRINT " NO SUCH FILE FOUND : ";Name$
1240 IF Z=2 THEN PRINT " WRONG FILE TYPE : ";Name$
1250 GOTO Manual
1260 Msrt:GOSUB Main
1270 GOSUB Exit
1280 STOP
1290 !
1300 ! #####
1310 ! MAIN MODELLING ROUTINE
1320 !
1330 Main:PRINT "ABC"&CHR$(12)&" PROGRAM VMODEL EXECUTING "
1340 ! Set up variable list
1350 MAT READ #1;Data
1360 Sdiam=Data(1,1)/10 ! (cm)
1370 Rdiam=Data(1,2)/10 ! (cm)
1380 L=Data(1,3)/10 ! (cm)
1390 Awdth=Data(1,4)/10 ! (cm)
1400 Aclar=Data(1,5)/10 ! (cm)
1410 Vwdth=Data(1,6)/10 ! (cm)
1420 Vclar=Data(1,7)/10 ! (cm)
1430 Pdiam=Data(1,8)/10 ! (cm)
1440 Pangl=Data(1,9)/180*PI ! (rad)
1450 Abrad=Data(1,10)/10 ! (cm)
1460 Aarad=Data(1,11)/10 ! (cm)
1470 Aorad=Data(1,12)/10 ! (cm)
1480 Angl=Data(1,13)/180*PI ! (rad)
1490 Eodiam=Data(1,14)/10 ! (cm)
1500 Eidiam=Data(1,15)/10 ! (cm)
1510 Eclar=Data(1,16)/10 ! (cm)
1520 Nseg=Data(1,17) ! Num of seg/cycle
1530 Speed=Data(2,1) ! (RPM)
1540 Ipsure=Data(2,2)*10 ! (N/cm2)
1550 Opsure=Data(2,3)*10 ! (N/cm2)
1560 Cpsure=Data(2,4)*10 ! (N/cm2)
1570 Rho=Data(2,5)*1E-8 ! (NS2/cm4)
1580 Eta=Data(2,6)*.0001 ! (NS/cm2)
1590 Beta=Data(2,7)*100 ! (N/cm2)
1600 Ildiam=Data(2,8)/10 ! (cm)
1610 Oldiam=Data(2,9)/10 ! (cm)
1620 Dcff=Data(2,10) ! Discharge coeff
1630 Pcav=Data(2,11)/10 ! N/cm2 Cav pres
1640 Gdpth(1,1)=Data(3,1)/10 ! (cm) Hemis inlet dpth
1650 Gdpth(2,1)=Data(4,1)/10 ! (cm) Hemis outlet dpth
1660 Gcdim1(1)=Data(3,2)/10 ! (cm) inlet cutter dim
1670 Gcdim1(2)=Data(4,2)/10 ! (cm) outlet cutter dim
1680 Gastr(1,1)=Data(3,3)/180*PI ! (rad) inlet start ang
1690 Gastr(2,1)=Data(4,3)/180*PI ! (rad) outlet start ang
1700 Gdpth(1,2)=Data(3,4)/10 ! (cm) Square inlet dpth
1710 Gdpth(2,2)=Data(4,4)/10 ! (cm) Square outlet dpth
1720 Gcwth2(1)=Data(3,5)/10 ! (cm) inlet wdth
1730 Gcwth2(2)=Data(4,5)/10 ! (cm) outlet wdth
1740 Gastr(1,2)=Data(3,6)/180*PI ! (rad) inlet start ang
1750 Gastr(2,2)=Data(4,6)/180*PI ! (rad) outlet start ang
1760 Gdpth(1,3)=Data(3,7)/10 ! (cm) Triang inlet dpth
1770 Gdpth(2,3)=Data(4,7)/10 ! (cm) Triang outlet dpth
1780 Gcang3(1)=Data(3,8)/180*PI ! (cm) inlet cutter ang

```

```

1790 Gcang3(2)=Data(4,8)/180*PI ! (cm) outlet cutter ang
1800 Gastr(1,3)=Data(3,9)/180*PI ! (rad) inlet start ang
1810 Gastr(2,3)=Data(4,9)/180*PI ! (rad) outlet start ang
1820 Gtype(1)=Data(3,10) ! Defines Inlet groove
1830 Gtype(2)=Data(4,10) ! Defines Outlet groove
1840 Vwang=2*ASN(Vwidth/Rdiam) ! (rad)
1850 Awang=2*ASN(Awidth/Rdiam) ! (rad)
1860 Phi=2*ASN(Pdiam/(Sdiam*COS(Pang1))) ! (rad)
1870 U=Sdiam*PI*Speed/600 ! (cm/s)
1880 Omega=PI*Speed/30 ! (rad/s)
1890 Erad=(Eodiam+Eidiam)/4 ! (cm) plate radius
1900 Ewth=(Eodiam-Eidiam)/2 ! (cm)
1910 Ite_err=5.0E-4 ! Permitted iteration error
1920 Maxpass=15 ! Maximum no. of passes
1930 Resftr=3 ! Resolution factor
1940 Resnum=Resftr*360 ! Total no. points
1950 Res=INT(Resnum/Nseg) ! No. points per sector
1960 Inc=PI/(4*Res) ! (rad)
1970 Secsrt(0)=-Res ! Start of Sector0
1980 Secsrt(1)=1 ! Start of Sector1
1990 Secsrt(2)=Res+1 ! Start of Sector2
2000 Secsrt(3)=Resnum-2*Res+1 ! Start of Sector3
2010 Secsrt(4)=Resnum-Res+1 ! Start of Sector4
2020 Modelart=(-(PI/Nseg)+.5*(Awang+Vwang))/Inc ! Start
2030 Modelend=(PI-.5*(Awang+Vwang))/Inc ! End
2040 Leakmax=1500/Res ! Max permitted leakage,Sub:Selso1
2050 Minvdlta=.5 ! Small Vdlta value ,Sub:Selso1
2060 Leakcont=.01 ! Leakage constant ,Sub:Selso1
2070 Checklist=0 ! Checklist not reqd:0
2080 Conftr_o=.1 ! Press. fluct. suppressor outlet
2090 Conftr_i=.1 ! Press. fluct. suppressor inlet
2100 Instat=0 ! No inlet pressure fluct.
2110 !
2120 ! *****
2130 ! This section generates the vane height array.
2140 DISP " PROCESSING VHEIGHT "
2150 CALL Vheight(Rang1,Rarad,Abrod,Aorad,Awang,Inc,Res,Rdiam,Sdiam,
Vclar,Vwang,H(*)
2160 ! *****
2170 ! This section cal. the ctl. vol. for all angles of rotation
2180 DISP " PROCESSING VCTL "
2190 CALL Vctl(Awang,Inc,L,Nseg,Rdiam,Res,Sdiam,Vwang,Vwidth,V(*),H
(*)
2200 ! *****
2210 ! This section calculates change in ctl. vol.
2220 DISP " PROCESSING VDLTA "
2230 CALL Vdlta(Awang,Inc,L,Nseg,Rdiam,Res,Sdiam,Vclar,Vwang,H(*),
Vdlta(*)
2240 ! *****
2250 ! This section calculates orifice flow areas.
2260 DISP " PROCESSING AREA "
2270 CALL Area(Awang,Gtype(*),Gcdim1(*),Gcwth2(*),Gcang3(*),Inc,L,
Nseg,Pang1,Pdiam,Phi,Res,Sdiam,Vwang,Gastr(*),Gdpth(*),Area(*)
2280 ! *****
2290 ! This section sets up starting values of pressure and flow.
2300 DISP " PROCESSING INITIAL "
2310 CALL Initial(Ipsure,Nseg,Opsure,Res,Resnum,Secsrt(*),P(*),Ip(
*),Op(*)
2320 !
2330 ! *****

```

```

2340 ! Start of iteration loop:Recalculates segment pressures till
2350 ! convergence criteria is met. Maximum number of permitted
2360 ! re-iteration is Maxpass
2370 PRINTER IS 0
2380 PRINT LIN(2)," PROCESSING :";Name$
2390 Pass=1
2400 !
2410 Repass:! Re_entry for next pass
2420 !
2430 PRINTER IS 0
2440 PRINT USING "/,14A,D,/";" PASS NUMBER :";Pass,CHR$(128)
2450 PRINTER IS 16
2460 !
2470 ! *****
2480 DISP " PROCESSING SEMENT DATA "
2490 Vcav=0 ! Reset cavitation Vol.
2500 !
2510 ! Determine initial value
2520 Idir=1
2530 Sector=1
2540 Pstat=1 ! 1:Inlet mode 2:Outlet mode
2550 Pstart=0
2560 FOR I=1 TO 5
2570 CALL Splin(Aclar,Awdth,Awang,Cpsure,Dir,Eclar,Enad,Ewth,Inc,I
dir,L,Nseg,Omega,Pangl,Phi,Pstat,Res,Sector,U,Vcav,Vclar,Vwang,Vwdth
,I)
2580 Pstart=Pstart+P(I)
2590 NEXT I
2600 Pstart1=Pstart*.2 ! Averages first 5 points
2610 P(0)=Pstart1
2620 IF P(0)<Ipsure THEN Scomp ! Improbable start check
2630 !
2640 ! + Escape routine :Alternative start value
2650 ! + Assigns start value as Ipsure less orifice losses.
2660 Area=Area(1)
2670 Q=Omega*Vdlt(1)
2680 K1=Q/(Dcff*Area)
2690 Ploss=Rho/2*(K1*K1)
2700 Ploss=Rho/2*(Q/(Dcff*Area))^2
2710 Pstart2=Ipsure-Ploss
2720 !
2730 Scomp:! Starts computing sector pressures.
2740 Csum=0 ! Reset Csum status
2750 IMAGE DDD,X,DDDD,XX,3(DDDD.DD,X),4(DDDD.DDD,X),X,D.DDDD
2760 IMAGE DDD,X,DDDD,XX,2(DDDD.DD,X),8X,4(DDDD.DDD,X),X,D.DDDD
2770 !
2780 ! *** PRE-SECTOR ***
2790 ! Pre-sector is calculated in reverse direction to motion.
2800 ! P(0)=P(Secart(1)-1) Value attained at start value.
2810 Idir=-1 ! Dir. of iteration :counter to motion
2820 Sector=0 ! Sector Identifier
2830 Pstat=1 ! 1:Inlet mode 2:Outlet mode
2840 FOR I=Secart(1)-3 TO Secart(0)+1 STEP -1
2850 GOSUB Selsol
2860 -Ii=I
2870 IF Ii<0 THEN Ii=Ii+Res
2880 PRINT USING 2760;0,I,P(I),P(I+Res),Area(I),Vdlt(I),L1(I),V(I
),H(Ii)
2890 NEXT I
2900 P(Secart(1)-2)=P(Secart(1)-3) ! Transition error

```

```
2910 P(Secsrt(0))=P(Secsrt(0)+1)
2920 ! *** FIRST SECTOR ***
2930 Idir=1
2940 Sector=1 ! Sector identifier
2950 Pstat=1 ! 1:Inlet mode 2:Outlet mode
2960 L1(Secsrt(1))=L1(Secsrt(1)-3)
2970 P(Secsrt(1))=P(Secsrt(1)-3)
2980 FOR I=Secsrt(1)+1 TO Secsrt(2)-2
2990 GOSUB Selsol
3000 PRINT USING 2750;1,I,P(I),P(I-Res),P(I+Res),Area(I),Vdlt(I),
L1(I),V(I),H(I)
3010 NEXT I
3020 P(Secsrt(1))=P(Secsrt(1)+1) ! Transition error
3030 P(Secsrt(2)-1)=P(Secsrt(2)-2)
3040 ! *** SECOND SECTOR ***
3050 Idir=1
3060 Sector=2 ! Sector identifier
3070 Pstat=1 ! 1:Inlet mode 2:Outlet mode
3080 L1(Secsrt(2))=L1(Secsrt(2)-2)
3090 P(Secsrt(2))=P(Secsrt(2)-2)
3100 FOR I=Secsrt(2)+1 TO Secsrt(3)-2
3110 IF Area(I)<=0 THEN Pstat=2 ! Change to outlet mode
3120 GOSUB Selsol
3130 PRINT USING 2750;2,I,P(I),P(I-Res),P(I+Res),Area(I),Vdlt(I),
L1(I),V(I),H(I)
3140 NEXT I
3150 P(Secsrt(2))=P(Secsrt(2)+1) ! Transition error
3160 P(Secsrt(3)-1)=P(Secsrt(3)-2)
3170 ! **** THIRD SECTOR ***
3180 Idir=1
3190 Sector=3 ! Sector identifier
3200 L1(Secsrt(3))=L1(Secsrt(3)-2)
3210 P(Secsrt(3))=P(Secsrt(3)-2)
3220 FOR I=Secsrt(3)+1 TO Secsrt(4)-2
3230 GOSUB Selsol
3240 PRINT USING 2750;3,I,P(I),P(I-Res),P(I+Res),Area(I),Vdlt(I),
L1(I),V(I),H(I)
3250 NEXT I
3260 P(Secsrt(3))=P(Secsrt(3)+1) ! Transition error
3270 P(Secsrt(4)-1)=P(Secsrt(4)-2)
3280 ! **** FOURTH SECTOR ***
3290 Idir=1
3300 Sector=4
3310 L1(Secsrt(4))=L1(Secsrt(4)-2)
3320 P(Secsrt(4))=P(Secsrt(4)-2)
3330 FOR I=Secsrt(4)+1 TO Resnum-1
3340 GOSUB Selsol
3350 PRINT USING 2760;4,I,P(I),P(I-Res),Area(I),Vdlt(I),L1(I),V(I),
H(I)
3360 NEXT I
3370 P(Secsrt(4))=P(Secsrt(4)+1)
3380 P(Resnum)=P(Resnum-1)
3390 !
3400 ! *****
3410 ! Smooths P array by moving point averaging.
3420 CALL Smooth(Resnum,.5,P(*))
3430 !
3440 ! *****
3450 ! Generates segment and inlet/outlet data arrays.
3460 DISP " PROCESSING INLET/ OUTLET CONDITIONS :GDAT1"
```

```

3470 CALL Gdat1(Aclar,Awdth,Ang, Cpsure,Eclar,Ernd,Erwth,Inc,L,Min
vdlt,a,Nseg, Omega, Pangl, Phi, Res, Resnum, Secsrt(*), U, Vclar, Vwang, Vwdth)
3480 !
3490 ! *****
3500 ! Smooths If and Of arrays by moving point averaging.
3510 CALL Smooth(Resnum,1,If(*))
3520 CALL Smooth(Resnum,1,Of(*))
3530 !
3540 ! *****
3550 ! This section generates pump line pressure from the Inlet
3560 ! and outlet flow.
3570 DISP " PROCESSING INLET/ OUTLET CONDITIONS :PSURE"
3580 CALL Psure(Beta,Conftr_i,Conftr_o,Instat,Ipsure,Ildiam,Oldiam
,Opsure,Resnum,Rho,0,Secsrt(*),Of(*),If(*),Op(*),Ip(*))
3590 !
3600 ! *****
3610 ! Smooths Ip and Op arrays by moving point averaging.
3620 CALL Smooth(Resnum,3,Ip(*))
3630 CALL Smooth(Resnum,3,Op(*))
3640 !
3650 ! Convergence check
3660 !
3670 IF Pass<2 THEN Store_of ! Skip check & store array.
3680 !
3690 ! Check Of array for convergence
3700 Ofdiff_1=Ofdiff
3710 Ofdiff=0
3720 FOR I=1 TO Res
3730 Ofdiff=Ofdiff+ABS(Dummy0(I)-Of(I))
3740 NEXT I
3750 PRINTER IS 0
3760 PRINT " Pass convergence indicator :";Ofdiff/Sumof
3770 PRINTER IS 16
3780 IF (Ofdiff/Sumof<Ite_err*Resftr) AND (Pass>3) THEN Mdl_corr
3790 IF (Ofdiff>Ofdiff_1) AND (Pass>4) THEN Mdl_corr
3800 IF Pass>4 THEN Mdl_corr
3810 !
3820 Store_of:! Store intm Of array & mean value over 1 vane pitch
3830 Sumof=0
3840 FOR I=1 TO Res
3850 Dummy0(I)=Of(I)
3860 Sumof=Sumof+Dummy0(I)
3870 NEXT I
3880 !
3890 Nextpass:! Check before next pass
3900 Pass=Pass+1
3910 IF Pass<=Maxpass THEN Repass
3920 !
3930 ! Failure to converge
3940 Csum=9999 ! Sets data check sum for invalid data.
3950 PRINTER IS 0
3960 PRINT " NO CONVERGENCE AFTER ";Maxpass;" iterations !!!! "
3970 PRINTER IS 16
3980 !
3990 Mdl_corr:! End model connections.
4000 !
4010 ! Characteristic line pressure
4020 CALL Psure(Beta,1,1,1,Ipsure,Ildiam,Oldiam,Opsure,Resnum,Rho,
1,Secsrt(*),Of(*),If(*),Op(*),Ip(*))
4030 !

```

```

4040 ! Abutment correction
4050 Endgrad=-(P(Modelend)-P(1))/(Resnum-Modelend)
4060 FOR I=INT(Modelend+1.5) TO Resnum
4070 P(I)=P(Modelend)+Endgrad*(I-Modelend)
4080 NEXT I
4090 !
4100 Checklist: ! Lists data arrays.
4110 IF Checklist=0 THEN GOTO Outfile ! Checklist not required.
4120 PRINTER IS 0
4130 IMAGE 3A,4X,6(X,11A)
4140 IMAGE DDD,6(X,M5D.4D)
4150 PRINT USING 4130;" I","P(I)","L1(I)","Vd1ta(I)"," Area(I)","
H(I)"," V(I)"
4160 Apos=1
4170 FOR I=1 TO 4*Res STEP 4*Res/360
4180 PRINT USING 4140;Apos,P(I),L1(I),Vd1ta(I),Area(I),H(I),V(I)
4190 Apos=Apos+1
4200 NEXT I
4210 PRINTER IS 16
4220 !
4230 ! Outputs the generated data into a data file (V)GDT%
4240 ! File format: sequential access, 360 elements in each array
4250 ! six arrays; P,L1,Q,Ip,Op,If,Of
4260 !
4270 Outfile: ! Generates output file
4280 Name1$[1,4]=Oname$
4290 Name1$[5,6]=Name$[5,6]
4300 Name1$[7,10]=Mstore$
4310 !
4320 ! Lists Input & Output filenames.
4330 PRINTER IS 0
4340 PRINT USING "28A,DD";" TOTAL NUMBER OF PASSES:",Pass
4350 IMAGE /,17A,10A,3X,17A,10A
4360 PRINT USING 4350;" Input Datafile: ";Name$,"Output Datafile;
",Name1$
4370 PRINTER IS 16
4380 !
4390 ! Prepares and outputs pump history to datafile.
4400 DISP " OUTPUTING DATA "
4410 ASSIGN Name1$ TO #2,Z
4420 IF Z=0 THEN PURGE Name1$
4430 IF Z=0 THEN Outfile2
4440 IF Z=1 THEN Outfile2
4450 PRINTER IS 0
4460 PRINT " DUPLICATE PROGRAM FILENAME !!!"
4470 PRINT " DATAFILE NOT GENERATED ";Name1$
4480 PRINTER IS 16
4490 GOTO Outend ! No file generated.
4500 !
4510 Outfile2: ! Reorder data array size
4520 SHORT Dummy0(360),Dummy1(360),Dummy2(360),Dummy3(360)
4530 SHORT Dummy4(360),Dummy5(360),Dummy6(360),Dummy7(360)
4540 FOR I=1 TO 360
4550 J=I*INT(Resnum/360)
4560 Dummy1(I)=P(J)
4570 Dummy2(I)=L1(J)
4580 Dummy3(I)=Q(J)
4590 Dummy4(I)=Ip(J)
4600 Dummy5(I)=Op(J)
4610 Dummy6(I)=If(J)

```

```

4620 Dummy7(I)=Of(J)
4630 NEXT I
4640 !
4650 ! Outputs pump history.
4660 CREATE Name1$,40
4670 ASSIGN Name1$ TO #2
4680 PRINT #2;Csum
4690 MAT PRINT #2;Dummy1,Dummy2,Dummy3,Dummy4,Dummy5,Dummy6,Dummy7
,END
4700 PRINTER IS 0
4710 PRINT LIN(1),TAB(2);RPT$("#",24);"END OF RUN";RPT$("#",25),LI
N(1)
4720 PRINTER IS 16
4730 !
4740 Outend:!! Closes logical assignment.
4750 ASSIGN * TO #1
4760 ASSIGN * TO #2
4770 Csum=0 ! Reset status checksum.
4780 RETURN
4790 !
4800 ! #####
4810 ! DETERMINES SOLUTION TYPE
4820 ! This subroutine check the parameters of change in swept vol
4830 ! and inst. port flow area; and determines the appropriate
4840 ! solution technique.
4850 !
4860 ! Solution : Sub "Spnlin"
4870 ! Non-Linear conditions and transition zones.
4880 ! a) Significant leakage condition
4890 ! Check : Vdlt*Omega>Leakcont*L1
4900 ! b) High change in leakage rate
4910 ! Check : Delta L1>Leakmax :Leakmax=1500/Res cm3/step
4920 ! c) Vdlt>0 in second sector.(Secsrt(2) to Secsrt(1)-1)
4930 !
4940 ! Solution: Sub "Spln"
4950 ! d) Vdlt=0 in second sector.(Secsrt(2) to Secsrt(1)-1)
4960 ! e) All remaining region
4970 !
4980 ! Solution:Approx
4990 ! P(I)=P(I-Idir)
5000 !
5010 ! f) Undefined region: X> Modelend , X< Modelst
5020 ! g) Very small Vdlt: Minvdlt in sector 0 & 4
5030 ! ** This approximation provides for a shorter program time
5040 ! there is no significant error as there is little pressure
5050 ! change in this region.
5060 ! #####
5070 !
5080 Selsol:!! Selects solution method.
5090 ON Sector+1 GOTO Sector0,Sector1,Sector2,Sector3,Sector4
5100 !
5110 Sector0:!! Pre Sector.
5120 IF I<=Modelst THEN Selsol3
5130 IF Area(I)<=0 THEN Selsol1
5140 IF (ABS(Vdlt(I))<Minvdlt) AND (I<Secsrt(0)+.75*Res) THEN GO
TO Selsol3
5150 IF ABS(Vdlt(I-Idir)*Omega)<Leakcont*ABS(L1(I-Idir)) THEN GOT
O Selsol2
5160 IF (ABS(L1(I-Idir)-L1(I-2*Idir))>Leakmax) AND (ABS(L1(I-2*Idi
r)-L1(I-3*Idir))>Leakmax) AND (ABS(L1(I-3*Idir)-L1(I-4*Idir))>Leakma
x) THEN Selsol2

```

```

5170 GOTO Selsol1
5180 Sector1!! First Sector.
5190 IF Area(I)<=0 THEN Selsol1
5200 IF ABS(Vdlt(I-Idir)*Omega)<Leakcont*ABS(L1(I-Idir)) THEN GOT
0 Selsol2
5210 IF (ABS(L1(I-Idir)-L1(I-2*Idir))>Leakmax) AND (ABS(L1(I-2*Idi
r)-L1(I-3*Idir))>Leakmax) AND (ABS(L1(I-3*Idir)-L1(I-4*Idir))>Leakma
x) THEN Selsol2
5220 GOTO Selsol1
5230 Sector2!! Second Sector.
5240 IF Area(I)>0 THEN GOTO Selsol2
5250 GOTO Selsol1
5260 Sector3!! Third Sector.
5270 IF Area(I)<=0 THEN Selsol1
5280 IF ABS(Vdlt(I-Idir)*Omega)<Leakcont*ABS(L1(I-Idir)) THEN GOT
0 Selsol2
5290 IF (ABS(L1(I-Idir)-L1(I-2*Idir))>Leakmax) AND (ABS(L1(I-2*Idi
r)-L1(I-3*Idir))>Leakmax) AND (ABS(L1(I-3*Idir)-L1(I-4*Idir))>Leakma
x) THEN Selsol2
5300 GOTO Selsol1
5310 Sector4!! Fourth Sector.
5320 IF I>=Modelend THEN Selsol3
5330 IF Area(I)<=0 THEN Selsol1
5340 IF (ABS(Vdlt(I))<Minvdlt) AND (I>Secsrt(4)+.25*Res) THEN GO
TO Selsol3
5350 IF ABS(Vdlt(I-Idir)*Omega)<Leakcont*ABS(L1(I-Idir)) THEN GOT
0 Selsol2
5360 IF (ABS(L1(I-Idir)-L1(I-2*Idir))>Leakmax) AND (ABS(L1(I-2*Idi
r)-L1(I-3*Idir))>Leakmax) AND (ABS(L1(I-3*Idir)-L1(I-4*Idir))>Leakma
x) THEN Selsol2
5370 Selsol1!! Linear condition.
5380 DISP "I= ";I;" Linear Sol"
5390 Err_stat=0
5400 ON ERROR CALL Err_rec
5410 CALL Splin(Aclar, Awang, Cpsure, Dir, Eclar, Erad, Ewth, Inc, I
dir, L, Nseg, Omega, Pangl, Phi, Pstat, Res, Sector, U, Vcav, Vclar, Vwang, Vwdth
, I)
5420 OFF ERROR
5430 IF Err_stat=1 THEN GOTO Recover1
5440 RETURN
5450 Selsol2!! Nonlinear condition.
5460 DISP "I= ";I;" Non-linear Sol"
5470 Err_stat=0
5480 ON ERROR CALL Err_rec
5490 CALL Spnlin(Aclar, Awang, Awdth, Cpsure, Eclar, Erad, Ewth, Idir, Inc
, L, Nseg, Omega, Pangl, Phi, Pstat, Sector, U, Vcav, Vclar, Vwang, Vwdth, Res, Cs
um, I)
5500 OFF ERROR
5510 IF Err_stat=1 THEN GOTO Recover2
5520 RETURN
5530 Selsol3!! Approx solution at model boundaries.
5540 DISP "I= ";I;" Approximate Sol"
5550 P(I)=P(I-Idir)
5560 RETURN
5570 Recover1!! Recovery for linear sol.
5580 Errm$="Linear"
5590 GOSUB Pnt_err
5600 GOTO Selsol2
5610 Recover2!! Recovery for non-linear sol.
5620 Errm$="Non-linear"

```

```

5630 GOSUB Prt_err
5640 GOTO Selsol3
5650 Prt_err!! Prints error messages
5660 PRINTER IS 0
5670 PRINT "Counter: ";I,TRIM$(ERRM$);" for "&Enrm$&" solution"
5680 PRINTER IS 16
5690 RETURN
5700 !
5710 ! *****
5720 ! PRINTS EXIT MESSAGES
5730 !
5740 Exit:PRINT "ABS"&CHR$(12)
5750 PRINT RPT$("*",80),LIN(2)
5760 PRINT RPT$("*",34);" COMPLETED ";RPT$("*",35)
5770 PRINT LIN(2),RPT$("*",80),LIN(5)
5780 PRINT " THIS MACHINE IS FREE FOR THE NEXT USER "
5790 PRINT LIN(2)
5800 PRINT "PLEASE PLACE DISK/CASSETTE IN APPROPRIATE CONTAINER"
5810 PRINT "THANK YOU"
5820 PRINT TAB(61);" G.SEET "
5830 DISP RPT$("*",80)
5840 DISP " "
5850 RETURN
5860 END !*****
5870 ! END OF MAIN PROGRAM SEGMENT
5880 ! *****
5890 ! ++++++ SUBROUTINE LEAK ++++++
5900 ! + Calculates vane tip leakages into the control volume. +
5910 ! ++++++
5920 SUB Leak(Aclar, Awang, Awdth, Cpsure, Eclar, Erad, Ewth, Inc, L, Nseg,
Omega, Res, Sector, U, Vclar, Vwang, Vwdth, I)
5930 COM Auto(1:3), Aprefix$(1), Err_stat
5940 COM SHORT Ip(-360:1440), Op(-360:1440), If(-360:1440), Of(-360:1
440)
5950 COM SHORT L1(-360:1440), P(-360:1440), Q(-360:1440)
5960 COM SHORT Qi0(360), Qi1(360), Qo1(360), Qo2(360), Qo3(360)
5970 COM SHORT Vdlt(-360:1440), V(-360:1440), Area(-360:1440), H(144
0)
5980 COM Beta, Dcff, Eta, Pcav, Rho
5990 P3=Cpsure-P(I)
6000 W3=Ewth
6010 H3=Eclar
6020 ON Sector+1 GOTO Leak0, Leak1, Leak2, Leak3, Leak4
6030 Leak0:!! ***** Sector0 *****
6040 Theta=-(Res*Inc)+.5*(Awang+Vwang)
6050 Lek01: IF Inc*I>Theta THEN Lek02
6060 L1(I)=0 ! Sector not defined
6070 SUBEXIT
6080 Lek02: W1=Vwdth
6090 H1=H(I+Res)
6100 P1=P(I+Res)-P(I)
6110 W2=Awdth
6120 H2=Aclar
6130 P2=P(Nseg*Res+I)-P(I)
6140 L3=Erad*(Inc*(I+Res)-.5*(Awang+Vwang))
6150 L1(I)=FNLeak1(Eta, H1, H2, H3, L, L3, P1, P2, P3, Sector, U, Vclar, W
1, W2, W3)
6160 SUBEXIT
6170 Leak1:!! ***** Sector1 *****
6180 Theta=.5*(Awang+Vwang)

```

```

6190      W1=Vwidth
6200      H1=H(I+Res)
6210      P1=P(I+Res)-P(I)
6220 Lek11: IF I*Inc>Theta THEN GOTO Lek12
6230      W2=Awidth
6240      H2=Aclar
6250      P2=P((Nseg-1)*Res+I)-P(I)
6260      L3=Erads*(Inc*(I+Res)-.5*(Awang+Vwang))
6270      L1(I)=FNLeak1(Eta,H1,H2,H3,L,L3,P1,P2,P3,Sector,U,Vclar,W
1,W2,W3)
6280      SUBEXIT
6290 Lek12:H2=H(I)
6300      W2=Vwidth
6310      P2=P(I-Res)-P(I)
6320      L3=Erads*(Inc*Res-Vwang)
6330      L1(I)=FNLeak1(Eta,H1,H2,H3,L,L3,P1,P2,P3,Sector,U,Vclar,W
1,W2,W3)
6340      SUBEXIT
6350 Leak2:! ***** Sector2 *****
6360      H1=H(I+Res)
6370      W1=Vwidth
6380      P1=P(Res+I)-P(I)
6390      H2=H(I)
6400      W2=Vwidth
6410      P2=P(I-Res)-P(I)
6420      L3=Erads*(Inc*Res-Vwang)
6430      L1(I)=FNLeak1(Eta,H1,H2,H3,L,L3,P1,P2,P3,Sector,U,Vclar,W
1,W2,W3)
6440      SUBEXIT
6450 Leak3:! ***** Sector3 *****
6460      Theta=(1-1/Nseg)*PI-.5*(Awang+Vwang)
6470      H2=H(I)
6480      W2=Vwidth
6490      P2=P(I-Res)-P(I)
6500      L3=Erads*(Inc*Res-Vwang)
6510 Lek31: IF Inc*I>Theta THEN GOTO Lek32
6520      H1=H(I+Res)
6530      W1=Vwidth
6540      P1=P(I+Res)-P(I)
6550      L1(I)=FNLeak1(Eta,H1,H2,H3,L,L3,P1,P2,P3,Sector,U,Vclar,W
1,W2,W3)
6560      SUBEXIT
6570 Lek32:H1=Aclar
6580      W1=Awidth
6590      P1=P(I-(Nseg-1)*Res)-P(I)
6600      L1(I)=FNLeak1(Eta,H1,H2,H3,L,L3,P1,P2,P3,Sector,U,Vclar,W
1,W2,W3)
6610      SUBEXIT
6620 Leak4:! ***** Sector4 *****
6630      Theta=PI-.5*(Awang+Vwang)
6640 Lek41: IF Inc*I>Theta THEN Lek42
6650      W1=Awidth
6660      H1=Aclar
6670      P1=P(I-Nseg*Res)-P(I)
6680      W2=Vwidth
6690      H2=H(I)
6700      P2=P(I-Res)-P(I)
6710      L3=Erads*(Theta-I*Inc)
6720      L1(I)=FNLeak1(Eta,H1,H2,H3,L,L3,P1,P2,P3,Sector,U,Vclar,W
1,W2,W3)

```

```

6730      SUBEXIT
6740 Lek42:L1(I)=0      ! Sector is undefined
6750      SUBEXIT
6760      SUBEND
6770      ! ++++++ SUBFUNCTION LEAK1 ++++++
6780      ! Calculates total leakage across the segment vane boundary
6790      ! ++++++
6800      DEF FNLeak1(Eta,H1,H2,H3,L,L3,P1,P2,P3,Sector,U,Vclar,W1,W2,W3
)
6810      CALL Chkh(H1,H2,Sector,Vclar,He1,He2,Hv1,Hv2)
6820      Qv=(L*(Hv1^3*P1/W1+Hv2^3*P2/W2)+2*L3*H3^3*P3/W3)/(12*Eta)
6830      Qe=(He1-He2)*U*L/2
6840      Q=Qv+Qe      ! mm3/S
6850      RETURN Q
6860      FNEND
6870      !
6880      ! ++++++ SUBROUTINE CHKH ++++++
6890      ! + Checks vane clearance to permitted values.      +
6900      ! + This is necessary to hold within bounds entrain effects +
6910      ! + and to avoid unnecessarily low vane tip resistances. +
6920      ! ++++++
6930      SUB Chkh(H1,H2,Sector,Vclar,He1,He2,Hv1,Hv2)
6940      Entftm=6      ! Entrained flow factor in main sectors
6950      Visftm=6      ! Viscous flow factor in main sectors
6960      Entfte=6      ! Entrained flow factor in end sectors
6970      Visfte=6      ! Viscous flow factor in end sectors
6980      He1=Hv1=H1
6990      He2=Hv2=H2
7000      ON Sector+1 GOTO Chk1,Chk2,Chk3
7010      Chk1:! Sector0
7020      IF He1>Entfte*Vclar THEN He1=Entfte*Vclar
7030      IF He2>Entftm*Vclar THEN He2=Entftm*Vclar
7040      IF Hv1>Visfte*Vclar THEN Hv1=Visfte*Vclar
7050      IF Hv2>Visftm*Vclar THEN Hv2=Visftm*Vclar
7060      SUBEXIT
7070      Chk2:! Main Sector
7080      Entftr=Entftm*Vclar
7090      Visftr=Visftm*Vclar
7100      IF He1>Entftr THEN He1=Entftr
7110      IF He2>Entftr THEN He2=Entftr
7120      IF Hv1>Visftr THEN Hv1=Visftr
7130      IF Hv2>Visftr THEN Hv2=Visftr
7140      SUBEXIT
7150      Chk3:! Sector4
7160      IF He1>Entftm*Vclar THEN He1=Entftm*Vclar
7170      IF He2>Entfte*Vclar THEN He2=Entfte*Vclar
7180      IF Hv1>Visftm*Vclar THEN Hv1=Visftm*Vclar
7190      IF Hv2>Visfte*Vclar THEN Hv2=Visfte*Vclar
7200      SUBEXIT
7210      SUBEND
7220      !
7230      ! ++++++ SUBROUTINE FLOW ++++++
7240      ! + Calculates nett flow into the control volume.      +
7250      ! ++++++
7260      SUB Flow(Awang,Dcwf,Inc,Idir,Minvdlta,Nseg,Pstat,Res,Rho,Secto
r,Vwang,I)
7270      COM Auto(1:3),Aprefix#[1],Err_stat
7280      COM SHORT Ip(-360:1440),Op(-360:1440),If(-360:1440),Of(-360:14
40)
7290      COM SHORT L1(-360:1440),P(-360:1440),Q(-360:1440)

```

```

7300 COM SHORT Qi0(360),Qi1(360),Qo1(360),Qo2(360),Qo3(360)
7310 COM SHORT Vd1ta(-360:1440),V(-360:1440),Area(-360:1440),H(1440)
7320 ON Sector+1 GOTO Flow0,Flow1,Flow2,Flow3,Flow4
7330 Flow0:! ***** Sector0 *****
7340 Theta=-(Res*Inc)+.5*(Awang+Vwang)
7350 Flw01:IF I*Inc>Theta THEN Flw02
7360 Qi0(I+Res)=0 ! Sector undefined
7370 Q(I)=0
7380 SUBEXIT
7390 Flw02:IF ABS(Vd1ta(I))>Minvd1ta THEN Flw03
7400 IF Theta/Inc-I+Idir=0 THEN Flw02a
7410 Q(I)=Q(I-Idir)+Q(I-Idir)/(Theta/Inc-I+Idir)
7420 IF Q(I)>0 THEN Flw02b
7430 Flw02a:Q(I)=0
7440 Flw02b:Qi0(I+Res)=-Q(I)+L1(I)
7450 SUBEXIT
7460 Flw03:P0=ABS(P(I)-Ip(I))
7470 P1=P(I)-Ip(I)
7480 Qi0(I+Res)=SGN(P1)*Dcff*Area(I)*SQR(2*P0/Rho)
7490 Q(I)=-Qi0(I+Res)+L1(I)
7500 SUBEXIT
7510 Flow1:! ***** Sector1 *****
7520 P0=ABS(P(I)-Ip(I))
7530 P1=P(I)-Ip(I)
7540 Qi1(I)=SGN(P1)*Dcff*Area(I)*SQR(2*P0/Rho)
7550 Q(I)=-Qi1(I)+L1(I)
7560 SUBEXIT
7570 Flow2:! ***** Sector2 *****
7580 Pp=Ip(I)*(Pstat=1)+Op(I)*(Pstat=2)
7590 P0=ABS(P(I)-Pp)
7600 P1=P(I)-Pp
7610 Qo1(I-Res)=SGN(P1)*Dcff*Area(I)*SQR(2*P0/Rho)
7620 Q(I)=-Qo1(I-Res)+L1(I)
7630 SUBEXIT
7640 Flow3:! ***** Sector3 *****
7650 P0=ABS(P(I)-Op(I))
7660 P1=P(I)-Op(I)
7670 Qo2(I-2*Res)=SGN(P1)*Dcff*Area(I)*SQR(2*P0/Rho)
7680 Q(I)=-Qo2(I-2*Res)+L1(I)
7690 SUBEXIT
7700 Flow4:! ***** Sector4 *****
7710 Theta=PI-.5*(Awang+Vwang)
7720 Flw41:IF (I*Inc>Theta) OR (ABS(Vd1ta(I))<=Minvd1ta) THEN Flw42
7730 P0=ABS(P(I)-Op(I))
7740 P1=P(I)-Op(I)
7750 Qo3(I-3*Res)=SGN(P1)*Dcff*Area(I)*SQR(2*P0/Rho)
7760 Q(I)=-Qo3(I-3*Res)+L1(I)
7770 SUBEXIT
7780 Flw42:IF I*Inc>Theta THEN Flw43
7790 IF Theta/Inc-I+Idir=0 THEN Flw42a
7800 Q(I)=Q(I-Idir)+Q(I-Idir)/(Theta/Inc-I+Idir)
7810 IF Q(I)<0 THEN Flw42b
7820 Flw42a:Q(I)=0
7830 Flw42b:Qo3(I-3*Res)=-Q(I)+L1(I)
7840 SUBEXIT
7850 Flw43:Qo3(I-3*Res)=0 ! Sector Undefined
7860 Q(I)=0
7870 SUBEXIT
7880 SUBEND

```

```

7890 !
7900 ! ++++++ SUBROUTINE SPNLIN ++++++
7910 ! + This subroutine solves the non-linear equations for +
7920 ! + pressure flow and leakage. +
7930 ! + +
7940 ! + Define max. stepsize: Maxstep +
7950 ! ++++++
7960 SUB Spnlin(Aclar, Awang, Awdth, Cpsure, Eclar, Erad, Ewth, Idir, Inc, L
, Nseg, Omega, Pangl, Phi, Pstat, Sector, U, Vcav, Vclar, Vwang, Vwdth, Res, Csum
, I)
7970 COM Auto(1:3), Aprefix$(1), Err_stat
7980 COM SHORT Ip(-360:1440), Op(-360:1440), If(-360:1440), Of(-360:14
40)
7990 COM SHORT L1(-360:1440), P(-360:1440), Q(-360:1440)
8000 COM SHORT Qi0(360), Qi1(360), Qo1(360), Qo2(360), Qo3(360)
8010 COM SHORT Vdlt a(-360:1440), V(-360:1440), Area(-360:1440), H(1440
)
8020 COM Beta, Dcff, Eta, Pcav, Rho
8030 SHORT Pite(0:512)
8040 Theta1=-(Res*Inc)+.5*(Awang+Vwang)
8050 Theta2=(1-1/Nseg)*PI-.5*(Awang+Vwang)
8060 Maxstep=512 ! Max step size
8070 Csum1=Sector
8080 !
8090 ! *****
8100 ! Solves for pressure using the Runge-Kutta-Merson method.
8110 ! Geometric variables are assumed linear between steps.
8120 N=4 ! Initial Substep.
8130 GOSUB Set
8140 Rungel: ! Start of solution.
8150 H=Inc/N
8160 Pite(0)=P(I-Idir)
8170 FOR Nstep=1 TO N
8180 Hstep=0
8190 Pc=Pite(Nstep-1)
8200 GOSUB Intval
8210 K1=H*FNFTn1(Area, Beta, Dcff, Eta, H1, H2, Eclar, L, L3, Omega, P1,
P2, Cpsure, Pc, Pport, Rho, Sector, U, V, Vclar, Vdlt a, W1, W2, Ewth)
8220 Hstep=H/3
8230 Pc=Pite(Nstep-1)+K1/3
8240 GOSUB Intval
8250 K2=H*FNFTn1(Area, Beta, Dcff, Eta, H1, H2, Eclar, L, L3, Omega, P1,
P2, Cpsure, Pc, Pport, Rho, Sector, U, V, Vclar, Vdlt a, W1, W2, Ewth)
8260 Hstep=H/3
8270 Pc=Pite(Nstep-1)+(K1+K2)/6
8280 GOSUB Intval
8290 K3=H*FNFTn1(Area, Beta, Dcff, Eta, H1, H2, Eclar, L, L3, Omega, P1,
P2, Cpsure, Pc, Pport, Rho, Sector, U, V, Vclar, Vdlt a, W1, W2, Ewth)
8300 Hstep=H/2
8310 Pc=Pite(Nstep-1)+(K1/8+3*K3/8)
8320 GOSUB Intval
8330 K4=H*FNFTn1(Area, Beta, Dcff, Eta, H1, H2, Eclar, L, L3, Omega, P1,
P2, Cpsure, Pc, Pport, Rho, Sector, U, V, Vclar, Vdlt a, W1, W2, Ewth)
8340 Hstep=H
8350 Pc=Pite(Nstep-1)+(K1/2-3*K3/2+2*K4)
8360 GOSUB Intval
8370 K5=H*FNFTn1(Area, Beta, Dcff, Eta, H1, H2, Eclar, L, L3, Omega, P1,
P2, Cpsure, Pc, Pport, Rho, Sector, U, V, Vclar, Vdlt a, W1, W2, Ewth)
8380 Pite(Nstep)=Pite(Nstep-1)+(K1+4*K4+K5)/6
8390 Pite(0)=Pite(Nstep)

```

```

8400      Error=(2*K1-9*K3+8*K4-K5)/30
8410      IF (ABS(Error)>.2) AND (N<Maxstep) THEN GOTO Recover1
8420      ! PRINT N,Error,Nstep,Pite(Nstep)
8430      IF Err_stat=1 THEN SUBEXIT ! Abort: Error occured
8440      NEXT Nstep
8450      Exit:P=Pite(Nstep-1) ! Nstep less one due to counter.
8460      !
8470      ! Cavitation check
8480      P(I)=FNPcav(Inc, Omega, P, Pcav, Vcav, Vdlt(I), L1(I))
8490      CALL Leak(Aclar, Awang, Awdth, Cpsure, Eclar, Erad, Ewth, Inc, L, Nseg, Omega, Res, Sector, U, Vclar, Vwang, Vwdth, I)
8500      SUBEXIT
8510      Recover1: ! Doubles no. steps and restarts
8520      N=N*2
8530      IF N>Maxstep THEN N=Maxstep
8540      IF N>=Maxstep THEN Csum=Quad
8550      GOTO Runge1
8560      !
8570      ! ++++++ Intval Functions ++++++
8580      ! These subroutines determines the parameter value at points
8590      ! within the interval.
8600      ! ++++++
8610      Intval: ! Start of subroutine Intval
8620      Area=Area(I)+Agrad*Hstep ! L3 deter. in "Intval 0-4"
8630      V=V(I)+Vgrad*Hstep
8640      Vdlt=Vdlt(I)+Vdgrad*Hstep
8650      ON Sector+1 GOTO Intval0, Intval1, Intval2, Intval3, Intval4
8660      Intval0: ! Sets interval value for pre-sector
8670      Pport=Ip(I+Res)+Ppgrad*Hstep
8680      H1=H(I+Res)+H1grad*Hstep ! H1grad=0
8690      P1=P(I+Res)+P1grad*Hstep
8700      W1=Vwdth
8710      H2=Aclar+H2grad*Hstep
8720      P2=P(Nseg*Res+I)+P2grad*Hstep
8730      W2=Awdth
8740      L3=Erad*(Inc*(I+Res)-.5*(Awang+Vwang))
8750      RETURN
8760      Intval1: ! Sets interval value for 1st sector
8770      Pport=Ip(I)+Ppgrad*Hstep
8780      H1=H(I+Res)+H1grad*Hstep
8790      P1=P(I+Res)+P1grad*Hstep
8800      W1=Vwdth
8810      Ival11: IF Inc*I>Theta1 THEN Ival12
8820      H2=Aclar+H2grad*Hstep ! H2grad=0
8830      P2=P((Nseg-1)*Res+I)+P2grad*Hstep
8840      W2=Awdth
8850      L3=Erad*(Inc*(I+Res)-.5*(Awang+Vwang))
8860      RETURN
8870      Ival12: H2=Vclar+H2grad*Hstep
8880      P2=P(I-Res)+P2grad*Hstep
8890      W2=Vwdth
8900      L3=Erad*(Inc*Res-Vwang)
8910      RETURN
8920      Intval2: ! Sets interval value for 2nd sector
8930      Pp=Ip(I)*(Pstat=1)+Op(I)*(Pstat=2)
8940      Pport=Pp+Ppgrad*Hstep
8950      H1=H(I+Res)+H1grad*Hstep
8960      P1=P(I+Res)+P1grad*Hstep
8970      W1=Vwdth
8980      H2=H(I)+H2grad*Hstep

```

```

8990      P2=P(I-Res)+P2grad*Hstep
9000      W2=Vwidth
9010      L3=Erads*(Inc*Res-Vwang)
9020      RETURN
9030 Intval3: ! Sets interval value for 3rd sector
9040      Pport=Op(I)+Ppgrad*Hstep
9050      H2=H(I)+H2grad*Hstep      ! H2grad=0
9060      P2=P(I-Res)+P2grad*Hstep
9070      W2=Vwidth
9080      L3=Erads*(Inc*Res-Vwang)
9090 Ival31: IF Inc*I>Theta2 THEN Ival32
9100      H1=H(I+Res)+H1grad*Hstep
9110      P1=P(I+Res)+P1grad*Hstep
9120      W1=Vwidth
9130      RETURN
9140 Ival32: H1=Awidth+H1grad*Hstep      ! H1grad=0
9150      P1=P(I-(Nseg-1)*Res)+P1grad*Hstep
9160      W1=Awidth
9170      RETURN
9180 Intval4: ! Sets interval value for 4th sector
9190      Pport=Op(I)+Ppgrad*Hstep
9200      H1=Aclar+H1grad*Hstep      ! H1grad=0
9210      P1=P(I-Nseg*Res)+P1grad*Hstep
9220      W1=Awidth
9230      H2=H(I)+H2grad*Hstep
9240      P2=P(I-Res)+P2grad*Hstep
9250      W2=Vwidth
9260      L3=Erads*(PI-.5*(Awang+Vwang)-I*Inc)
9270      RETURN
9280      !
9290      ! ++++++ Set functions ++++++
9300      ! These functions determine the gradient between the next
9310      ! interval. Linear function assumed over the interval step.
9320      ! ++++++
9330 Set: ! Start of subroutine set
9340      Agrad=(Area(I+Idir)-Area(I))/Inc
9350      Vgrad=(V(I+Idir)-V(I))/Inc
9360      Vdgrad=(Vdlt(I+Idir)-Vdlt(I))/Inc
9370      ON Sector+1 GOTO Set0,Set1,Set2,Set3,Set4
9380 Set0: ! Set interval grad. for pre-sector
9390      Ppgrad=(Ip(I+Res+Idir)-Ip(I+Res))/Inc
9400      H1grad=(H(I+Res+Idir)-H(I+Res))/Inc
9410      P1grad=(P(I+Res+Idir)-P(I+Res))/Inc
9420      H2grad=0      ! Aclar:Const
9430      P2grad=(P(Nseg*Res+I+Idir)-P(Nseg*Res+I))/Inc
9440      RETURN
9450 Set1: ! Set interval grad. for 1st sector
9460      Ppgrad=(Ip(I+Idir)-Ip(I))/Inc
9470      H1grad=(H(I+Res+Idir)-H(I+Res))/Inc
9480      P1grad=(P(I+Res+Idir)-P(I+Res))/Inc
9490 St11: IF Inc*I>Theta1 THEN St12
9500      H2grad=0      ! Aclar:Const
9510      P2grad=(P((Nseg-1)*Res+I+Idir)-P((Nseg-1)*Res+I))/Inc
9520      RETURN
9530 St12: H2grad=(H(I+Idir)-H(I))/Inc
9540      P2grad=(P(I-Res+Idir)-P(I-Res))/Inc
9550      RETURN
9560 Set2: ! Set interval grad. for 2nd sector
9570      Ppgrad=(Ip(I+Idir)-Ip(I))*(Pstat=1)+(Op(I+Idir)-Op(I))*(Pstat=2)

```

```

9580 Ppgrad=Ppgrad/Inc
9590 H1grad=(H(I+Res+Idir)-H(I+Res))/Inc
9600 P1grad=(P(I+Res+Idir)-P(I+Res))/Inc
9610 H2grad=(H(I+Idir)-H(I))/Inc
9620 P2grad=(P(I-Res+Idir)-P(I-Res))/Inc
9630 RETURN
9640 Set3:! Set interval grad. for 3rd sector
9650 Ppgrad=(Op(I+Idir)-Op(I))/Inc
9660 H2grad=(H(I+Idir)-H(I))/Inc
9670 P2grad=(P(I-Res+Idir)-P(I-Res))/Inc
9680 St31:IF I*Inc>Theta2 THEN GOTO St32
9690 H1grad=(H(I+Res+Idir)-H(I+Res))/Inc
9700 P1grad=(P(I+Res+Idir)-P(I+Res))/Inc
9710 RETURN
9720 St32:H1grad=0
9730 P1grad=(P(I-(Nseg-1)*Res+Idir)-P(I-(Nseg-1)*Res))/Inc
9740 RETURN
9750 Set4:! Set interval grad. for 4th sector
9760 Ppgrad=(Op(I+Idir)-Op(I))/Inc
9770 H1grad=0
9780 P1grad=(P(I-Nseg*Res+Idir)-P(I-Nseg*Res))/Inc
9790 H2grad=(H(I+Idir)-H(I))/Inc
9800 P2grad=(P(I-Res+Idir)-P(I-Res))/Inc
9810 RETURN
9820 SUBEND
9830 !
9840 ! ++++++ SUBFUNCTION FTN1 ++++++
9850 ! This subfunction defines the main differential equation for
9860 ! the rate of change of cell pressure w.r.t angular position.
9870 ! ++++++
9880 DEF FNFTn1(Area,Beta,Dcff,Eta,H1,H2,Eclar,L,L3,Omega,P1,P2,Cps
ure,Pc,Pport,Rho,Sector,U,V,Vclar,Vdlt,W1,W2,Ewth)
9890 COM Auto(1:3),Aprefix$[1],Err_stat
9900 CALL Chkh(H1,H2,Sector,Vclar,He1,He2,Hv1,Hv2)
9910 Dltap=Pport-Pc
9920 Y1=SGN(Dltap)*Dcff*Area*SQR(2*ABS(Dltap)/Rho) ! Orifice
9930 Y1=Y1+U*L/2*(He1-He2) ! Entrain
9940 Y2=L*(Hv1^3*(P1-Pc)/W1+Hv2^3*(P2-Pc)/W2)
9950 Y2=(Y2+2*L3*Eclar^3*(Cpsure-Pc)/Ewth)/(12*Eta)
9960 Y=(Y1+Y2-Omega*Vdlt)*Beta/(Omega*V)
9970 RETURN Y
9980 FNEND
9990 !
10000 ! ++++++ End of routines for non-linear solutions ++++++
10010 !
10020 ! ++++++ SUBROUTINE SPLIN ++++++
10030 ! + Solves linear equations for pressure,flow and leakage +
10040 ! + This routine is valid for the conditions; +
10050 ! + a) Insignificant leakage comp. with port flow :Solve1 +
10060 ! + b) Significant leakage comp. but no port flow. :Solve2 +
10070 ! ++++++
10080 SUB Splin(Aclar,Awdth,Awang,Cpsure,Dir,Eclar,Erad,Ewth,Inc,Idi
r,L,Nseg,Omega,Pangl,Phi,Pstat,Res,Sector,U,Vcav,Vclar,Vwang,Vwdth,I
)
10090 COM Auto(1:3),Aprefix$[1],Err_stat
10100 COM SHORT Ip(-360:1440),Op(-360:1440),If(-360:1440),Of(-360:14
40)
10110 COM SHORT L1(-360:1440),P(-360:1440),Q(-360:1440)
10120 COM SHORT Qi0(360),Qi1(360),Qo1(360),Qo2(360),Qo3(360)
10130 COM SHORT Vdlt(-360:1440),V(-360:1440),Area(-360:1440),H(1440
)

```

```

10140 COM Beta,Dcff,Eta,Pcav,Rho
10150 ON 2+SGN(Area(I)) GOSUB Bcond,Bcond,Acond ! Select: Solve 1/2
10160 P(I)=FNPCav(Inc, Omega, P, Pcav, Vcav, Vdlt(I), L1(I))
10170 SUBEXIT
10180 Acond: ! With significant port flow
10190     Cstat=0 ! Re-iteration check.
10200     C1=Inc*I
10210     K=I-Idir
10220     CALL Leak(Aclar, Awang, Awdth, Cpsure, Eclar, Erad, Ewth, Inc, L,
Nseg, Omega, Res, Sector, U, Vclar, Vwang, Vwdth, K)
10230     L1=L1(K)
10240     CALL Pcons(Beta, K12, Dcff, K11, Eta, Inc, Idir, L1, Omega, P1, Pr,
Pstat, Res, Rho, Sector, I, Area(*), Ip(*), Op(*), P(*), V(*), Vdlt(*))
10250 Start:Dir=SGN(P1)
10260     IF Dir=0 THEN Dir=SGN(K11)
10270     IF Dir<>0 THEN Splin1
10280     P=P(K) ! Solved
10290     RETURN
10300 Splin1:U1=SQR(ABS(P1))
10310     Z1=K11-Dir*K12*U1
10320     P=P(K)
10330     CALL Solve1(K12, Dir, K11, P, Pr, Inc, Z1, I) ! K12 def.+ve
10340     IF Err_stat=1 THEN SUBEXIT ! Abort : Error occured
10350 Check1: ! Checks for accuracy of K11, K12 estimate values.
10360     K=I
10370     P(K)=P
10380     CALL Leak(Aclar, Awang, Awdth, Cpsure, Eclar, Erad, Ewth, Inc, L,
Nseg, Omega, Res, Sector, U, Vclar, Vwang, Vwdth, K)
10390     Val1=L1
10400     Val2=L1(I)
10410     IF SGN(Val1)<>SGN(Val2) THEN Check2
10420     IF (ABS(Val2-Val1)>ABS(1.5*Val1)) OR (ABS(Val2-Val1)<ABS(
.5*Val1)) THEN GOTO Check2
10430     RETURN
10440 Check2: ! New values for K11, K12 and re-iterate.
10450     L1=L1(I)
10460     Cstat=Cstat+1
10470     IF Cstat>=3 THEN RETURN ! Max permitted 3 Iterations
10480     CALL Pcons(Beta, K12, Dcff, K11, Eta, Inc, Idir, L1, Omega, P1, Pr,
Pstat, Res, Rho, Sector, I, Area(*), Ip(*), Op(*), P(*), V(*), Vdlt(*))
10490     GOTO Start
10500 Bcond: ! No port flow
10510     CALL Solve2(Aclar, Awdth, Awang, Beta, Cpsure, Eclar, Erad, Eta,
Ewth, Inc, Idir, L, Nseg, Omega, P, Res, Sector, U, Vclar, Vwang, Vwdth, I, H(*), P
(*), V(*), Vdlt(*))
10520     IF Err_stat=1 THEN SUBEXIT ! Abort : Error occured
10530     P(I)=P
10540     CALL Leak(Aclar, Awang, Awdth, Cpsure, Eclar, Erad, Ewth, Inc, L,
Nseg, Omega, Res, Sector, U, Vclar, Vwang, Vwdth, I)
10550     RETURN
10560 SUBEND
10570 !
10580 ! ++++++ SUBROUTINE Solve1 ++++++
10590 ! + Selects appropriate routines for differing conditions of +
10600 ! + suction and delivery flow. +
10610 ! ++++++
10620 SUB Solve1(K12, Dir, K11, P, Pr, Inc, Z1, I)
10630 COM Auto(1:3), Aprefix#[1], Err_stat
10640 Zstol=1E-4 ! Sufficiently small Zs
10650 C1=Inc*I

```

```

10660 Theta1=C1
10670 Theta2=C1+Inc
10680 X=2-Dir*SGN(K11)
10690 ON X GOSUB Con1,Con2,Con3
10700 SUBEXIT
10710 Con1: X=2-Dir*SGN(Z1)
10720 ON X GOSUB Scon11,Scon12,Scon13
10730 RETURN
10740 Scon11:Zs=FNZs(2,K12,Dir,K11,Theta1,Theta2,Z1)
10750 IF ABS(Zs)>Zstol THEN Scon11a
10760 Z2=0
10770 P=FNPprt(2,K12,Dir,K11,Pr,Z2)
10780 RETURN
10790 Scon11a:Xmin=Zs
10800 Xmax=Z1
10810 IF Xmin<Xmax THEN GOTO Scon11b
10820 Xmin=Z1
10830 Xmax=Zs
10840 Scon11b:Z2=FNSfn(1,K12,Dir,K11,Theta1,Theta2,Z1,Zs,Xmin,Xmax,I
)
10850 P=FNPprt(2,K12,Dir,K11,Pr,Z2)
10860 RETURN
10870 Scon12:P=P ! P initialised at P(I-1)
10880 RETURN
10890 Scon13:Zs=FNZs(3,K12,Dir,K11,Theta1,Theta2,Z1)
10900 IF ABS(Zs)>1E-19 THEN Sscon1
10910 Exp=-((Theta2-Theta1)*K12*K12/(2*Dir*K11)+Z1/K11)
10920 IF Exp<=LOG(ABS(1E-19/Z1)) THEN Sscon2
10930 Zs=Z1
10940 Ssrt: Zs=.5*Zs
10950 Zss=Zs
10960 Xmin=K11
10970 Xmax=Z1
10980 IF Xmin<Xmax THEN GOTO Scon13a
10990 Xmin=Z1
11000 Xmax=K11
11010 Scon13a:Az=FNSfn(1,K12,K11,Dir,Theta1,Theta2,Z1,Zss,Xmin,Xmax,
I)
11020 IF ABS(Az)<Zstol THEN Sscon4
11030 IF Az<0 THEN Ssrt
11040 IF Az>0 THEN Sscon3
11050 Sscon1:IF ABS(Zs)>Zstol THEN Sscon1a
11060 Z2=0
11070 P=FNPprt(2,K12,Dir,K11,Pr,Z2)
11080 RETURN
11090 Sscon1a:Xmin=Z1
11100 Xmax=Zs
11110 IF Xmin<Xmax THEN Sscon1b
11120 Xmin=Zs
11130 Xmax=Z1
11140 Sscon1b:Z2=FNSfn(1,K12,Dir,K11,Theta1,Theta2,Z1,Zs,Xmin,Xmax,I
)
11150 P=FNPprt(2,K12,Dir,K11,Pr,Z2)
11160 RETURN
11170 Sscon2:Z2=Z1*EXP(Exp)
11180 P=FNPprt(2,K12,Dir,K11,Pr,Z2)
11190 RETURN
11200 Sscon3:Zs=Az
11210 Zz=FNSfn(1,K12,Dir,K11,Theta1,Theta2,Z1,Zs,Xmin,Xmax,I)
11220 Z2=Zz

```

```

11230     P=FNPprt(2,K12,Dir,K11,Pr,Z2)
11240     RETURN
11250 Scon4:Z2=Az
11260     P=FNPprt(2,K12,Dir,K11,Pr,Z2)
11270     RETURN
11280 Con2: X=SGN(Theta2-(Theta1-Dir*2*Z1/(K12*K12)))
11290     IF Dir*X<=0 THEN P=Pr
11300     IF Dir*X>0 THEN P=FNPprt(3,K12,Dir,K11,Pr,Z2)
11310     RETURN
11320 Con3: Thetae=Theta1+Dir*2/(K12*K12)*(K11-Z1-K11*LOG(K11/Z1))
11330     X=2-SGN(Theta2-Thetae)
11340     IF (Thetae<Theta2+.01*Inc) AND (Thetae>Theta2-.01*Inc)
THEN X=2
11350     ON X GOSUB Scon31,Scon32,Scon33
11360     RETURN
11370 Scon31:Zs=FNZs(1,K12,Dir,K11,Theta1,Theta2,Z1)
11380     IF ABS(Zs)>Zstol THEN Scon31a
11390     Z2=0
11400     P=FNPprt(1,K12,Dir,K11,Pr,Z2)
11410     RETURN
11420 Scon31a:Xmin=K11
11430     Xmax=Zs
11440     IF Xmin<Xmax THEN GOTO Scon31b
11450     Xmin=Zs
11460     Xmax=K11
11470 Scon31b:Z2=FNSfn(2,K12,Dir,K11,Theta1,Theta2,Z1,Zs,Xmin,Xmax,I
)
11480     P=FNPprt(1,K12,Dir,K11,Pr,Z2)
11490     RETURN
11500 Scon32:P=Pr
11510     RETURN
11520 Scon33:Zs=Z1
11530     IF ABS(Zs)>Zstol THEN Scon33a
11540     Z2=0
11550     P=FNPprt(2,K12,Dir,K11,Pr,Z2)
11560     RETURN
11570 Scon33a:Xmin=K11
11580     Xmax=Z1
11590     IF Xmin<Xmax THEN GOTO Scon33b
11600     Xmin=Z1
11610     Xmax=K11
11620 Scon33b:Z2=FNSfn(1,K12,Dir,K11,Theta1,Theta2,Z1,Zs,Xmin,Xmax,I
)
11630     P=FNPprt(2,K12,Dir,K11,Pr,Z2)
11640     RETURN
11650     SUBEND
11660 !
11670 ! ++++++ SUBROUTINE Solve2 ++++++
11680 ! + This subroutine solves for segment pressure directly, +
11690 ! + when the outlet port is closed. +
11700 ! + The routine assumes vane clearances at Vclar for forward +
11710 ! + and trailing vane. +
11720 ! + Note: Non defined area checks in Selsol +
11730 ! ++++++
11740 SUB Solve2(Aclar,Awdth,Awang,Beta,Cpsure,Eclar,Erad,Eta,Ewth,I
nc,Idir,L,Nseg,Omega,P,Res,Sector,U,Vclar,Vwang,Vwdth,I,SHORT H(*),P
(*),V(*),Vdlt(*))
11750 COM Auto(1:3),Aprefix#[1],Err_stat
11760 K=I-Idir
11770 ON Sector+1 GOSUB Sol0,Sol1,Sol2,Sol3,Sol4

```

```

11780 CALL Chkh(H1,H2,Sector,Vc1ar,He1,He2,Hv1,Hv2)
11790 K1=Beta/(V(K)*Omega)
11800 K2=1/(12*Eta)
11810 K3=L*(Hv1^3*Pf/W1+Hv2^3*Pr/W1)+2*L3*Ec1ar^3*Cpsure/Ewth
11820 A=K1*(K2*K3+U*L/2*(He1-He2)-Omega*Vd1ta(K))
11830 B=K1*K2*(L*(Hv1^3/W1+Hv2^3/W2)+L3*Ec1ar^3/Ewth)
11840 Zz1=A-B*P(K)
11850 Zz2=Zz1*EXP(-B*Inc)
11860 P=(A-Zz2)/B
11870 SUBEXIT
11880 Sol0:!! Sector 0
11890     W1=Vwdth
11900     H1=H(K+Res)
11910     Pf=P(K+Res)
11920     W2=Awdth
11930     H2=Ac1ar
11940     Pr=P(Nseg*Res+K)
11950     L3=Erاد*(Inc*(I+Res)-.5*(Awang+Vwang))
11960     RETURN
11970 Sol1:!! Sector 1
11980     Theta=.5*(Awang+Vwang)
11990 Sol11: W1=Vwdth
12000     H1=H(K+Res)
12010     Pf=P(K+Res)
12020     IF I*Inc>Theta THEN GOTO Sol12
12030     W2=Awdth
12040     H2=Ac1ar
12050     Pr=P((Nseg-1)*Res+K)
12060     L3=Erاد*(Inc*(I+Res)-.5*(Awang+Vwang))
12070     RETURN
12080 Sol12: W2=Vwdth
12090     H2=H(K)
12100     Pr=P(K-Res)
12110     L3=Erاد*(Inc*Res-Vwang)
12120     RETURN
12130 Sol2:!! Sector 2
12140     H1=H(K+Res)
12150     W1=Vwdth
12160     Pf=P(K+Res)
12170     H2=H(K)
12180     W2=Vwdth
12190     Pr=P(K-Res)
12200     L3=Erاد*(Inc*Res-Awang)
12210     RETURN
12220 Sol3:!! Sector 3
12230     Theta=(1-1/Nseg)*PI-.5*(Awang+Vwang)
12240 Sol31: H2=H(K)
12250     W2=Vwdth
12260     Pr=P(K-Res)
12270     L3=Erاد*Inc*Res
12280     IF I*Inc>Theta THEN GOTO Sol32
12290     H1=H(K+Res)
12300     W1=Vwdth
12310     Pf=P(K+Res)
12320     RETURN
12330 Sol32: H1=Ac1ar
12340     W1=Awdth
12350     Pf=P(K-(Nseg-1)*Res)
12360     L3=Erاد*(PI-Theta-.5*(Awang+Vwang))
12370     RETURN

```

```

12380 Sol4: ! Sector 4
12390      W1=Awdth
12400      H1=Aclar
12410      Pf=P(K-Nseg*Res)
12420      W2=Vwdth
12430      H2=H(K)
12440      Pr=P(K-Res)
12450      L3=Erاد*(PI-Theta-.5*(Awang+Vwang))
12460      RETURN
12470      SUBEND
12480 !
12490 ! ++++++ SUBFUNCTION SFN ++++++
12500 ! Solves for the root Z2 of the non linear equation using the
12510 ! methods of 'Modified Regula Falsi' and 'Newton-Raphson'.
12520 ! ++++++
12530 DEF FNSfn(Eqn,K12,Dir,K11,Theta1,Theta2,Z1,Zs,Xmin,Xmax,I)
12540 COM Auto(1:3),Aprefix$[1],Err_stat
12550 Acount=1
12560 Ftol=.01 ! Acceptable function value
12570 IF FNYfn(Eqn,K12,Dir,K11,Theta1,Theta2,Z1,Zs)<=Ftol THEN GOTO
Newton
12580 Regfals: ! Set up trip parameters
12590      Ntol=20 ! Max iteration
12600      Xtol=1E-5 ! Acceptable Z1,Z2 difference
12610 Regsrt: ! Start of routine proper & entry for error routine
12620      A=Xmin
12630      B=Xmax
12640      W=A
12650      Fa=FNYfn(Eqn,K12,Dir,K11,Theta1,Theta2,Z1,A)
12660      Fb=FNYfn(Eqn,K12,Dir,K11,Theta1,Theta2,Z1,B)
12670      IF Fa#Fb>0 THEN GOTO Error1 ! Same sign at endpoints
12680      Fw=Fa
12690      FOR N=1 TO Ntol
12700      IF (ABS((B-A)/2)>Xtol) AND (ABS(Fw)>Ftol) THEN GOTO Srg
f1s
12710      IF ABS((B-A)/2)<=Xtol THEN Zs=(B-A)/2
12720      IF ABS(Fw)<=Ftol THEN Zs=W
12730      GOTO Newton
12740 Srgf1s: W=(Fb*A-Fa*B)/(Fb-Fa)
12750      Prevfw=Fw
12760      Fw=FNYfn(Eqn,K12,Dir,K11,Theta1,Theta2,Z1,W)
12770      ! Change to new interval
12780      IF Fa#Fw>0 THEN GOTO Srgf1s2
12790      A=W
12800      Fa=Fw
12810      IF Fw#Prevfw>0 THEN Fb=Fb/2
12820      GOTO Srgf1s3
12830 Srgf1s2: B=W
12840      Fb=Fw
12850      IF Fw#Prevfw>0 THEN Fa=Fa/2
12860 Srgf1s3: NEXT N
12870      GOTO Error2
12880 Error1: PRINTER IS 0
12890      PRINT "I :";I,"Same sign at end points"
12900      PRINTER IS 16
12910      ! Widen Xmin,Xax limits
12920      Xmin=Xmin-.25*(Xmax-Xmin)
12930      Xmax=Xmax+.25*(Xmax-Xmin)
12940      IF Acount>5 THEN GOTO Newton
12950      Acount=Acount+1

```

```

12960           GOTO Regsrt
12970 Error2:PRINTER IS 0
12980           PRINT "I :";I,"Max permitted iteration"
12990           PRINTER IS 16
13000           ! Attempt to solve with 'Newton"
13010 Newton:! Solves by Newton-Raphson Method
13020           Irate=1
13030           Nitol=20
13040           Nftol=1E-5
13050           Nerr=.001
13060 Newton2:Yfn=FNYfn(Eqn,K12,Dir,K11,Theta1,Theta2,Z1,Zs)
13070           IF ABS(Yfn)>Nftol THEN Newton3
13080           RETURN Zs
13090 Newton3:Ydfn=FNYdfn(Eqn,K12,Dir,K11,Zs)
13100           Ydlta=Yfn/Ydfn
13110           Z2=Zs-Ydlta
13120           IF (ABS(Ydlta)<Nerr) OR (Irate>Nitol) THEN RETURN Z2
13130           Irate=Irate+1
13140           Zs=Z2
13150           GOTO Newton2
13160           SUBEND
13170 !
13180 ! ++++++ SUBFUNCTIONs YFN ++++++
13190 ! Defines the non-linear equations.
13200 ! ++++++
13210 DEF FNYfn(Eqn,K12,Dir,K11,Theta1,Theta2,Z1,Z2)
13220 COM Auto(1:3),Aprefix#[1],Err_stat
13230 ON Eqn GOTO Eqn1,Eqn2
13240 Eqn1:Yfn=2*Dir/(K12*K12)*(Z2-Z1-K11*LOG(Z2/Z1))-(Theta2-Theta1)
13250           RETURN Yfn
13260 Eqn2:Yfn=-((2*Dir)/(K12*K12))*(Z1+Z2-2*K11+2*LOG(K11*K11/(Z1*Z2)))-
13270           (Theta2-Theta1)
13270           RETURN Yfn
13280           FNEND
13290 !
13300 ! ++++++ SUBFUNCTIONS YDFN ++++++
13310 ! Defines the derivative of the equations
13320 ! ++++++
13330 DEF FNYdfn(Eqn,K12,Dir,K11,Z2)
13340 COM Auto(1:3),Aprefix#[1],Err_stat
13350 ON Eqn GOTO Eqn1,Eqn2
13360 Eqn1:Ydfn=2*Dir/(K12*K12)*(1-K11/Z2)
13370           RETURN Ydfn
13380 Eqn2:Ydfn=-2*Dir/(K12*K12)*(1-K11/Z2)
13390           RETURN Ydfn
13400           FNEND
13410 !
13420 ! ++++++ SUBFUNCTION ZS ++++++
13430 ! Determines start values
13440 ! ++++++
13450 DEF FNZs(Eqn,K12,Dir,K11,Theta1,Theta2,Z1)
13460 COM Auto(1:3),Aprefix#[1],Err_stat
13470 ON Eqn GOTO Eqn1,Eqn2,Eqn3
13480 Eqn1: Zs=K11*K11/Z1*EXP(-2+Z1/K11+(Theta2-Theta1)*K12*K12/(2*Dir*K11))
13490           RETURN Zs
13500 Eqn2: Zs=Z1*EXP(-((Theta2-Theta1)*K12*K12/(2*Dir*K11)+Z1/K11))
13510           RETURN Zs
13520 Eqn3: Zs=Z1*EXP(-((Theta2-Theta1)*K12*K12/(2*Dir*K11)))

```

```

13530      RETURN Zs
13540      FNEND
13550 !
13560 ! ++++++ SUBFUNCTION PSRT ++++++
13570 ! Evaluates P value
13580 ! ++++++
13590 DEF FNPprt(Eqn,K12,Dir,K11,Pr,Z2)
13600 COM Auto(1:3),Aprefix#[1],Err_stat
13610 ON Eqn GOTO Eqn1,Eqn2,Eqn3
13620 Eqn1: X=(Z2-K11)/K12
13630      P=Pr-Dir*X*X
13640      RETURN P
13650 Eqn2: X=(Z2-K11)/K12
13660      P=Pr+Dir*X*X
13670      RETURN P
13680 Eqn3: X=-(Theta2-Thets1)*K12/2+Z1/K12
13690      P=Pr+Dir*X*X
13700      RETURN P
13710      FNEND
13720 !
13730 ! ++++++ SUBROUTINE Pcons ++++++
13740 ! + Sets constants K12,K11,P1,Pr. (Ref Documentation) +
13750 ! ++++++
13760 SUB Pcons(Beta,K12,Dcff,K11,Eta,Inc,Idir,L1,Omega,P1,Pr,Pstat,
13770 Res,Rho,Sector,I,SHORT Area(*),Ip(*),Op(*),P(*),V(*),Vdlt(*))
13780 COM Auto(1:3),Aprefix#[1],Err_stat
13790 K=I-Idir
13790 K12=Beta/(V(K)*Omega)*Dcff*Area(K)*SQR(2/Rho)
13800 Ep=-Beta*Vdlt(K)/V(K)
13810 K11=Beta*L1/(V(K)*Omega)+Ep
13820 ON Pstat GOTO Input,Output
13830 Input:P1=P(K)-Ip(K)
13840      Pr=Ip(K)
13850      SUBEXIT
13860 Output:P1=P(K)-Op(K)
13870      Pr=Op(K)
13880      SUBEND
13890 !
13900 ! ++++++ End of routines for linear solutions ++++++
13910 !
13920 !
13930 ! ++++++ SUBFUNCTION PCAV ++++++
13940 ! Cavitation check
13950 ! Pressures assigned to cavitation values if the calculated
13960 ! pressure is less than the cavitation pressure and/or the
13970 ! cavitation volume is greater than zero.
13980 ! ++++++
13990 DEF FNPcav(Inc,Omega,P,Pcav,Vcav,SHORT Vdlt,L1)
14000 COM Auto(1:3),Aprefix#[1],Err_stat
14010 IF (P>Pcav) AND (Vcav<=0) THEN RETURN P
14020 Vdir=1 ! Increasing cavitation vol.
14030 IF P>Pcav THEN Vdir=-1
14040 Ivca=(Vdlt-L1/Omega)*Inc
14050 Vcav=Vcav+Vdir+Ivca
14060 IF Vcav<0 THEN Vcav=0
14070 PRINT " CAVITATION Vcav=" ;Vcav
14080 RETURN Pcav
14090 FNEND
14100 !
14110 ! ++++++ SUBROUTINE GDAT1 ++++++

```

```

14120 ! + Calculates leakage, net flow out of the control volume +
14130 ! + and segment port flow at each angular position. +
14140 ! + Summed segment port flows produces the inlet and outlet +
14150 ! + flow arrays. +
14160 ! ++++++
14170 SUB Gdat1(Aclar,Awdth,Awang,Cpsure,Eclar,Ernd,Ewth,Inc,L,Minvd
lta,Nseg,Omega,Pangl,Phi,Res,Resnum,Secsrt(*),U,Vclar,Vwang,Vwdth)
14180 COM Auto(1:3),Aprefix#[1],Err_stat
14190 COM SHORT Ip(-360:1440),Op(-360:1440),If(-360:1440),Of(-360:14
40)
14200 COM SHORT L1(-360:1440),P(-360:1440),Q(-360:1440)
14210 COM SHORT Qi0(360),Qi1(360),Qo1(360),Qo2(360),Qo3(360)
14220 COM SHORT VdltA(-360:1440),V(-360:1440),Area(-360:1440),H(1440
)
14230 COM Beta,Dcff,Eta,Pcav,Rho
14240 !
14250 ! Generate leakage and flow arrays.
14260 ! *** PRE-SECTOR ***
14270 Sector=0
14280 Pstat=1
14290 FOR I=Secsrt(1)-1 TO Secsrt(0) STEP -1
14300 C1=I*Inc
14310 CALL Leak(Aclar,Awang,Awdth,Cpsure,Eclar,Ernd,Ewth,Inc,L,Nseg,
Omega,Res,Sector,U,Vclar,Vwang,Vwdth,I)
14320 CALL Flow(Awang,Dcff,Inc,Idir,MinvdltA,Nseg,Pstat,Res,Rho,Sect
or,Vwang,I)
14330 NEXT I
14340 ! *** FIRST SECTOR ***
14350 Sector=1
14360 Pstat=1
14370 FOR I=Secsrt(1) TO Secsrt(2)-1
14380 C1=I*Inc
14390 CALL Leak(Aclar,Awang,Awdth,Cpsure,Eclar,Ernd,Ewth,Inc,L,Nseg,
Omega,Res,Sector,U,Vclar,Vwang,Vwdth,I)
14400 CALL Flow(Awang,Dcff,Inc,Idir,MinvdltA,Nseg,Pstat,Res,Rho,Sect
or,Vwang,I)
14410 NEXT I
14420 ! *** SECOND SECTOR ***
14430 Sector=2
14440 Pstat=1
14450 FOR I=Secsrt(2) TO Secsrt(3)-1
14460 IF Area(I)<=0 THEN Pstat=2
14470 C1=I*Inc
14480 CALL Leak(Aclar,Awang,Awdth,Cpsure,Eclar,Ernd,Ewth,Inc,L,Nseg,
Omega,Res,Sector,U,Vclar,Vwang,Vwdth,I)
14490 CALL Flow(Awang,Dcff,Inc,Idir,MinvdltA,Nseg,Pstat,Res,Rho,Sect
or,Vwang,I)
14500 NEXT I
14510 ! *** THIRD SECTOR ***
14520 Sector=3
14530 FOR I=Secsrt(3) TO Secsrt(4)-1
14540 C1=I*Inc
14550 CALL Leak(Aclar,Awang,Awdth,Cpsure,Eclar,Ernd,Ewth,Inc,L,Nseg,
Omega,Res,Sector,U,Vclar,Vwang,Vwdth,I)
14560 CALL Flow(Awang,Dcff,Inc,Idir,MinvdltA,Nseg,Pstat,Res,Rho,Sect
or,Vwang,I)
14570 NEXT I
14580 ! *** FOURTH SECTOR ***
14590 Sector=4
14600 FOR I=Secsrt(4) TO Resnum

```

```

14610 C1=I*Inc
14620 CALL Leak(Aclar, Awang, Awdth, Cpsure, Eclar, Enad, Ewth, Inc, L, Nseg,
Omega, Res, Sector, U, Vclar, Vwang, Vwdth, I)
14630 CALL Flow(Awang, Dcff, Inc, Idir, Minvdlta, Nseg, Pstat, Res, Rho, Sect
or, Vwang, I)
14640 NEXT I
14650 !
14660 ! Sets output array for Inlet and Outlet flow.
14670 Enderr=INT(.05*Res) ! End correction factor
14680 !
14690 ! *** PRE-SECTOR ***
14700 FOR I=Secsrt(0)+Enderr TO Secsrt(1)-1-Enderr
14710 If(I)=Qi1(I+Res)+Qi0(I+Res)
14720 Of(I)=Qo1(I+Res)+Qo2(I+Res)+Qo3(I+Res)
14730 NEXT I
14740 FOR I=Secsrt(0) TO Secsrt(0)+Enderr-1 ! End correction
14750 If(I)=If(Secsrt(0)+Enderr)
14760 Of(I)=Of(Secsrt(0)+Enderr)
14770 NEXT I
14780 FOR I=Secsrt(1)-Enderr TO Secsrt(1)-1
14790 If(I)=If(Secsrt(1)-Enderr-1)
14800 Of(I)=Of(Secsrt(1)-Enderr-1)
14810 NEXT I
14820 !
14830 ! *** FIRST TO FOURTH SECTOR ***
14840 Kcount=1
14850 FOR J=1 TO Nseg
14860 FOR I=Secsrt(0) TO Secsrt(1)-2
14870 If(Kcount)=If(I)
14880 Of(Kcount)=Of(I)
14890 Kcount=Kcount+1
14900 NEXT I
14910 NEXT J
14920 SUBEND
14930 !
14940 ! ++++++ SUBROUTINE PSURE ++++++
14950 ! + Calculates port pressures from the inlet and outlet flow.+
14960 ! + The routine models a lossless anechoic line and dominant +
14970 ! + source impedance +
14980 ! + Intermediate fluctuation are suppressed to aid conv. +
14990 ! ++++++
15000 SUB Psure(Beta, Conftr_i, Conftr_o, Instat, Ipsure, Ildiam, Oldiam, O
psure, Resnum, Rho, Type, Secsrt(*), SHORT Of(*), If(*), Op(*), Ip(*))
15010 ! Process Output
15020 CALL Psure1(Beta, Conftr_o, Instat, Oldiam, Opsure, Resnum, Rho, Type
, Secsrt(*), Of(*), Op(*))
15030 ! Process Input
15040 IF Instat=0 THEN SUBEXIT
15050 CALL Psure1(Beta, Conftr_i, Instat, Ildiam, Ipsure, Resnum, Rho, Type
, Secsrt(*), If(*), Ip(*))
15060 SUBEND
15070 SUB Psure1(Beta, Conftr, Instat, Diam, Mpsure, Resnum, Rho, Type, Secs
rt(*), SHORT Flow(*), Press(*))
15080 K=PI*Diam^2
15090 K=4*SQR(Rho*Beta)/K
15100 K=Conftr*K
15110 Sum=0
15120 Count=Resnum-Secsrt(0)+1
15130 FOR I=Secsrt(0) TO Resnum
15140 Sum=Sum+Flow(I)

```

```

15150     NEXT I
15160     Nout1=Sum/Count
15170     ON Type+1 GOTO Sort1,Sort2
15180 Sort1:! Sort intermediate array
15190     FOR I=Secsrt(0) TO Resnum
15200     Press(I)=(Press(I)+Mpsure+K*(Flow(I)-Nout1))*0.5
15210     NEXT I
15220     Press(0)=Press(Secsrt(0))
15230     SUBEXIT
15240 Sort2:! Sort final array
15250     FOR I=Secsrt(0) TO Resnum
15260     Press(I)=Mpsure+K*(Flow(I)-Nout1)
15270     NEXT I
15280     Press(0)=Press(Secsrt(0))
15290     SUBEXIT
15300 SUBEND
15310 !
15320 ! ++++++ SUBROUTINE SMOOTH ++++++
15330 ! + Waveform smoothing: a simple moving point averaging : +
15340 ! + which is a low pass digital filter. +
15350 ! + Excessive smoothing masks the characteristic behavior. +
15360 ! + Level of smoothing is controlled by parameter: Smooth +
15370 ! ++++++
15380 SUB Smooth(Resnum,Smooth,SHORT Array(*))
15390 Int=INT(Resnum/180*Smooth)
15400 FOR I=Int TO Resnum-Int
15410 Array=0
15420 FOR J=-Int TO Int
15430 Array=Array+Array(I+J)
15440 NEXT J
15450 Array(I)=Array/(2*Int+1)
15460 NEXT I
15470 FOR I=Resnum-Int+1 TO Resnum
15480 Array(I)=Array(Resnum-Int)
15490 NEXT I
15500 FOR I=0 TO Int-1
15510 Array(I)=Array(Int)
15520 NEXT I
15530 SUBEND
15540 !
15550 ! ++++++ SUBROUTINE ERR_REC ++++++
15560 ! + Recovery routine for numerical errors in Selsol routines.+
15570 ! + Sets err_stat to 1 on error and returns call. +
15580 ! ++++++
15590 SUB Err_rec
15600 COM Auto(1:3),Aprefix#[1],Err_stat
15610 Err_stat=1
15620 SUBEND
15630 !
15640 ! ++++++ SUBROUTINE VCTL ++++++
15650 ! + Calculates the control volume for each rotational position
15660 ! ++++++
15670 SUB Vct1(Awang,Inc,L,Nseg,Rdiam,Res,Sdiam,Vwang,Vwidth,SHORT V(*),H(*))
15680 Theta1=-(PI/Nseg)+.5*(Awang+Vwang)
15690 Theta2=.5*(Awang+Vwang)
15700 Theta3=(1-1/Nseg)*PI-.5*(Awang+Vwang)
15710 Theta4=PI-.5*(Awang+Vwang)
15720 Theta5=PI
15730 V=(Sdiam^2-Rdiam^2)*L/8

```

```

15740 Vol=V*(PI/Nseg-Vwang)
15750 Thetaa=PI-.5*(Awang+Vwang)
15760 I=-Res
15770 C1=Inc*I
15780 Loop1:IF C1>Theta1 THEN Loop2
15790     V(I)=0
15800     I=I+1
15810     C1=I*Inc
15820     GOTO Loop1
15830 Loop2:IF C1>Theta2 THEN Loop3
15840     V(I)=V*(C1-Theta1)
15850     I=I+1
15860     C1=Inc*I
15870     GOTO Loop2
15880 Loop3:IF C1>Theta3 THEN Loop4
15890     V(I)=Vol
15900     I=I+1
15910     C1=Inc*I
15920     GOTO Loop3
15930 Loop4:IF C1>Theta4 THEN Loop5
15940     V(I)=V*(Thetaa-C1)
15950     I=I+1
15960     C1=Inc*I
15970     GOTO Loop4
15980 Loop5:IF C1>Theta5 THEN Exit1
15990     V(I)=0
16000     I=I+1
16010     C1=Inc*I
16020     GOTO Loop5
16030 Exit1:SUBEND
16040 !
16050 ! ++++++ SUBROUTINE AREA ++++++
16060 ! + Calculates the effective flow area for each rotational +
16070 ! + position.The routine also permits the inclusion of three +
16080 ! + types of 'relief grooves' to provide for a controlled +
16090 ! + leakage path to the outlet port. +
16100 ! + +
16110 ! + Defined groove types; a) Hemispherical :Gtype 1 +
16120 ! + b) Square sloping :Gtype 2 +
16130 ! + c) Triangular sloping :Gtype 3 +
16140 ! + +
16150 ! + No overlap of relieve grooves is permitted. +
16160 ! + Virtual flow areas are defined in sector 0 and 4 .This +
16170 ! + is presented as a percentage of the maximum flow area +
16180 ! + and consistent with a scolloped port configuration. +
16190 ! ++++++
16200 SUB Area(Awang,Gtype(*),Gcdim1(*),Gcwth2(*),Gcang3(*),Inc,L,Ns
eg,Pangl,Pdiam,Phi,Res,Sdiam,Vwang,Gastr(*),Gdpth(*),SHORT Area(*))
16210 DIM Y(250),A(250),Gmax(1:2)
16220 Virftr=.30 ! Virtual flow area factor
16230 N=Phi/Inc
16240 N=INT((N+1)/2)
16250 N=2*N
16260 Step1=Pdiam/N
16270 Arcac=Sdiam*ASN(Pdiam/(Sdiam*COS(Pangl)))
16280 Step2=Arcac/N
16290 FOR I=0 TO N/2
16300 X=I*Step1
16310 Y(I)=2*SQR(Pdiam*X-X^2)
16320 NEXT I

```

```

16330 FOR I=N/2 TO N
16340 X=I*Step1
16350 Y(I)=Y(N-I)
16360 NEXT I
16370 A(0)=0
16380 FOR I=1 TO N
16390 A(I)=A(I-1)+.5*(Y(I)+Y(I-1))*Step2
16400 NEXT I
16410 Oarea=A(N)
16420 Voarea=Vinftr*Oarea
16430 I=-Res
16440 J=K=L1=M=0
16450 C1=Inc*I
16460 Theta1=-(PI/Nseg)+.5*(Awang+Vwang)
16470 Theta2=-(PI/Nseg)+(Pang1-.5*(Phi-Vwang))
16480 Theta3=-(PI/Nseg)+(Pang1+.5*(Phi+Vwang))
16490 Theta4=Pang1-.5*(Phi+Vwang)
16500 Theta5=Pang1+.5*(Phi-Vwang)
16510 Theta6=(1-1/Nseg)*PI-(Pang1+.5*(Phi-Vwang))
16520 Theta7=(1-1/Nseg)*PI-(Pang1-.5*(Phi+Vwang))
16530 Theta8=PI-(Pang1+.5*(Phi+Vwang))
16540 Theta9=PI-(Pang1-.5*(Phi-Vwang))
16550 Theta10=PI-.5*(Awang+Vwang)
16560 Theta11=PI
16570 Segang=PI/Nseg
16580 Gmaxang=Theta8-Segang+Vwang
16590 Gmax(1)=Gmax(2)=0
16600 IF Gtype(1)<>0 THEN Gmax(1)=FNGroove(1,Segang,Vwang,Pang1,Phi,
Gtype(*),Gcdim1(*),Gcwth2(*),Gcang3(*),Theta5,Gastr(*),Gdpth(*))
16610 IF Gtype(2)<>0 THEN Gmax(2)=FNGroove(2,Segang,Vwang,Pang1,Phi,
Gtype(*),Gcdim1(*),Gcwth2(*),Gcang3(*),Gmaxang,Gastr(*),Gdpth(*))
16620 IF Gtype(1) THEN End_groove1=Theta5+Gastr(1,Gtype(1))
16630 Loop1:IF C1>Theta1 THEN Loop2
16640 Area(I)=0 ! Seg. undef. flow set to zero
16650 I=I+1
16660 C1=Inc*I
16670 GOTO Loop1
16680 Loop2:IF C1>Theta2 THEN Loop3
16690 Area(I)=Voarea ! Virtual i/flow area
16700 I=I+1
16710 C1=Inc*I
16720 GOTO Loop2
16730 Loop3:IF C1>Theta3 THEN Loop4
16740 Area(I)=A(M)
16750 IF Area(I)>Oarea THEN Area(I)=Oarea
16760 IF Area(I)<Voarea THEN Area(I)=Voarea
16770 M=M+1
16780 I=I+1
16790 C1=Inc*I
16800 GOTO Loop3
16810 Loop4:IF C1>Theta4 THEN Loop5
16820 Area(I)=Oarea
16830 I=I+1
16840 C1=Inc*I
16850 GOTO Loop4
16860 Loop5:IF C1>Theta5 THEN Loop5a
16870 Area(I)=A(N-J)
16880 IF Area(I)>Oarea THEN Area(I)=Oarea
16890 IF Area(I)<Gmax(1) THEN Area(I)=Gmax(1)
16900 J=J+1

```

```

16910     I=I+1
16920     C1=Inc*I
16930     GOTO Loop5
16940 Loop5a:IF Gtype(1)=0 THEN Loop6
16950 Loop5b:IF C1>End_groove1 THEN Loop6
16960     Area(I)=FNGroove(1,Segang,Vwang,Pangl,Phi,Gtype(*),Gcdim1
(*) ,Gcwth2(*),Gcang3(*),C1,Gastr(*),Gdpth(*))
16970     I=I+1
16980     C1=Inc*I
16990     GOTO Loop5b
17000 Loop6:IF C1>Theta6 THEN Loop7
17010     Area(I)=0 ! Assumes no groove
17020     IF Gtype(2)<>0 THEN Area(I)=FNGroove(2,Segang,Vwang,Pangl
,Phi,Gtype(*),Gcdim1(*),Gcwth2(*),Gcang3(*),C1,Gastr(*),Gdpth(*))
17030     I=I+1
17040     C1=Inc*I
17050     GOTO Loop6
17060 Loop7:IF C1>Theta7 THEN Loop8
17070     Area(I)=A(K)
17080     IF Area(I)<Gmax(2) THEN Area(I)=Gmax(2) ! Transition are
a.
17090     K=K+1
17100     I=I+1
17110     C1=Inc*I
17120     GOTO Loop7
17130 Loop8:IF C1>Theta8 THEN Loop9
17140     Area(I)=Oarea
17150     I=I+1
17160     C1=Inc*I
17170     GOTO Loop8
17180 Loop9:IF C1>Theta9 THEN Loop10
17190     Area(I)=A(N-L1)
17200     IF Area(I)>Oarea THEN Area(I)=Oarea
17210     IF Area(I)<Voarea THEN Area(I)=Voarea
17220     L1=L1+1
17230     I=I+1
17240     C1=Inc*I
17250     GOTO Loop9
17260 Loop10:IF C1>Theta10 THEN Loop11
17270     Area(I)=Voarea ! Virtual o/flow path
17280     I=I+1
17290     C1=Inc*I
17300     GOTO Loop10
17310 Loop11:IF C1>Theta11 THEN Exit
17320     Area(I)=0 ! Seg. undef. flow set to zero
17330     I=I+1
17340     C1=Inc*I
17350     GOTO Loop11
17360 Exit:SUBEND
17370 !
17380 ! Defines groove area
17390 DEF FNGroove(Idenpt,Segang,Vwang,Pangl,Phi,Gtype(*),Gcdim1(*),
Gcwth2(*),Gcang3(*),C1,Gastr(*),Gdpth(*))
17400 ON Idenpt GOTO Inlet,Outlet
17410 Inlet: ! Inlet port groove
17420     Gtype=Gtype(1)
17430     Vrang=C1+.5*Vwang
17440     Astrt=Pangl+.5*Phi+Gastr(1,Gtype)
17450     K=Astrt-Vrang
17460     IF K<=0 THEN RETURN 0

```

```

17470 Igdpth=Gdpth(1,Gtype)/Gastr(1,Gtype)*K
17480 ON Gtype GOSUB Groove1,Groove2,Groove3
17490 RETURN Garea
17500 Outlet!! Outlet port groove.
17510 Gtype=Gtype(2)
17520 Vrang=C1+Segang-.5*Vwang
17530 Astrt=PI-Pangl-.5*Phi-Gastr(2,Gtype)
17540 K=Vrang-Astrt
17550 IF K<=0 THEN RETURN 0
17560 Igdpth=Gdpth(2,Gtype)/Gastr(2,Gtype)*K
17570 ON Gtype GOSUB Groove1,Groove2,Groove3
17580 RETURN Garea
17590 Groove1!! Hemispherical groove.
17600 Beta=ACS(1-Igdpth/(.5*Gcdim1(Idenpt)))
17610 Carea=.25*PI*Gcdim1(Idenpt)^2
17620 Sarea=2*Beta/PI*Carea
17630 Tarea=.5*Gcdim1(Idenpt)^2*COS(Beta)*SIN(Beta)
17640 Garea=Sarea-Tarea
17650 RETURN
17660 Groove2!! Square sloping.
17670 Garea=Igdpth*Gcwth2(Idenpt)
17680 RETURN
17690 Groove3!! Triangular sloping.
17700 Garea=Igdpth^2*TAN(.5*Gcang3(Idenpt))
17710 RETURN
17720 FNEND
17730 !
17740 ! ++++++ SUBROUTINE VHEIGHT ++++++
17750 ! + Calculates the vane clearance at each angular position. +
17760 ! + The array is defined in the angular position 0 to .5*PI +
17770 ! + Vane clearance is calculated for 0<=angle<=.5*PI +
17780 ! + The array is mirrored about the .5*PI +
17790 ! ++++++
17800 SUB Vheight(Rangl,Rarad,Abrad,Aorad,Awang,Inc,Res,Rdiam,Sdiam,
Vclar,Vwang,SHORT H(*)
17810 I=0
17820 C1=0
17830 Ee=(Aorad-Rarad)*SIN(Rangl)
17840 Aa=(Aorad-Rarad)*COS(Rangl)
17850 Gama=ASN(Ee/(Abrad-Rarad))
17860 Rofs=(Abrad-Rarad)*COS(Gama)-Aa
17870 Theta1=.5*(Awang+Vwang)
17880 Theta2=Abrad*SIN(Gama)
17890 Theta2=Theta2/(Abrad*COS(Gama)-Rofs)
17900 Theta2=ATN(Theta2)
17910 Theta3=Rangl
17920 Theta4=.5*PI
17930 Theta5=PI
17940 Crise=.5*(Sdiam-Rdiam)
17950 Loop1:IF C1>Theta1 THEN Loop2
17960 H(I)=Crise
17970 I=I+1
17980 C1=I*Inc
17990 GOTO Loop1
18000 Loop2:IF C1>Theta2 THEN Loop3
18010 D=(2*Rofs*COS(C1))^2-4*(Rofs^2-Abrad^2)
18020 D=SQR(D)
18030 B=2*Rofs*COS(C1)
18040 X1=(-B+D)/2
18050 X2=(-B-D)/2

```

```

18060      X=X1
18070      IF (X>Aorad) OR (X<0) THEN X=X2
18080      H(I)=Aorad-X+Vclar
18090      IF H(I)>Crise THEN H(I)=Crise
18100      I=I+1
18110      C1=I*Inc
18120      GOTO Loop2
18130 Loop3: IF C1>Theta3 THEN Loop4
18140      B=-2*(Aorad-Arad)*COS(Theta3-C1)
18150      D=B^2-4*((Aorad-Arad)^2-Arad^2)
18160      D=SQR(D)
18170      X1=(-B+D)/2
18180      X2=(-B-D)/2
18190      X=X1
18200      IF (X>Aorad) OR (X<0) THEN X=X2
18210      H(I)=Aorad-X+Vclar
18220      I=I+1
18230      C1=I*Inc
18240      GOTO Loop3
18250 Loop4: IF C1>Theta4 THEN Loop5
18260      H(I)=Vclar
18270      I=I+1
18280      C1=I*Inc
18290      GOTO Loop4
18300 !
18310 ! Sets array for other quadrants.
18320 Loop5: Lastpt=I-1
18330      J=0
18340 Loop6: IF C1>Theta5 THEN Exit
18350      H(I)=H(Lastpt-J)
18360      J=J+1
18370      I=I+1
18380      C1=I*Inc
18390      GOTO Loop6
18400 Exit: SUBEND
18410 !
18420 ! ++++++ SUBROUTINE INITIAL ++++++
18430 ! + Calculates initial estimate of pressure for segment +
18440 ! + and the inlet/outlet ports. +
18450 ! + Start values assume constant port pressures set to mean +
18460 ! + values and negligible compressibility effects. +
18470 ! ++++++
18480 SUB Initial(Ipsure,Nseg,Opsure,Res,Resnum,Secsrt(*),SHORT P(*),
,Ip(*),Op(*))
18490      Dltap=(Opsure-Ipsure)/(Nseg-2)
18500      FOR I=Secsrt(0) TO Secsrt(2)-1
18510      P(I)=Ipsure
18520      NEXT I
18530      FOR I=Secsrt(2) TO Secsrt(3)-1
18540      P(I)=Ip+Dltap*(INT((I-Res)/Res)+1)
18550      NEXT I
18560      FOR I=Secsrt(3) TO Resnum
18570      P(I)=Opsure
18580      NEXT I
18590      MAT Ip=(Ipsure)
18600      MAT Op=(Opsure)
18610 SUBEND
18620 !
18630 ! ++++++ SUBROUTINE VDLTA ++++++
18640 ! + Calculates the change in swept volume for each angular +

```

```

18650 ! + position. +
18660 ! + Changes in swept vol. is kept to zero until the forward +
18670 ! + vane retracts to 1.25* normal vane clearance. This +
18680 ! + produces the effect of attributing all the flow to the +
18690 ! + dominant segment communicating with the port. +
18700 ! ++++++
18710 SUB VdltA(Awang, Inc, L, Nseg, Rdiam, Res, Sdiam, Vclar, Vwang, SHORT H
(*), VdltA(*))
18720 Min_h=1.25*Vclar ! See note above.
18730 Theta1=-(PI/Nseg)+.5*(Awang+Vwang)
18740 Theta2=.5*(Awang+Vwang)
18750 Theta3=PI/Nseg
18760 Theta4=PI*(1-2/Nseg)
18770 Theta5=PI*(1-1/Nseg)
18780 Theta6=PI-.5*(Awang+Vwang)
18790 Theta7=PI
18800 Odiam=Sdiam-2*Vclar
18810 Vmax=(Odiam^2-Rdiam^2)*L/8
18820 I=-Res
18830 C1=I*Inc
18840 Loop1:IF C1>Theta1 THEN Loop2
18850 VdltA(I)=0 ! Seg. undefined
18860 I=I+1
18870 C1=I*Inc
18880 GOTO Loop1
18890 Loop2:IF C1>Theta2 THEN Loop3
18900 Idiam=Sdiam-2*H(I+Res)
18910 VdltA(I)=(Idiam^2-Rdiam^2)*L/8
18920 IF H(I+Res)<Min_h THEN VdltA(I)=Vmax
18930 I=I+1
18940 C1=I*Inc
18950 GOTO Loop2
18960 Loop3:IF C1>Theta3 THEN GOTO Loop4
18970 Idiam=Sdiam-2*H(I)
18980 VdltA(I)=(Odiam^2-Idiam^2)*L/8
18990 IF H(I)<Min_h THEN VdltA(I)=0
19000 I=I+1
19010 C1=I*Inc
19020 GOTO Loop3
19030 Loop4:IF C1>Theta4 THEN GOTO Loop5
19040 VdltA(I)=0
19050 I=I+1
19060 C1=I*Inc
19070 GOTO Loop4
19080 Loop5:IF C1>Theta5 THEN Loop6
19090 Idiam=Sdiam-2*H(I+Res)
19100 VdltA(I)=- (Odiam^2-Idiam^2)*L/8
19110 IF H(I+Res)<Min_h THEN VdltA(I)=0
19120 I=I+1
19130 C1=I*Inc
19140 GOTO Loop5
19150 Loop6:IF C1>Theta6 THEN Loop7
19160 Idiam=Sdiam-2*H(I)
19170 VdltA(I)=- (Idiam^2-Rdiam^2)*L/8
19180 IF H(I)<Min_h THEN VdltA(I)=-Vmax
19190 I=I+1
19200 C1=I*Inc
19210 GOTO Loop6
19220 Loop7:IF C1>Theta7 THEN Exit
19230 VdltA(I)=0

```

```
19240      I=I+1
19250      C1=I*Inc
19260      GOTO Loop7
19270 Exit:SUBEND
```

### C.3 PROGRAM VPLOT

```

10  ! RE-STORE"VPLOT:F8"
20  ! ***** PROGRAM VPLOT *****
30  ! *
40  ! * The program outputs the vane M/C dynamic characteristic *
50  ! * in a graphical form. *
60  ! *
70  ! * The program provides a choice of three plotting media: *
80  ! * Benson,HP 9872A & VDU *
90  ! * Data is read from datafiles "%GDT%" *
100 ! *
110 ! * The program operates in two modes AUTO & MANUAL: *
120 ! * AUTO: Batch processing of data specified between upper *
130 ! * and lower limits. *
140 ! * MANUAL:Individual input of data filenames *
150 ! *
160 ! * Revision#1:18:OCT:1982 *
170 ! * Re-structured and added A5 size plot option *
180 ! *
190 ! * ORIGIN: G.SEET MECH. ENG. ASTON VARSITY *
200 ! * DATE: 22 JULY 81 *
210 ! *
220 ! *****
230 COM Auto(1:3),Aprefix$(1)
240 DIM Name1$(10),Mstore$(4),Messag1$(30),Messag2$(10)
250 SHORT Vcp(360),Vlf(360),Vcf(360),Ip(360),Op(360),If(360),Of(360)
260 PRINTER IS 16
270 EXIT GRAPHICS
280 PRINT "ABC"&CHR$(12)
290 PRINT " PROGRAM VPLOT EXECUTING "
300 Mstore$=":T14" ! Define mass storage device.
310 Chk=2 ! 1:Gaphics 2:Benson 3:9872A
320 Pcount=1 ! Initialize plot count
330 IF Auto(1)=1 THEN Auto4 ! Auto sequence mode
340 !
350 ! Select plotting device
360 Splot:LINPUT " DO YOU REQUIRE VIDEO GRAPHICS (Y/N) :",Y$
370 IF Y$="Y" THEN Chk=1
380 IF Y$="Y" THEN Input
390 IF Y$="N" THEN Splot1
400 GOTO Splot
410 Splot1:LINPUT " DO YOU REQUIRE BENSON (Y/N) :",Y$
420 IF Y$="Y" THEN Chk=2
430 IF Y$="Y" THEN Input
440 IF Y$="N" THEN Splot2
450 GOTO Splot1
460 Splot2:LINPUT " DO YOU REQUIRE 9872A PLOTTER ",Y$
470 IF Y$="Y" THEN Chk=3
480 IF Y$="Y" THEN Input
490 IF (Y$<>"Y") AND (Y$<>"N") THEN Splot2
500 GOTO Splot
510 !
520 ! Select mode
530 Input:LINPUT " IS AUTO SEQUENCE REQUIRED (Y/N): ",Y$
540 IF Y$="N" THEN Manual
550 IF Y$="Y" THEN Auto
560 GOTO Input
570 !
580 ! #####
590 ! AUTO SEQUENCE ROUTINE

```

```

600 ! This routine permits batch processing of the VGDT%% data.
610 ! The datafiles stored at the specified mass-storage device
620 ! are accessed and plotted sequentially between specified
630 ! upper and lower limits.
640 Auto: Auto(1)=1
650   Aprefix$="V"
660 Auto1: INPUT "INPUT DATAFILE PREFIX (Default 'V'):", Aprefix$
670 Auto2: INPUT "INPUT LOWEST DATAFILE NO. (>=0);", Auto(2)
680   IF (Auto(2)<0) OR (Auto(2)>99) THEN Auto2
690 Auto3: INPUT "INPUT HIGHEST DATAFILE NO. (<=99):", Auto(3)
700   IF (Auto(3)<0) OR (Auto(3)>99) THEN Auto3
710   IF Auto(2)>Auto(3) THEN Auto2
720 Auto4: ! Entry for linked call.
730   Count=Auto(2)
740   Mode=1
750   Name1$[1,1]=Aprefix$
760   Name1$[2,4]="GDT"
770 Auto5: T=Count DIV 10
780   I=Count MOD 10
790   Name1$[5]=CHR$(48+T)
800   Name1$[6]=CHR$(48+I)
810   Name1$[7,10]=Mstore$
820   ASSIGN Name1$ TO #1,Z
830   IF Z=0 THEN Auto6
840   Count=Count+1
850   IF Count>Auto(3) THEN GOTO Aend
860   GOTO Auto5
870 Auto6: GOSUB Plot
880   Count=Count+1
890   IF (Count>Auto(3)) OR (Count)=100 THEN Aend
900   GOTO Auto5
910 Aend: Auto(1)=0
920   GOSUB Exit
930   STOP
940 ! #####
950 ! MANUAL SEQUENCE ROUTINE
960 ! The routine requires individual input of data filenames
970 Manual: ! Manual mode
980   Mode=2
990   LINPUT " INPUT DATA FILENAME (%GDT%): ", Name1$[1,6]
1000   Name1$[7,10]=Mstore$
1010   ASSIGN Name1$ TO #1,Z
1020   IF Z=0 THEN Mplot
1030   BEEP
1040   PRINT "ABC"&CHR$(12)
1050   PRINT USING "#,K";CHR$(27)&"&a23r0C"
1060   IF Z=1 THEN PRINT " NO SUCH FILE FOUND ; ";Name1$
1070   IF Z=2 THEN PRINT " WRONG FILE TYPE ; ";Name1$
1080   GOTO Manual
1090 Mplot: GOSUB Plot
1100   ASSIGN #1 TO *
1110   GOSUB Exit
1120   STOP
1130 ! #####
1140 ! MAIN GRAPHING ROUTINE
1150 Plot: ! Reads graphical data.
1160   READ #1;Csum
1170   MAT READ #1;Vcp,Vlf,Vcf,Ip,Op,If,Of
1180   ! Convert to output units.
1190   MAT Vcp=(.1)*Vcp ! bar

```

```
1200     MAT V1f=(1000)*V1f      ! mm3/S
1210     MAT Vcf=(1000)*Vcf      ! mm3/S
1220     MAT Ip=(.1)*Ip          ! bar
1230     MAT Op=(.1)*Op          ! bar
1240     MAT If=(1000)*If        ! mm3/S
1250     MAT Of=(1000)*Of        ! mm3/S
1260     !
1270     ! *****
1280     ! This routine checks the data status.
1290     IF Csum=0 THEN Plot2
1300     PRINTER IS 0
1310     PRINT " CAUTION DATA FAULTY ** :";Name1$
1320     PRINT
1330     PRINT " DATA STATUS VALUE :";Csum
1340     PRINTER IS 16
1350     Plot2: ! Plots graphical data.
1360     !
1370     ! *****
1380     ! Outputs the plot VANE SEGMENT PRESSURE Vs ANGULAR
1390     ! POSITION ". Data is Vcp.
1400     Iset=1
1410     CALL Set(Iset,Mode,Chk,Pcount,2)
1420     Messag1$="VANE SEGMENT PRESSURE x1E"
1430     Messag2$="(bar) "
1440     CALL Pltsg1(Name1$,Vcp(*),Messag1$,Messag2$)
1450     CALL Reset(Iset,Mode,Chk,Pcount,2)
1460     Pcount=Pcount+1
1470     !
1480     ! *****
1490     ! Outputs the plot " VANE LEAKAGE FLOW Vs ANGULAR
1500     ! POSITION ". Data is V1f.
1510     Iset=2
1520     CALL Set(Iset,Mode,Chk,Pcount,2)
1530     Messag1$="VANE LEAKAGE FLOW x1E"
1540     Messag2$="(mm3/S)"
1550     CALL Pltsg1(Name1$,V1f(*),Messag1$,Messag2$)
1560     CALL Reset(Iset,Mode,Chk,Pcount,2)
1570     Pcount=Pcount+1
1580     !
1590     ! *****
1600     ! Outputs the plot "VANE SEGMENT FLOW Vs ANGULAR
1610     ! POSITION" Data is Vcf.
1620     Iset=3
1630     CALL Set(Iset,Mode,Chk,Pcount,2)
1640     Messag1$="VANE SEGMENT FLOW x1E"
1650     Messag2$="(mm3/S)"
1660     CALL Pltsg1(Name1$,Vcf(*),Messag1$,Messag2$)
1670     CALL Reset(Iset,Mode,Chk,Pcount,2)
1680     Pcount=Pcount+1
1690     !
1700     ! *****
1710     ! Outputs the plot "INLET/OUTLET FLOW Vs ANGULAR
1720     ! POSITION" Data is If and Of.
1730     Iset=4
1740     CALL Set(Iset,Mode,Chk,Pcount,2)
1750     Messag1$=" INLET / OUTLET FLOW x1E"
1760     Messag2$="(mm3/S)"
1770     CALL Pltdb1(Name1$,If(*),Of(*),Messag1$,Messag2$)
1780     CALL Reset(Iset,Mode,Chk,Pcount,2)
1790     Pcount=Pcount+1
```

```
1800 !
1810 ! *****
1820 ! Outputs the plot "INLET /OUTLET PRESSURE
1830 ! Vs ANGULAR POSITION " . Data is Ip and Op.
1840 Iset=5
1850 CALL Set(Iset,Mode,Chk,Pcount,2)
1860 Messag1$="INLET / OUTLET PRESSURES x1E"
1870 Messag2$="(bar) "
1880 CALL Pltdbl(Name1$,Ip(*),Op(*),Messag1$,Messag2$)
1890 CALL Reset(Iset,Mode,Chk,Pcount,2)
1900 Pcount=Pcount+1
1910 !
1920 RETURN
1930 !
1940 ! *****
1950 ! PRINTS EXIT MESSAGES
1960 Exit:EXIT GRAPHICS
1970 PRINT "ABC"&CHR$(12)
1980 PRINT CHR$(128)
1990 PRINT RPT$("*",80)
2000 PRINT LIN(1)
2010 PRINT RPT$("*",34);" COMPLETED ";RPT$("*",34)
2020 PRINT LIN(1)
2030 PRINT RPT$("*",80)
2040 PRINT LIN(1)
2050 PRINT "FOR ANOTHER EXECUTION PRESS /RUN/"
2060 PRINT LIN(3)
2070 PRINT " THIS MACHINE IS FREE FOR THE NEXT USER "
2080 PRINT
2090 PRINT "PLEASE PLACE DISK/CASSETTE IN APPROPRIATE CONTAINER"
2100 PRINT "THANK YOU"
2110 PRINT TAB(61);"G.SEET"
2120 DISP " "
2130 RETURN
2140 END !#####
2150 ! END OF MAIN PROGRAM SEGMENT
2160 ! #####
2170 !
2180 ! ++++++ SUBROUTINE SET ++++++
2190 ! + Sets plotter limit for "GRAPHICS" facility +
2200 ! ++++++
2210 SUB Set(Iset,Mode,Chk,Pcount,Size)
2220 PRINT "ABC"&CHR$(12)
2230 PRINT " PROGRAM VPLOT PLOTTING "
2240 ON Chk GOSUB Plt1,Plt2,Plt3
2250 SUBEXIT
2260 Plt1: ! Graphics
2270 PLOTTER IS 13,"GRAPHICS"
2280 GRAPHICS
2290 LIMIT 0,184.47,10,135
2300 FRAME
2310 RETURN
2320 Plt2: ! Benson plotter
2330 ! 1:A4 , 2:A6
2340 PLOTTER IS 5,"INCREMENTAL",.05
2350 IF FRACT(Pcount/(4*Size))=1/(4*Size) THEN LIMIT 0/Size,297
/Size,20/Size,230/Size
2360 IF FRACT(Pcount/(4*Size))<>1/(4*Size) THEN LIMIT 0/Size,29
7/Size,230/Size,440/Size
2370 FRAME
```

```

2380     RETURN
2390 P1t3: ! 9872A Plotter
2400     PLOTTER IS 7,5,"9872A"
2410     LIMIT 5,275,10,180
2420     IF FRACT(Iset/4)=1/4 THEN FRAME
2430     IF FRACT(Iset/4)=1/4 THEN LIMIT 5,140,10,95
2440     IF FRACT(Iset/4)=2/4 THEN LIMIT 5,140,95,180
2450     IF FRACT(Iset/4)=3/4 THEN LIMIT 140,275,10,95
2460     IF FRACT(Iset/4)=0 THEN LIMIT 140,275,95,180
2470     FRAME
2480     RETURN
2490 SUBEND
2500 !
2510 ! ++++++ SUBROUTINE RESET ++++++
2520 ! + Resets graphic facility. +
2530 ! ++++++
2540 SUB Reset(Iset,Mode,Chk,Pcount,Size)
2550 ON Mode GOSUB Dmode,Manual
2560 SUBEXIT
2570 Dmode: ! Directory mode
2580     ON Chk GOSUB Dplt1,Dplt2,Dplt3
2590     RETURN
2600 Manual: ! Manual mode
2610     ON Chk GOSUB Mplt1,Mplt2,Mplt3
2620     RETURN
2630 Dplt1: ! Graphics
2640     DUMP GRAPHICS
2650     RETURN
2660 Dplt2: ! Benson
2670     BEEP
2680     IF FRACT(Pcount/(4*Size))<>0 THEN RETURN
2690     LIMIT 0,317/Size,-710,0
2700     MOVE 100,0
2710     RETURN
2720 Dplt3: ! 9872A
2730     IF (FRACT(Iset/4)<>0) AND (Iset<>5) THEN RETURN
2740     PRINT "ABC"&CHR$(12)
2750     BEEP
2760     PRINT CHR$(131)&" PLEASE CHANGE PAPER "
2770     PAUSE
2780     RETURN
2790 Mplt1: ! Graphics
2800     BEEP
2810     PAUSE
2820     RETURN
2830 Mplt2: ! Benson
2840     BEEP
2850     IF FRACT(Pcount/(4*Size))<>0 THEN RETURN
2860     LIMIT 0,317/Size,-710,0
2870     MOVE 100,0
2880     RETURN
2890 Mplt3: ! 9872A
2900     IF (FRACT(Iset/4)<>0) AND (Iset<>5) THEN RETURN
2910     PRINT "ABC"&CHR$(12)
2920     PRINT LIN(2)
2930     BEEP
2940     PRINT CHR$(131)&" PLEASE CHANGE PAPER "
2950     RETURN
2960 SUBEND
2970 !

```

```

2980 ! ++++++ SUBROUTINE PLTSG1 ++++++
2990 ! + Generates single plots. +
3000 ! ++++++
3010 SUB Pltsg1(Name1$,SHORT Sp(*),Messag1$,Messag2$)
3020 Ymax=0
3030 Ymin=0
3040 FOR I=1 TO 360 STEP 2
3050 IF Sp(I)>Ymax THEN Ymax=Sp(I)
3060 IF Sp(I)<Ymin THEN Ymin=Sp(I)
3070 NEXT I
3080 D=Ymax
3090 IF ABS(Ymin)>D THEN D=ABS(Ymin)
3100 D=LGT(D)
3110 D=INT(D-1)
3120 Div=10^D
3130 Ymax=Ymax/Div
3140 Ymin=Ymin/Div
3150 Inc=INT((Ymax-Ymin+10)/10)
3160 Ymax=INT((Ymax+1.5*Inc)/Inc)
3170 Ymax=Inc*Ymax
3180 Ymin=INT((Ymin-Inc)/Inc)
3190 Ymin=Inc*Ymin
3200 IF Ymin1>0 THEN Ymin=0
3210 LOCATE 25,135,15,85
3220 SCALE 0,720+.25,1.001*Ymin,1.001*Ymax
3230 AXES 30,1,0,0,3,Inc
3240 LORG 6
3250 FOR I=45 TO 360 STEP 45
3260 MOVE 2*I,-((Ymax+ABS(Ymin))/20)
3270 LABEL I
3280 NEXT I
3290 LORG 8
3300 FOR I=0 TO Ymax STEP Inc
3310 MOVE 4.5,I
3320 LABEL USING "MDDDDXX";I*10
3330 NEXT I
3340 FOR I=0 TO Ymin STEP -Inc
3350 MOVE 4.5,I
3360 LABEL USING "MDDDDXX";I*10
3370 NEXT I
3380 LINE TYPE 1
3390 MOVE 0,0
3400 FOR I=1 TO 360
3410 PLOT I,Sp(I)/Div,-1
3420 NEXT I
3430 FOR I=1 TO 360
3440 PLOT I+360,Sp(I)/Div,-1
3450 NEXT I
3460 SETGU
3470 LORG 1
3480 MOVE 50,6.5
3490 LABEL "ROTOR ANGULAR POSITION (deg)"
3500 DEG
3510 LDIR 90
3520 MOVE 5,10
3530 IMAGE 25A,"-",D,8A
3540 IMAGE 25A,"+",D,8A
3550 Exp=D-1
3560 IF Exp>-1 THEN LABEL USING 3530;Messag1$;ABS(Exp);Messag2$
3570 IF Exp<0 THEN LABEL USING 3540;Messag1$;ABS(Exp);Messag2$

```

```
3580 LDIR 0
3590 MOVE 15,95
3600 LABEL Name1$
3610 MOVE 0,0
3620 SUBEND
3630 !
3640 ! ++++++SUBROUTINE PLTDBL ++++++
3650 ! + Generates double plots. +
3660 ! ++++++
3670 SUB Pltdbl(Name1$,SHORT Dp1(*),Dp2(*),Messag1$,Messag2$)
3680 Ymax=0
3690 Ymin=0
3700 FOR I=1 TO 360 STEP 2
3710 IF Dp1(I)>Ymax THEN Ymax=Dp1(I)
3720 IF Dp2(I)>Ymax THEN Ymax=Dp2(I)
3730 IF Dp1(I)<Ymin THEN Ymin=Dp1(I)
3740 IF Dp2(I)<Ymin THEN Ymin=Dp2(I)
3750 NEXT I
3760 D=Ymax
3770 IF ABS(Ymin)>D THEN D=ABS(Ymin)
3780 D=LGT(D)
3790 D=INT(D-1)
3800 Div=10^D
3810 Ymax=Ymax/Div
3820 Ymin=Ymin/Div
3830 Inc=INT((Ymax-Ymin+10)/10)
3840 Ymax=INT((Ymax+1.5*Inc)/Inc)
3850 Ymin=INT((Ymin-Inc)/Inc)
3860 Ymin=Inc*Ymin
3870 Ymin=Inc*Ymin
3880 LOCATE 25,135,15,85
3890 SCALE 0,720+.25,1.001*Ymin,1.001*Ymax
3900 AXES 30,1,0,0,3,Inc
3910 LORG 6
3920 FOR I=45 TO 360 STEP 45
3930 MOVE 2*I,-((Ymax+ABS(Ymin))/20)
3940 LABEL I
3950 NEXT I
3960 LORG 8
3970 FOR I=0 TO Ymax STEP Inc
3980 MOVE 4.0,I
3990 LABEL USING "MDDDDXX";I*10
4000 NEXT I
4010 FOR I=0 TO Ymin STEP -Inc
4020 MOVE 4.0,I
4030 LABEL USING "MDDDDXX";I*10
4040 NEXT I
4050 MOVE 0,0
4060 LINE TYPE 1
4070 !
4080 ! Plots Input pressures (Ip)
4090 FOR I=1 TO 360
4100 PLOT I,Dp2(I)/Div,-1
4110 NEXT I
4120 FOR I=1 TO 360
4130 PLOT I+360,Dp2(I)/Div,-1
4140 NEXT I
4150 MOVE 0,0
4160 !
4170 ! Outputs second plot
```

```
4180 FOR I=1 TO 360
4190 PLOT I,Dp1(I)/Div,-1
4200 NEXT I
4210 FOR I=1 TO 360
4220 PLOT I+360,Dp1(I)/Div,-1
4230 NEXT I
4240 SETGU
4250 LORG 1
4260 MOVE 50,6.5
4270 LABEL "ROTOR ANGULAR POSITION (deg)"
4280 DEG
4290 LDIR 90
4300 MOVE 5,16
4310 IMAGE 28A,"-",D,8A
4320 IMAGE 28A,"+",D,8A
4330 Exp=D-1
4340 IF Exp>-1 THEN LABEL USING 4310;Messag1$;ABS(Exp);Messag2$
4350 IF Exp<0 THEN LABEL USING 4320;Messag1$;ABS(Exp);Messag2$
4360 LDIR 0
4370 MOVE 15,95
4380 LABEL Name1$
4390 MOVE 0,0
4400 SUBEND
```

**APPENDIX D : SIMULATION RUN**

- D.1 Introduction
- D.2 Datafile Preparation
- D.3 Process Simulation
- D.4 Graphical Output

## D.1 Introduction

The aim of this appendix is to guide the user through a typical simulation run giving details of the required operations and the expected outputs. Within these sections, only very basic knowledge of computer keyboard skills is assumed. The user will be guided through the three stages of; parameter file preparation, process simulation and finally on to graphical output generation.

The following processes assume the default mass-storage device is the HP9885M flexible disk drive set to select code 8 and that the relevant programs VFLGEN, VMODEL and VPLOT are stored on disk. It is essential that the 'PRT ALL' key is latched up, for proper operation of the display facility.

In the documentation quantities bounded by '< >' are acceptable inputs which serve as example values.

## D.2 Datafile Preparation

Program : VFLGEN

User Instructions:

- 1) Insert flexible disk into disk drive.
- 2) Load the program:
  - a. Type: LOAD 'VFLGEN:F8'
  - b. Press: EXECUTE
- 3) Start the program:
  - a. Press: RUN
- 4) When 'INPUT DATA FILENAME (%DAT%%):' appears on CRT display:  
Enter: A filename <ADAT01>

PUMP GEOMETRY

1	STATOR DIAMETER (mm) :	121.4000
2	ROTOR DIAMETER (mm) :	115.0000
3	ASSEMBLY LENGTH (mm) :	50.0000
4	ABUTMENT WIDTH (mm) :	10.0000
5	ABUT. CLEARANCE (mm) :	.0290
6	VANE WIDTH (mm) :	7.0000
7	VANE CLEARANCE (mm) :	.0400
8	PORT DIAMETER (mm) :	25.4000
9	PORT ANGLE(deg) :	27.7900
10	CAM ABUT. RAD. (mm) :	93.7100
11	CAM ACT. RAD. (mm) :	22.3500
12	CAM OP. RAD. (mm) :	49.6600
13	CAM ACT. ANGLE(deg) :	38.2500
14	ENDPLATE O/Diam.(mm) :	127.5000
15	ENDPLATE I/Diam.(mm) :	121.4000
16	ENDPLATE Clear. (mm) :	0.0000
17	NUMBER OF SEGMENTS :	4.0000

OPERATING ENVELOPE

1	SHAFT SPEED (RPM):	2100.0000
2	INLET PRESSURE (bar):	6.2000
3	OUTLET PRESSURE (bar):	138.0000
4	CASE PRESSURE (bar):	1.5000
5	FLUID DENSITY (Kg/m3):	861.0000
6	FLUID VISCOSITY(NS/m2):	.0250
7	BULK MODULUS (MN/m2):	1766.0000
8	INPUT LINE DIAM. (mm):	31.7500
9	OUTPUT LINE DIAM. (mm):	31.7500
10	DISCHARGE COEFF. :	.7000
11	CAVITATION PRESS.(bar):	.6800

INLET GROOVE PARAMETERS

1)Hemisphere:Groove depth (mm):	1.0000
Cutter diam. (mm):	4.0000
Start angle (deg):	10.0000
2)Square :Groove depth (mm):	.6000
Groove width (mm):	4.0000
Start angle (deg):	2.0000
3)Triangular:Groove depth (mm):	3.6000
Cutter angle(deg):	60.0000
Start angle (deg):	10.0000
INLET GROOVE TYPE (0-3) :	0.0000

OUTLET GROOVE PARAMETERS

1)Hemisphere:Groove depth (mm):	1.5000
Cutter diam. (mm):	6.0000
Start angle (deg):	30.0000
2)Square :Groove depth (mm):	1.2500
Groove width (mm):	6.0000
Start angle (deg):	30.0000
3)Triangular:Groove depth (mm):	3.6000
Cutter angle(deg):	60.0000
Start angle (deg):	30.0000
OUTLET GROOVE TYPE (0-3) :	0.0000

FIG.D.2.1 PARAMETER DATAFILE CONTENTS

Press: CONT

5) If no such file exists on disk, the program enters into the mode which requests the necessary input values for file generation, If a file already exists, editing can be performed, for which section (5.5) highlights the process. It will be assumed here, that the simulation proceeds from scratch. In this case the display will show the pump geometry page with the cursor at item 1.

a: Enter: The parameter value <121.4>

b: Press: CONT

6) Continue until all three pages of data are filled. Suitable values are shown in figure (D.2.1), which is an actual print out from the program.

7) On completion of input process.

a: Press: Key 9

8) Display shows 'SAME FILENAME (DEFAULT:Y):'

a: Press: CONT

Program prints list shown in figure (D.2.1) and outputs to disk.

9) Terminate from program.

a: Press: Key 15

First stage complete proceed to next 'Process Simulation'

Editing:

Selection of Key 7 defines the functions.

Select function key as required and proceed, whilst following program prompts.

### D.3 Process Simulation

Program : VMODEL

User Instructions:

- 1) Insert flexible disk into disk drive.
- 2) Load the program:
  - a. Type: LOAD 'VMODEL:F8'
  - b. Press: EXECUTE
- 3) Start the program:
  - a. Press: RUN
- 4) When 'IS AUTO SEQUENCE REQUIRED (Y/N):' appears on CRT display:
  - a. Enter: N (for manual mode or Y for auto mode)
  - b. Press: CONT
- 5a) For manual mode:

When 'ENTER DATA FILENAME (VDAT%%):' appears on CRT:

  - a. Enter: Filename <ADAT01>
  - b. Press: CONT

If datafile entry is correct the program executes and performs simulation. At the end of the run the datafile <AGDT01> is output and the program stops. Proceed on to 'Graphical Output'

OR

- 5b) For auto mode:

When 'INPUT FILENAME PREFIX:Default (V)DAT:' appears on CRT:

  - a. Enter: File prefix <A>
  - b. Press: CONT
- 6) When 'OUTPUT FILENAME PREFIX:Default (V)GDT:' appears on CRT:
  - a. Enter: File prefix <B>
  - b. Press: CONT
- 7) When 'INPUT LOWEST DATAFILE NO. (>=0):' appears on CRT:

- a. Enter: Lowest number <1>
  - b. Press: CONT
- 8) When 'INPUT HIGHEST DATAFILE NO. (<=99):' appears on CRT:
- a. Enter: Highest number <5>
  - b. Press: CONT
- 9) When 'IS PLOT REQUIRED :' appears on CRT:
- a. Enter: N (for no plot or Y for plot)
  - b. Press: CONT

The suggested entry assumes the existence of five datafiles with filenames ADAT01 to ADAT05 on disk. The successful run would result in the generation of five files BGDT01 to BGDT05 and no graphical output, as yet. If 'Y' was input for 9 above, the program VPLOT would have been loaded automatically with outputs to the drum plotter, otherwise proceed to 'Graphical output'.

#### Running Outputs:

During execution the program prints out on the CRT the current results and progress indicators which inform on the progress of the simulation.

#### D.4 Graphical Output

Program : VPLOT

User Instructions:

- 1) Insert flexible disk into disk drive.
- 2) Load the program:
  - a. Type: LOAD 'VPLOT:F8'
  - b. Press: EXECUTE
- 3) Start the program:

a. Press: RUN

4a) When 'DO YOU REQUIRE VIDEO GRAPHICS (Y/N):' appears on CRT display

a. Type: Y (for graphics or N for other medium)

b. Press: CONT

If 'Y' goto 5

4b) When 'DO YOU REQUIRE BENSON (Y/N):' appears on CRT display

a. Type: Y (for Benson or N for other medium)

b. Press: CONT

If 'Y' goto 5

4c) When 'DO YOU REQUIRE 9872A (Y/N):' appears on CRT display

a. Type: Y (for 9872A or N for other medium)

b. Press: CONT

If 'Y' goto 5

5) When 'IS AUTO SEQUENCE REQUIRED (Y/N):' appears on CRT display:

a. Enter: N (for manual mode or Y for auto mode)

b. Press: CONT

5a) For manual mode:

When 'ENTER DATA FILENAME (VDAT%%):' appears on CRT:

a. Enter: Filename <AGDT01>

b. Press: CONT

If datafile entry is correct the program executes and performs plotting. End of simulation run.

OR

5b) For auto mode:

When 'INPUT DATAFILE PREFIX (Default 'V'):' appears on CRT:

a. Enter: File prefix <B>

b. Press: CONT

6) When 'INPUT LOWEST DATAFILE NO. (>=0):' appears on CRT:

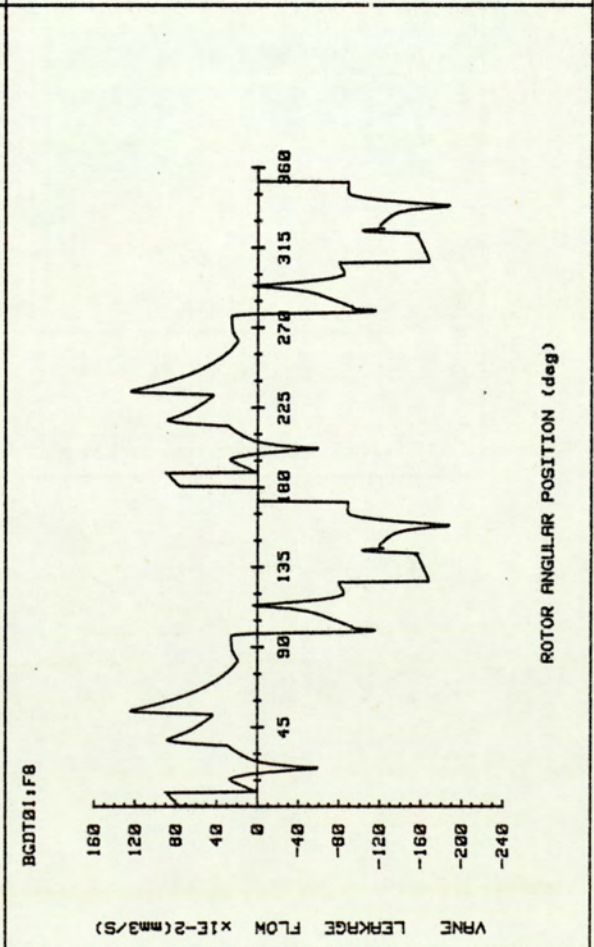
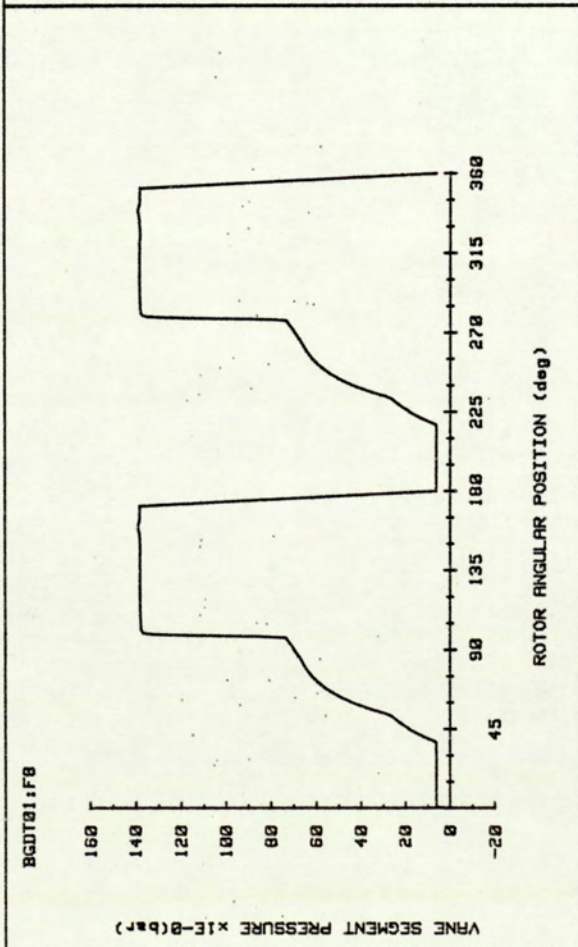
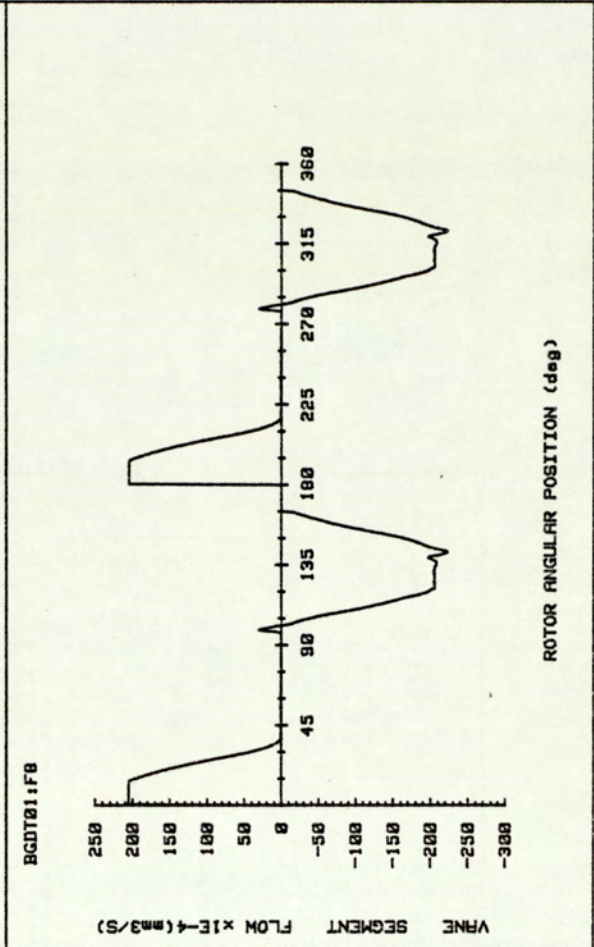
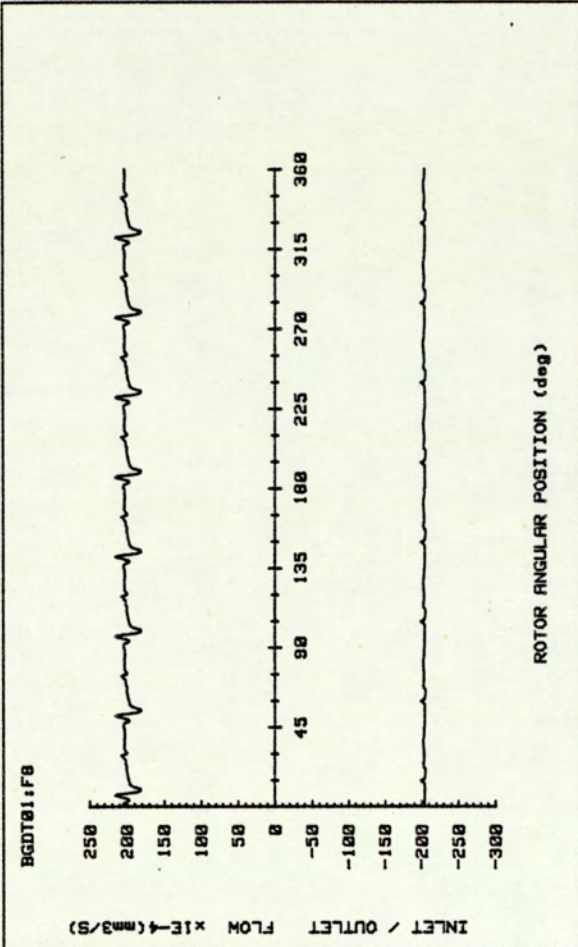


FIG.D.4.1 GRAPHICAL OUTPUT OF PUMP PROCESS - SHEET 1

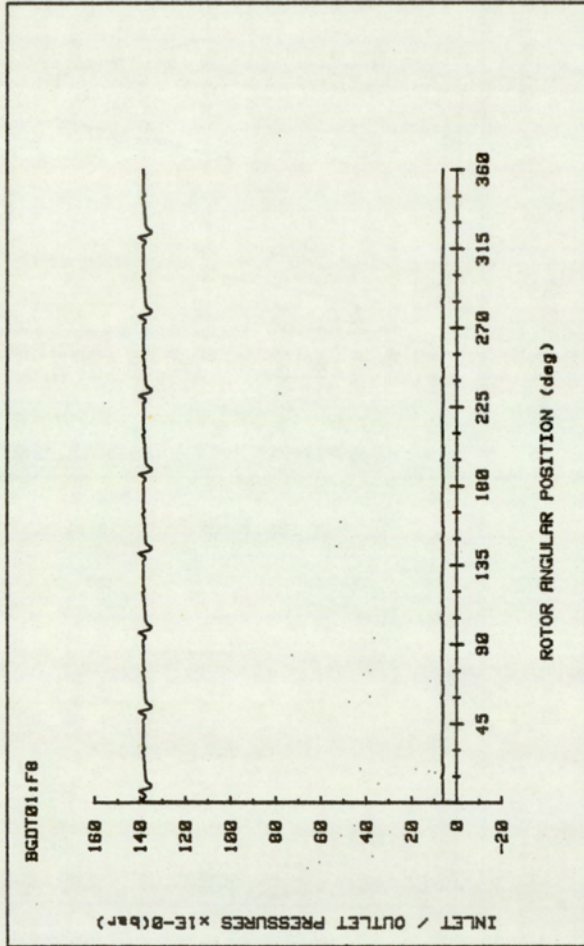


FIG.D.4.2 GRAPHICAL OUTPUT OF PUMP PROCESS - SHEET 2

- a. Enter: Lowest number <1>
  - b. Press: CONT
- 7) When 'INPUT HIGHEST DATAFILE NO. (<=99):' appears on CRT:
- a. Enter: Highest number <5>
  - b. Press: CONT

The suggested entry assumes the existence of five datafiles of filenames BGD01 to BGD05 on disk. The successful run would result in the generation of five sets of graphical output. The figure (D.4.1) and (D.4.2) shows one such set of graphical output.

## **REFERENCES**

List of Abbreviations

List of References

## LIST OF ABBREVIATIONS

AHEM	Association of Hydraulic Equipment Manufacturers
ASME	American Society of Mechanical Engineers
BFPR	British Fluid Power Research
BHRA	British Hydrodynamic Research Association
Conf.	Conference on
Dept.	Department of
Engng.	Engineering
Engrs	Engineers
IASTED	International Association of Science and Test for Development
IFIPS	International Federation for Information Processing Society
IMechE	Institution of Mechanical Engineering
Int.	International
J.	Journal
JSME	Japan Society of Mechanical Engineers
Mech.	Mechanical
Proc.	Proceedings
Pt.	Part
Symp.	Symposium
Trans.	Transactions
Vol.	Volume

## LIST OF REFERENCES

- 1 Jones , R. 'Hydraulic Propulsion Motor'. Normalair Garrett Ltd. Report T.P.1490. (1976).
- 2 Burgess, C.K. 'Hydraulic Pump-Preliminary Designs'. Normalair Garrett Ltd. Report, (1978).
- 3 Wuerzer, N.J. 'The Design of a Radial Vane Pump'. MSc., thesis. Dept. Mech. Engng, University of Birmingham, 1979.
- 4 Stecki, J,S. 'Noise of Hydraulic Positive Displacement'. Conf. Vibration and Noise in Pumps, Fans and Compressors. Southampton University, 1975.
- 5 BISHOPP, B.E. 'Some Aspects of Pre-compression Variation and the Effects on Pump Noise'. National Conf. Fluid Power, 1972.
- 6 Iyengar, S.K.R. 'Review of Computer Software for Simulating Hydraulic Systems'. BFPR. J., 1979, Vol. 12, Pt. 4
- 7 Foster, K. 'Computer-Aided Design of Positive Displacement Pumps'. Seminar on Applied control and Identification. Copenhagen, Denmark, 28 Jun.- 1 Jul., 1983, IASTED.
- 8 Hooke, C., Madera, G. and Foster, K. 'CAD for the Port Plate of a Two-Bearing Axial Piston Pump Motor'. Seminar on Computer Aided Design in High Pressure Hydraulic Systems. 21 Nov., 1983, IMechE.
- 9 O'Neal, D.L. and Maroney, G.E. 'Measuring Pump Fluidborne Noise Generation Potential'. BFPR., J., 1978, Vol. 11, Pt. 2.
- 10 Crook, A. and Hansford, I. 'Oil Hydraulic Relief Valve Noise'. Seminar on Quiet Oil Hydraulics. 2-3 Nov., 1977. IMechE.

- 11 Heron, R.A. and Hansford, I. 'Airborne Noise Due to Structure Borne Vibrations Transmitted Through Pump Mountings and Along Circuits'. Seminar on Quiet Oil Hydraulics. 2-3 Nov., 1977, IMechE.
- 12 Longmore, D.K. 'The Transmission and Attenuation of Fluid Borne Noise in Hydraulic Hose'. Seminar on Quiet Oil Hydraulics. 2-3 Nov., 1977, IMechE.
- 13 Crook, A., and Heron, R.A. 'Airborne Noise From Hydraulic Lines Due to Liquid Borne Noise'. Seminar on Quiet Oil Hydraulics, 2-3 Nov., 1977, IMechE.
- 14 Hughes, M.L. 'Flexural Vibrations in Rigid Pipework Due to Liquid Borne Noise'. Seminar on Quiet Oil Hydraulics. 2-3, Nov., 1977, IMechE.
- 15 Donaldson, C. 'A Quiet Valve'. Quieter Fluid Power Handbook. BHRA, 1980.
- 16 Helgestead, B.O, Foster, K. and Bannister, F.K. 'Noise in an Axial Piston Pump'. Seminar on Noise Emitted by Fluid Power equipment - Its Causes and Control. 1973. IMechE.
- 17 Martin, M.J. and Taylor, R. 'Optimised Port plate Timing for an Axial Piston Pump'. 5th Int. Symp. Fluid Power. 13-15 Sept., 1978, BHRA.
- 18 Kelsey, J., Taylor, R. and Foster, K. 'Fluid Properties: The Effects of the Fluid Being Pumped on the Noise Emitted by an Axial Piston Pump'. Seminar on Quieter Oil Hydraulics. 29-30 Oct., 1980, IMechE.
- 19 Brown, David and Sons Limited. 'Roloid Pump Gears'. Mechanical World. Vol. 80, 1926.

- 20 Meldahl, A. 'A Theory of Gear Pumps'. Brown-Boveri Review.  
Vol. 26, 1939.
- 21 Fielding, D., Taylor, R. and Foster, K. 'Notes on the Selection  
of a Standard Delivery Condition for the  
Theoretical Prediction and Experimental  
Measurement of Pressure Ripple'. 5th. International  
Fluid Power Symp. 13-15 Sept., 1978.
- 22 Mukerjee, P. and Bhattachryya. 'Analysis of Gear Pumps'.  
J. Inst. Engs. India, Vol. 52,9, Pt. NE5.
- 23 Merritt, H.E. 'Gears', Pitman 19.
- 24 Hadekel 'Displacement Pumps and Motors'. Pitman and Sons.
- 25 Bloch, P. 'Theoretical and Experimental Investigation in  
Connection with a Fluid Transmission Mechanism  
(The Hydro-Titan transmission)'.  
Von Roll Mitteilungen. 1953, Vol. 12, Pt. (1/2).
- 26 Zaichenko, I.Z. and Boltyanskii, A.D. 'Reducing Noise Level of  
Axial Piston Pumps'. Russian Engng. J. Vol. XLIX,  
Pt. 4, 1969.
- 27 Yamaguchi, A. 'Studies on the characteristics of Axial Plunger  
Pumps and Motors'. (1st. and 2nd. reports).  
Bulletin of Japanese Society of Mech. Engrs.,  
Vol. 9, Pt. 34, 1966.
- 28 Helgestad, B.O, Foster, K and Bannister, F.K. 'Pressure  
Transients in an Axial Piston Hydraulic Pump'.  
Proc. IMechE. Vol. 180, Pt. 17/74, 1974.
- 29 Kakoullis, Y.P. 'An Investigation of the Torque Characteristics  
of an Axial Piston Pump'. B.Sc., thesis, Dept.  
Mech. Eng., University of Birmingham, 1974.

- 30 Hannan, D.M. 'Flow, Pressure and Flow Pulsations in a Hydraulic Axial Piston Pump'. MSc., thesis. Dept. Mech. Engng., University of Birmingham, 1976.
- 31 Foster, K. and Hannan, D.M. 'Fundamental Fluidborne and Airborne Noise Generation of Axial Piston Pumps'. Seminar on Quiet Oil Hydraulics. 2-3 Nov., 1977, IMechE.
- 32 Willekens, F.A.M. 'Fluid Borne Noise in Hydraulic Systems'. 1st. European Fluid Power Conf., East Kilbride, U.K., 1973.
- 33 Kogima, E and Nagakura, H. 'Characteristics of Fluid Borne Noise Generated by Fluid Power Pumps', (1st Report, Mechanism of Generation of Pressure Pulsations in Axial Piston Pump). JSME. B., Vol. 25, No.199, Jan. 1982.
- 34 Fielding, D. and Hooke, C.J. 'Sources of Pressure Pulsation From a Gear Pump'. Seminar on Quiet Oil Hydraulics. 2-3 Nov., 1977, IMechE.
- 35 Bidhendi, I.M., Foster, K., Taylor, R. 'Computer Predictions of Cyclic Excitation Sources for an External Gear Pump'. Seminar on Computer Aided Design in High Pressure Hydraulic Systems. 21 Nov., 1983, IMechE., AHEM. and BHRA.
- 36 Fielding, D., Taylor, R. and Hooke, C.J. 'An Investigation into the Effects of Sideplate Clearance on the Delivery Flow Ripple Produced by an Enternal Gear Pump'. Seminar on Quieter Oil Hydraulics. 29-30 Oct., 1980. IMechE.

- 37 Kogima, E., Shinada. M. and Yoshino. T. 'Characteristics of Fluid Borne Noise Generated by Fluid Power Pumps', (2nd Report, Pressure Pulsations in Balanced Vane Pump). JSME. B., Vol. 27, No.225, Mar. 1984.
- 38 Constantinesco, G. 'Theory of Wave Transmission, a Treatise on Transmission of Power by Sinusoidal Wave Motion Through Hydraulic Oil in a Uniform Pipe'. Walter Haddon, 1922.
- 39 Bowns, D.E. and McCandlish, D. 'Pressure Ripple Propagation'. Seminar on Quiet Oil Hydraulics. 2-3 Nov., 1977, IMechE.
- 40 Bowns, D.E. and Edge, K.A. 'The Assessment of Pump Fluid Borne Noise', Seminar on Quiet Oil Hydraulics. 2-3 Nov., 1977, IMechE.
- 41 Edge, K. 'Positive Displacement Pumps as Generators of Fluid-Borne Noise'. Quieter Fluid Power Handbook. BHRA., 1980.
- 42 Iyengar, S.K.R. and Maroney, G.E. 'Estimation of the "Blocked Pressure" ripple for a Fixed Displacement Pump'. BFPR. J. 1979, Vol. 12, pt. 4.
- 43 Conesco Inc. 'Study of Fluidborne Noise and the Development of Fluid Acoustic Filter Test Specification and Rules'. Conesco, Cambridge, Massachusetts. May, 1964.
- 44 O'Neal, D.L. and Maroney, G.E. 'Performance Evaluation of Fluidborne Noise Attenuators'. National Conf. Fluid Power, 1976.

- 45 O'Neal, D.L. and Maroney, G.E. 'A Computer Aided Stationary Transducer Fluidborne Noise Measurement Technique'. BFP.R., J., 1978, Vol. 11, Pt. 1.
- 46 Henderson, A.R. 'Measuring the Performance of Fluid-Borne Noise Attenuators'. Seminar on Quiet Oil Hydraulics. 2-3 Nov., 1977, IMechE.
- 47 McCandlish, D., Edge, K.A. and Tilley, D.G. 'Fluid Borne Noise Generated by Positive Displacement Pumps. Seminar on Quiet Oil Hydraulics. 2-3 Nov., 1977, IMechE.
- 48 Tilley, D. 'Fluid Borne Noise in Hydraulic Systems'. Quieter Oil Fluid Power Handbook. BHRA., 1980.
- 49 Taylor, R., Penny, J.E.T. and Seet, G. 'Pressure Ripple Effects with Two Pump Outputs Connected'. Hydraulic and Air Engineering, Oct., 1982.
- 50 Massey, B.S. 'Mechanics of Fluids'. Von Nostrand Reinhold Company, London, 1971.
- 51 Gear, C.W. 'The Automatic Integration of Stiff Differential Equations'. Proc. IFIPS. Conf. Edinburgh, 1968.
- 52 Foster, K. Lecture notes on 'Advanced Phase Dissemination Notes on Quieter Hydraulic Systems and Hydraulic Pumps'. Dept. Mech. Engng. University of Aston in Birmingham. 1981.
- 53 Foster, K., and Parker, G.A. 'Transmission of Power by Sinusoidal Wave Motion Through Hydraulic Oil in a Uniform Pipe'. Proc. IMechE. Vol. 179, Pt.1, No.19, 1964-65.
- 54 Oldenburger, R. and Goodson, R.E. 'Simplification of Hydraulic Line by Use of Infinite Products'. ASME. Trans. J. Basic Engng., March 1964.

- 55 Iyengar, S.K.R. 'Pressure Ripple Calculations in Fluid Power Systems Using Linear Systems Theory'. BFPR. J., 1978, Vol. 11, Pt. 3.
- 56 Otnes, R.K. and Enochson, L. 'Applied Time Series Analysis'. Vol. 1. Basic Techniques. John Wiley and Sons. 1978.
- 57 McCalla, T.R. 'Introduction to Numerical Methods and Fortran Programming'. John Wiley & Sons, Inc. 1967.
- 58 Wusthof, P., and Rexroth, G.L. 'An Analysis of Pump Parameters Influence on Noise Level'. Proc. Symp. Fluid Power Testing. Fluid Power Society. 16-18 Aug., 1976.
- 59 Taylor, R. 'Pump Noise and its Treatment'. Quieter Fluid Power Handbook. BHRA., 1980.
- 60 Kelsey, K., Taylor, R. and Wood, K. 'The Practical Benefits of Optimising the Port Timing for an Axial Piston Pump'. Seminar on Quieter Oil Hydraulics. 29-30 Oct., 1980. IMechE.
- 61 Williams, P.W. 'Numerical Computation'. Thomas Nelson and Sons, Great Britain, 1979.
- 62 Bowns, D.E, Edge, K.A and McCandlish, D. 'Factors Affecting the Choice of a Standard Method for the Determination of Pump Pressure Ripple'. Seminar on Quieter Oil Hydraulics. 29-30 Oct., 1980. IMechE.